

**Development of Organocatalyzed Enantioselective  
Conjugate Addition and Application to the Total  
Synthesis of Cannabinoids**

by  
Jirong Luo

A dissertation submitted to the Department of Chemistry,  
College of Natural Sciences and Mathematics  
in partial fulfillment of the requirements for the degree of

DOCTOR OF PHILOSOPHY

in Chemistry

Chair of Committee: Dr. Jeremy A. May

Committee Member: Dr. Olafs Daugulis

Committee Member: Dr. Eva Harth

Committee Member: Dr. Barbara Czako

Committee Member: Dr. Arnold Guloy

University of Houston  
May 2022

*In memory of Jiahua Yang,*

*You were always a caring and inspiring figure in our family,*

*Your virtues will be remembered,*

*Your legacy will be carried on.*

## ACKNOWLEDGEMENTS

I would like to acknowledge my advisor, Dr. Jeremy May. Accomplishing the total synthesis of a natural product has always been my dream since college, this dream would never come true without your support and guidance.

I would like to acknowledge my committee, Dr. Olafs Daugulis, Dr. Barbara Czako, Dr. Eva Harth, and Dr. Arnold Guloy for their support and advice. You are all great chemists that I look up to. I have no doubt that everything I've learnt from you will help me succeed in my future career.

I would like to acknowledge all my past and present group members for their support. Especially Dr. Po-An Chen, Dr. Sasha Sundstrom, and Dr. Qinxuan Wang, you have always been good friends to talk to, and good scientists to learn from.

I would like to thank my parents who offered unconditional love and support as I pursued my degree. I would not be able to focus on my research without you taking care of everything back at home.

I would like to thank my grandaunt Jiahuang Ji and granduncle Jiahua Yang for their love during my five years of study in Houston. Thank you for sharing me a taste of home when I'm thousands of miles away from my motherland. My heart was shattered when Jiahua passed. I believe he has found peace by the side of God.

I would like to dedicate my special thanks to the love of my life, Ms. Lining Feng. Your love and gentle encouragement carried me through the most desperate days in my research.

## ABSTRACT

(-)- $\Delta^9$ -Tetrahydrocannabinol (THC) and cannabidiol (CBD) were synthesized via an organocatalyzed tandem enantioselective conjugate addition/enolate alkylation annulation with a novel ambiphilic trifluoroborate in 7 steps (longest linear steps; 10 steps overall with 23% yield for THC and 18% yield for CBD) from inexpensive commercially available starting materials. Both vinyl and aryl ambiphilic trifluoroborates were synthesized and showed great compatibility with various functional group, high yields, and excellent stereoselectivity. To demonstrate how these qualities will facilitate synthesizing THC and CBD analogs that were previously difficult to access with existing methods, we completed the synthesis of a novel benzo-fused A-ring analog of THC. Tandem reaction product containing all-carbon quaternary centers were also obtained with good to excellent enantioselectivity.

## Table of Contents

Acknowledgements.....	iii
Abstracts.....	iv
Table of Contents.....	v
List of Figures.....	ix
List of Schemes .....	xi
List of Tables.....	xii
List of Abbreviations .....	xiii
<b>Chapter 1 Organocatalyzed Enantioselective Conjugate Addition Reactions and Enantioselective Total Synthesis of Cannabinoids .....</b>	<b>1</b>
1.1 Conjugate Addition Reaction (Michael Addition).....	1
1.2 Transition Metal Catalyzed Enantioselective Conjugate Addition Reactions .....	2
1.3 Organocatalyzed Enantioselective Conjugate Addition with Organoboronates as Nucleophile .....	4
1.3.1 BINOL-derivative Catalyzed Enantioselective Conjugate Addition Reported by J. Michael Chong .....	4
1.3.2 Thiourea-derivatives Catalyzed Enantioselective Conjugate Addition Reported by Takemoto.....	5
1.3.3 O-monoacylatartaric Acid Catalyzed Enantioselective Conjugate Addition Reported by Sugiura .....	6
1.3.4 Further Reaction Development in the May Group .....	6
1.4 Introduction to Cannabinoids .....	9

1.5 Total Synthesis of Cannabinoids via Enantioselective Catalysis Routes.....	11
1.5.1 Enantioselective Diels-Alder Route Developed by the Evans Group .....	11
1.5.2 Asymmetric Allylic Alkylation Route Developed by the Trost Group.....	11
1.5.3 Asymmetric Hydrogenation Route Developed by the Zhou Group.....	12
1.5.4 Stereodivergent Route Developed by the Carreira Group.....	13
1.5.5 Enzyme Controlled Reduction Route Developed by the Leahy Group.....	14
1.5.6 NHC Catalysis Route Developed by the Lupton Group.....	15
1.7 Limitation of Existing Routes and Proposed Retrosynthetic Analysis.....	16
1.8 Focus of This Thesis .....	17
1.9 Bibliography .....	18
<b>Chapter 2 Development of Ambiphilic Organoboronates.....</b>	<b>23</b>
2.1 Ambiphilic Molecules and Their Application in Organic Synthesis.....	23
2.2 Design of Ambiphilic Organoboronates .....	24
2.3 Synthesis of Type A Ambiphilic Organoboronates .....	26
2.4 Synthesis of Type B Ambiphilic Organoboronates .....	29
2.5 Synthesis of Type C Ambiphilic Organoboronates .....	30
2.6 Conclusion.....	33
2.7 Experimental.....	34
2.7.1 Material and Methods.....	34
2.7.2 Synthesis of Vinyl Ambiphilic Trifluoroborate ( <b>2.38</b> ) from 3-butyn-1-ol ( <b>2.30</b> )....	35
2.7.3 Synthesis of Cyclic Ambiphilic Boronates <b>2.44</b> and <b>2.51</b> .....	38
2.7.4 Synthesis of <b>2.54</b> and <b>2.55</b> .....	41
2.7.5 Synthesis of Geminal Ambiphilic Trifluoroborate <b>2.60</b> .....	42

2.7.6 Synthesis of Aryl Ambiphilic Trifluoroborates <b>2.63</b> , <b>2.69</b> , <b>2.77</b> , and <b>2.82</b> .....	45
2.8 Bibliography .....	52
Chapter 2 Appendix .....	56
<b>Chapter 3 Conjugate Addition Enolate Alkylation Reaction Development</b> .....	<b>92</b>
3.1 Reaction Discovery and Optimization .....	92
3.2 Conjugate Addition Scope.....	99
3.3 Conjugate Addition Enolate Alkylation Scope.....	102
3.4 Conclusion .....	105
3.5 Experimental.....	106
3.5.1 Material and Methods .....	106
3.5.2 HPLC Columns .....	107
3.5.3 Synthesis of the Catalysts .....	107
3.5.4 Synthesis of Enones.....	108
3.5.5 General procedure of the BINOL-catalyzed conjugate addition reactions between ( <i>Z</i> )- (4-bromo-2-methylbut-1-en-1-yl)trifluoro- $\lambda^4$ -borane, potassium salt ( <b>3.2</b> ) and various enones (0.2 mmol scale) .....	111
3.5.6 General procedure of the BINOL-catalyzed conjugate addition reactions between (2- (2-bromoethyl)-4-methoxyphenyl)trifluoro- $\lambda^4$ -borane, potassium salt ( <b>3.19</b> ) and various enones (0.2 mmol scale) .....	120
3.5.7 General procedure of the tandem BINOL-catalyzed conjugate addition enolate alkylation annulation between ( <i>Z</i> )-(4-bromo-2-methylbut-1-en-1-yl)trifluoro- $\lambda^4$ -borane, potassium salt ( <b>3.2</b> ) and various enones (0.2 mmol scale).....	125

3.5.8 General procedure of the BINOL-catalyzed conjugate addition tandem enolate alkylation annulation between (2-(2-bromoethyl)-4-methoxyphenyl)trifluoro- $\lambda^4$ -borane, potassium salt ( <b>3.19</b> ) and various enones (0.2 mmol scale).....	133
3.6 Bibliography .....	136
Chapter 3 Appendix .....	139
<b>Chapter 4 Total Synthesis of Cannabinoids</b> .....	<b>247</b>
4.1 Retrosynthetic Analysis.....	247
4.2 Total Synthesis of THC ( <b>4.1</b> ) and CBD ( <b>4.2</b> ).....	249
4.3 Total Synthesis of Novel THC Analog <b>4.13</b> .....	252
4.4 Conclusion.....	253
4.5 Experimental.....	254
4.5.1 Material and Methods .....	254
4.5.2 Synthesis of CBD <b>4.2</b> .....	255
4.5.3 Synthesis of THC <b>4.1</b> .....	257
4.5.4 Synthesis of Analog <b>4.13</b> .....	258
4.6 Bibliography .....	259
Chapter 4 Appendix .....	261

## List of Figures

<b>Figure 1.1</b> Conjugate Addition/Michael Addition/1,4-Addition .....	1
<b>Figure 1.2</b> Diastereoselective Conjugate Addition with Enantiopure Starting Materials .....	2
<b>Figure 1.3</b> Copper Catalysis for Enantioselective Conjugate Addition .....	2
<b>Figure 1.4</b> Copper Oxazoline Thiolate Catalyzed Asymmetric Conjugate Addition .....	3
<b>Figure 1.5</b> Palladium-Catalyzed Asymmetric Conjugate Addition .....	3
<b>Figure 1.6</b> First Use of Organoboronate Conjugate Addition Reported by Suzuki .....	4
<b>Figure 1.7</b> Chong's Report of Organocatalyzed Enantioselective Conjugate Addition .....	4
<b>Figure 1.8</b> Thiourea-derived Catalysts Developed by the Takemoto Group .....	5
<b>Figure 1.9</b> Tartaric Acid-derived Catalyst Developed by the Sugiura Group .....	6
<b>Figure 1.10</b> BINOL Catalyzed Enantioselective Conjugate Addition to Unprotected Indolyl Enone .....	7
<b>Figure 1.11</b> Expanded Enone Scope .....	7
<b>Figure 1.12</b> Expanded Trifluoroborate Salt Scope .....	8
<b>Figure 1.13</b> Key Step of Banwell's Synthesis of Discoipyrrole D .....	8
<b>Figure 1.14</b> Proposed Key Step for Mucronatin Synthesis .....	9
<b>Figure 1.15</b> Selected Natural and Synthetic Cannabinoids .....	10
<b>Figure 1.16</b> Dethe Cannabinoid Synthesis via Chiral Pool Strategy .....	10
<b>Figure 1.17</b> Key Step of Evans' THC Synthesis .....	11
<b>Figure 1.18</b> Key Transformations in Trost's THC Synthesis .....	12
<b>Figure 1.19</b> Key Transformations in Zhou's THC Synthesis .....	13
<b>Figure 1.20</b> Stereodivergent Dual Catalysis Strategy in Carreira's THC Synthesis .....	14
<b>Figure 1.21</b> Key Transformations in Leahy's THC Synthesis .....	15

<b>Figure 1.22</b> Key Step of Lupton's THC Synthesis .....	15
<b>Figure 2.1</b> Wittig Reaction .....	23
<b>Figure 2.2</b> Corey-Chaykovsky Epoxidation/Cyclopropanation and 1,3-Dipolar Cycloaddition Reaction.....	24
<b>Figure 2.3</b> Catalytic Cycle of BINOL-Derivative Catalyzed Conjugate Addition/Enolate Alkylation Reaction with Ambiphilic Organoboronate.....	25
<b>Figure 2.4</b> Design of Ambiphilic Organoboronates.....	26
<b>Figure 3.1</b> Proposed Conjugate Addition Enolate Alkylation Mechanism .....	94
<b>Figure 3.2</b> Conjugate Addition with Ambiphilic Aryl Trifluoroborates.....	100
<b>Figure 3.3</b> Conjugate Addition Scope with Ambiphilic Vinyl Trifluoroborate <b>2</b> .....	101
<b>Figure 3.4</b> Conjugate Addition/Enolate Alkylation Annulation Tandem Reaction .....	102
<b>Figure 4.1.</b> Retrosynthetic Analysis of THC ( <b>1</b> ) and CBD ( <b>2</b> ).....	247
<b>Figure 4.2.</b> Retrosynthetic analysis of novel THC analog <b>13</b> .....	249

## List of Schemes

<b>Scheme 2.1</b> Synthesis of Ambiphilic Trifluoroborate <b>2.34</b> .....	27
<b>Scheme 2.2</b> Synthesis of Ambiphilic Trifluoroborate <b>2.38</b> .....	27
<b>Scheme 2.3</b> Synthesis of Ambiphilic Trifluoroborate <b>2.45</b> .....	28
<b>Scheme 2.4</b> Synthesis of Ambiphilic Trifluoroborate <b>2.52</b> .....	29
<b>Scheme 2.5</b> Attempt for the Synthesis of <b>56</b> .....	29
<b>Scheme 2.6</b> Synthesis of Ambiphilic Trifluoroborate <b>2.60</b> .....	30
<b>Scheme 2.7</b> Synthesis of Ambiphilic Aryl Trifluoroborate <b>2.63</b> .....	31
<b>Scheme 2.8</b> Synthesis of Ambiphilic Trifluoroborate <b>2.69</b> .....	31
<b>Scheme 2.9</b> Synthesis of <b>2.73</b> .....	32
<b>Scheme 2.10</b> Synthesis of Ambiphilic Trifluoroborate <b>2.77</b> .....	32
<b>Scheme 2.11</b> Synthesis of Ambiphilic Trifluoroborate <b>82</b> .....	33
<b>Scheme 3.1</b> Conjugate Addition with Geminal Trifluoroborate <b>13</b> .....	99
<b>Scheme 3.2</b> Double Alkylation to Form a <i>cis</i> -Decalin with Quaternary Carbon .....	104
<b>Scheme 3.3</b> Double Alkylation to Form a Decalin with Aryl Trifluoroborate.....	105
<b>Scheme 4.1</b> Synthesis of ambiphilic vinyl trifluoroborate <b>4</b> .....	250
<b>Scheme 4.2</b> Synthesis of enone <b>4.5</b> .....	250
<b>Scheme 4.3</b> Synthesis of key intermediate <b>4.3</b> .....	251
<b>Scheme 4.4</b> Synthesis of THC and CBD .....	251
<b>Scheme 4.5</b> Synthesis of ambiphilic aryl trifluoroborate <b>4.15</b> .....	252
<b>Scheme 4.6</b> Synthesis of aryl-fused intermediate <b>4.14</b> .....	253
<b>Scheme 4.7</b> Synthesis of novel THC analog <b>4.13</b> .....	253

## List of Tables

<b>Table 3.1</b> Solvent Screen for Conjugate Addition .....	92
<b>Table 3.2</b> Catalyst and Time Screen for Conjugate Addition in DCE .....	93
<b>Table 3.3</b> Base Screen with Conjugate Addition in DCE .....	95
<b>Table 3.4</b> Enolate Alkylation Optimization.....	96
<b>Table 3.5</b> Optimization of the Conjugate Addition in 2-MeTHF .....	97
<b>Table 3.6</b> Optimization of Combined Reaction .....	98

## List of Abbreviations

2-MeTHF	2-methyltetrahydrofuran
9-BBN	9-benzobicyclononane
aq	aqueous
Ar	aryl
BINOL	1,1'-bi-2-naphthol
Bn	benzyl
Boc	tert-butoxycarbonyl
Bpin	pinacolborane
<i>t</i> -Bu	<i>tert</i> -butyl
cat.	catalyst
Cbz	carboxybenzyl
DCE	1,2-dichloroethane
LDA	lithium diisopropyl amine
MOM	methoxymethyl
<i>n</i> -Bu	<i>n</i> -butyl
NMR	nuclear magnetic resonance
Nu	nucleophile
PCC	pyridinium chlorochromate
Ph	phenyl
PhMe	toluene
RT	room temperature
SM	starting material

Tf	triflate
TFA	trifluoroacetic acid
THF	tetrahydrofuran
TLC	thin layer chromatography
TMEDA	tetramethylethylenediamine
TMS	trimethylsilyl
Ts	tosyl

# Chapter 1

## Organocatalyzed Enantioselective Conjugate Addition Reactions and Enantioselective Total Synthesis of Cannabinoids

### 1.1 Conjugate Addition Reaction (Michael Addition)

Carbon-Carbon bond formation is always a popular topic in organic synthesis. Methods that allow the reaction to take place in a selective manner are highly sought. Conjugate addition (also known as 1,4 addition or Michael addition) is one of the most powerful tools in organic synthesis for forming new carbon-carbon bonds selectively. In 1887, Arthur Michael systematically studied formation of substituted pentanedioic acid diesters in a reaction using diethyl malonate as a nucleophile and  $\alpha,\beta$ -unsaturated ethyl cinnamate as an electrophile (Figure 1.1).<sup>1</sup> During his study, the diethyl malonate added across the double bond of ethyl cinnamate. Later in 1894, he found that electron-deficient triple bonds would also react in the same fashion.<sup>2</sup> Consequently, this method became extremely popular in the 1900s for organic synthesis. Today, all reactions that involve the 1,4-addition of any nucleophile (including enolates, Grignard reagents, organolithium reagents, and organoboronates) to activated  $\pi$  systems are referred to as Michael additions.<sup>3</sup>

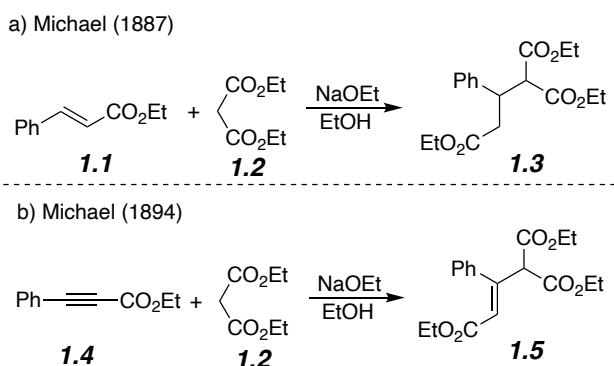


**Figure 1.1** Conjugate Addition/Michael Addition/1,4-Addition

## 1.2 Transition Metal Catalyzed Enantioselective Conjugate Addition Reactions

The original discovery of conjugate additions addressed the regioselectivity as it was a selective 1,4-addition. As the conjugate addition forms new stereocenters in many cases, several approaches were developed to enable the stereoselective formation of the new carbon-carbon bonds.<sup>4</sup> One classic way to control this type of stereocenter formation was to utilize an existing stereocenter on the starting material to dictate the selectivity of the formation of the second stereocenter (Figure 1.2).<sup>5</sup>

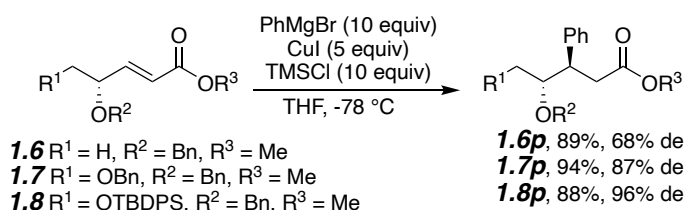


**Figure 1.2** Diastereoselective Conjugate Addition with Enantiopure Starting Materials

However, applications of these reaction were limited due to their need for enantiopure starting material in the first place. Also, the sizes of substituents on the pre-existing stereocenter had to be different enough to be influenced by one more than the other. Thus, an enantioselective catalysis route would significantly benefit synthesis efforts. One good example of such an approach is the enantioselective conjugate addition developed by Feringa using a BINOL-derived chiral phosphorous amidite for copper catalysis (Figure 1.3).<sup>4</sup> In this case, an alkylzinc nucleophile was incorporated with good enantioselectivity.

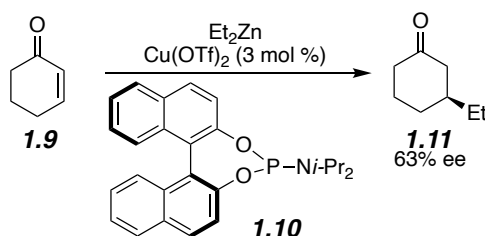


**Figure 1.3** Copper Catalysis for Enantioselective Conjugate Addition

Besides the BINOL-derived ligands, chiral aryl-thiolates also showed good selectivity in a similar system using strong nucleophiles such as the alkyl Grignard reagents (Figure 1.4).<sup>5</sup>

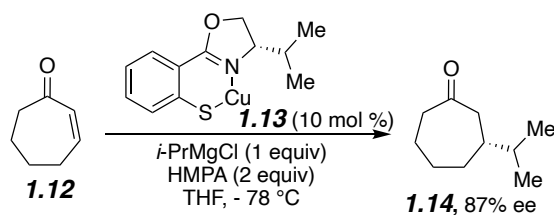


**Figure 1.4** Copper Oxazoline Thiolate Catalyzed Asymmetric Conjugate Addition

Other transition metal catalysis systems, such as the widely applied palladium catalysts, also showed outstanding performance for conjugate addition. For example, the Stoltz group developed an all-carbon quaternary center forming method using conjugate addition and a chiral palladium complex (Figure 1.5).<sup>6</sup> It is worth pointing out that all-carbon quaternary center formation has always been a hot topic in the organic synthesis community due to the difficulty of the reaction. Having such quaternary centers formed in high yield and great selectivity definitely demonstrates the effectiveness of conjugate addition as a tool in stereoselective organic synthesis.

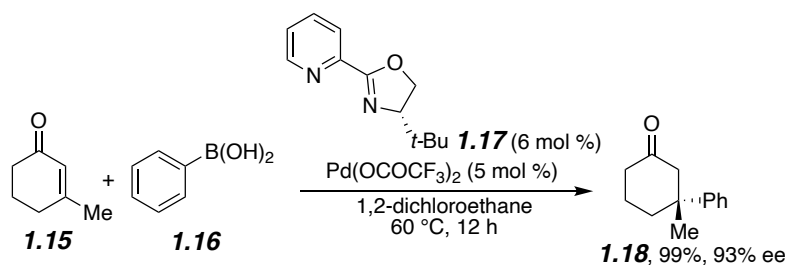


**Figure 1.5** Palladium-Catalyzed Asymmetric Conjugate Addition

Notably, an aryl boronic acid was used as the nucleophile in the conjugate addition above. Organoboronate reagents are not only very well-known participants in cross coupling reactions such as the Suzuki coupling,<sup>7</sup> but are also considered to be chemically stable and selective nucleophiles in conjugate addition reactions. Additionally, they are significantly more stable and easier to synthesize than stronger nucleophiles such as Grignard reagents and organolithium

reagents.<sup>8</sup> It was first discovered by Suzuki that these organoboronates could add to enone double bonds in an enone (Figure 1.6).<sup>9</sup>

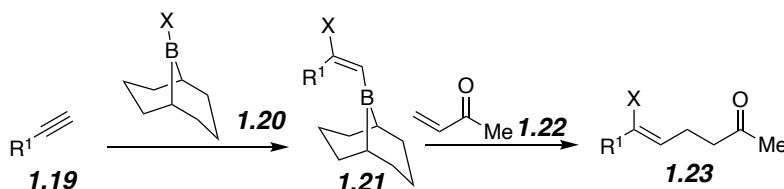


**Figure 1.6** First Use of Organoboronate Conjugate Addition Reported by Suzuki

Although the enantioselective conjugate addition were well developed using transition metal catalysis, the toxicity and functional group compatibility of metal catalysts might limit the application of these methods.<sup>10,11</sup> Thus, developing a route using an organocatalyst in lieu of a transition metal could be extremely beneficial to the organic synthesis community.

### 1.3 Organocatalyzed Enantioselective Conjugate Addition With Organoboronates as Nucleophile

#### 1.3.1 BINOL-derivative Catalyzed Enantioselective Conjugate Addition Reported by J. Michael Chong

Inspired by Suzuki's pioneering work, J. Michael Chong reported enantioselective conjugate additions with organoboronate nucleophiles and BINOL-derived catalyst (Figure 1.7).<sup>12</sup> In their proposed mechanism, the reaction started with binding between the BINOL-derived catalyst and a boronic ester. The reactive BINOL-boron complex then formed a new C–C bond at the  $\beta$ -position of the enone. The stereoselectivity of the carbon-carbon bond formation was dictated by the chirality of the BINOL-catalyst.

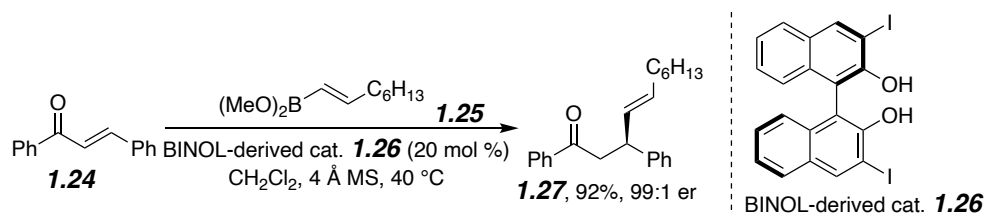


**Figure 1.7** Chong's Report of Organocatalyzed Enantioselective Conjugate Addition

While the reaction provided products in high yield and great enantioselectivity, it still suffered from several drawbacks such as limited substrate scope and long reaction times. It did demonstrate the promising potential of BINOL-derived catalysts and organoboronate nucleophiles in enantioselective conjugate addition reactions.

### 1.3.2 Thiourea-derivatives Catalyzed Enantioselective Conjugate Addition Reported by Takemoto

Besides BINOL-derivatives, other organic molecules, such as the thioureas-derivatives discovered by the Takemoto group,<sup>13,14</sup> were also found to be good catalysts in conjugate additions. The first Michael reaction they observed with their catalyst was the Michael reaction of malonates to nitroolefins (Figure 1.8a). After further modification of their thiourea catalyst, it could catalyze enantioselective conjugate addition of alkenyl boronic acids to  $\alpha,\beta$ -unsaturated ketones (Figure 1.8b). Yield of their conjugate products would be as high as 99% with an excellent enantioselectivity.

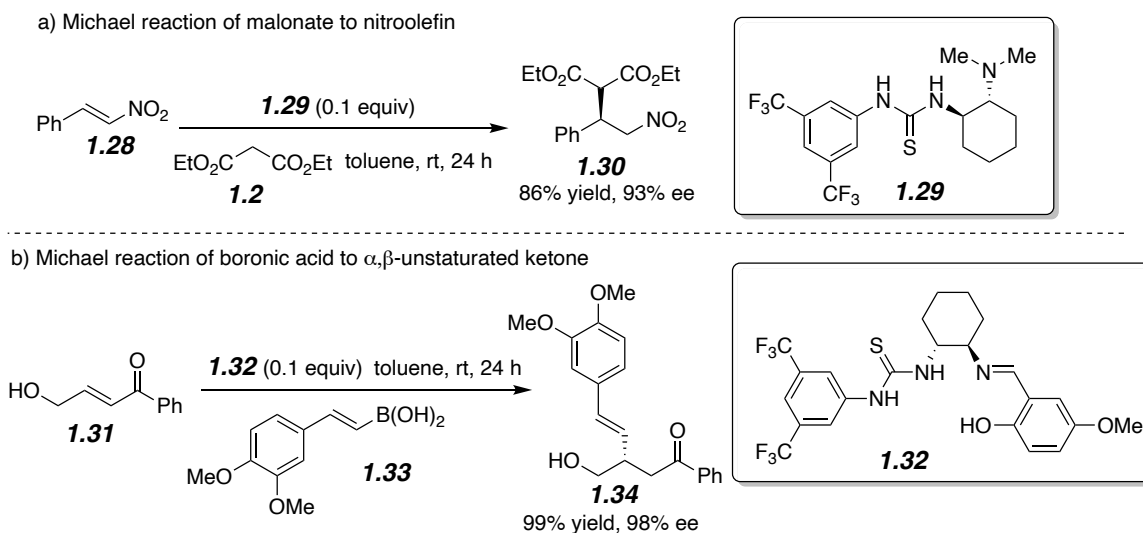


**Figure 1.8** Thiourea-derived Catalysts Developed by the Takemoto Group

### 1.3.3 O-monoacyltartaric Acid Catalyzed Enantioselective Conjugate Addition Reported by Sugiura

In 2014, the Sugiura group reported an enantioselective conjugate addition of boronic acids to dienones catalyzed by O-monoacyltartaric acid catalysts developed in their lab (Figure 1.9).<sup>16</sup> This catalyst effectively catalyzed the conjugate addition of boronic acid to both symmetrical and asymmetrical dienones to provide product in good yields and enantioselectivity. They could selectively synthesize the mono-adduct in good yield and enantioselectivity via modification of the dienone substrate.

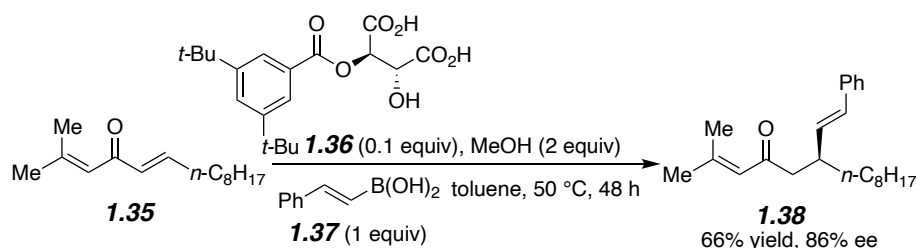


**Figure 1.9** Tartaric Acid-derived Catalyst Developed by the Sugiura Group

### 1.3.4 Further Reaction Development in the May Group

The research in the May lab has always been focused on developing methods to access novel structures that would allow further transformation into biologically active natural products. Our initial exploration in organocatalyzed conjugate addition was expected to provide methods to generate stereocenters adjacent to unprotected indole structures (Figure 1.10), which are essential structural components in many biologically active molecules as well as natural products.<sup>17</sup> In this example, the 3,3'-bis(pentafluorophenyl)-BINOL was used as the catalyst to enable the conjugate addition of vinyl boronic acid to 3-indolyl-enones in high yields and outstanding stereoselectivity.

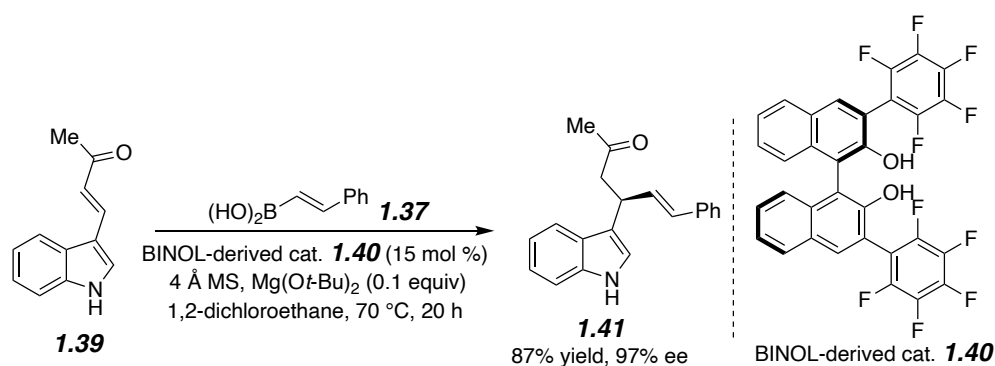
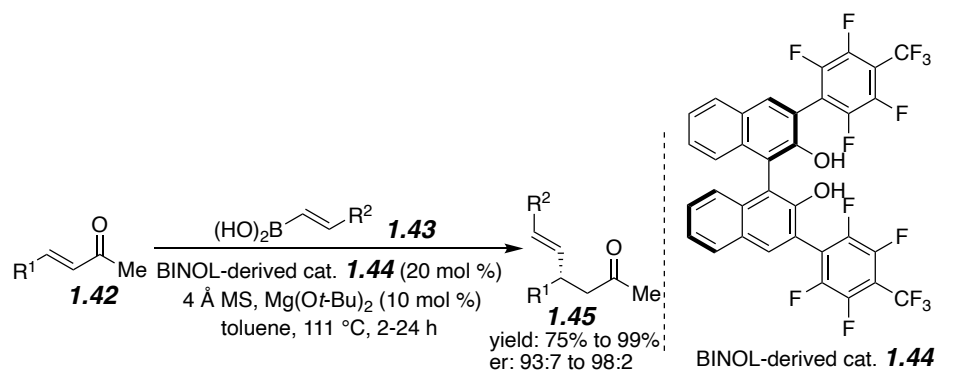


**Figure 1.10** BINOL Catalyzed Enantioselective Conjugate Addition to Unprotected Indolyl Enone

With this successful precedent, we conducted further investigations and expanded our enone scope to those bearing various heteroaryl substituents (Figure 1.11).<sup>18</sup> This methodology could generate a stereocenter adjacent to various unprotected sensitive heteroaryl groups, which was a difficult transformation previously.



list of R<sup>1</sup>:

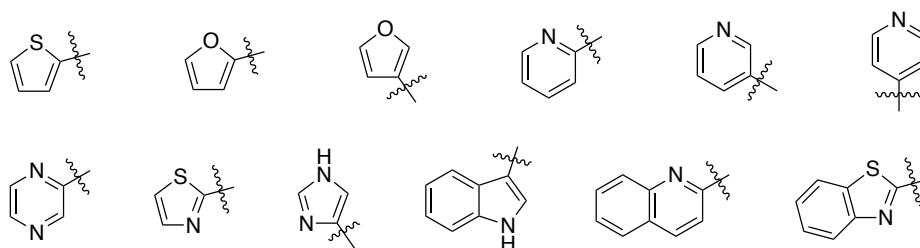
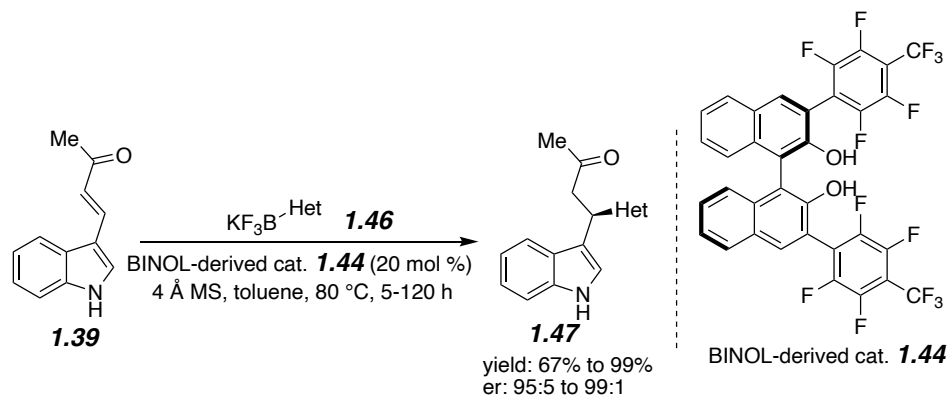


**Figure 1.11** Expanded Enone Scope

In 2015, an elegant method that would allow enantioselective formation of stereocenters bearing two heteroaryl substituents was developed by Jiun-Le Shih (Edward) and Thien Nguyen in the May group (Figure 1.12).<sup>19</sup> The revolutionary application of trifluoroborate salts in this

reaction proved essential for reliable reproducibility with high yields and excellent enantioselectivity.



selected list of heteroaryl trifluoroborate salts:

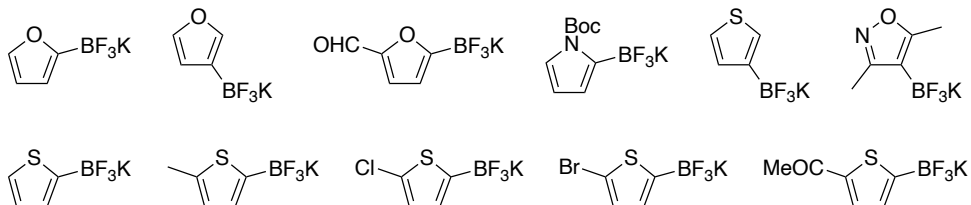


**Figure 1.12** Expanded Trifluoroborate Salt Scope

This method proved to be extremely useful in natural product synthesis as it was further applied in the total synthesis of a natural product, discoipyrrole D, by the Banwell group (Figure 1.13).<sup>19</sup>

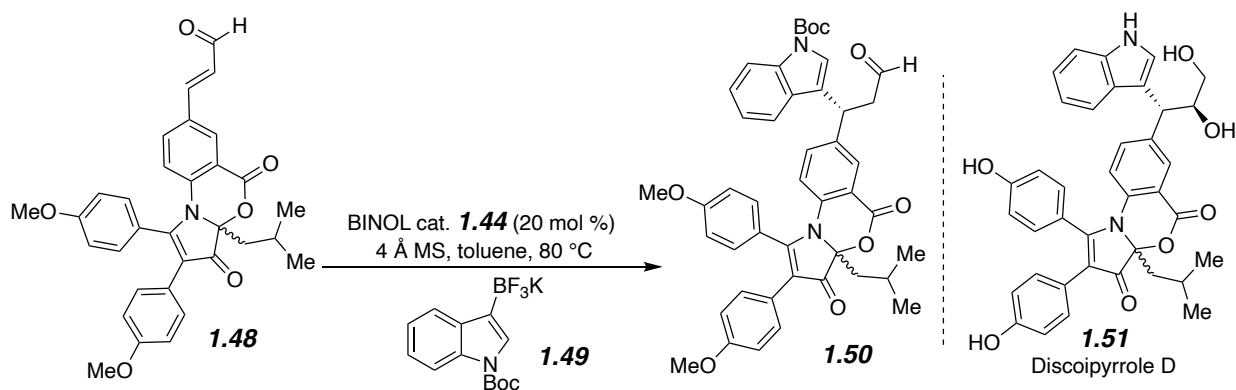
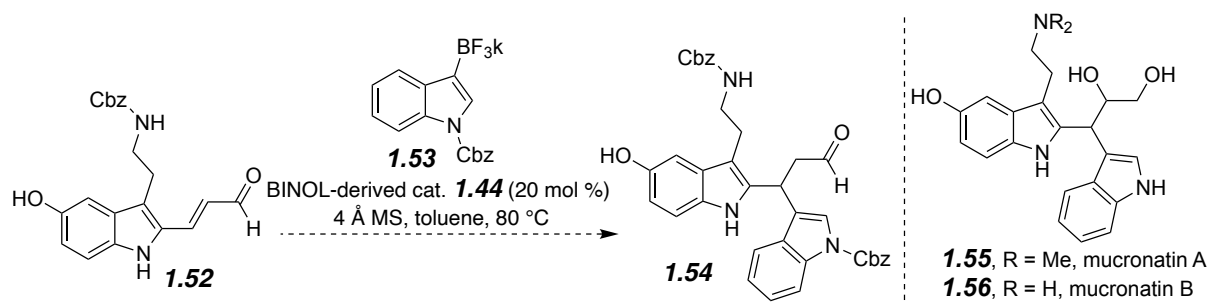


**Figure 1.13** Key Step of Banwell's Synthesis of Discoipyrrole D

Today, natural product total synthesis is being conducted using this BINOL-catalyzed enantioselective conjugate addition in the May group. Synthetic routes toward biologically active natural products such as mucronatins A and B are under prompt exploration (Figure 1.14).



## 1.4 Introduction to Cannabinoids

Ever since the discovery of  $\Delta^9$ -tetrahydrocannabinol (THC) (**47**, Figure 1.15) in 1964,<sup>20</sup> it has attracted great interest from both biochemists and synthetic chemists due to its fascinating structure and biological activity (Figure 1.15). The binding between cannabinoids, like THC and cannabidiol (CBD, **1.58**), and the central cannabinoid receptors CB1 and CB2 contributes to most of the observed pharmacological effects.<sup>21</sup> Many analogs, including those containing heterocycles (see **1.59** and **1.60**), have been synthesized for use in SAR studies to probe receptor binding interactions (Figure 1.15).<sup>22</sup> Importantly, the stereochemistry in analogs like **1.60** was found to play an important role in the receptor binding affinities.<sup>23</sup> This highlights a need for the development of a general strategy to access both natural and synthetic cannabinoids stereoselectively in high yield. Therefore, the cyclohexene ring A that contains two adjacent stereocenters is one of the most intriguing potential sites of modification for both synthetic and biological reasons. The following describes a concise high-yielding enantioselective and

diastereoselective synthesis of THC and CBD via a novel organocatalyzed ambiphilic annulation reaction of a haloalkylated vinylboronate that allows for cyclohexene modification.

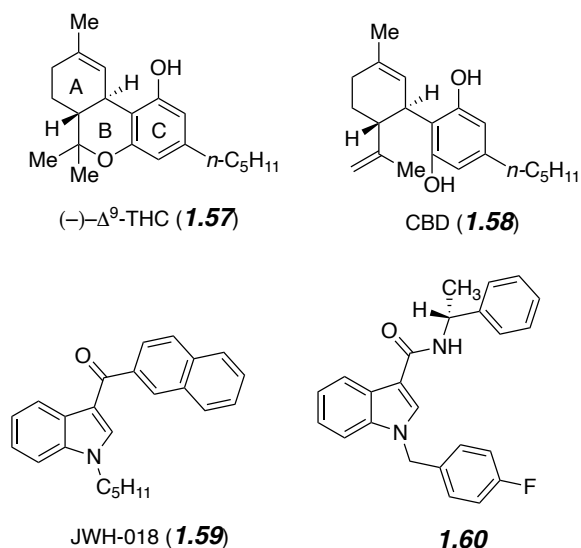


**Figure 1.15** Selected Natural and Synthetic Cannabinoids

### 1.5 Total Synthesis of Cannabinoids via Enantioselective Catalysis Routes

Although the cyclohexene ring of THC and CBD can be installed as a complete unit by Lewis acid catalysis using a chiral pool strategy (Figure 1.16),<sup>24</sup> enantioselective ring-forming approaches have been investigated by several groups to try and provide synthetic analogs.

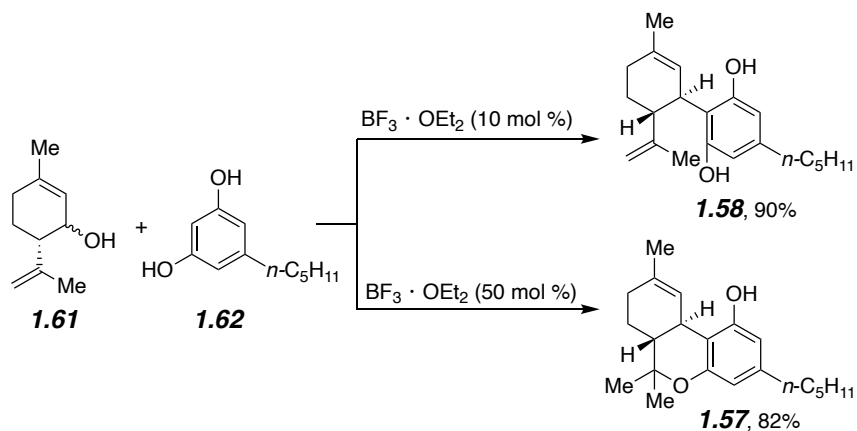


**Figure 1.16** Dethe Cannabinoid Synthesis via Chiral Pool Strategy

### 1.5.1 Enantioselective Diels-Alder Route Developed by the Evans Group

In 1997, Evans reported the first catalytic enantioselective route to THC via a chiral bis(oxazoline)Cu(II) catalyzed enantioselective Diels-Alder reaction (Figure 1.17).<sup>25</sup> With the catalyst, the Diels-Alder reaction gave the *exo*-product **1.66** in 57% yield with outstanding enantioselectivity (98% ee). This transformation had very high efficiency as it set two stereocenters in a single step. The only drawback of this reaction was that it also produced a considerable portion of *endo*-product which could neither be recycled nor used in the next step, causing some waste of the starting material. Nevertheless, they were able to obtain the enantiomer of naturally occurring THC in 7 steps, which has been the shortest enantioselective catalysis route even to today.

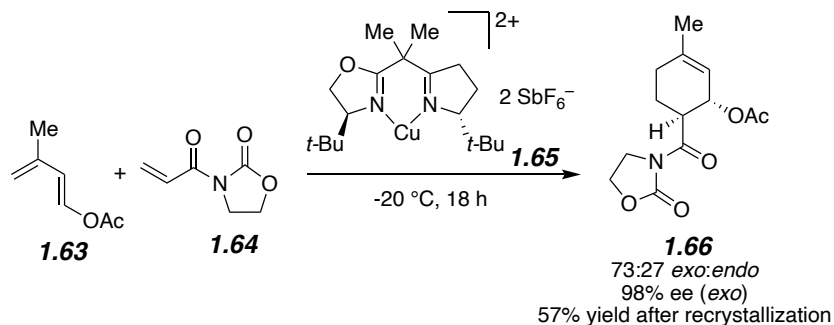


**Figure 1.17** Key Step of Evans' THC synthesis

### 1.5.2 Asymmetric Allylic Alkylation Route Developed by the Trost Group

Trost and Dogra installed the correct stereochemistry via a molybdenum catalyzed asymmetric alkylation in 2006 (Figure 1.18).<sup>26</sup> With the chiral ligand they designed and synthesized, the key intermediate **1.69** could be obtained in high yield and excellent enantioselectivity. However, the subsequent alkylation to add the other tethered alkene for olefin metathesis gave another stereocenter that was not controlled by the previously incorporated stereocenter in the asymmetric allylic alkylation. Consequently, they had to take a detour to close

the cyclohexene ring first using olefin metathesis and then conducting a thermodynamic epimerization to convert the *cis*-product into the *trans*-product. It is worth emphasizing that no material was wasted in this synthesis since they were able to transform the disfavored stereoisomer into the favored one.

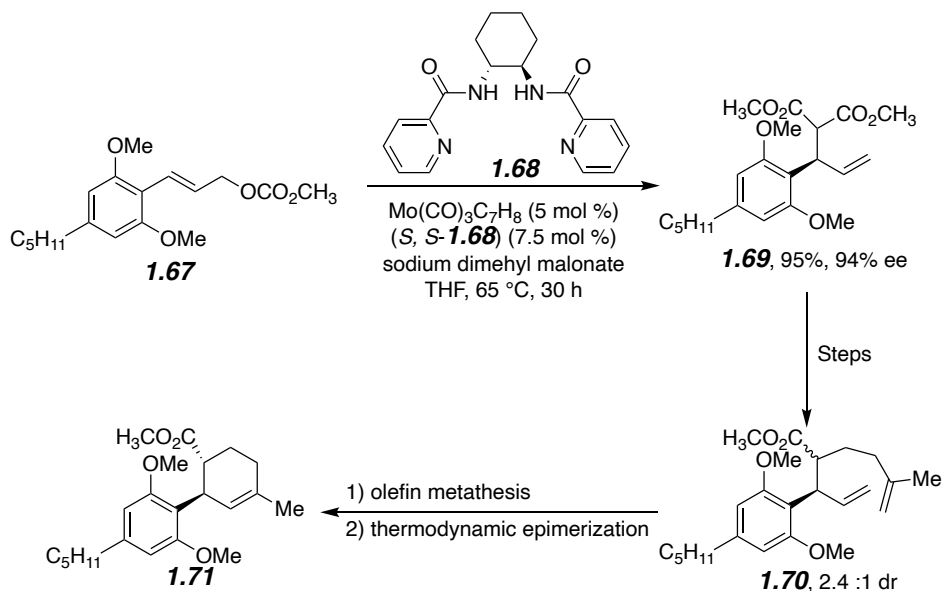


**Figure 1.18** Key Transformations in Trost's THC Synthesis

### 1.5.3 Asymmetric Hydrogenation Route Developed by the Zhou Group

In 2013, Zhou reported a THC synthesis using asymmetric hydrogenation to set the key stereocenter (Figure 1.19).<sup>27</sup> They could access enantiopure alcohols using a highly efficient Ru-catalyzed asymmetric hydrogenation of racemic ketones via a dynamic kinetic resolution developed in their lab. Their method could efficiently utilize racemic starting materials as shown in the transformation from **1.75** to **1.77** in Figure 1.19. However, in terms of synthesizing THC, this route suffered from the large amount of steps it was taking. For example, the synthesis of the starting material **1.74** required two complicated coupling components, **1.72** and **1.73**, which were

very hard to synthesize. Additionally, after setting the first stereocenters, six more steps were needed to set the other stereocenter, which made this route less concise than previous routes.

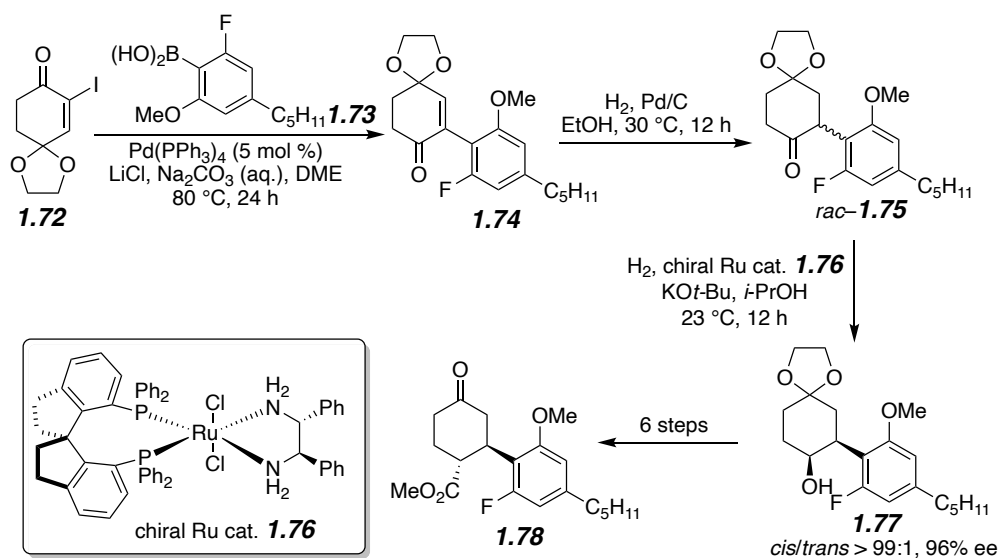


**Figure 1.19** Key Transformations in Zhou's THC Synthesis

#### 1.5.4 Stereodivergent Route Developed by the Carreira Group

Shortly afterwards, Carreira synthesized all four stereoisomers of THC via an elegant stereodivergent dual catalysis strategy (Figure 1.20).<sup>28</sup> Following their original report of a similar dual system,<sup>29</sup> they accessed all stereoisomers of THC by simply switching the ligand and amine. This reaction could set two adjacent stereocenters at a time in good yield with high diastereoselectivity and outstanding enantioselectivity. All stereoisomers of naturally occurring THC could be obtained after the same sequence of treatment as in Trost's synthesis, which involved olefin metathesis for cyclohexene ring formation.

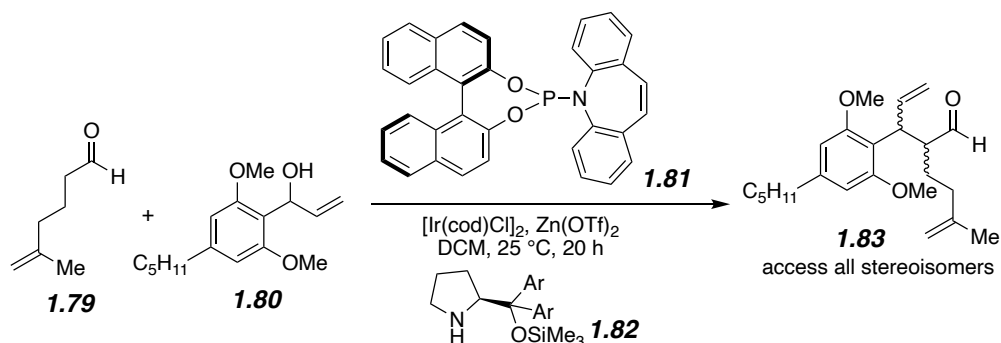


**Figure 1.20** Stereodivergent Dual Catalysis Strategy in Carreira's THC Synthesis

### 1.5.5 Enzyme Controlled Reduction Route Developed by the Leahy Group

In 2018, Leahy reported the enantioselective total synthesis of THC using an enzyme controlled ketone reduction followed by an Ireland-Claisen rearrangement (Figure 1.21).<sup>30</sup> The initial reduction was conducted with CBS oxazaborolidine **1.86**. While it offered almost quantitative transformation from the ketone **1.84** to alcohol **1.85**, the enantioselectivity was not ideal. An enzyme controlled reduction could give an excellent enantioselectivity, but it came with a relatively low yield. In modern organic synthesis, stereocontrol is often considered more important than obtaining a higher quantity of the material, but both are better. The Leahy group chose selectivity as their goal, and they moved forward to the Ireland-Claisen rearrangement following the enzyme controlled reduction pathway. The Ireland-Claisen rearrangement followed with typically high levels of stereoselectivity, with the first stereocenter set in extremely high enantiopurity. A serendipitous finding in their research was that intermediate **1.88** could be recrystallized with high enantiopurity, which meant that the low enantioselectivity they obtained from the CBS oxazaborolidine controlled reduction would also be useful in later stages. From intermediate **1.88**, THC could be synthesized following a similar sequence to Trost and Carreira's synthesis.

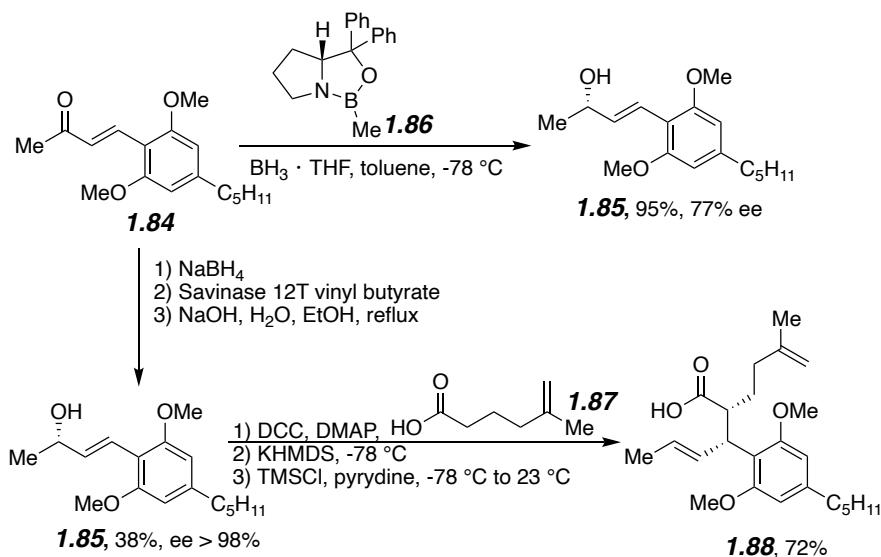


**Figure 1.21** Key Transformations in Leahy's THC Synthesis

### 1.5.6 NHC Catalysis Route Developed by the Lupton Group

Recently, in 2019, Lupton reported an enantioselective total synthesis of THC using asymmetric NHC catalysis (Figure 1.22).<sup>31</sup> Following their procedure, the key intermediate **1.92** could be obtained in 45% yield with 20:1 dr and 98:2 er. Despite the fact that they successfully formed three stereocenters in one reaction, only the one that was attached to the aryl group was preserved until they finished the synthesis. The other two stereocenters on the lactone were quickly eliminated in subsequent steps of the synthesis

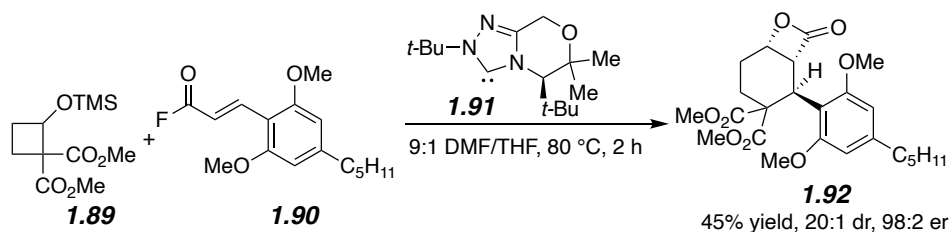


**Figure 1.22** Key Step of Lupton's THC Synthesis

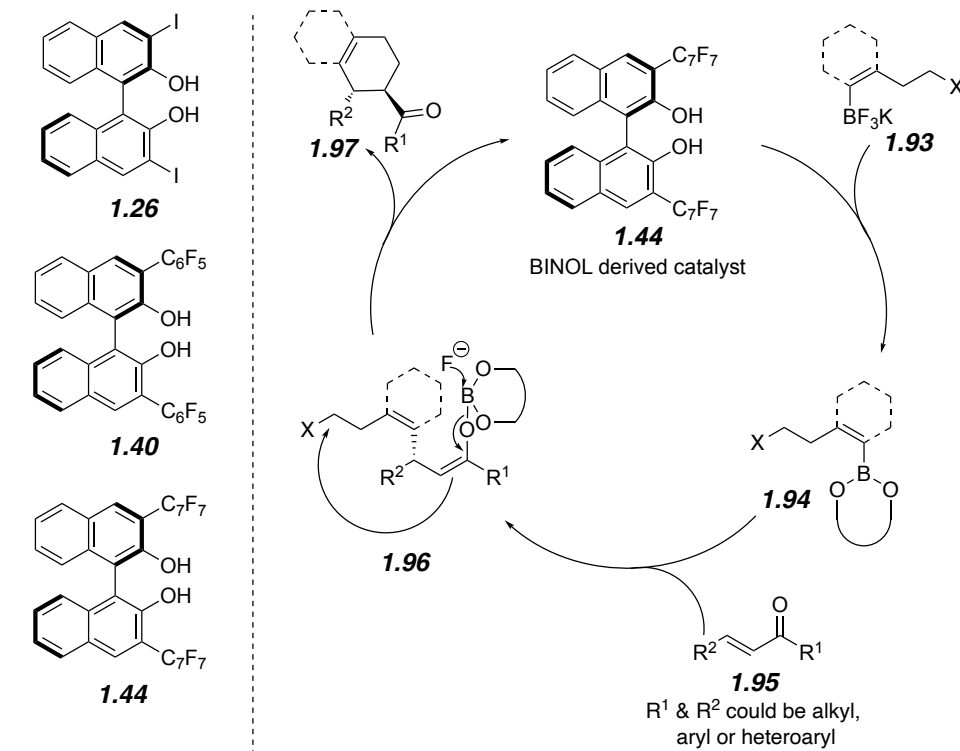
## 1.7 Limitation of Existing Routes and Proposed Retrosynthetic Analysis

While synthetic approaches to  $\Delta^9$ -THC have flourished, many of them require transition metal catalysis to set stereocenters or ring closing metathesis to construct the cyclohexene. In terms of Structure Activity Relationship (SAR) studies, transition metal catalysis can limit analog exploration due to lack of compatibility with heterocycles, halides, and other sensitive groups.<sup>10,11</sup> Additionally, it would be impossible to make analogs containing a fused aryl/heteroaryl ring in the place of the double bond by all the reported enantioselective catalysis routes. Thus, having a metal-free method to afford key stereocenters would be tremendously beneficial for analog development of cannabinoids. We hypothesized that an organocatalyzed tandem annulation reaction would provide that enantioselective method for synthesizing the cannabinoid core with maximum flexibility.

As previously discussed, the conjugate addition reactions of organoboron nucleophiles to  $\alpha,\beta$ -unsaturated ketones have been rigorously explored in the May group.<sup>16-18</sup> This metal-free conjugate addition method uses BINOL-derived catalysts (**1.26**, **1.40**, **1.44**, Figure 1.23a) to synthesize tertiary beta-stereocenters with excellent enantioselectivity and outstanding compatibility with heterocycles. The nucleophilic vinyl borate group **1.93** is activated by fluoride loss and then binding first to the chiral BINOL-derived catalyst **1.44** and then to the enone carbonyl. Given the resulting switchable reactivity, we believed that an electrophilic functionality could be incorporated in the nucleophilic organoboronate to provide a novel ambiphilic alkyl halide organoborate reagent (**1.93**). Such an arrangement is impossible with other strong nucleophiles such as Grignard and organolithium reagents and is typically only seen in transition metal intermediates or 1,3-dipole cycloadditions.<sup>32</sup> The powerful annulation in Figure 1.23 would

provide rapid access to the cyclohexene (or other-sized) ring in THC and derivatives (Figure 1.23b), including those containing heterocyclic bioisosteres.

**a) BINOL-derived catalysts and catalytic cycle of BINOL derivative catalyzed conjugate addition**



**b) Proposed convergent retrosynthesis of THC**

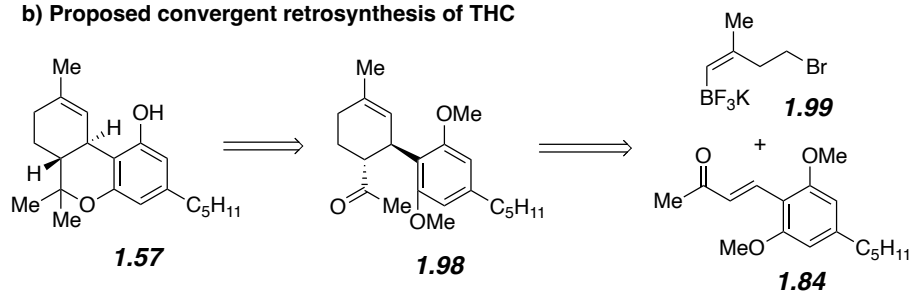


**Figure 1.23** Proposed Conjugate Addition/Enolate Alkylation Reaction and Retrosynthetic Analysis of THC

**1.8 Focus of This Thesis**

The remainder of this thesis will focus on the development of novel ambiphilic organoboronate reagents and an enantioselective conjugate addition/enolate alkylation annulation

methodology. The total synthesis of natural cannabinoids and a structural analog will also be demonstrated in later chapters.

## 1.9 Bibliography

1. Michael, A. *J. Prakt. Chem./Chem.-Ztg.* **1887**, *35*, 349.
2. Michael, A. Addition of Sodium Acetate and Sodium Diethyl Malonate to Unsaturated Acids *J. Prakt. Chem./Chem.-Ztg.* **1894**, *49*, 20.
3. Kürti, L.; Czako, B. *Strategic Applications of Named Reactions in Organic Synthesis*. Elsevier, Burlington, MA, USA, 2005.
4. Rossiter, B. E.; Swingle, N. M. Asymmetric Conjugate Addition. *Chem. Rev.* **1992**, *92*, 771–806.
5. Harutyunyan, S. R.; den Hartog, T.; Geurts, K.; Minnaard, A. J.; Feringa, B. L. Catalytic Asymmetric Conjugate Addition and Allylic Alkylation with Grignard Reagents *Chem. Rev.* **2008**, *108*, 2824–2852.
6. Shockley, S. E.; Holder, J. C.; Stoltz, B. M. Palladium-Catalyzed Asymmetric Conjugate Addition of Arylboronic Acids to  $\alpha,\beta$ -Unsaturated Cyclic Electrophiles *Org. Process Res. Dev.* **2015**, *19*, 974–981.
7. Miyaura, N.; Suzuki, A. Palladium-Catalyzed Cross-Coupling Reactions of Organoboron Compounds *Chem. Rev.* **1995**, *95*, 2457–2483.
8. Molander, G. A.; Petrillo, D. E. Oxidation of Hydroxyl-Substituted Organotrifluoroborates *J. Am. Chem. Soc.* **2006**, *128*, 9634–9635.

9. Hara, S.; Hyuga, S.; Aoyama, M.; Sato, M.; Suzuki, A. BF<sub>3</sub> Etherate Mediate 1,4-Addition of 1-Alkenyldialkoxyboranes to  $\alpha,\beta$ -Unsaturated Ketones. A Stereoselective Synthesis of  $\gamma,\delta$ -Unsaturated Ketones. *Tetrahedron Lett.* **1990**, *31*, 247–250.
10. Ananikove, V. P. Nickel: The “Spirited Horse” of Transition Metal Catalysis. *ACS Catal.* **2015**, *5*, 1964–1971.
11. Zhou, Q-L. Transition-Metal Catalysis and Organocatalysis: Where Can Progress Be Expected? *Angew. Chem. Int. Ed.* **2016**, *55*, 5352–5353.
12. a) Wu, T. R.; Chong, J. M. Ligand-Catalyzed Asymmetric Alkynylboration of Enones: A New Paradigm for Asymmetric Synthesis Using Organoboranes. *J. Am. Chem. Soc.* **2005**, *127*, 3244–3245; b) Wu, T. R.; Chong, J. M. Asymmetric Conjugate Alkenylation of Enones Catalyzed by Chiral Diols. *J. Am. Chem. Soc.* **2007**, *129*, 4908–4909.
13. Okino, T.; Hoashi, Y.; Takemoto, Y. Enantioselective Michael Reaction of Malonates to Nitroolefins Catalyzed by Bifunctional Organocatalysts. *J. Am. Chem. Soc.* **2003**, *125*, 12672–12673.
14. Inokuma, T.; Takasu, K.; Sakaeda, T.; Takemoto, Y. Hydroxyl Group-Directed Organocatalytic Asymmetric Michael Addition of  $\alpha,\beta$ -Unsaturated Ketones with Alkenylboronic Acids. *Org. Lett.* **2009**, *11*, 2425–2428.
15. Sugiura, M.; Kinoshita, R.; Nakajima, M. O-Monoacyltartaric Acid Catalyzed Enantioselective Conjugate Addition of a Boronic Acid to Dienones: Application to the Synthesis of Optically active Cyclopentenones. *Org. Lett.* **2014**, *16*, 5172–5175.
16. Lundy, B. J.; Jansone-Popova, S.; May, J. A. The Enantioselective Conjugate Addition of Alkenylboronic Acids to Indole-Appended Enones. *Org. Lett.* **2011**, *13*, 4958–4951.

17. Le, P. Q.; Nguyen, T. S.; May, J. A. A General Method for the Enantioselective Synthesis of  $\alpha$ -Chiral Heterocycles. *Org. Lett.* **2012**, *14*, 6104-6107.
18. Shih, J.-L.; Nguyen, T. S.; May, J. A. Organocatalyzed Asymmetric Conjugate Addition of Heteroary and Aryl Trifluoroborates: a Synthetic Strategy for Discoipyrrole D. *Angew. Chem. Int. Ed.* **2015**, *54*, 9931–9935.
19. Zhang, Y.; Banwell, M. G. A Total Synthesis of the Marine Alkaloid Discoipyrrole D. *J. Org. Chem.* **2017**, *82*, 9328–9334.
20. Mechoulam, R.; Gaoni, Y. A Total Synthesis of dl- $\Delta^1$ -Tetrahydrocannabinol, the Active Constituent of Hashish. *J. Am. Chem. Soc.* **1965**, *87*, 3273–3275.
21. Romero, J.; Lastres-Becker, L.; de Miguel, R.; Berrendero, F.; Ramos, J. A.; Fernández-Ruiz, J. The Endogenous Cannabinoid System and the Basal Ganglia: Biochemical, Pharmacological, and Therapeutic Aspects *Pharmacol. Ther.* **2002**, *95*, 137–152.
22. a) Worob, A.; Wenthur, C. DARK Classics in Chemical Neuroscience: Synthetic Cannabinoids (Spice/K2). *ACS Chem. Neurosci.* **2020**, *11*, 3881–3892; b) Banister, S. D.; Moir, M.; Stuart, J.; Kevin, R. C.; Wood, K. E.; Longworth, M.; Wilkinson, S. M.; Beinart, C.; Buchanan, A. S.; Glass, M.; Connor, M.; McGregor, I. S.; Kassiou, M. Pharmacology of Indole and Indazole Synthetic Cannabinoid Designer Drugs AB-FUBINACA, ADB-FUBINACA, AB-PINACA, ADB-PINACA, 5F-AB-PINACA, 5F-ADB-PINACA, ADBICA, and 5F-ADBICA. *ACS Chem. Neurosci.* **2015**, *6*, 1546–1559.
23. Ametovski, A.; Macdonald, C.; Manning, J. J.; Haneef, S. A. S.; Santiago, M.; Martin, L.; Sparkes, E.; Reckers, A.; Gerona, R. R.; Connor, M.; Glass, M.; Banister, S. D. Exploring Stereochemical and Conformational Requirements at Cannabinoid Receptors for Synthetic

Cannabinoids Related to SDB-006, 5F-SDB-006, CUMYL-PICA, and 5F-CUMYL-PICA. *ACS Chem. Neurosci.* **2020**, *11*, 3672–3682.

24. For representative chiral pool strategy (a) Klotter, F.; Studer, A. Short and Divergent Total Synthesis of (+)-Machaeriol B, (+)-Machaeriol D, (+)- $\Delta^8$ -THC, and Analogues. *Angew. Chem. Int. Ed.* **2015**, *54*, 8547–8550; (b) Dethe, D. H.; Erande, R. D.; Mahapatra, S.; Das, S.; Kumar B., V.

Protecting Group Free Enantiospecific Total Syntheses of Structurally Diverse Natural Products of the Tetrahydrocannabinoid Family. *Chem. Commun.* **2015**, *51*, 2871–2873.

25. Evans, D. A.; Shaughnessy, E. A.; Barnes, D. M. Cationic Bis(oxazoline)Cu(II) Lewis Acid Catalysts. Application to the Asymmetric Synthesis of ent- $\Delta^1$ -Tetrahydrocannabinol. *Tetrahedron Lett.* **1997**, *38*, 3193–3194.

26. Trost, B. M.; Dogra, K. Synthesis of (–)- $\Delta^9$ -trans-Tetrahydrocannabinol: Stereocontrol via Mo-Catalyzed Asymmetric Allylic Alkylation Reaction. *Org. Lett.* **2007**, *9*, 861–863.

27. Cheng, L.-J.; Xie, J.-H.; Chen, Y.; Wang, L.-X.; Zhou, Q.-L. Enantioselective Total Synthesis of (–)- $\Delta^8$ -THC and (–)- $\Delta^9$ -THC via Catalytic Asymmetric Hydrogenation and S<sub>N</sub>Ar Cyclization. *Org. Lett.* **2013**, *15*, 764–767.

28. Schafroth, M. A.; Zuccarello, G.; Krautwald, S.; Sarlah, D.; Carreira, E. M. Stereodivergent Total Synthesis of  $\Delta^9$ -Tetrahydrocannabinols. *Angew. Chem. Int. Ed.* **2014**, *53*, 13898–13901.

29. Krautwald, S.; Sarlah, D.; Schafroth, M. A.; Carreira, E. M. Enantio- and Diastereodivergent Dual Catalysis:  $\alpha$ -Allylation of Branched Aldehydes *Science*. **2013**, *340*, 1065–1068.

30. Shultz, Z. P.; Lawrence, G. A.; Jacobson, J. M.; Cruz, E. J.; Leahy, J. W. Enantioselective Total Synthesis of Cannabinoids—A Route for Analogue Development. *Org. Lett.* **2018**, *20*, 381–384.

31. Ametovski, A.; Lupton, D. W. Enantioselective Total Synthesis of (-)- $\Delta^9$ -Tetrahydrocannabinol via N-Heterocyclic Carbene Catalysis. *Org. Lett.* **2019**, *21*, 1212–1215.
32. For reviews on 1,3-dipole cycloadditions, see a) T. Hashimoto, K. Maruoka, *Chem. Rev.* **2015**, *115*, 5366; b) K. V. Gothelf, K. A. Jorgensen, *Chem. Rev.* **1998**, *98*, 863. For recent development of ambiphilic boron species in transition metal chemistry, see M. Sc. M. Wienhold, J. J. Molloy, C. G. Daniliuc, R. Gilmour, *Angew. Chem. Int. Ed.* **2021**, *60*, 685.

## Chapter 2 Development of Ambiphilic Organoboronates

### 2.1 Ambiphilic Molecules and Their Application in Organic Synthesis

In the world of organic chemistry, the word “ambiphilic” is used when a molecule has both electrophilic and nucleophilic character. Due to such unique properties, ambiphilic reagents are often effective in forming multiple chemical bonds in a single transformation, which largely increases the efficiency in organic synthesis. However, this distinctive type of molecule is very rare due to its conflicted nature. This arrangement is impossible with some well-known strong nucleophiles such as Grignard or organolithium reagents and is typically only seen in bench-stable compounds as ylides.<sup>1</sup> One representative example can be found in the Wittig reaction, using phosphorus ylide **2.3** (Figure 2.1).

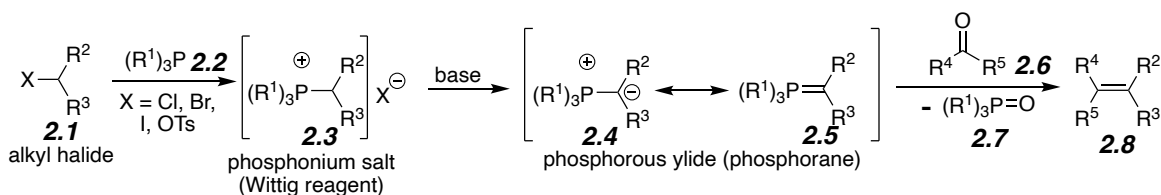
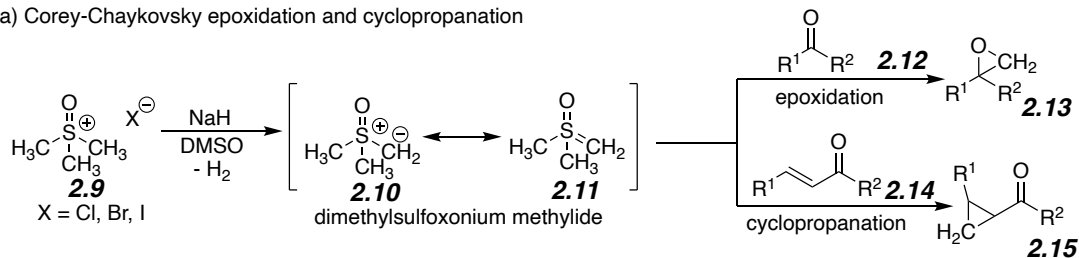


**Figure 2.1** Wittig Reaction

Other than bench- and air-stable ylides, ambiphilic reactivity is only available in transient reaction intermediates, such as those in Corey-Chaykovsky epoxidation/cyclopropanation<sup>1</sup> and 1,3-dipolar cycloaddition reactions (Figure 2.2).<sup>2</sup>

a) Corey-Chaykovsky epoxidation and cyclopropanation



b) 1,3-dipolar cycloaddition reaction

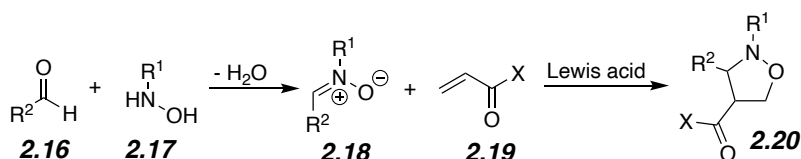


**Figure 2.2** Corey-Chaykovsky Epoxidation/Cyclopropanation and 1,3-Dipolar Cycloaddition Reaction

## 2.2 Design of Ambiphilic Organoboronates

One of the major reasons for the scarcity of stable ambiphilic reagents is chemoselectivity. A non-selective strong nucleophile would target any electrophile in its surrounding environment intermolecularly and/or intramolecularly if conformational geometry permitted. Due to such non-selective reactivity, strong nucleophiles such as Grignard reagents, organolithium reagents, or stabilized enolates are not a good fit for providing the nucleophilic character in an ambiphilic molecule. However, as was found in a mechanistic study,<sup>3</sup> the nucleophilicity of organoboronates used in organocatalyzed enantioselective conjugate addition reactions is not activated until the effective binding between boron and the BINOL-derived catalyst (Figure 2.3). Additionally, the nucleophile has a specific chemoselectivity toward Michael acceptors after the binding event. Therefore, we hypothesized that an electrophilic functionality could also be incorporated to trap the transient enolate intermediate in the reaction, thus providing a novel bench- and air-stable ambiphilic reagent.

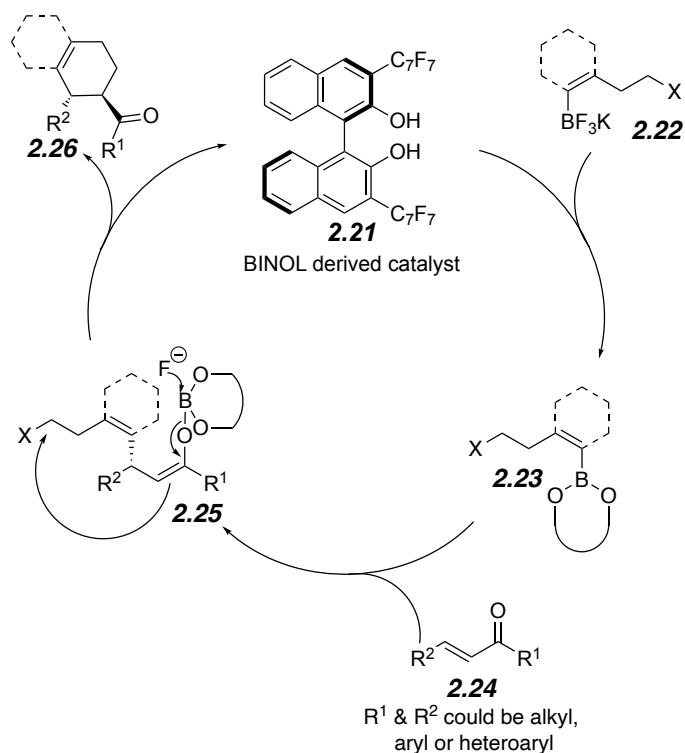


**Figure 2.3** Catalytic Cycle of BINOL-Derivative Catalyzed Conjugate Addition/Enolate Alkylation Reaction with Ambiphilic Organoboronate

To provide a concise total synthesis of THC and also rapid access to various analogs, a general model of this ambiphilic organoboronate was established (Figure 4). Possible targets were divided into three major types based on their structure and functional groups. Type A included the most common cyclic and acyclic vinyl organoboronates with an alkyl chain containing up to 3 methylenes and a *Z*-olefin in order to set the stage for the intramolecular enolate alkylation. Type B contained vinyl organoboronates with a slightly different connection, as the alkyl chain containing the electrophilic leaving group was attached to the same carbon as the boron. It was therefore named the “vinyl geminal” type. Type C expanded the ambiphile cope to the aryl/heteroaryl based structures, granting access to novel THC analogs which were inaccessible via synthetic routes using olefin metathesis for the ring closure.<sup>4-6</sup>

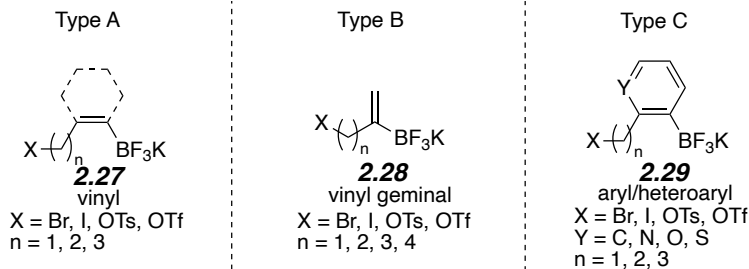
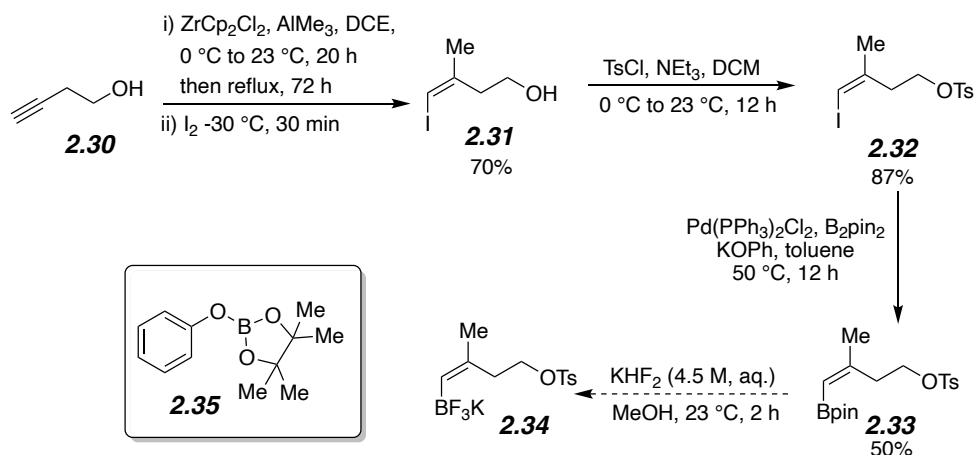


**Figure 2.4** Design of Ambiphilic Organoboronates

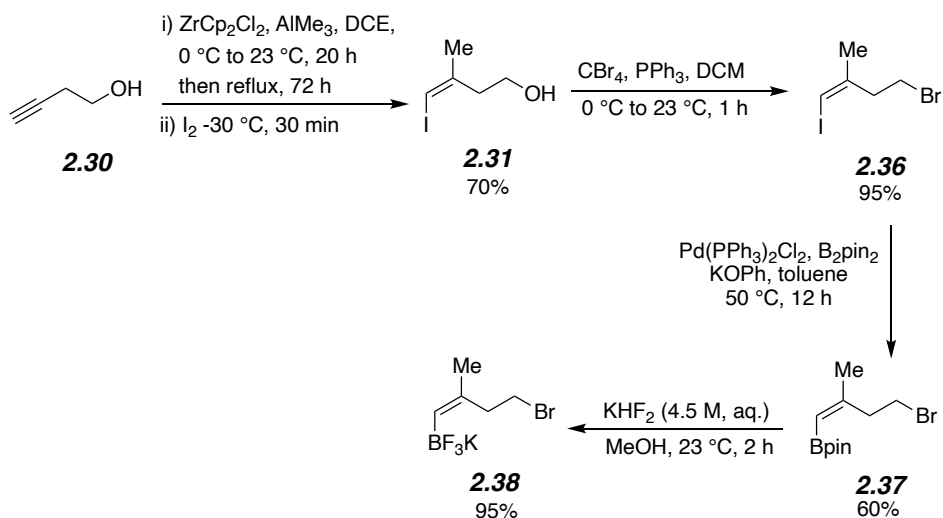
### 2.3 Synthesis of Type A Ambiphilic Organoboronates

Among all three types of ambiphilic organoboronates, type A had the closest structural similarity to with the natural product target. Therefore, we decided to start with the synthesis of the vinyl trifluoroborate alkyl tosylate **2.34** (Scheme 2.1). Following a procedure reported by Negishi,<sup>7</sup> the vinyl iodide alcohol **2.31** was successfully obtained in 70% yield. The tosylation was also smooth, giving the tosylated product in 87% yield. Miyaura borylation was troublesome during the first several trials due to an inseparable impurity, which turned out to be an inevitable byproduct, phenyl boronic ester **2.35**, generated in the catalytic cycle. After a few examinations of various aqueous washes, it was found that this byproduct would undergo hydrolysis after treatment with 1 *N* aqueous NaOH solution. Pure vinyl pinacolborane alkyl tosylate **2.33** was then obtained in 50% yield. After several failed attempts to transform **2.33** into the corresponding trifluoroborate **2.34**,<sup>8</sup> it was hypothesized that the lone pair electrons on the oxygen atom, which was six atoms away from the empty p orbital on boron, could potentially coordinate to boron thus making the molecule more vulnerable to protodeboronation. This type of Lewis acid-base interaction was observed in many systems containing similar elements and geometry.<sup>9,10</sup>



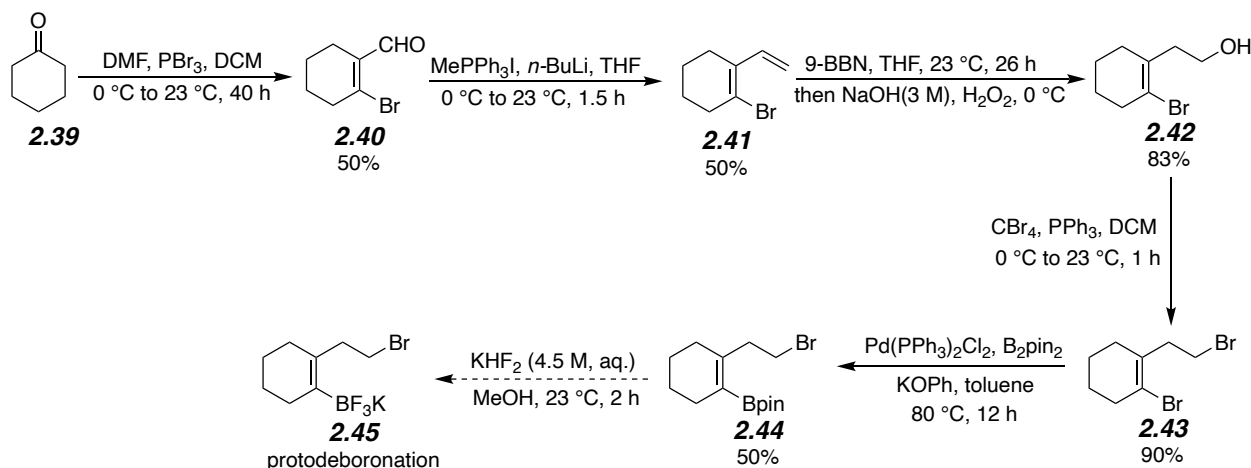
**Scheme 2.1** Synthesis of Ambiphilic Trifluoroborate **2.34**

We then sought the electrophilic character from a non-oxygen based leaving group, namely bromide or iodide (Scheme 2.2). After obtaining vinyl iodide **2.31**, the Appel reaction incorporated the bromide, giving **2.36** in almost quantitative yield. Miyaura borylation successfully delivered the vinyl pinacolborane alkyl bromide **2.37** in 60% yield. The most important transformation from **2.37** to the ambiphilic trifluoroborate **2.38** was not prohibited by protodeboration at all, and the target molecule was obtained in 95% yield. This successful transformation supported our coordination hypothesis.



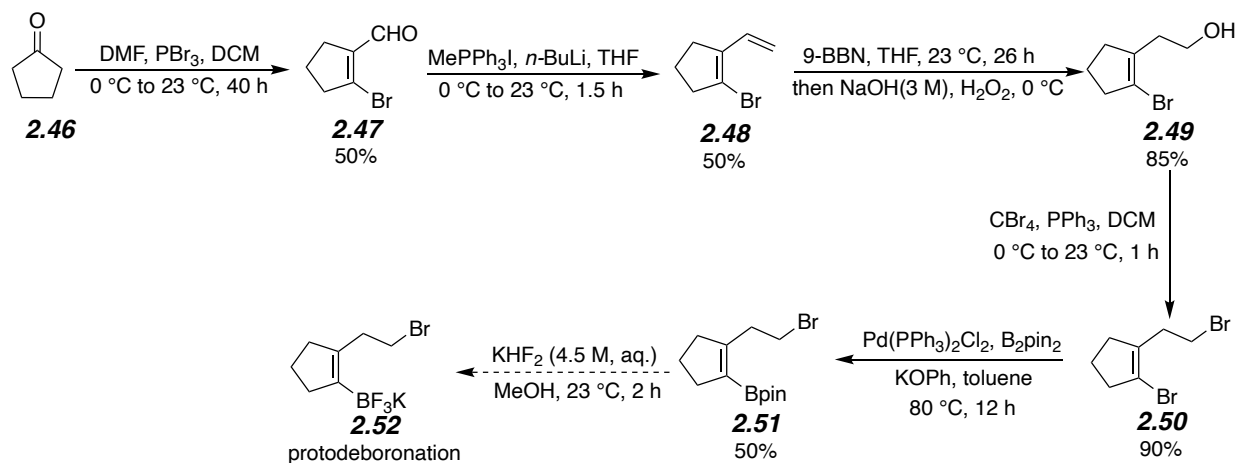
**Scheme 2.2** Synthesis of Ambiphilic Trifluoroborate **2.38**

After successfully obtaining this ambiphilic trifluoroborate, we then tried to expand the substrate scope to include the cyclic vinyl building blocks (Scheme 2.3). The cyclohexenyl bromide alcohol **2.42** was synthesized following reported procedures.<sup>11</sup> After a sequence of Appel reaction and Miyaura borylation, the cyclic vinyl pinacolborane alkyl bromide **2.44** was obtained. However, the transformation of this pinacolborane to its corresponding trifluoroborate **2.45** was again hindered due to rapid and inevitable protodeboronation.



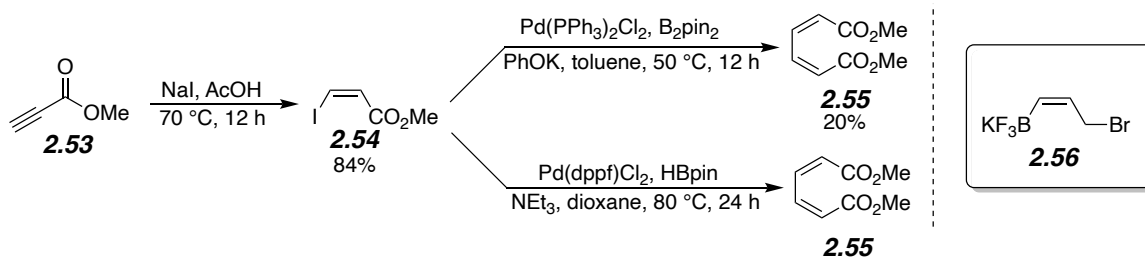
**Scheme 2.3** Synthesis of Ambiphilic Trifluoroborate **2.45**

An adjustment from a 6-membered ring to a 5-membered ring didn't help, and protodeboronation still prevented access to the desired trifluoroborate (Scheme 4.4). We then hypothesized that electronic effects might be introduced due to the alignment of orbitals in such a cyclic structure or that the trialkyl substituted alkene was too electron-rich, making it vulnerable to protodeboronation.



**Scheme 2.4** Synthesis of Ambiphilic Trifluoroborate **2.52**

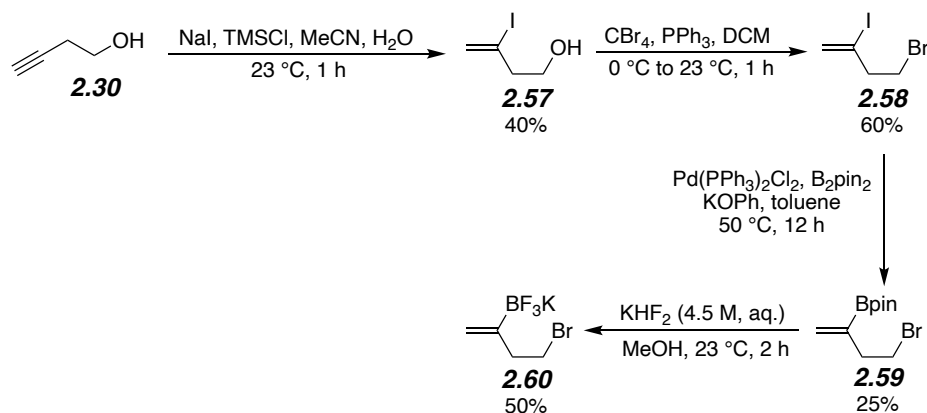
We also tried to obtain building blocks for THC analogs bearing a cyclopentenyl ring. The iodination of methyl propiolate (**2.53**) with sodium iodide and acetic acid gave *Z*-vinyl iodide ester **2.54** in 84% yield. However, using previously successful conditions or even when using less hindered boron sources, the subsequent Miyaura borylation gave only the dimerized product **2.55**.



**Scheme 2.5** Attempt for the Synthesis of **56**

## 2.4 Synthesis of Type B Ambiphilic Organoboronates

Due to the influence of the allylic substituent on the vinyl iodide, Miyaura borylation was not effective in synthesizing *Z*-vinyl trifluoroborate alkyl bromides such as **2.56**. Additionally, given the reactive nature of the allylic position, methods requiring the use of strong nucleophiles such as lithium were considered unfeasible. We then turned our sights to a potential alternative building block for a THC analog with a 5-membered ring, the type B ambiphilic trifluoroborate **2.60** (Scheme 2.6).



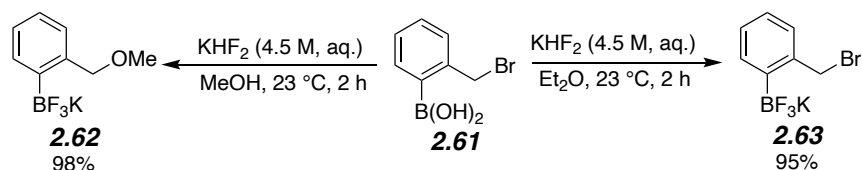
**Scheme 2.6** Synthesis of Ambiphilic Trifluoroborate **2.60**

After treating 3-butyn-1-ol (**2.30**) with sodium iodide and TMSCl in a mixture of acetonitrile and water, the iodide was successfully introduced to the same carbon as the alkyl chain. The Appel reaction then incorporated the bromide to give **2.58** in 60% yield. The yield of vinyl pinacolborane compound **2.59** after Miyaura borylation was relatively low due to potential steric hinderance from the geminal alkyl chain. Nonetheless, the geminal ambiphilic trifluoroborate **2.60** was successfully synthesized in 50% yield after treating **2.59** with aqueous KHF<sub>2</sub> solution.

## 2.5 Synthesis of Type C Ambiphilic Organoboronates

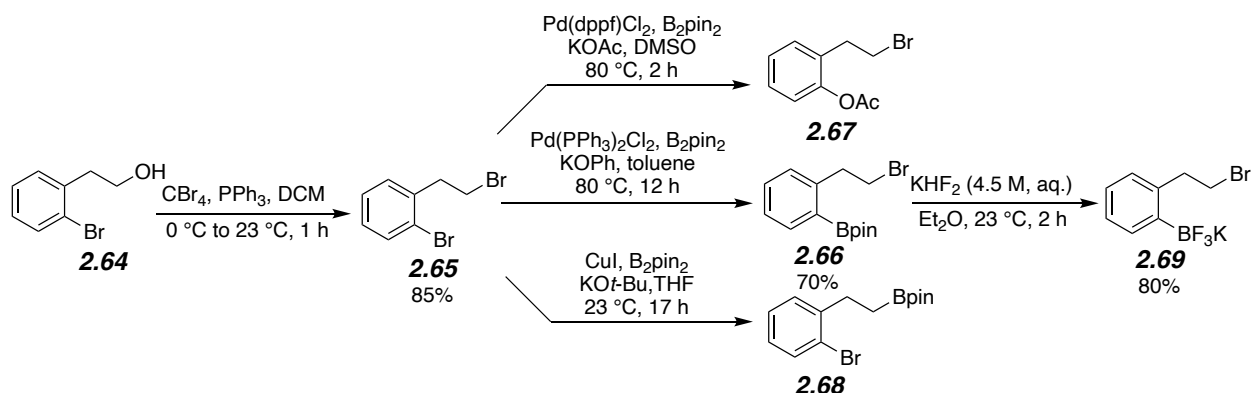
After exploring vinyl ambiphilic trifluoroborates, we started pursuing aryl ambiphilic trifluoroborates, which could potentially provide access to previously inaccessible THC analogs.

Our first target was ambiphilic trifluoroborate **2.63** because the boronic acid precursor **2.61** was an inexpensive commercially available compound (Scheme 2.7). Surprisingly, the most common method for trifluoroborate synthesis, using methanol as the solvent, was not ideal for this specific substrate. Because the benzylic bromide was too reactive, methanol was a strong enough nucleophile to attack the benzylic bromide giving the methyl benzyl ether **2.62**. After switching the solvent to ethyl ether, trifluoroborate **2.63** was successfully obtained in 95% yield.



**Scheme 2.7** Synthesis of Ambiphilic Aryl Trifluoroborate **2.63**

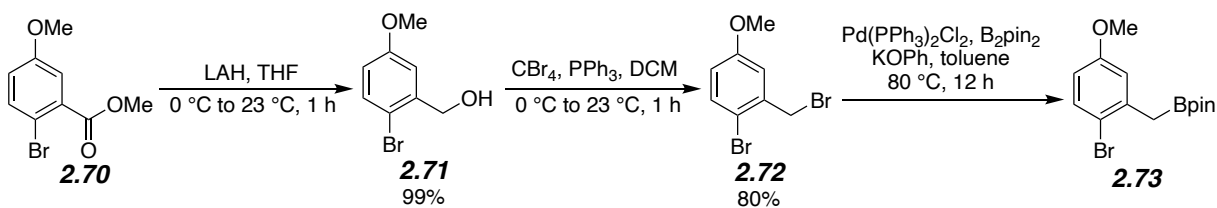
We then moved on to the synthesis of ambiphilic aryl trifluoroborate **2.69**, which was designed with a homo-benzylic bromide (Scheme 2.8). Incorporation of the bromide was successful via Appel reaction from the homo-benzylic alcohol **2.64**. The borylation step was somewhat challenging. Instead of pinacolborane, the acetate base was introduced to the aryl ring via the typical Miyaura borylation conditions for aryl substrates. The copper catalysis was more selective toward oxidative insertion into the homo-benzylic bromide, giving the alkyl pinacolborane as the final product while leaving the aryl bromide untouched. We then modified three facets of the Miyaura borylation; using a less reactive catalyst, a less reactive solvent environment, and a bulkier base to prevent the insertion. These modifications turned out to be very effective as the target aryl Bpin alkyl bromide **2.66** was successfully obtained in 70% yield. Recrystallization after treatment with aqueous  $\text{KHF}_2$  solution gave the ambiphilic aryl trifluoroborate **2.69** in 80% yield.



**Scheme 2.8** Synthesis of Ambiphilic Trifluoroborate **2.69**

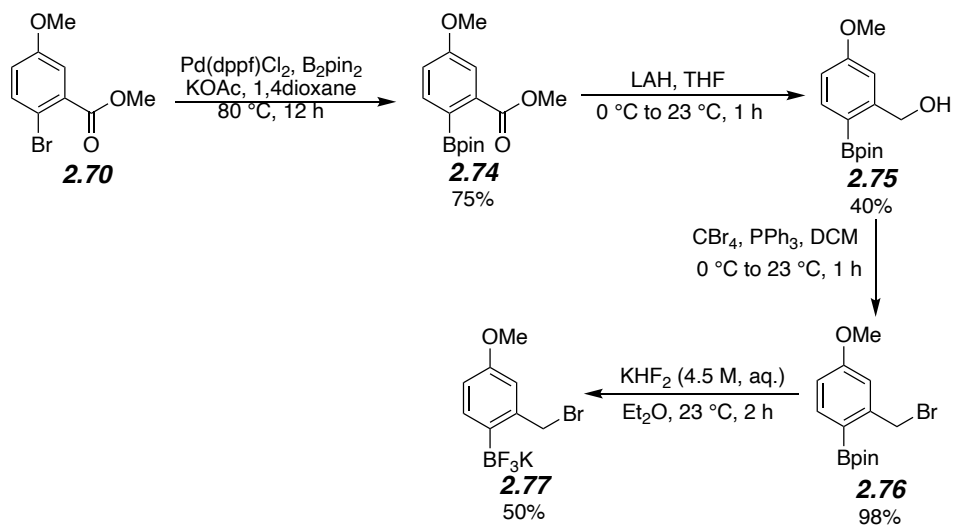
With **2.63** and **2.69** in hand, we were concerned that the electron-withdrawing benzylic-/homo-benzylic bromides in these molecules might hurt the nucleophilicity. Consequently, the

decision was made to introduce an electron-donating methoxy group with para relationship. The benzyl alcohol **2.71** was obtained in almost quantitative yield after reducing the ester **2.70** with LAH (Scheme 2.9). Incorporation of bromide via Appel reaction gave **2.72** in 80% yield. The slight difference in structure turned out to have great impact on the reactivity as the oxidative insertion is much slower on electron-rich aryl rings. The selectivity of Miyaura borylation switched from the aryl bromide to the allylic bromide, giving **2.73** as the borylation product.



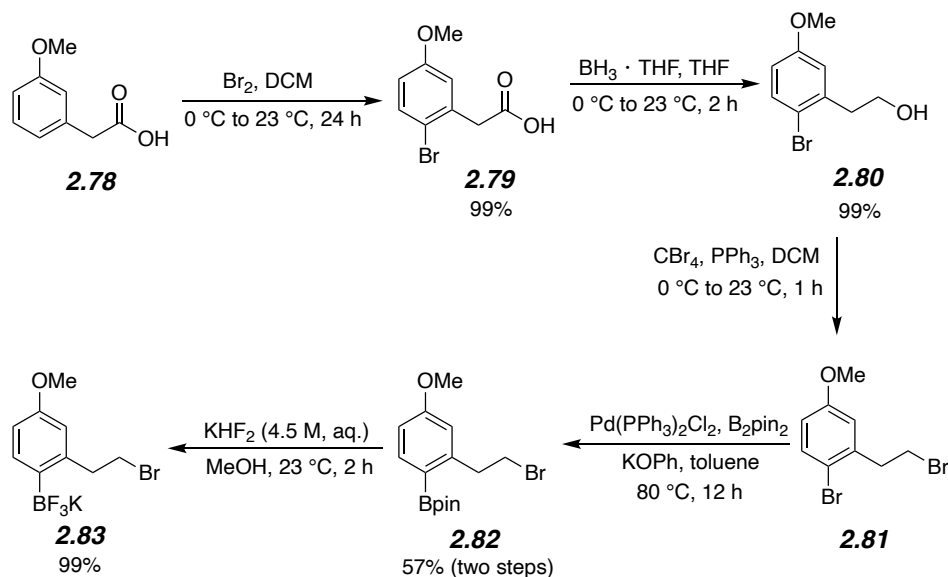
**Scheme 2.9** Synthesis of **2.73**

Based on this observation, we considered altering the order of events by conducting borylation before introducing the bromide leaving group (Scheme 2.10). The aryl Bpin ester **2.74** was synthesized in 75% yield from **2.70** via Miyaura borylation. Reduction of ester **2.74** with LAH gave alcohol **2.75** in 40% yield due to a side reaction between the boronic ester and the hydride. The sequence of Appel reaction and aqueous  $\text{KHF}_2$  treatment was effective and the target trifluoroborate **2.77** was obtained in 50% yield after two steps.



**Scheme 2.10** Synthesis of Ambiphilic Trifluoroborate **2.77**

Previous explorations clarified the route toward the ambiphilic aryl trifluoroborate with homobenzylic bromide (Scheme 2.11). The homobenzylic alcohol **2.80** was prepared following literature reported procedure in quantitative yield.<sup>12</sup> Aryl pinacolborane alkyl halide **2.82** was obtained in 57% yield using another Appel reaction and Miyaura borylation. After treatment with aqueous  $\text{KHF}_2$ , aryl ambiphilic trifluoroborate **2.83** was obtained in 99% yield.



## 2.6 Conclusion

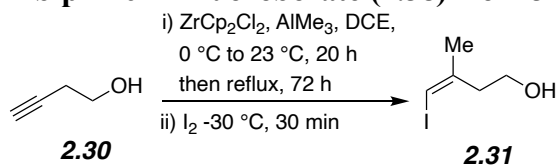
Eight bench- and air-stable ambiphilic organoboronates were successfully synthesized despite the challenges arising from the conflicted nature of these unique molecules. These ambiphilic coupling partners were applied in conjugate addition reactions (Chapter 3). For those ambiphilic boronic esters that could not be transformed into the corresponding trifluoroborates due to rapid protodeboration, further investigation will be conducted to overcome the issues using boronic esters and explore their potential application in conjugate addition conditions.

## 2.7 Experimental

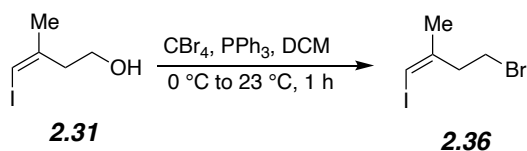
### 2.7.1 Material and Methods

All reactions were carried out in flame- or oven-dried glassware under a positive pressure of argon unless the reaction contained water as a solvent. Dichloromethane, toluene, THF and acetonitrile were purged with argon and dried over activated alumina columns. 1,2-dichloroethane was freshly distilled from CaH<sub>2</sub> before use. Flash chromatography was performed using 60 Å silica gel (Sigma Aldrich). Preparative and analytical plate chromatography was performed on Sigma Aldrich silica gel plates, 250 µm thickness, 60 Å pore size, with UV light at 254 nm used to visualize the plates. Chemical names were generated using Cambridge Soft ChemBioDraw Ultra 12.0. Analysis by HPLC was performed on a Shimadzu Prominence LC (LC-20AB) equipped with an SPD-20A UV-Vis detector (190 nm–400 nm) and a Chiralpak or Chiralcel (250 mm x 4.6 mm) column (see below for column details). The <sup>1</sup>H, <sup>13</sup>C, <sup>11</sup>B, and <sup>19</sup>F NMR spectra were recorded on a JEOL ECA-600, ECA-500, or ECX-400P spectrometer using the residual solvent peak as an internal standard (CDCl<sub>3</sub>: 7.25 ppm for <sup>1</sup>H NMR and 77.00 ppm for <sup>13</sup>C NMR). NMR yields were determined by addition of 1 equivalent of methyl (4-nitrophenyl) carboxylate or *trans*-stilbene as an internal standard to the crude reaction mixture. IR spectra were obtained using a ThermoNicolet Avatar 370 FT-IR instrument. HRMS analyses were performed under contract by UT Austin's mass spectrometric facility via an Agilent 6546 Q-TOF LC/MS (high res ESI), Agilent 6530 Q-TOF LC/MS (high resolution CI, APCI or APPI), or Waters Autospec GC/MS (high resolution CI) instrument. Commercially available compounds were purchased from Sigma Aldrich, Acros, Combi-Blocks, Oakwood Chemical, Alfa Aesar, Ambeed, ArkPharm, Beantown Chemical, TCI, and Cambridge Isotope Laboratories and were used without further purification.

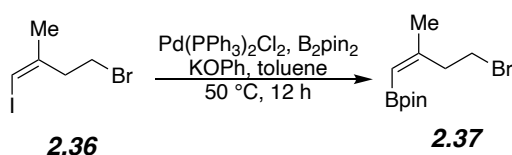
## 2.7.2 Synthesis of Vinyl Ambiphilic Trifluoroborate (**2.38**) from 3-butyn-1-ol (**2.30**)



(*Z*)-4-iodo-3-methylbut-3-en-1-ol (**2.31**) was synthesized by modifying conditions originally reported by Negishi.<sup>7</sup> To a flame dried round bottom flask equipped with a stir bar was added zirconocene dichloride (3.65 g, 12.5 mmol). 1,2-Dichloroethane (150 mL) was then added to the flask and the solution was cooled to  $0\text{ }^\circ\text{C}$  before trimethyl aluminum (50 mL, 2 M solution in toluene) was added dropwise. The solution was allowed to stir for 15 minutes at  $0\text{ }^\circ\text{C}$ , then 3-butyn-1-ol (**2.30**, 3.54 g, 50 mmol) was added dropwise (a considerable quantity of gas is generated, use care to allow its release). This mixture was warmed to room temperature and stirred for 20 hours and then heated to  $90\text{ }^\circ\text{C}$  for 3 days. The resulting solution was cooled to  $-30\text{ }^\circ\text{C}$  and quenched by the addition of a solution of iodine (14 g, 55 mmol) in THF (30 mL). After being stirred at room temperature for 30 minutes, the reaction mixture was cooled to  $0\text{ }^\circ\text{C}$ , and 4 mL water was added dropwise followed by the slow addition of 15% aqueous sodium hydroxide solution (4 mL) and water (10 mL). The resulting suspension was allowed to stir 15 minutes at room temperature followed by addition of anhydrous magnesium sulfate. This mixture was stirred for 15 minutes until the emulsion had dissipated. Filtration followed by chromatography on silica gel (30% ethyl acetate in hexanes) afforded (*Z*)-4-iodo-3-methylbut-3-en-1-ol (**2.31**) as a dark red oil in 70% yield (7.39 g). All spectral data matched literature reports.<sup>7</sup>

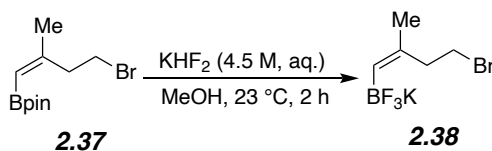


**(Z)-4-bromo-1-iodo-2-methylbut-1-ene (2.36).** In a flame dried round bottom flask equipped with a stir bar, tetrabromomethane (10.2 g, 26 mmol) and (Z)-4-iodo-3-methylbut-3-en-1-ol (**2.31**, 5 g, 23.6 mmol) were dissolved in dichloromethane (100 mL). After being cooled to 0 °C, triphenylphosphine (6.8 g, 26 mmol) was added in 3 portions. The resulting mixture was allowed to warm up to room temperature and stirred for 1 hour. After completion, the reaction mixture was concentrated and added dropwise to an agitated mixture of silica gel (20 g) in hexanes, then passed through a silica plug to remove triphenyl phosphine oxide. The filtrate was concentrated and chromatography on silica gel (100% hexanes) afforded (Z)-4-bromo-1-iodo-2-methylbut-1-ene (**2.36**) in 95% yield (6.2 g) as a pink oil. <sup>1</sup>H-NMR (500 MHz, chloroform-d) δ 6.06 (s, 1H), 3.44 (t, *J* = 7.7 Hz, 2H), 2.79 (t, *J* = 7.4 Hz, 2H), 1.94 (d, *J* = 1.1 Hz, 3H). <sup>13</sup>C-NMR (126 MHz, chloroform-d) δ 144.5, 77.4, 41.8, 28.9, 23.5. IR 3270, 2391, 2274, 1448, 1266, 1200, 1167, 783, 637, 545 cm<sup>-1</sup>. HRMS-Cl *m/z* calcd. for C<sub>5</sub>H<sub>8</sub><sup>79</sup>BrI [M]<sup>+</sup> 273.8854, found 273.8852; calcd. for C<sub>5</sub>H<sub>8</sub><sup>81</sup>BrI [M]<sup>+</sup> 275.8834, found 275.8832.



**(Z)-2-(4-bromo-2-methylbut-1-en-1-yl)-4,4,5,5-tetramethyl-1,3,2-dioxaborolane (2.37)** was synthesized by modifying conditions originally reported by Miyaura.<sup>13</sup> In a flame dried round bottom flask (Z)-4-bromo-1-iodo-2-methylbut-1-ene (**2.36**, 2.75 g, 10 mmol), bis(pinacolato)diboron (aka B<sub>2</sub>pin<sub>2</sub>, 3.81 g, 15 mmol), bis(triphenylphosphine)palladium(II) dichloride (210.6 mg, 0.3 mmol), and potassium phenolate (1.98 g, 15 mmol) were dissolved in toluene (60 mL). The reaction mixture was degassed for 10 minutes before being heated to 50 °C, then stirred for 12 hours. Water (100 mL) was added, and the reaction mixture was extracted with

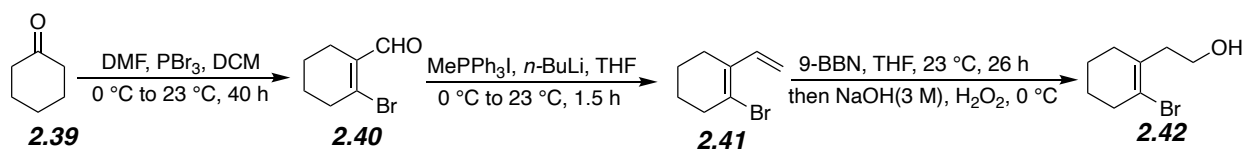
Et<sub>2</sub>O (3 x 20 mL). The combined organic layers were washed with 1 M aqueous sodium hydroxide solution (30 mL), brine (100 mL), then dried over anhydrous magnesium sulfate. The solution was concentrated under reduced pressure. The crude mixture was purified by chromatography on silica gel (2% ethyl acetate in hexanes) to yield (*Z*)-2-(4-bromo-2-methylbut-1-en-1-yl)-4,4,5,5-tetramethyl-1,3,2-dioxaborolane (**2.37**, 1.67 g, 60% yield) as a colorless oil. <sup>1</sup>H-NMR (400 MHz, chloroform-d) δ 5.26 (s, 1H), 3.44 (t, *J* = 7.6 Hz, 2H), 2.92 (t, *J* = 7.6 Hz, 2H), 1.88 (s, 3H), 1.23 (s, 12H). <sup>13</sup>C-NMR (101 MHz, chloroform-d) δ 157.2, 81.3, 37.5, 30.3, 25.0, 23.3. <sup>11</sup>B-NMR (128 MHz, chloroform-d) δ 26.9. IR 2976, 2932, 1636, 1442, 1378, 1256, 1141, 968, 850cm<sup>-1</sup>. HRMS-**CI** *m/z* calcd. for C<sub>11</sub>H<sub>21</sub><sup>11</sup>BO<sub>2</sub><sup>79</sup>Br [M]<sup>+</sup> 275.0818, found 275.0808; calcd. for C<sub>11</sub>H<sub>21</sub><sup>11</sup>BO<sub>2</sub><sup>81</sup>Br [M]<sup>+</sup> 277.0798, found 277.0800



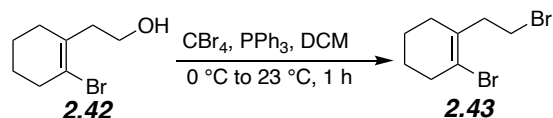
**(*Z*)-(4-bromo-2-methylbut-1-en-1-yl)trifluoro-λ<sup>4</sup>-borane, potassium salt (2.38).** In a round bottom flask equipped with a stir bar, (*Z*)-2-(4-bromo-2-methylbut-1-en-1-yl)-4,4,5,5-tetramethyl-1,3,2-dioxaborolane (**2.37**, 1.1 g, 4 mmol) were dissolved in methanol (20 mL). Potassium hydrogen fluoride solution (3.6 mL, 4.5 M in water) was added dropwise. The reaction mixture was then stirred vigorously at room temperature for 2 hours. The mixture was concentrated to dryness under reduced pressure then dissolved in acetone (20 mL). The solution was filtered, and the solid was washed with acetone (3 x 10 mL). The acetone solution was concentrated to 5 mL, then ether was added until no further precipitation was observed. The crystals were then filtered and washed with ether to yield (*Z*)-(4-bromo-2-methylbut-1-en-1-yl)trifluoro-λ<sup>4</sup>-borane, potassium salt (**2.38**, 970 mg, 95% yield) as a white crystal. <sup>1</sup>H-NMR (500 MHz, acetone-d<sub>6</sub>) δ

5.20 (d,  $J = 4.6$  Hz, 1H), 3.45 (t,  $J = 8.3$  Hz, 2H), 2.66 (t,  $J = 8.3$  Hz, 2H), 1.67 (s, 3H).  $^{13}\text{C-NMR}$  (126 MHz, acetone- $d_6$ )  $\delta$  39.5, 33.5, 25.8.  $^{11}\text{B-NMR}$  (160 MHz, acetone- $d_6$ )  $\delta$  1.8, 1.5.  $^{19}\text{F-NMR}$  (470 MHz, acetone- $d_6$ )  $\delta$  -136.9. **IR** 2963, 2922, 1643, 1449, 1117, 1085, 929, 848, 729, 635, 607  $\text{cm}^{-1}$ . **HRMS-ESI m/z** calcd. for  $\text{C}_5\text{H}_8^{11}\text{B}^{79}\text{BrF}_3$   $[\text{M}]^-$  214.9861, found 214.9861; calcd. for  $\text{C}_5\text{H}_8^{11}\text{B}^{81}\text{BrF}_3$   $[\text{M}]^-$  216.9841, found 216.9841 (Note: This compound must be tested with very gentle source conditions and injected into a flow of 100% acetonitrile for HRMS.)

### 2.7.3 Synthesis of Cyclic Ambiphilic Boronates 2.44 and 2.51

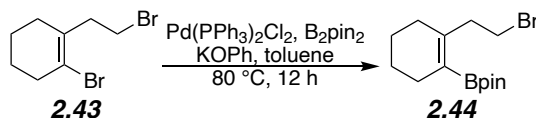


2-(2-bromocyclohex-1-enyl)ethanol (2.42) was prepared following literature procedure from cyclohexanone (2.39).<sup>11</sup> All spectral data matched literature reports.<sup>11</sup>

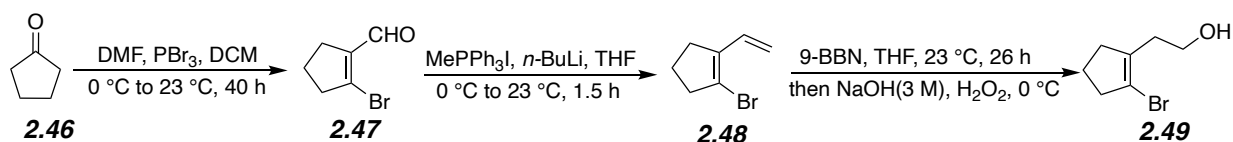


**1-bromo-2-(2-bromoethyl)cyclohex-1-ene (2.43).** In a flame dried round bottom flask equipped with a stir bar, tetrabromomethane (888.8 mg, 2.68 mmol) and 2-(2-bromocyclohex-1-enyl)ethanol (2.42) (500 mg, 2.44 mmol) were dissolved in dichloromethane (15 mL). After being cooled to 0 °C, triphenylphosphine (702.9 mg, 2.68 mmol) was added in three portions. The resulting mixture was allowed to warm up to room temperature and stirred for 1 hour. After completion, the reaction mixture was concentrated and added dropwise to an agitated mixture of silica gel (5 g) in hexanes, then passed through a silica plug to remove triphenyl phosphine oxide. The filtrate was concentrated and chromatography on silica gel (100% hexanes) afforded 1-bromo-

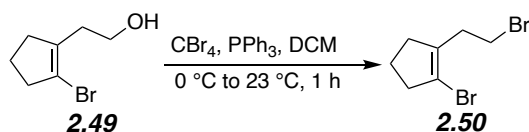
2-(2-bromoethyl)cyclohex-1-ene (**2.43**) in 90% yield (585.2 mg) as an oil. <sup>1</sup>H-NMR (500 MHz, chloroform-d) δ 3.43 (t, *J* = 8.0 Hz, 2H), 2.73 (t, *J* = 7.7 Hz, 2H), 2.48 (s, 2H), 2.14 (s, 2H), 1.67 (s, 4H).



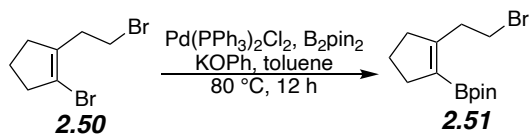
**2-(2-(2-bromoethyl)cyclohex-1-enyl)-4,4,5,5-tetramethyl-1,3,2-dioxaborolane (2.44)** was synthesized by modifying conditions originally reported by Miyaura.<sup>13</sup> In a flame dried round bottom flask 1-bromo-2-(2-bromoethyl)cyclohex-1-ene (**2.43**) (1.34 g, 5 mmol), bis(pinacolato)diboron (aka B<sub>2</sub>pin<sub>2</sub>, 1.9 g, 7.5 mmol), bis(triphenylphosphine)palladium(II) dichloride (175.5 mg, 0.25 mmol), and potassium phenolate (1.3 g, 10 mmol) were dissolved in toluene (30 mL). The reaction mixture was degassed for 10 minutes before being heated to 80 °C, then stirred for 12 hours. Water (50 mL) was added, and the reaction mixture was extracted with Et<sub>2</sub>O (3 x 15 mL). The combined organic layers were washed with 1 M aqueous sodium hydroxide solution (30 mL), brine (100 mL), then dried over anhydrous magnesium sulfate. The solution was concentrated under reduced pressure. The crude mixture was purified by chromatography on silica gel (2% ethyl acetate in hexanes) to yield 2-(2-(2-bromoethyl)cyclohex-1-enyl)-4,4,5,5-tetramethyl-1,3,2-dioxaborolane (**2.44**, 787.4 mg, 50% yield) as a colorless oil. <sup>1</sup>H-NMR (400 MHz, chloroform-d) δ 3.40 (t, *J* = 8.0 Hz, 2H), 2.81 (t, *J* = 8.0 Hz, 2H), 2.14-2.04 (m, 4H), 1.62-1.49 (m, 4H), 1.26 (s, 12H).



2-(2-bromocyclopent-1-enyl)ethanol (2.49) was prepared following literature procedure from cyclopentanone (2.46).<sup>14</sup> All spectral data matched literature reports.<sup>14</sup>



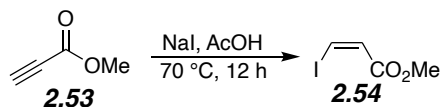
1-bromo-2-(2-bromoethyl)cyclopent-1-ene (2.50). In a flame dried round bottom flask equipped with a stir bar, tetrabromomethane (1.53 g, 4.62 mmol) and 2-(2-bromocyclopent-1-enyl)ethanol (2.49) (800 mg, 4.2 mmol) were dissolved in dichloromethane (30 mL). After being cooled to 0 °C, triphenylphosphine (1.21 g, 4.62 mmol) was added in three portions. The resulting mixture was allowed to warm up to room temperature and stirred for 1 hour. After completion, the reaction mixture was concentrated and added dropwise to an agitated mixture of silica gel (5 g) in hexanes, then passed through a silica plug to remove triphenyl phosphine oxide. The filtrate was concentrated and chromatography on silica gel (100% hexanes) afforded 1-bromo-2-(2-bromoethyl)cyclopent-1-ene (2.36) in 90% yield (960.3 mg) as an oil. <sup>1</sup>H-NMR (400 MHz, chloroform-d)  $\delta$  3.43 (t,  $J = 7.3$  Hz, 2H), 2.75 (t,  $J = 7.3$  Hz, 2H), 2.64 (t,  $J = 7.1$  Hz, 2H), 2.36 (t,  $J = 7.1$  Hz, 2H), 1.99-1.92 (m, 2H)



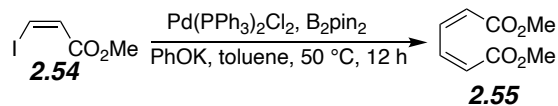
### 2-(2-(2-bromoethyl)cyclopent-1-enyl)-4,4,5,5-tetramethyl-1,3,2-dioxaborolane (2.44)

was synthesized by modifying conditions originally reported by Miyaura.<sup>Error! Bookmark not defined.</sup> In a flame dried round bottom flask 1-bromo-2-(2-bromoethyl)cyclopent-1-ene (**2.50**) (507.0 mg, 2 mmol), bis(pinacolato)diboron (aka B<sub>2</sub>pin<sub>2</sub>, 762.0 mg, 3 mmol), bis(triphenylphosphine)palladium(II) dichloride (70.2 mg, 0.1 mmol), and potassium phenolate (528.8 mg, 4 mmol) were dissolved in toluene (12 mL). The reaction mixture was degassed for 10 minutes before being heated to 80 °C, then stirred for 12 hours. Water (30 mL) was added, and the reaction mixture was extracted with Et<sub>2</sub>O (3 x 10 mL). The combined organic layers were washed with 1 M aqueous sodium hydroxide solution (10 mL), brine (30 mL), then dried over anhydrous magnesium sulfate. The solution was concentrated under reduced pressure. The crude mixture was purified by chromatography on silica gel (2-5% ethyl acetate in hexanes) to yield 2-(2-(2-bromoethyl)cyclopent-1-enyl)-4,4,5,5-tetramethyl-1,3,2-dioxaborolane (**2.44**, 301.4 mg, 50% yield) as a colorless oil. <sup>1</sup>H-NMR (500 MHz, chloroform-d) δ 3.45 (t, *J* = 7.2 Hz, 2H), 3.00 (t, *J* = 7.2 Hz, 2H), 2.45-2.38 (m, 4H), 1.83-1.77 (m, 2H), 1.26 (s, 12H).

### 2.7.4 Synthesis of 2.54 and 2.55

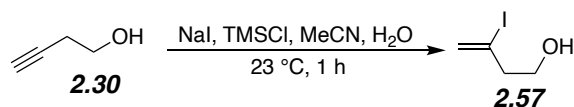


(*Z*)-methyl 3-iodoacrylate (**2.54**) was prepared following literature procedure.<sup>15</sup> All data matched the literature reports.<sup>15</sup>

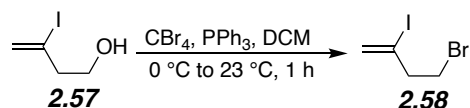


**(2Z,4Z)-dimethyl hexa-2,4-dienedioate (2.55).** In a flame dried round bottom flask (*Z*)-methyl 3-iodoacrylate (**2.54**) (846.4 mg, 4 mmol), bis(pinacolato)diboron (aka B<sub>2</sub>pin<sub>2</sub>, 1.53 g, 6 mmol), bis(triphenylphosphine)palladium(II) dichloride (85.8 mg, 0.12 mmol), and potassium phenolate (1.06 g, 8 mmol) were dissolved in toluene (24 mL). The reaction mixture was degassed for 10 minutes before being heated to 50 °C, then stirred for 12 hours. Water (30 mL) was added, and the reaction mixture was extracted with Et<sub>2</sub>O (3 x 15 mL). The combined organic layers were washed with 1 M aqueous sodium hydroxide solution (20 mL), brine (50 mL), then dried over anhydrous magnesium sulfate. The solution was concentrated under reduced pressure. The crude mixture was purified by chromatography on silica gel (2-5% ethyl acetate in hexanes) to yield (*2Z,4Z*)-dimethyl hexa-2,4-dienedioate (**2.55**, 67.7 mg, 20% yield) as a colorless oil. <sup>1</sup>H-NMR (400 MHz, chloroform-*d*) δ 7.90 (dd, *J* = 8.2, 1.8 Hz, 2H), 5.99 (dd, *J* = 8.2, 1.8 Hz, 2H), 3.75 (s, 6H). All data matched the literature reports.<sup>16</sup>

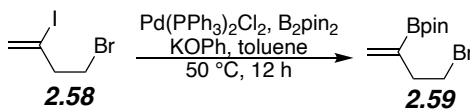
### 2.7.5 Synthesis of Geminal Ambiphilic Trifluoroborate 2.60



**3-iodobut-3-en-1-ol (2.57)** was prepared following literature procedure.<sup>17</sup> All data matched the literature reports.<sup>17</sup>

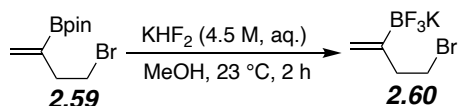


**4-bromo-2-iodobut-1-ene (2.58).** In a flame dried round bottom flask equipped with a stir bar, tetrabromomethane (3.26 g, 9.8 mmol) and 3-iodobut-3-en-1-ol (**2.57**) (1.5 g, 7.6 mmol) were dissolved in dichloromethane (40 mL). After being cooled to 0 °C, triphenylphosphine (2.58 g, 9.8 mmol) was added in 3 portions. The resulting mixture was allowed to warm up to room temperature and stirred for 1 hour. After completion, the reaction mixture was concentrated and added dropwise to an agitated mixture of silica gel (10 g) in hexanes, then passed through a silica plug to remove triphenyl phosphine oxide. The filtrate was concentrated and chromatography on silica gel (100% hexanes) afforded 4-bromo-2-iodobut-1-ene (**2.58**) in 60% yield (1.2 g) as a pink oil. <sup>1</sup>H-NMR (400 MHz, chloroform-d) δ 6.16 (s, 1H), 5.85 (s, 1H), 3.48 (t, *J* = 6.9 Hz, 2H), 2.89 (t, *J* = 6.6 Hz, 2H).



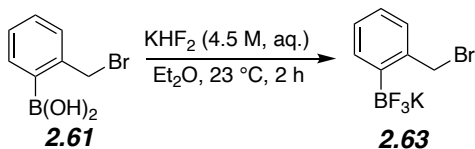
**2-(4-bromobut-1-en-2-yl)-4,4,5,5-tetramethyl-1,3,2-dioxaborolane (2.59).** In a flame dried round bottom flask 4-bromo-2-iodobut-1-ene (**2.58**) (1.13 g, 4 mmol), bis(pinacolato)diboron (aka B<sub>2</sub>pin<sub>2</sub>, 2.03 g, 8 mmol), bis(triphenylphosphine)palladium(II) dichloride (85.2 mg, 0.12 mmol), and potassium phenolate (1.33 g, 10 mmol) were dissolved in toluene (24 mL). The reaction mixture was degassed for 10 minutes before being heated to 50 °C, then stirred for 12 hours. Water (30 mL) was added, and the reaction mixture was extracted with Et<sub>2</sub>O (3 x 15 mL). The combined organic layers were washed with 1 M aqueous sodium hydroxide solution (20 mL), brine (40 mL), then dried over anhydrous magnesium sulfate. The solution was concentrated under reduced pressure. The crude mixture was purified by chromatography on silica

gel (2% ethyl acetate in hexanes) to yield 2-(4-bromobut-1-en-2-yl)-4,4,5,5-tetramethyl-1,3,2-dioxaborolane (**2.59**, 271.2 mg, 25% yield) as a colorless oil.  $^1\text{H-NMR}$  (400 MHz, chloroform-d)  $\delta$  5.91 (d,  $J = 3.2$  Hz, 1H), 5.70 (s, 1H), 3.49 (t,  $J = 7.3$  Hz, 2H), 2.70 (t,  $J = 7.3$  Hz, 2H), 1.25-1.27 (12H).

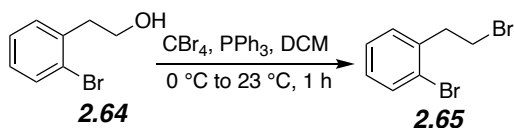


**2-(4-bromobut-1-en-2-yl)trifluoro- $\lambda^4$ -borane, potassium salt (2.60).** In a round bottom flask equipped with a stir bar, 2-(4-bromobut-1-en-2-yl)-4,4,5,5-tetramethyl-1,3,2-dioxaborolane (**2.59**, 1.0 g, 3.8 mmol) were dissolved in methanol (16 mL). Potassium hydrogen fluoride solution (4.2 mL, 4.5 M in water) was added dropwise. The reaction mixture was then stirred vigorously at room temperature for 2 hours. The mixture was concentrated to dryness under reduced pressure then dissolved in acetone (20 mL). The solution was filtered, and the solid was washed with acetone (3 x 10 mL). The acetone solution was concentrated to 2 mL, then ether was added until no further precipitation was observed. The crystals were then filtered and washed with ether to yield 2-(4-bromobut-1-en-2-yl) trifluoro- $\lambda^4$ -borane, potassium salt (**2.60**, 458.9 mg, 50% yield) as a white crystal.  $^1\text{H-NMR}$  (400 MHz, ACETONE-D6)  $\delta$  5.03 (s, 1H), 4.86 (s, 1H), 3.47 (t,  $J = 8.5$  Hz, 2H), 2.53 (t,  $J = 8.2$  Hz, 2H).

## 2.7.6 Synthesis of Aryl Ambiphilic Trifluoroborates 2.63, 2.69, 2.77, and 2.82

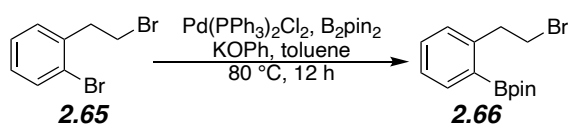


**2-(bromomethyl)phenyltrifluoro- $\lambda^4$ -borane, potassium salt (2.63).** In a round bottom flask equipped with a stir bar, 2-(bromomethyl)phenylboronic acid (**2.61**, 430.5 mg, 2 mmol) were dissolved in diethyl ether (8 mL). Potassium hydrogen fluoride solution (1.75 mL, 4.5 M in water) was added dropwise. The reaction mixture was then stirred vigorously at room temperature for 2 hours. The mixture was concentrated to dryness under reduced pressure then dissolved in acetone (20 mL). The solution was filtered, and the solid was washed with acetone (3 x 10 mL). The acetone solution was concentrated to 2 mL, then ether was added until no further precipitation was observed. The crystals were then filtered and washed with ether to yield 2-(bromomethyl)phenyltrifluoro- $\lambda^4$ -borane, potassium salt (**2.63**, 527.1 mg, 95% yield) as a white crystal.  $^1\text{H-NMR}$  (400 MHz, acetone- $d_6$ )  $\delta$  7.49 (d,  $J = 6.4$  Hz, 1H), 7.26 (s, 1H), 7.04-6.99 (m, 3H), 4.90 (s, 2H).

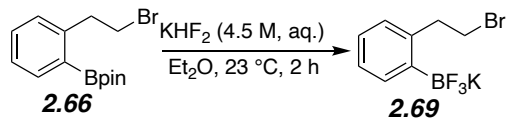


**1-bromo-2-(2-bromoethyl)benzene (2.65).** In a flame dried round bottom flask equipped with a stir bar, tetrabromomethane (1.8 g, 5.5 mmol) and 2-bromophenylethyl alcohol (**2.64**, 1.00 g, 5.0 mmol) were dissolved in dichloromethane (30 mL). After being cooled to  $0^\circ\text{C}$ , triphenylphosphine (1.44 g, 5.5 mmol) was added in 3 portions. The resulting mixture was allowed to warm up to room temperature and stirred for 1 hour. After completion, the reaction mixture was concentrated and added dropwise to an agitated mixture of silica gel (10 g) in hexanes, then passed

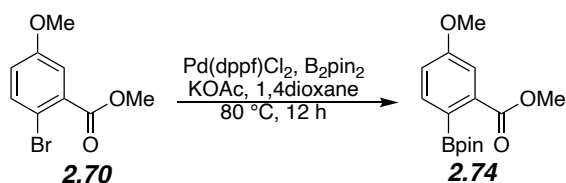
through a silica plug to remove triphenyl phosphine oxide. The filtrate was concentrated and chromatography on silica gel (100% hexanes) afforded 1-bromo-2-(2-bromoethyl)benzene (**2.65**) in 85% yield (1.12 g) as a thick oil. <sup>1</sup>H-NMR (400 MHz, chloroform-d) δ 7.54 (d, *J* = 7.8 Hz, 1H), 7.26 (d, *J* = 4.6 Hz, 2H), 7.14-7.10 (m, 1H), 3.58 (t, *J* = 7.6 Hz, 2H), 3.28 (t, *J* = 7.6 Hz, 2H). <sup>13</sup>C-NMR (101 MHz, CHLOROFORM-D) δ 136.6, 131.6, 129.8, 127.3, 126.1, 122.9, 75.9, 75.6, 75.3, 38.1, 29.6



**2-(2-(2-bromoethyl)phenyl)-4,4,5,5-tetramethyl-1,3,2-dioxaborolane (2.66).** In a flame dried round bottom flask (1-bromo-2-(2-bromoethyl)benzene (**2.65**) (527.9 mg, 2 mmol), bis(pinacolato)diboron (aka B<sub>2</sub>pin<sub>2</sub>, 761.8 mg, 3 mmol), bis(triphenylphosphine)palladium(II) dichloride (42 mg, 0.06 mmol), and potassium phenolate (528.8 mg, 4 mmol) were dissolved in toluene (12 mL). The reaction mixture was degassed for 10 minutes before being heated to 50 °C, then stirred for 12 hours. Water (20 mL) was added, and the reaction mixture was extracted with Et<sub>2</sub>O (3 x 15 mL). The combined organic layers were washed with 1 M aqueous sodium hydroxide solution (20 mL), brine (30 mL), then dried over anhydrous magnesium sulfate. The solution was concentrated under reduced pressure. The crude mixture was purified by chromatography on silica gel (2-5% ethyl acetate in hexanes) to yield 2-(2-(2-bromoethyl)phenyl)-4,4,5,5-tetramethyl-1,3,2-dioxaborolane (**2.66**, 436.2 mg, 70% yield) as a colorless oil. <sup>1</sup>H-NMR (400 MHz, chloroform-d) δ 7.81 (d, *J* = 7.3 Hz, 1H), 7.38 (t, *J* = 7.3 Hz, 1H), 7.26-7.19 (m, 3H), 3.54 (t, *J* = 7.6 Hz, 2H), 3.40 (t, *J* = 7.8 Hz, 2H), 1.34 (s, 12H). <sup>13</sup>C-NMR (101 MHz, CHLOROFORM-D) δ 144.1, 135.0, 129.7, 128.5, 124.8, 82.2, 75.9, 75.6, 75.2, 38.1, 33.0, 23.4

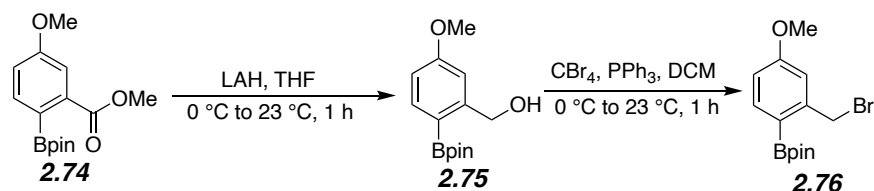


**2-(2-(2-bromoethyl)phenyl)trifluoro- $\lambda^4$ -borane, potassium salt (2.69).** In a round bottom flask equipped with a stir bar, 2-(2-(2-bromoethyl)phenyl)-4,4,5,5-tetramethyl-1,3,2-dioxaborolane (**2.66**, 622.0 mg, 2 mmol) were dissolved in methanol (8 mL). Potassium hydrogen fluoride solution (1.8 mL, 4.5 M in water) was added dropwise. The reaction mixture was then stirred vigorously at room temperature for 2 hours. The mixture was concentrated to dryness under reduced pressure then dissolved in acetone (20 mL). The solution was filtered, and the solid was washed with acetone (3 x 10 mL). The acetone solution was concentrated to 2 mL, then ether was added until no further precipitation was observed. The crystals were then filtered and washed with ether to yield 2-(2-(2-bromoethyl)phenyl)trifluoro- $\lambda^4$ -borane, potassium salt (**2.69**, 465.0 mg, 80% yield) as a white crystal. <sup>1</sup>H-NMR (400 MHz, acetone-d<sub>6</sub>)  $\delta$  7.50 (d,  $J$  = 5.0 Hz, 1H), 6.95 (t,  $J$  = 8.9 Hz, 3H), 3.61 (t,  $J$  = 8.2 Hz, 2H), 3.28 (t,  $J$  = 8.2 Hz, 2H). <sup>13</sup>C-NMR (101 MHz, ACETONE-D<sub>6</sub>)  $\delta$  204.1, 203.9, 140.5, 131.1, 127.0, 123.9, 123.2, 38.5, 33.5, 28.0, 27.8, 27.6, 27.4, 27.2, 27.0, 26.8



**Methyl 5-methoxy-2-(4,4,5,5-tetramethyl-1,3,2-dioxaborolan-2-yl)benzoate (2.74).** In a flame dried round bottom flask methyl 2-bromo-5-methoxybenzoate (**2.70**, 2.45 g, 10 mmol), bis(pinacolato)diboron (aka B<sub>2</sub>pin<sub>2</sub>, 2.45 g, 10 mmol), [1,1'-bis(diphenylphosphino)ferrocene]

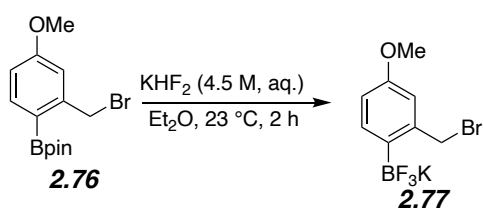
dichloropalladium (II) (219.5 mg, 0.3 mmol), and potassium acetate (1.47 g, 15 mmol) were dissolved in 1,4-dioxane (60 mL). The reaction mixture was degassed for 10 minutes before being heated to 80 °C, then stirred for 12 hours. Water (100 mL) was added, and the reaction mixture was extracted with Et<sub>2</sub>O (3 x 20 mL). The combined organic layers were washed with 1 M aqueous sodium hydroxide solution (30 mL), brine (100 mL), then dried over anhydrous magnesium sulfate. The solution was concentrated under reduced pressure. The crude mixture was purified by chromatography on silica gel (5% ethyl acetate in hexanes) to yield methyl 5-methoxy-2-(4,4,5,5-tetramethyl-1,3,2-dioxaborolan-2-yl)benzoate (**2.74**, 2.18 g, 75% yield) as a colorless oil. <sup>1</sup>H-NMR (400 MHz, chloroform-d) δ 7.44-7.42 (m, 2H), 7.04 (dd, *J* = 8.2, 2.3 Hz, 1H), 3.89 (s, 3H), 3.83 (s, 3H), 1.39 (s, 12H).



### 2-(2-(bromomethyl)-4-methoxyphenyl)-4,4,5,5-tetramethyl-1,3,2-dioxaborolane

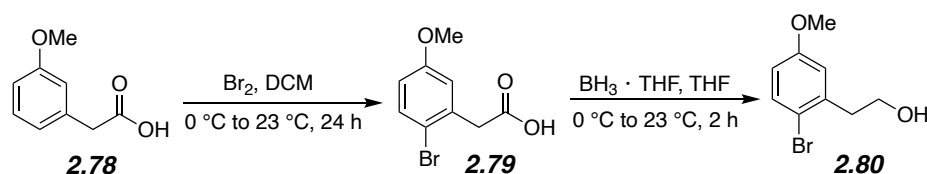
**(2.76)**. In a flame dried round bottom flask equipped with a stir bar, lithium aluminum hydride (198.8 mg, 5 mmol) was added to THF (6 mL), the suspended mixture was cool to 0 °C. Then a THF (5 mL) solution of methyl 5-methoxy-2-(4,4,5,5-tetramethyl-1,3,2-dioxaborolan-2-yl)benzoate (**2.74**, 584.3 mg, 2 mmol) was added dropwise. The solution was allowed to warm up to room temperature and stirred for 1 hour. After completion, the reaction mixture was quenched with saturated NH<sub>4</sub>Cl solution (5 mL). The layers were separated and the aqueous layer was extracted with Et<sub>2</sub>O (3 x 10 mL). The combined organic layer was washed with brine (30 mL), dried with anhydrous MgSO<sub>4</sub>, and concentrated. Chromatography on silica gel (5-10% ethyl

acetate in hexanes) afforded (5-methoxy-2-(4,4,5,5-tetramethyl-1,3,2-dioxaborolan-2-yl)phenyl)methanol (**2.75**, 40% yield calculated based on crude weight and  $^1\text{H-NMR}$ ) as an inseparable mixture with impurities which won't affect the next step. In a flame dried round bottom flask equipped with a stir bar, tetrabromomethane (656.6 mg, 1.98 mmol) and crude mixture from the previous step were dissolved in dichloromethane (10 mL). After being cooled to 0 °C, triphenylphosphine (519.3 mg, 1.98 mmol) was added in three portions. The resulting mixture was allowed to warm up to room temperature and stirred for 1 hour. After completion, the reaction mixture was concentrated and added dropwise to an agitated mixture of silica gel (5 g) in hexanes, then passed through a silica plug to remove triphenyl phosphine oxide. The filtrate was concentrated and chromatography on silica gel (5% ethyl acetate in hexanes) afforded 2-(2-(bromomethyl)-4-methoxyphenyl)-4,4,5,5-tetramethyl-1,3,2-dioxaborolane (**2.76**) in 98% yield (573.8 mg) as a white solid.  $^1\text{H-NMR}$  (500 MHz, chloroform- $d$ )  $\delta$  7.76 (d,  $J$  = 8.0 Hz, 1H), 6.92 (s, 1H), 6.81 (d,  $J$  = 11.5 Hz, 1H), 4.89 (s, 2H), 3.82 (s, 3H), 1.35 (s, 12H)

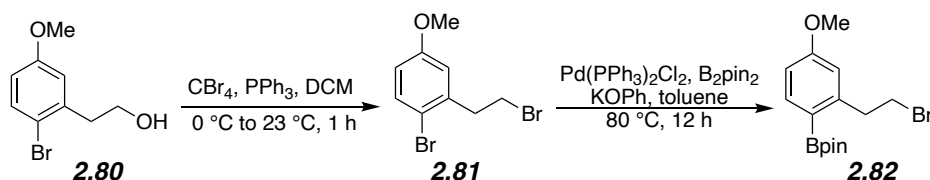


**2-(2-(bromomethyl)-4-methoxyphenyl)trifluoro- $\lambda^4$ -borane, potassium salt (2.77).** In a round bottom flask equipped with a stir bar, 2-(2-(bromomethyl)-4-methoxyphenyl)-4,4,5,5-tetramethyl-1,3,2-dioxaborolane (**2.76**, 241.0 mg, 0.74 mmol) were dissolved in diethyl ether (3 mL). Potassium hydrogen fluoride solution (0.65 mL, 4.5 M in water) was added dropwise. The reaction mixture was then stirred vigorously at room temperature for 2 hours. The mixture was concentrated to dryness under reduced pressure then dissolved in acetone (5 mL). The solution

was filtered, and the solid was washed with acetone (3 x 5 mL). The acetone solution was concentrated to 1 mL, then ether was added until no further precipitation was observed. The crystals were then filtered and washed with ether to yield 2-(2-(bromomethyl)-4-methoxyphenyl)trifluoro- $\lambda^4$ -borane, potassium salt (**2.77**, 86.9 mg, 50% yield) as a white crystal.  $^1\text{H-NMR}$  (400 MHz, acetone- $d_6$ )  $\delta$  7.41 (d,  $J = 11.9$  Hz, 1H), 6.86 (d,  $J = 2.3$  Hz, 1H), 6.59 (d,  $J = 8.2$  Hz, 1H), 4.90 (d,  $J = 6.0$  Hz, 2H), 3.70 (s, 3H).



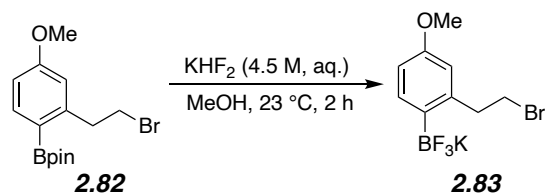
**2-(2-bromo-5-methoxyphenyl)ethan-1-ol (2.79)** was prepared from 3-methoxyphenylacetic acid (**2.77**) following a literature procedure.<sup>18</sup> All spectral data matched literature reports.<sup>18,19</sup>



**2-(2-bromo-5-methoxyphenyl)ethyl bromide (2.81)**. In a flame dried round bottom flask equipped with a stir bar, tetrabromomethane (5.1 g, 13 mmol) and 2-(2-bromo-5-methoxyphenyl)ethan-1-ol (**2.80**, 2.31 g, 10 mmol) were dissolved in dichloromethane (50 mL). After being cooled to 0 °C, triphenylphosphine (3.4 g, 13 mmol) was added in 3 portions. The resulting mixture was allowed to warm to room temperature and stir for 1 hour. After completion, the reaction was concentrated under reduced pressure. Chromatography on silica gel (15% ethyl acetate in hexanes) afforded 2-(2-bromo-5-methoxyphenyl)ethyl bromide (**2.81**) as a mixture

containing a small amount of bromoform. This mixture was used directly in the following step. A single, pure fraction from the column was isolated and characterized, and all spectral data matched the literature reports.<sup>20</sup>

**2-(2-(2-bromoethyl)-4-methoxyphenyl)-4,4,5,5-tetramethyl-1,3,2-dioxaborolane (2.82)** was synthesized by modifying conditions originally reported by Miyaura.<sup>21</sup> In a flame dried round bottom flask the 2-(2-bromo-5-methoxyphenyl)ethyl bromide (**2.81**) mixture from the previous step, bis(pinacolato)diboron (aka B<sub>2</sub>pin<sub>2</sub>, 3.81 g, 15 mmol), bis(tripheynylphosphine)palladium(II) dichloride (210.6 mg, 0.3 mmol), and potassium phenolate (1.98 g, 15 mmol) were dissolved in toluene (60 mL). The reaction mixture was degassed for 10 minutes before being heated up to 80 °C then stirred for 12 hours. Water (100 mL) was added, and the reaction mixture was extracted with Et<sub>2</sub>O (3 x 20 mL). The combined organic layers were washed with 1 M aqueous sodium hydroxide solution (30 mL), brine (100 mL), then dried over anhydrous magnesium sulfate. The solution was concentrated under reduced pressure. The crude mixture was purified by chromatography on silica gel (2-5% ethyl acetate in hexanes) to yield 2-(2-(2-bromoethyl)-4-methoxyphenyl)-4,4,5,5-tetramethyl-1,3,2-dioxaborolane (**2.82**) (1.94 g, 57% yield over 2 steps) as a white solid. **<sup>1</sup>H-NMR** (400 MHz, chloroform-d) δ 7.76 (d, *J* = 8.2 Hz, 1H), 6.79-6.73 (m, 2H), 3.81 (s, 3H), 3.54 (t, *J* = 7.6 Hz, 2H), 3.39 (t, *J* = 7.8 Hz, 2H), 1.33 (s, 12H). **<sup>13</sup>C-NMR** (126 MHz, chloroform-d) δ 161.9, 148.0, 138.5, 116.0, 111.5, 83.5, 55.2, 39.8, 34.5, 24.9. **<sup>11</sup>B-NMR** (160 MHz, chloroform-d) δ 29.9. **IR** 2975, 2933, 2836, 1602, 1587, 1366, 1239, 1162, 1074, 964, 926, 892, 858, 753, 658, 595, 584, 457 cm<sup>-1</sup>. **HRMS-Cl** *m/z* calcd. for C<sub>15</sub>H<sub>22</sub><sup>11</sup>B<sup>79</sup>BrO<sub>3</sub> [M]<sup>+</sup> 340.0845, found 340.0859; calcd. for C<sub>15</sub>H<sub>22</sub><sup>11</sup>B<sup>81</sup>BrO<sub>3</sub> [M]<sup>+</sup> 342.0825, found 342.0850.



**(2-(2-bromoethyl)-4-methoxyphenyl)trifluoro- $\lambda^4$ -borane, potassium salt (2.83).** In a round bottom flask equipped with a stir bar, 2-(2-(2-bromoethyl)-4-methoxyphenyl)-4,4,5,5-tetramethyl-1,3,2-dioxaborolane (**2.82**, 1.36 g, 4 mmol) was dissolved in methanol (50 mL). Potassium hydrogen fluoride solution (3.6 mL, 4.5 M in water) was added dropwise. The reaction mixture was then stirred vigorously at room temperature for 2 hours. The mixture was concentrated to dryness under reduced pressure then dissolved in acetone (20 mL). The solution was filtered, and the solid was washed with acetone (3 x 10 mL). The acetone solution was concentrated to 5 mL then hexanes was added until there's no more solid crashing out from the solution. The crystal was then filtered and washed with hexanes to yield (2-(2-bromoethyl)-4-methoxyphenyl)trifluoro- $\lambda^4$ -borane, potassium salt (**2.83**) (1.27 g, 99% yield) as a white crystal.  **$^1\text{H-NMR}$**  (400 MHz, acetone- $d_6$ )  $\delta$  7.41 (d,  $J = 8.2$  Hz, 1H), 6.62 (s, 1H), 6.56 (d,  $J = 8.2$  Hz, 1H), 3.69 (s, 3H), 3.62 (t,  $J = 8.2$  Hz, 2H), 3.26 (t,  $J = 8.0$  Hz, 2H).  **$^{13}\text{C-NMR}$**  (101 MHz, acetone- $d_6$ )  $\delta$  156.8, 142.1, 132.4, 113.1, 108.8, 52.8, 38.9, 33.6.  **$^{11}\text{B-NMR}$**  (128 MHz, acetone- $d_6$ )  $\delta$  1.6, 1.3.  **$^{19}\text{F-NMR}$**  (376 MHz, acetone- $d_6$ )  $\delta$  -138.6. **IR** 2940, 2836, 1597, 1558, 1484, 1451, 1288, 1241, 1129, 1042, 1009, 920, 870, 842, 767, 669, 599, 522  $\text{cm}^{-1}$ . **HRMS-ESI  $m/z$**  calcd. for  $\text{C}_9\text{H}_{10}^{11}\text{B}^{79}\text{BrF}_3\text{O} [\text{M}]^-$  280.9967, found 280.9967; calcd. for  $\text{C}_9\text{H}_{10}^{11}\text{B}^{81}\text{BrF}_3\text{O} [\text{M}]^-$  282.9947, found 282.9948

## 2.8 Bibliography

1. For information regarding Wittig reaction and Corey ylides see Kürti, L.; Czako, B. Strategic Applications of Named Reactions in Organic Synthesis. Elsevier, Burlington, MA, USA, 2005.

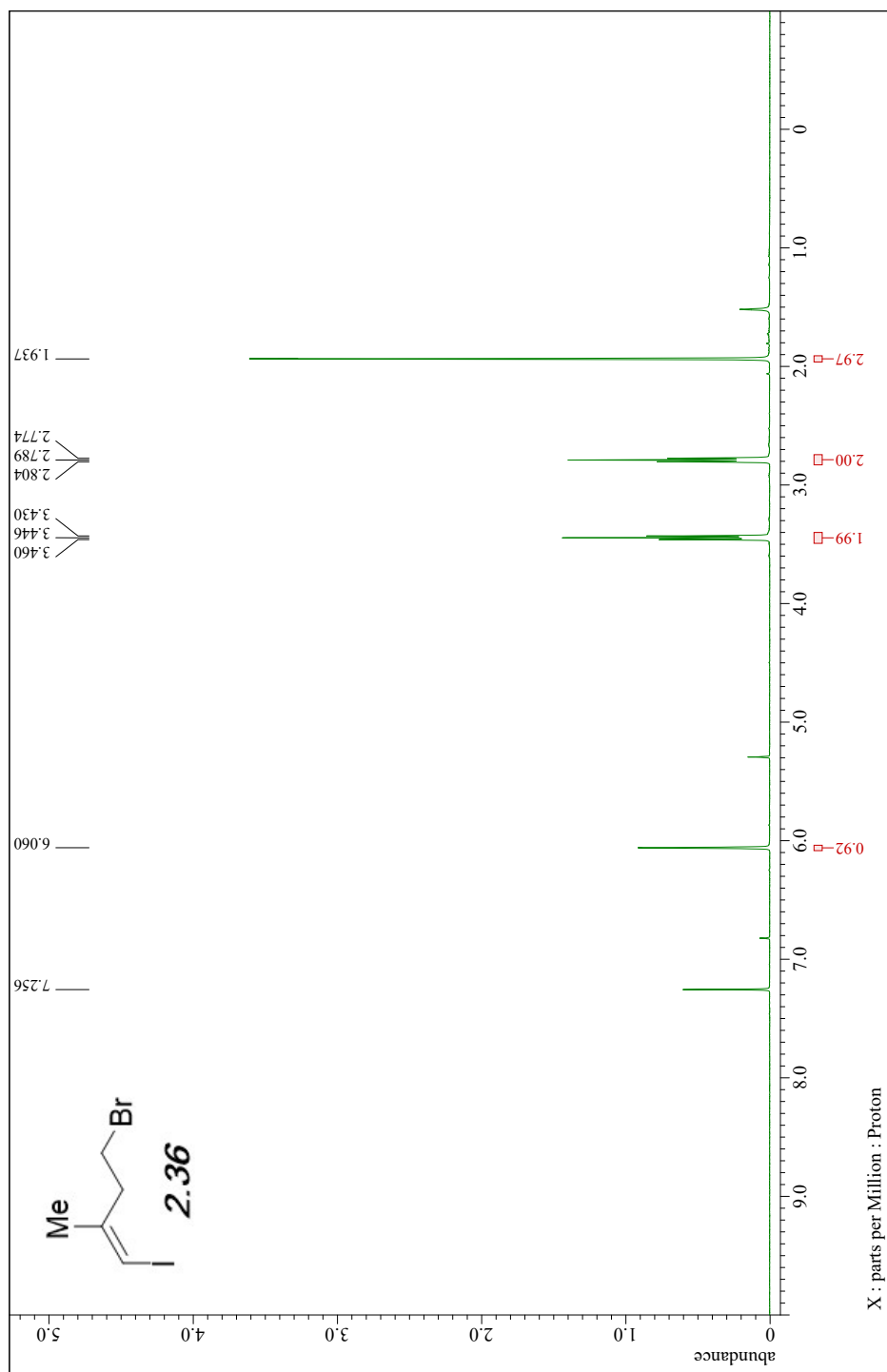
2. For reviews on 1,3-dipole cycloadditions, see a) Hashimoto, T.; Maruoka, K. Recent Advances of Catalytic Asymmetric 1,3-Dipolar Cycloadditions. *Chem. Rev.* **2015**, *115*, 5366–5412; b) Gothelf, K. V.; Jørgensen, K. A. Asymmetric 1,3-Dipolar Cycloaddition Reactions. *Chem. Rev.* **1998**, *98*, 863–910.
3. Thien S. Nguyen, Michelle S. Yang, Jeremy A. May. Experimental mechanistic insight into the BINOL-catalyzed enantioselective conjugate addition of boronates to enones. *Tetrahedron Lett.* **2015**, *56*, 3337-3341.
4. Trost, B. M.; Dogra, K. Synthesis of (–)- $\Delta^9$ -trans-Tetrahydrocannabinol: Stereocontrol via Mo-Catalyzed Asymmetric Allylic Alkylation Reaction. *Org. Lett.* **2007**, *9*, 861–863.
5. Schafroth, M. A.; Zuccarello, G.; Krautwald, S.; Sarlah, D.; Carreira, E. M. Stereodivergent Total Synthesis of  $\Delta^9$ -Tetrahydrocannabinols. *Angew. Chem. Int. Ed.* **2014**, *53*, 13898–13901.
6. Shultz, Z. P.; Lawrence, G. A.; Jacobson, J. M.; Cruz, E. J.; Leahy, J. W. Enantioselective Total Synthesis of Cannabinoids—A Route for Analogue Development. *Org. Lett.* **2018**, *20*, 381–384.
7. Ma, S.; Negishi, E. Anti-Carbometalation of Homopropargyl Alcohols and Their Higher Homologues via Non-Chelation-Controlled Syn-Carbometalation and Chelation-Controlled Isomerization. *J. Org. Chem.* **1997**, *62*, 784–785.
8. Please see Experimental Section for detail.
9. Fritzeimer, R. G.; Medici, E. J.; Szwetkowski, C.; Wonilowicz, L. G.; Sibley, C. D.; Slobodnick, C.; Santos, W. L. Route to Air and Moisture Stable  $\beta$ -Difluoroboryl Acrylamides. *Org. Lett.* **2019**, *21*, 8053-8057.
10. Molloy, J. J.; Schäfer, M.; Wienhold, M.; Morack, T.; Daniliuc, C. G.; Gilmour, R. Boron-Enabled Geometric Isomerization of Alkenes via Selective Energy-Transfer Catalysis. *Science.* **2020**, *369*, 302-306.

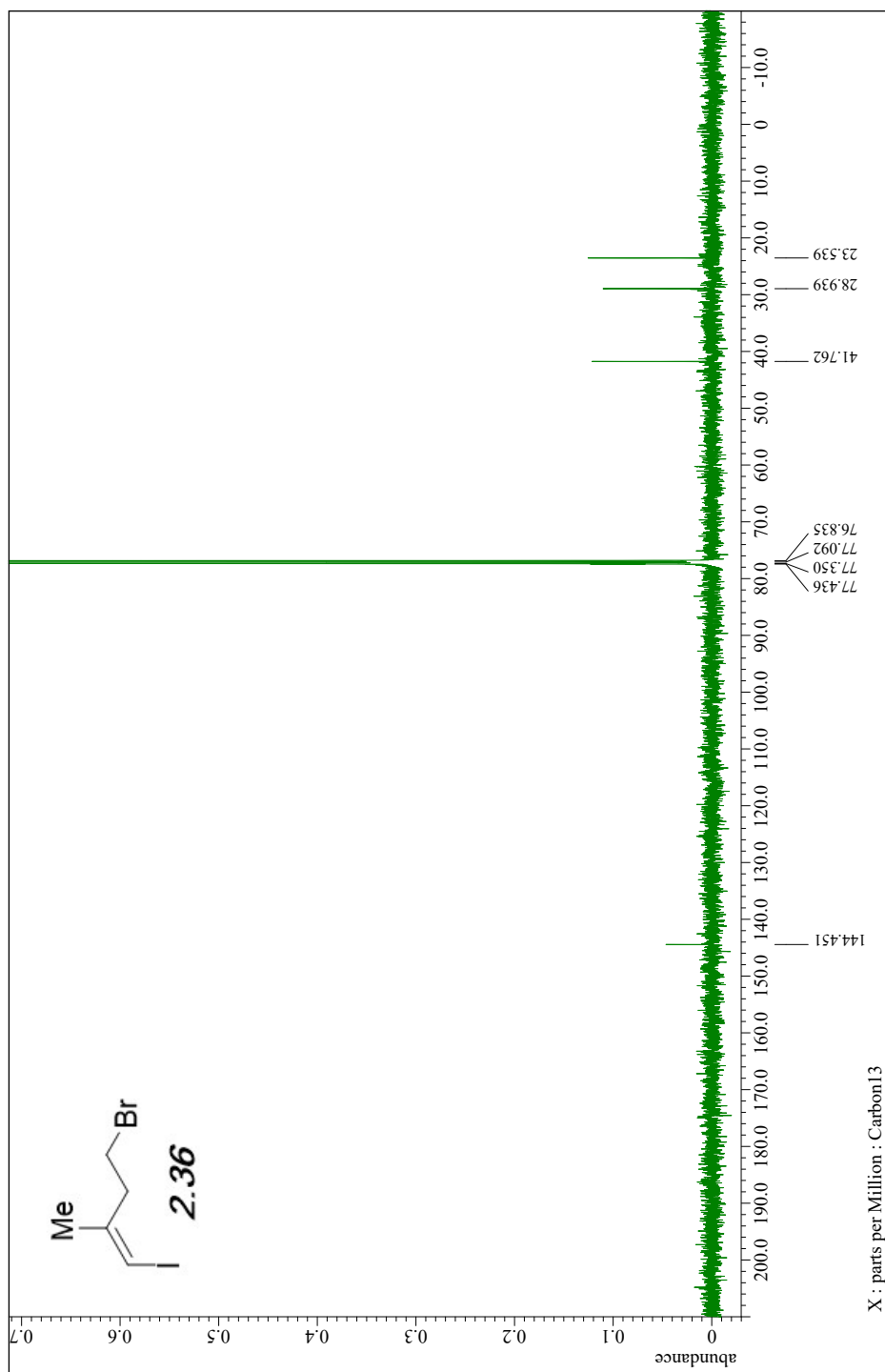
11. Bhunia, S.; Ghorpade, S.; Huple, D. B.; Liu, R.-S. Gold-Catalyzed Oxidative Cyclizations of *cis*-3-En-1-yne to Form Cyclopentenone Derivatives. *Angew. Chem. Int. Ed.* **2012**, *51*, 2939-2942.
12. Adams, H.; Gilmore, N. J.; Jones, S.; Muldowney, M. P.; von Reuss, S. H.; Vemula, R. Asymmetric Synthesis of Corsifuran A by an Enantioselective Oxazaborolidine Reduction. *Org. Lett.* **2008**, *10*, 1457-1460.
13. Takagi, J.; Takahashi, K.; Ishiyama, T.; Miyaura, N. Palladium-Catalyzed Cross-Coupling Reaction of Bis(pinacolato)diboron with 1-Alkenyl Halides or Triflates: Convenient Synthesis of Unsymmetrical 1,3-Dienes via the Borylation-Coupling Sequence. *J. Am. Chem. Soc.* **2002**, *124*, 8001–8006.
14. Iwai, T.; Ueno, M.; Okochi, H.; Sawamura, M. Synthesis of Cyclobutene-Fused Eight-Membered Carbocycles through Gold-Catalyzed Intramolecular Enyne [2+2] Cycloaddition. *Adv. Synth. Catal.* **2018**, *360*, 670–675.
15. Spino, C.; Rezaei, H.; Dupont-Gaudet, K.; Belanger, F. Inter- and Intramolecular [4+1]-Cycloadditions Between Electron-Poor Dienes and Electron-Rich Carbenes. *J. Am. Chem. Soc.* **2004**, *126*, 9926–9927.
16. Walsh, J. G.; Furlong, P. J.; Byrne, L. A.; Gilheany, D. G. Studies in the Oxidative Ring-Opening of Catachols and *o*-Benzoquinones. Lead Tetraacetate Versus the Copper(I) Chloride/Pyridine/Methanol System. *Tetrahedron*, **1999**, *55*, 11519–11536.
17. Zheng, J.-S.; Chang, H.-N.; Wang, F.-L.; Liu, L. Fmoc Synthesis of Peptide Thioesters without Post-Chain-Assembly Manipulation. *J. Am. Chem. Soc.* **2011**, *133*, 11080–11083.
18. Adams, H.; Gilmore, N. J.; Jones, S.; Muldowney, M. P.; von Reuss, S. H.; Vemula, R. Assymmetric Synthesis of Corsifuran A by an Enantioselective Oxazaborolidine Reduction. *Org. Lett.* **2008**, *10*, 1457–1460.

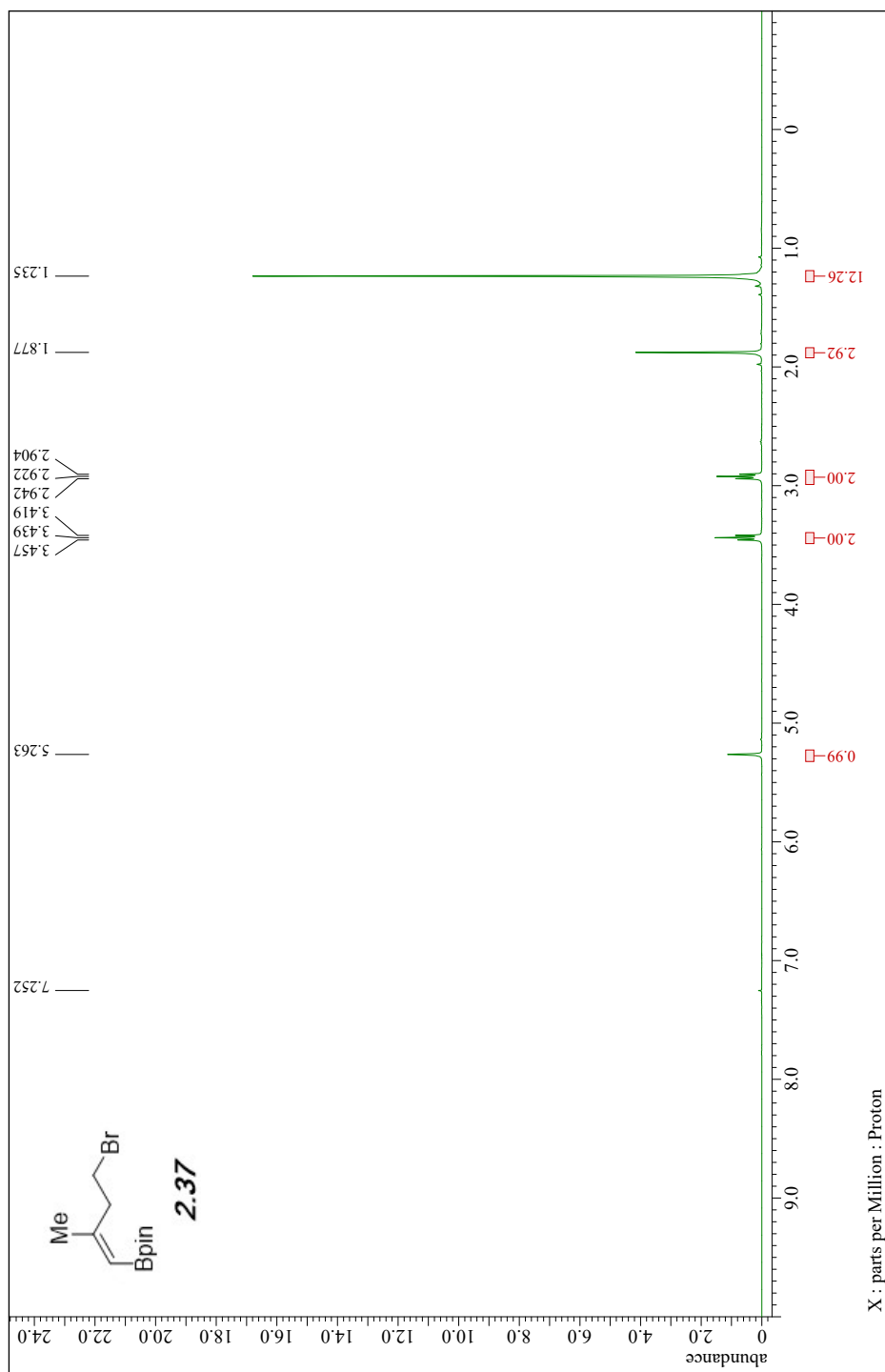
19. Snyder, L.; Meyers, A. I. Synthesis of Enantiomerically Pure Hydrinden-2-ones and Benz[e]inden-2-ones via Asymmetric Alkylations of Chiral Bicyclic Lactams. *J. Org. Chem.* **1993**, *58*, 7507–7515.
20. Ghosh, A. K.; Mukhopadhyaya, J. K.; Ghatak, U. R. Regioselective Aryl Radical Cyclisation. Part 2.1 Synthesis of Octahydro-1H-dibenzo[a,d]cycloheptenes Through 7-Endo Ring Closure. *J. Chem. Soc., Perkin Trans. 1*, **1997**, 2747–2756.
21. Ishiyama, T.; Murata, M.; Miyaura, N. Palladium(0)-Catalyzed Cross-Coupling Reaction of Alkoxydiboron with Haloarenes: A Direct Procedure for Arylboronic Ester. *J. Org. Chem.* **1995**, *60*, 7508–7510.

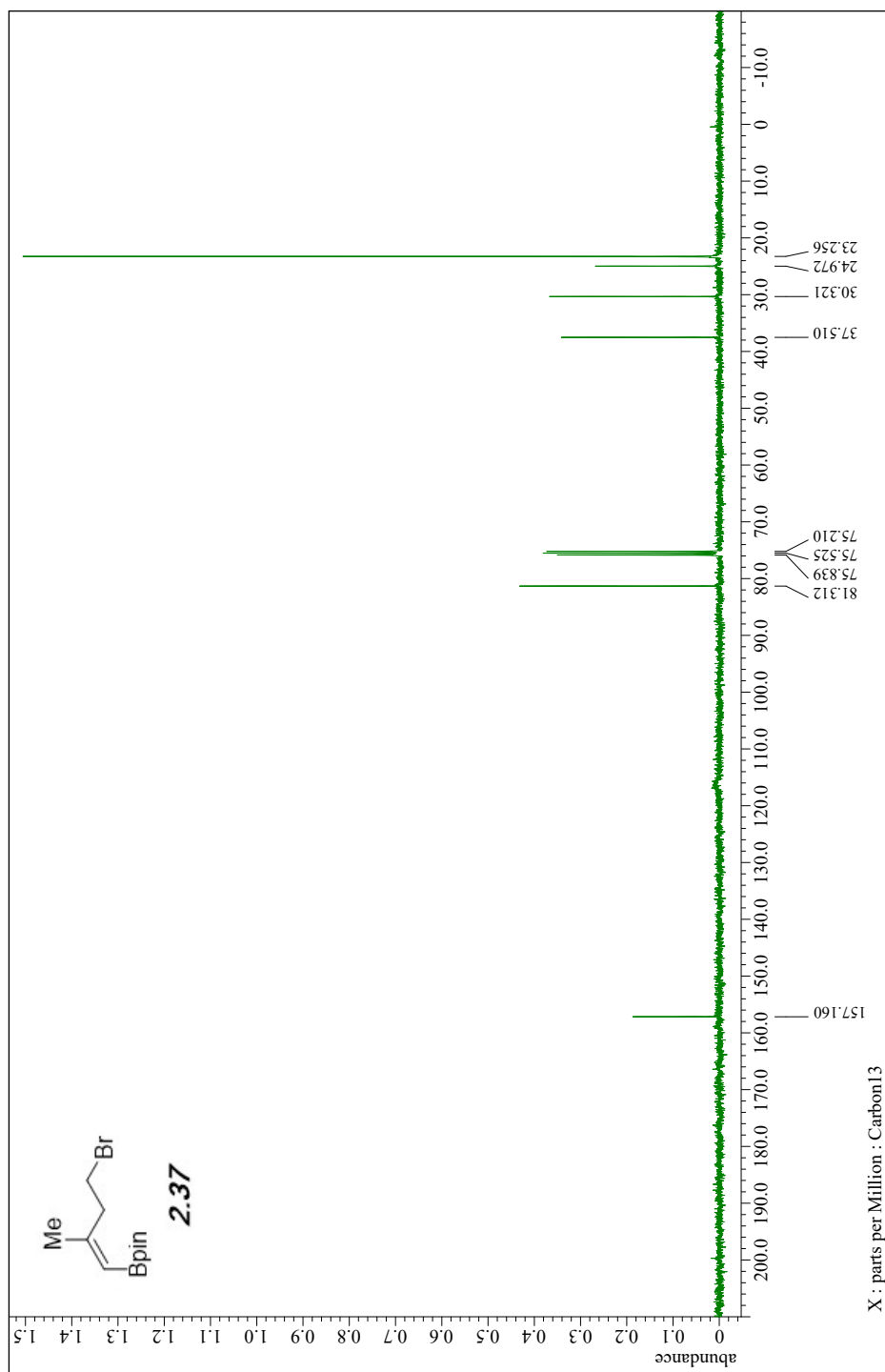
## **Chapter 2**

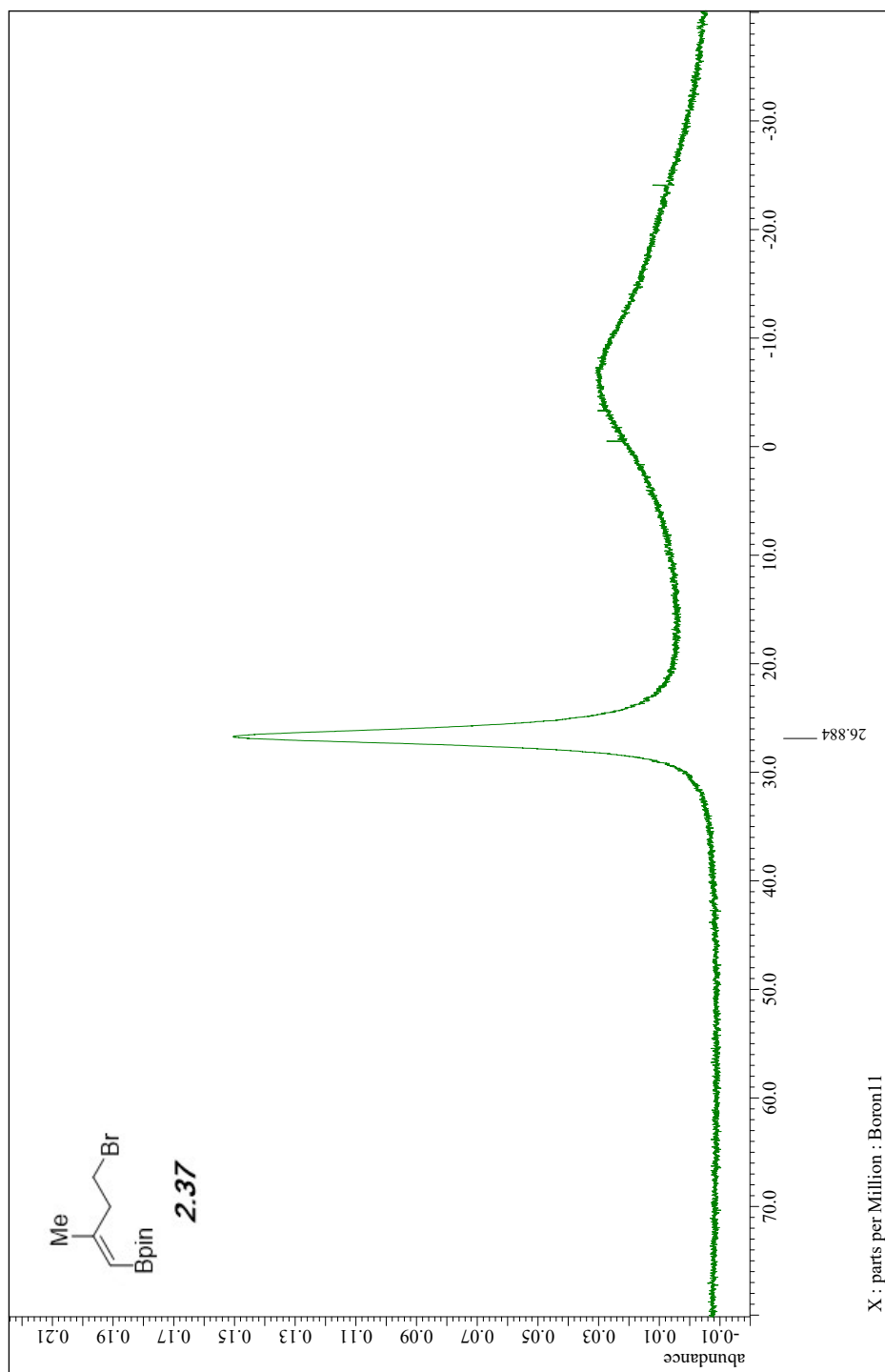
## **Appendix**



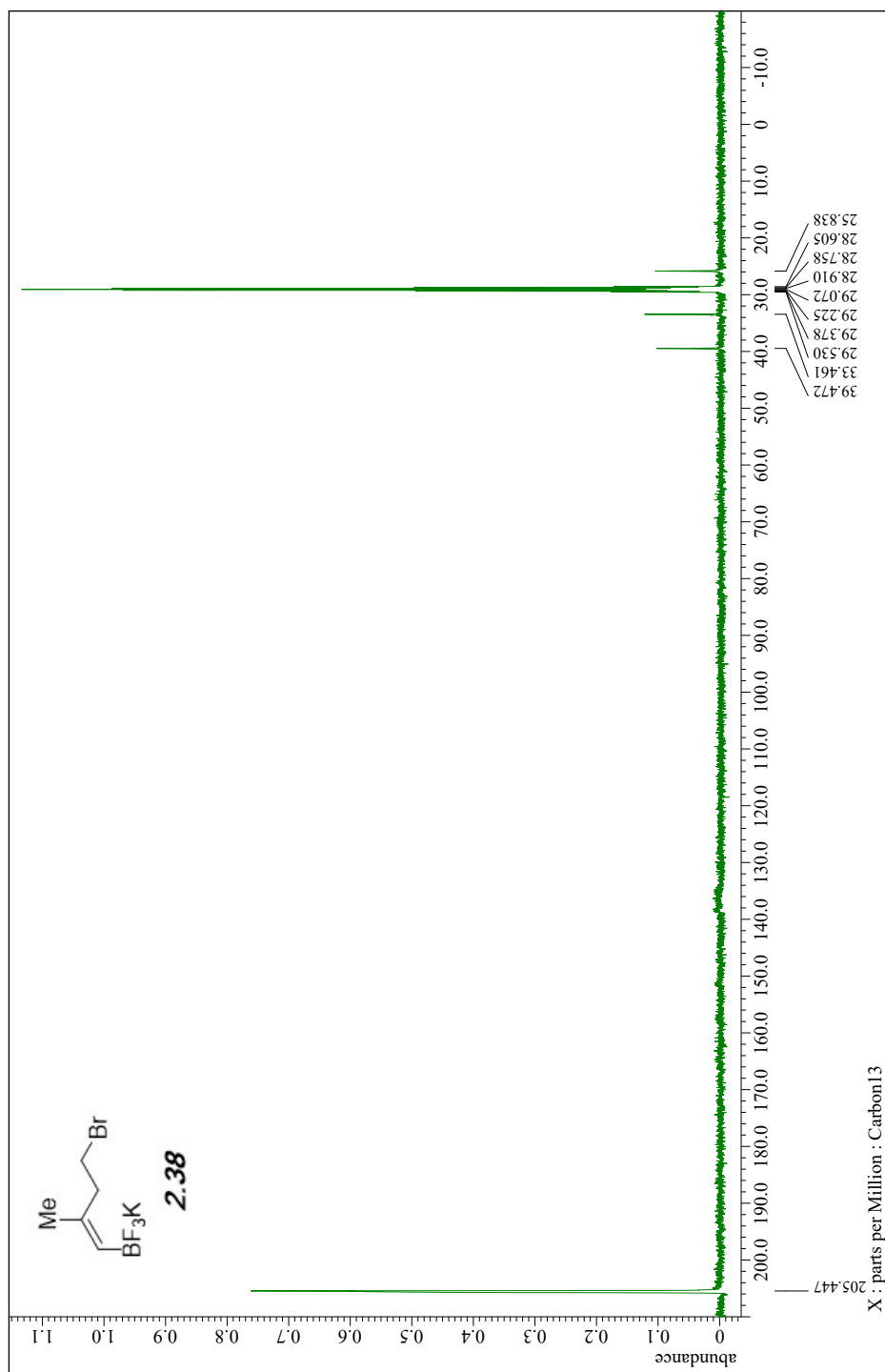


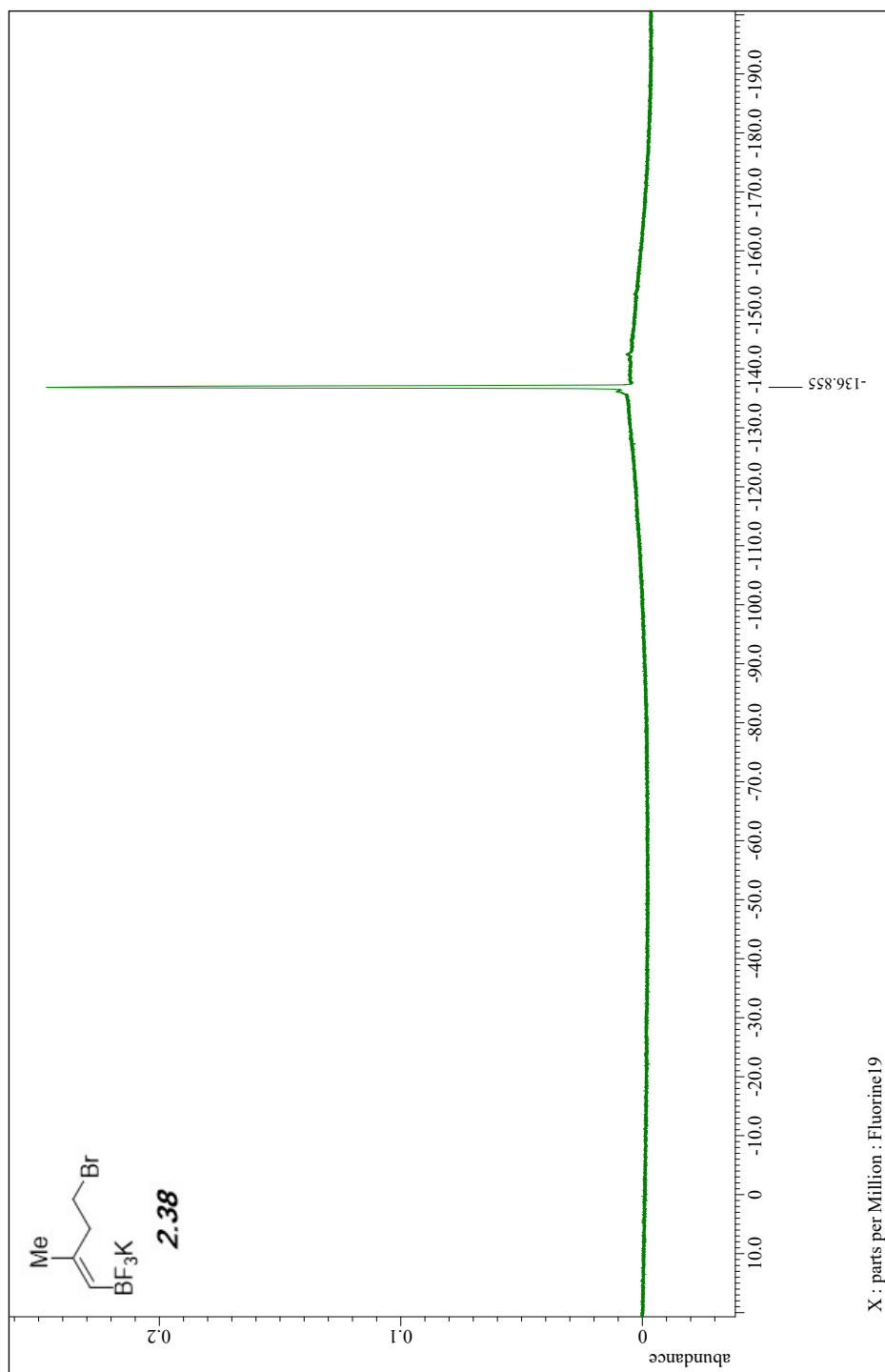


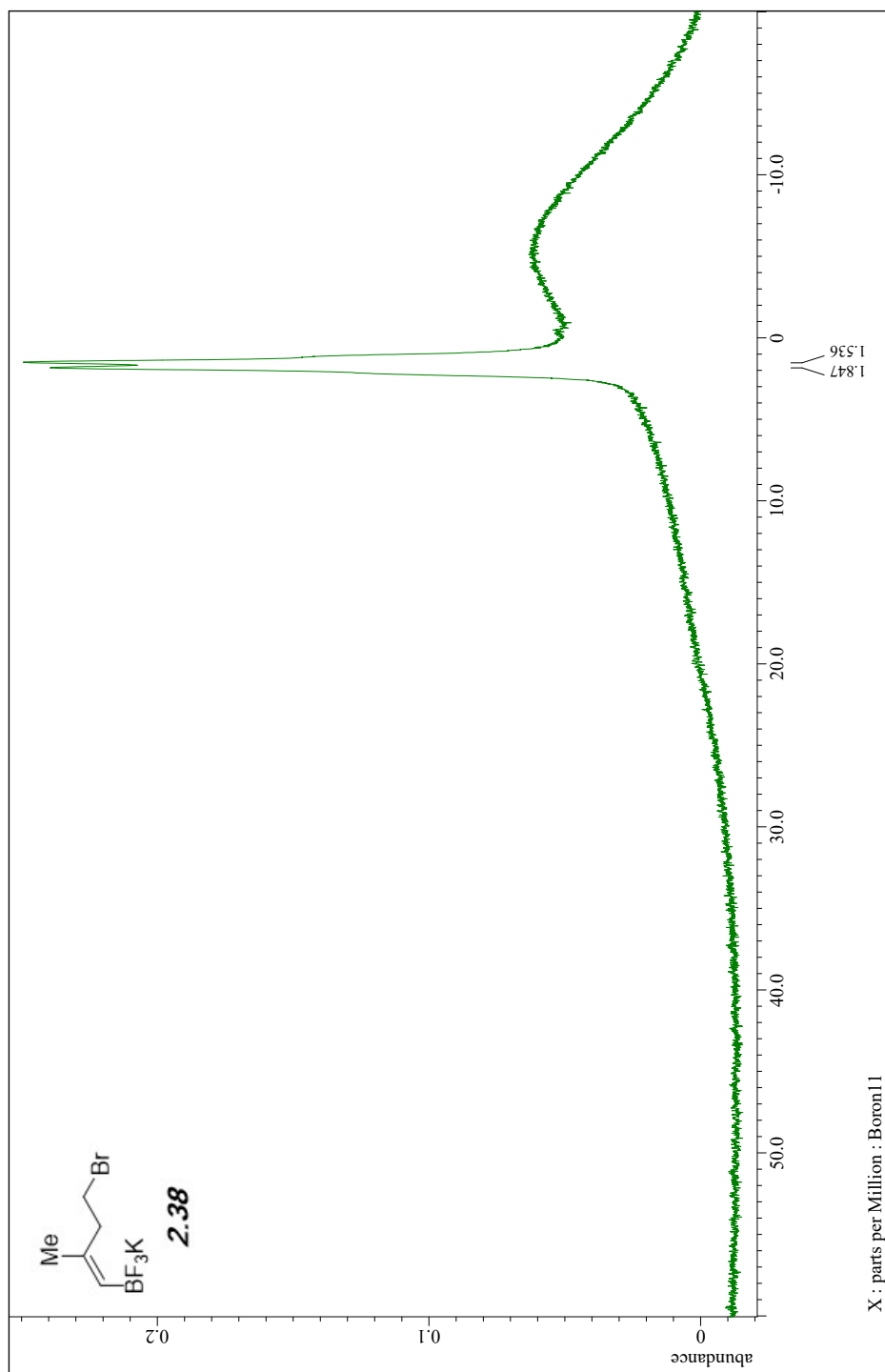


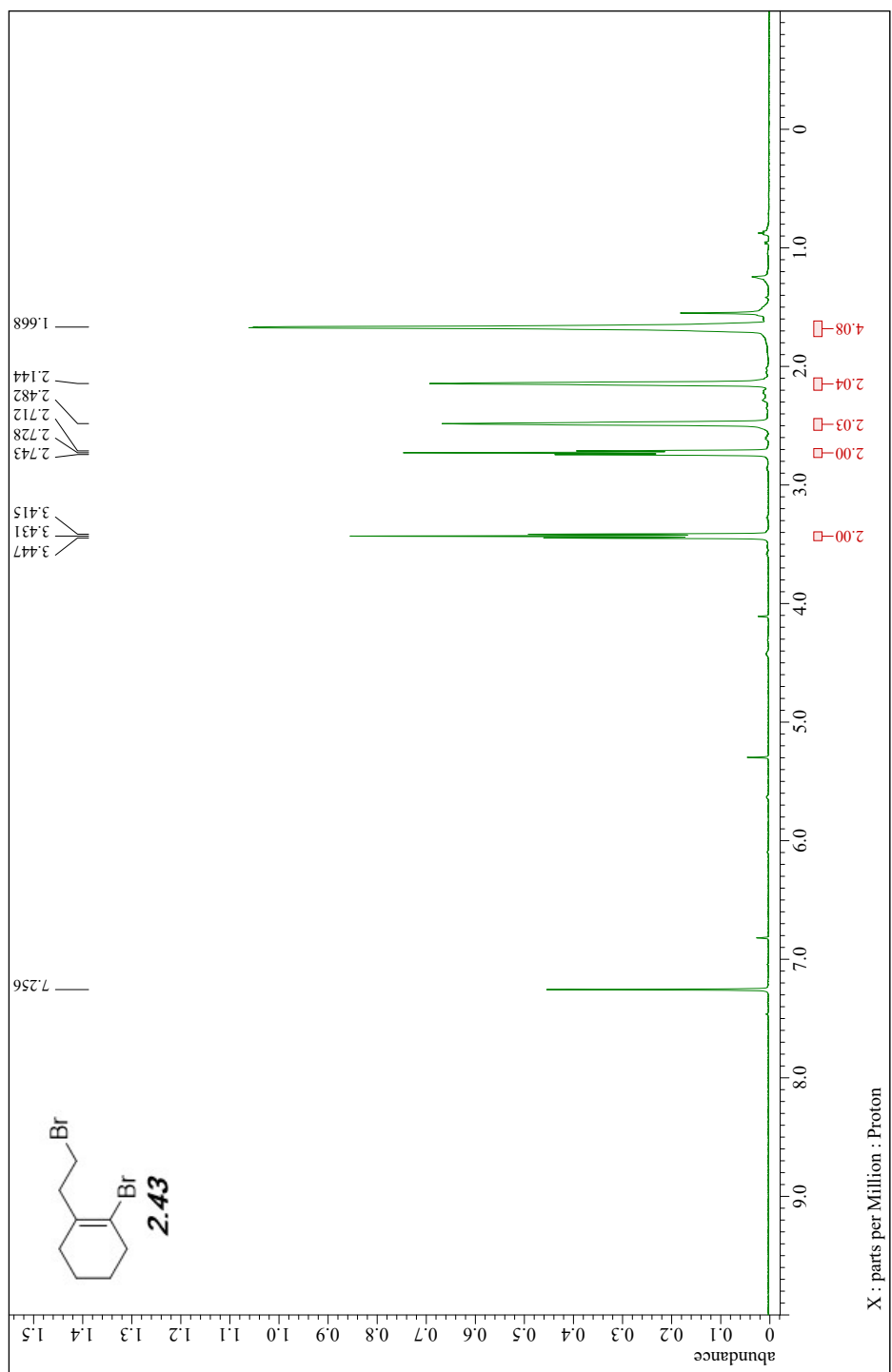


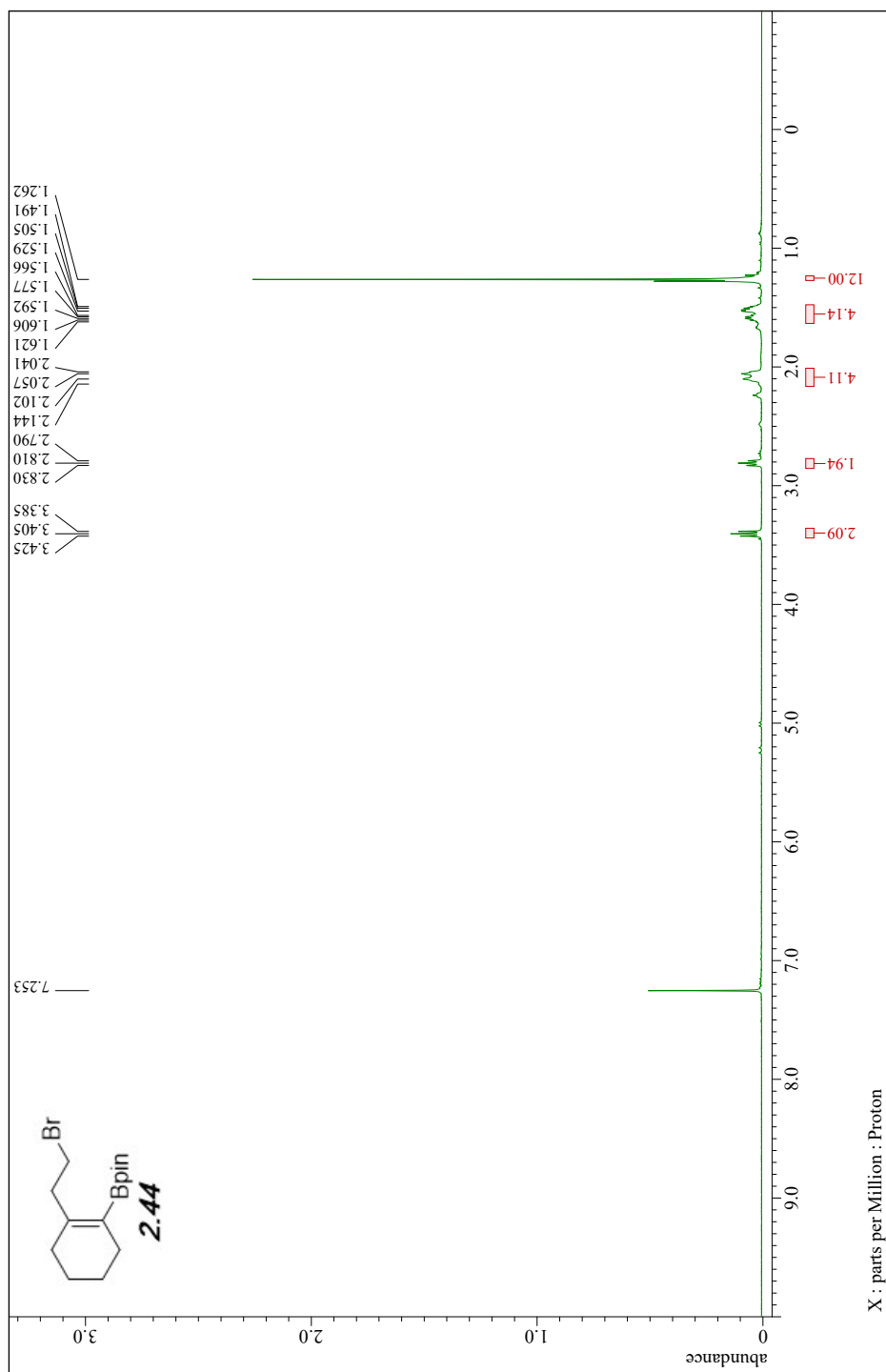


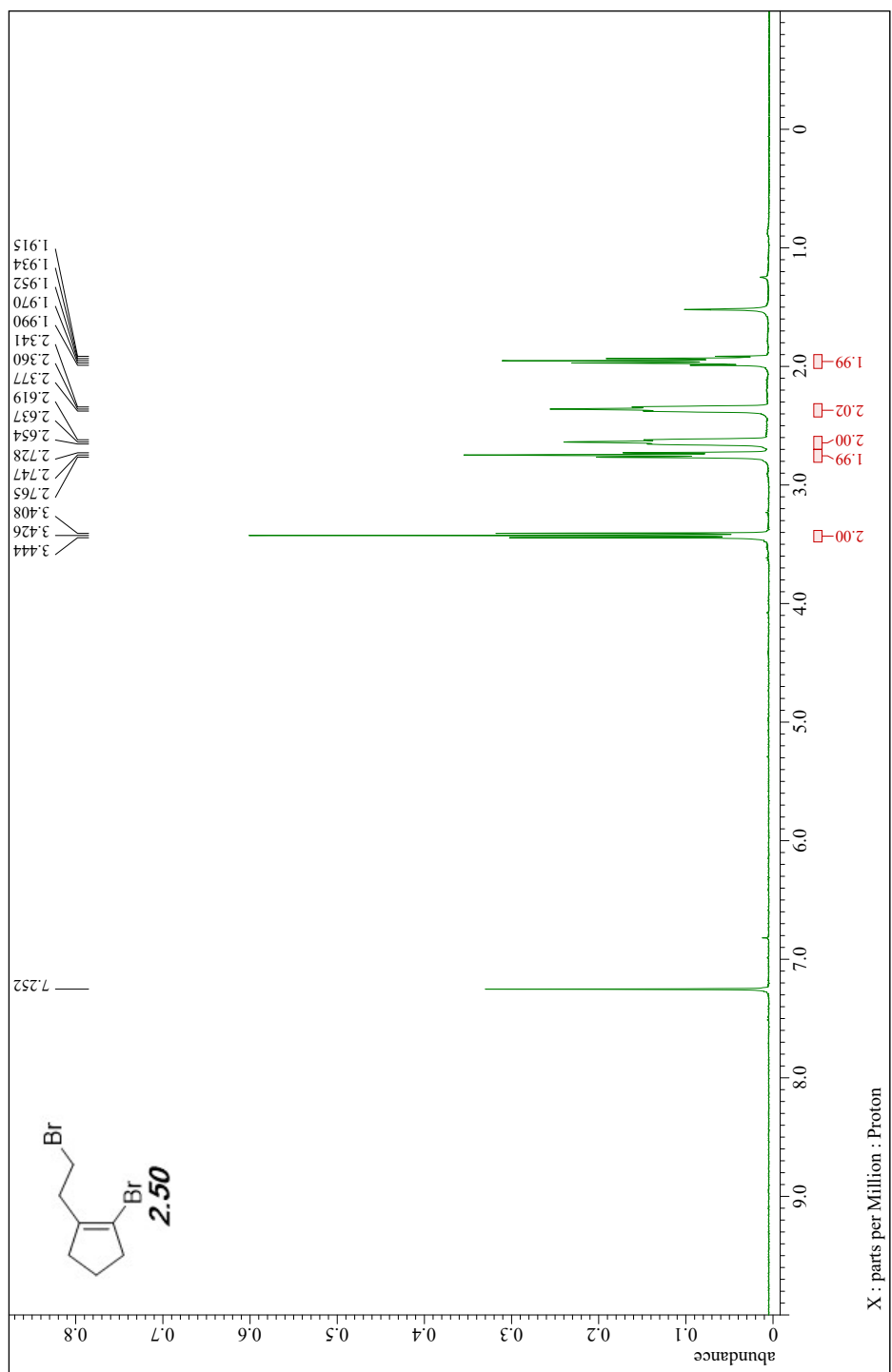


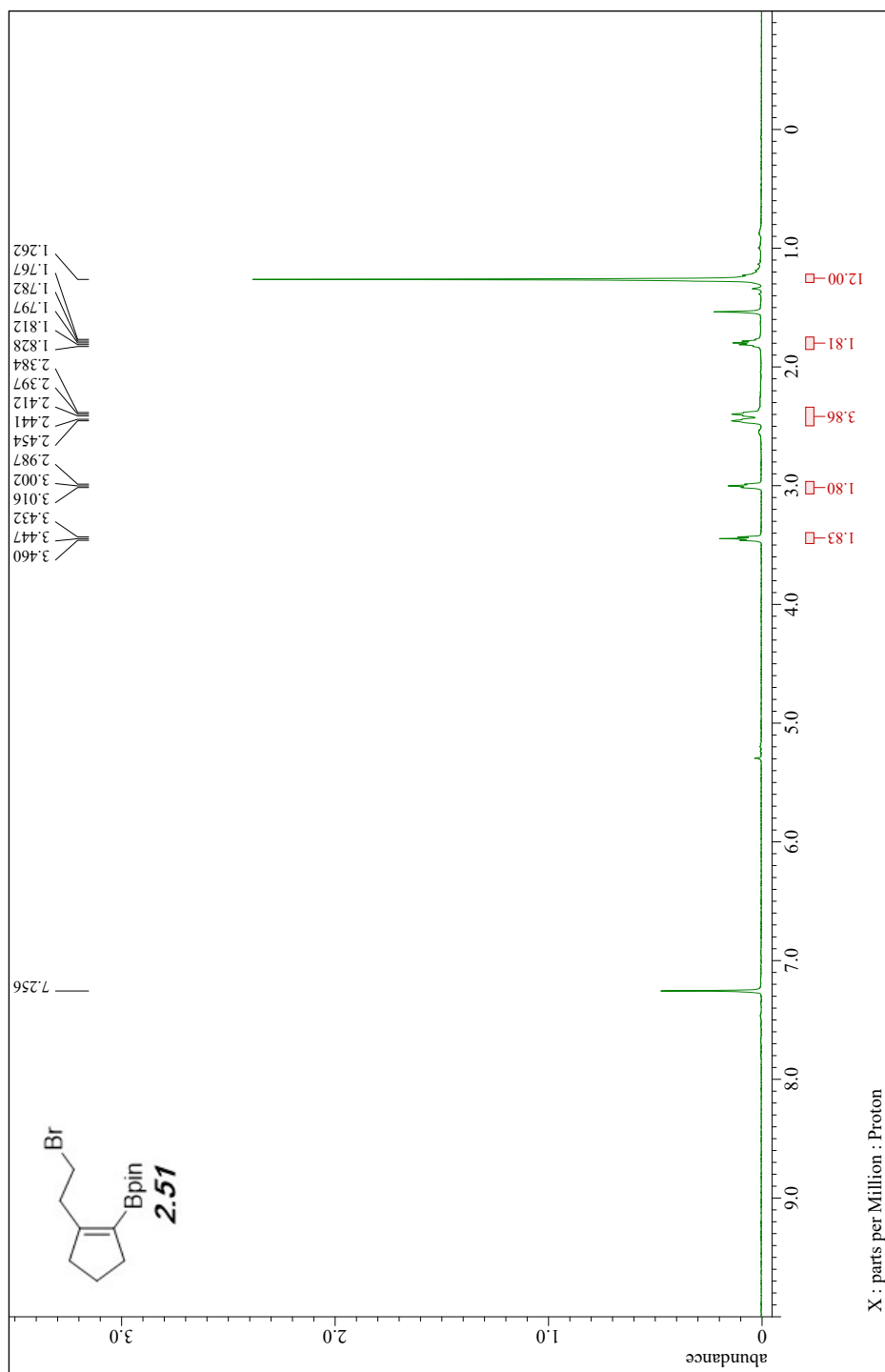


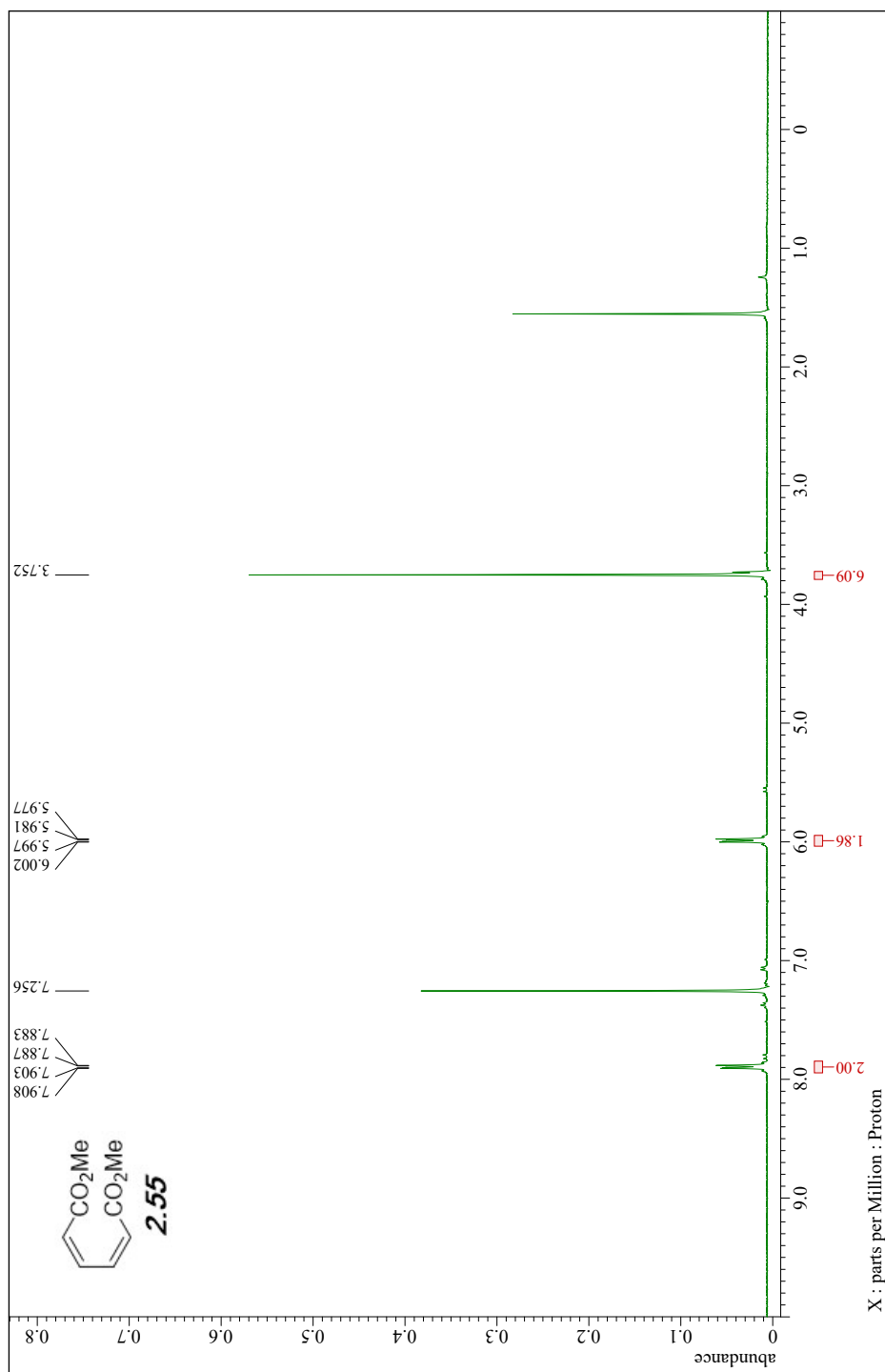


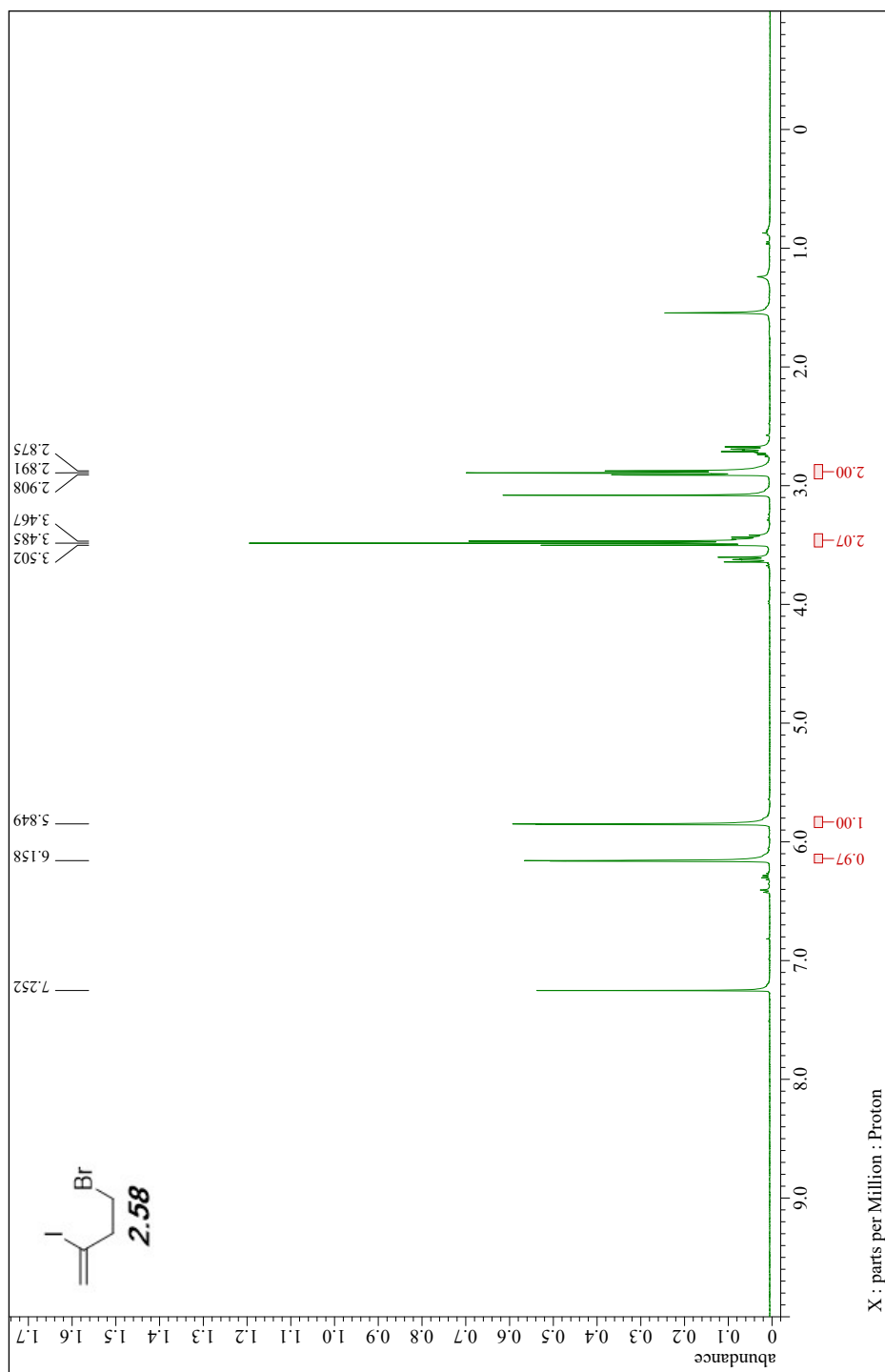


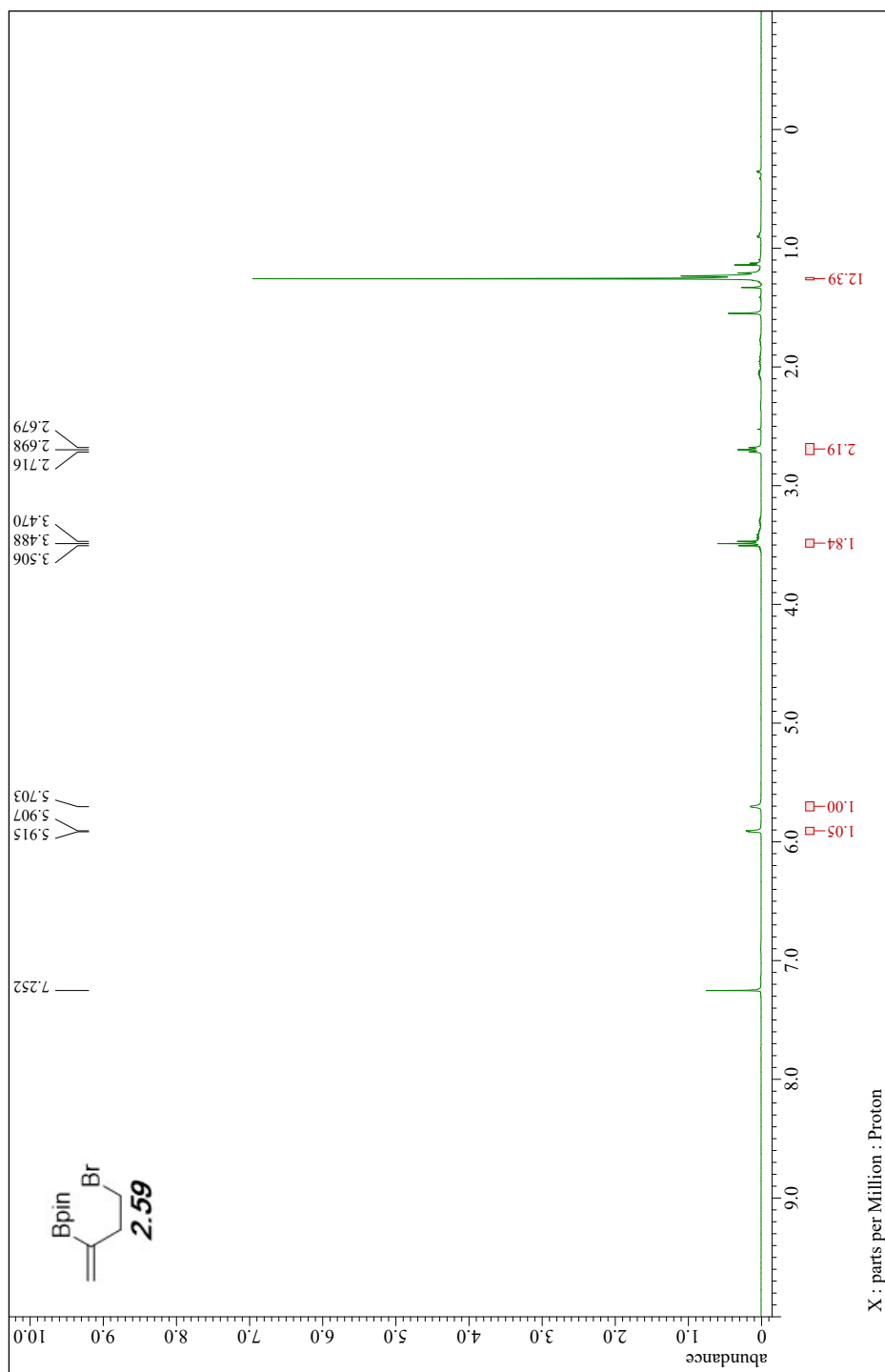


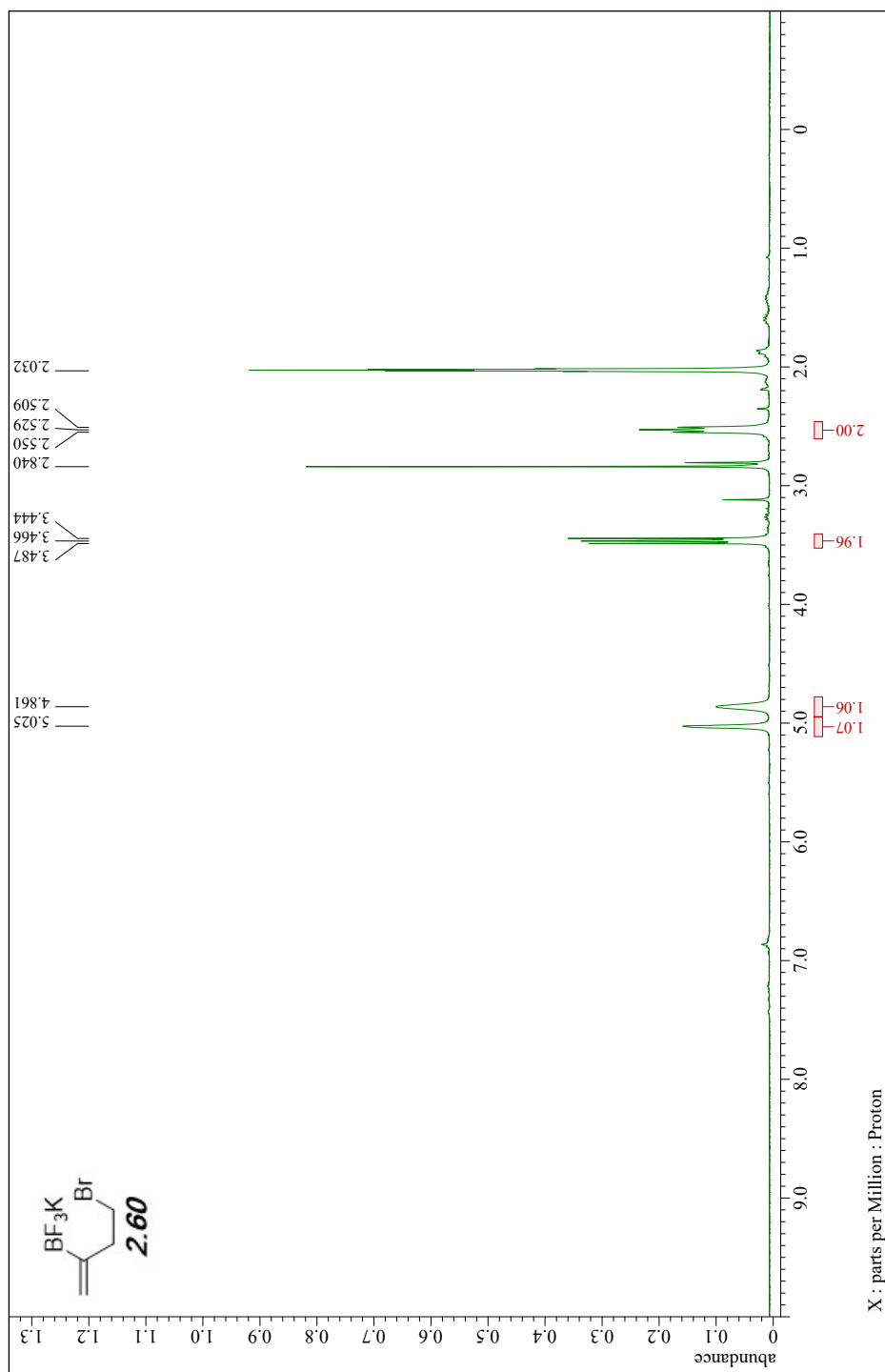


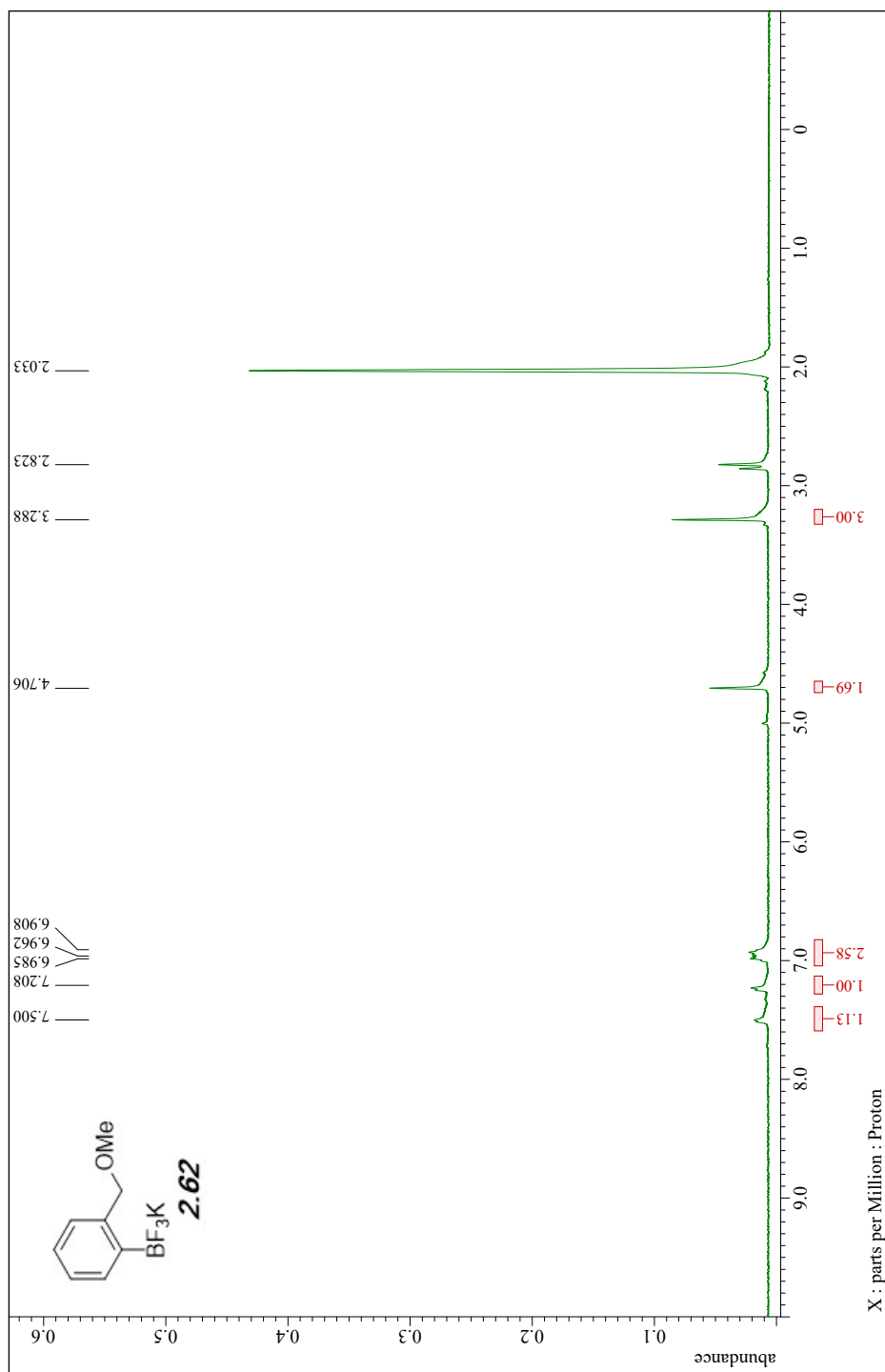


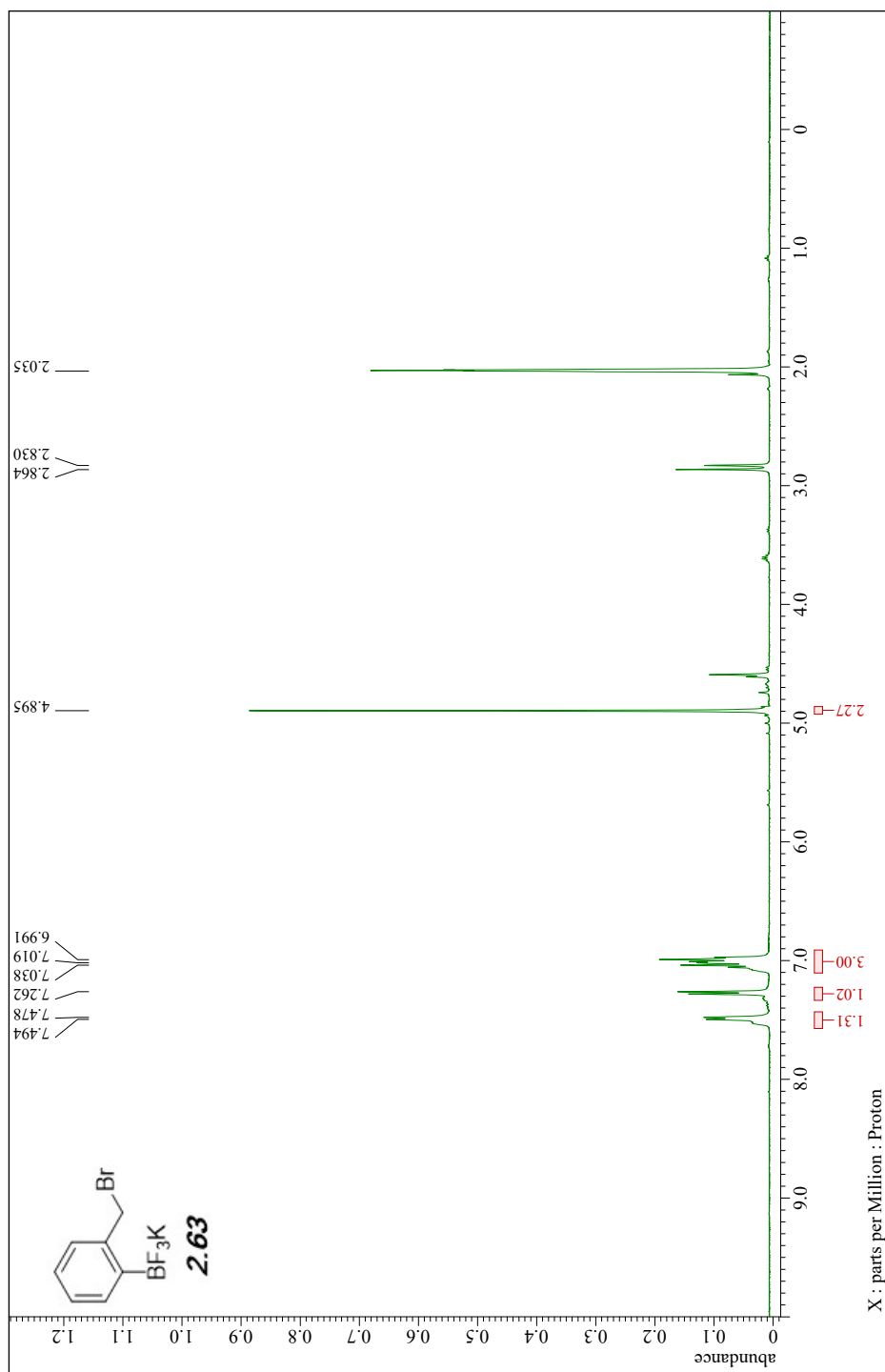


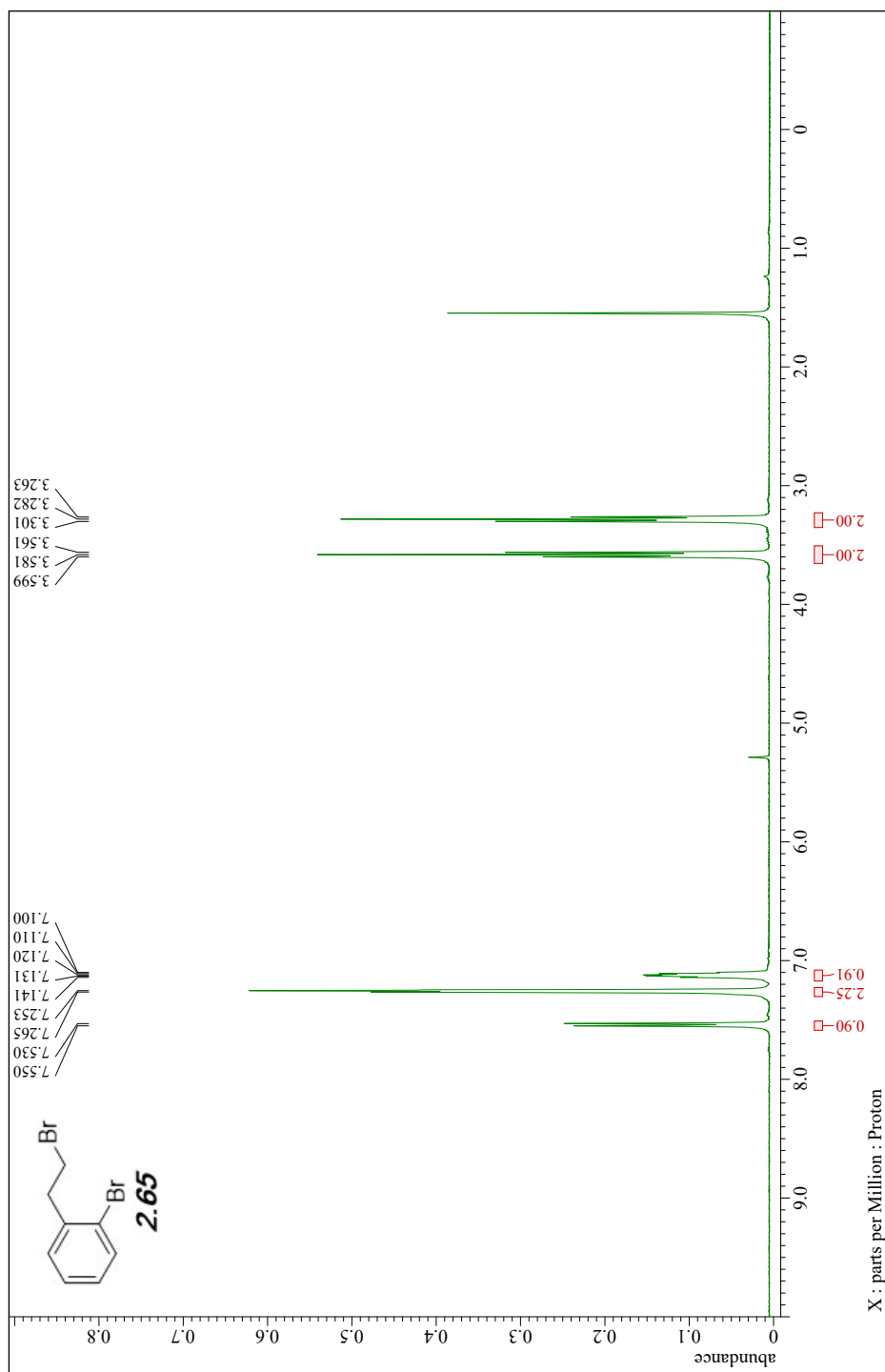


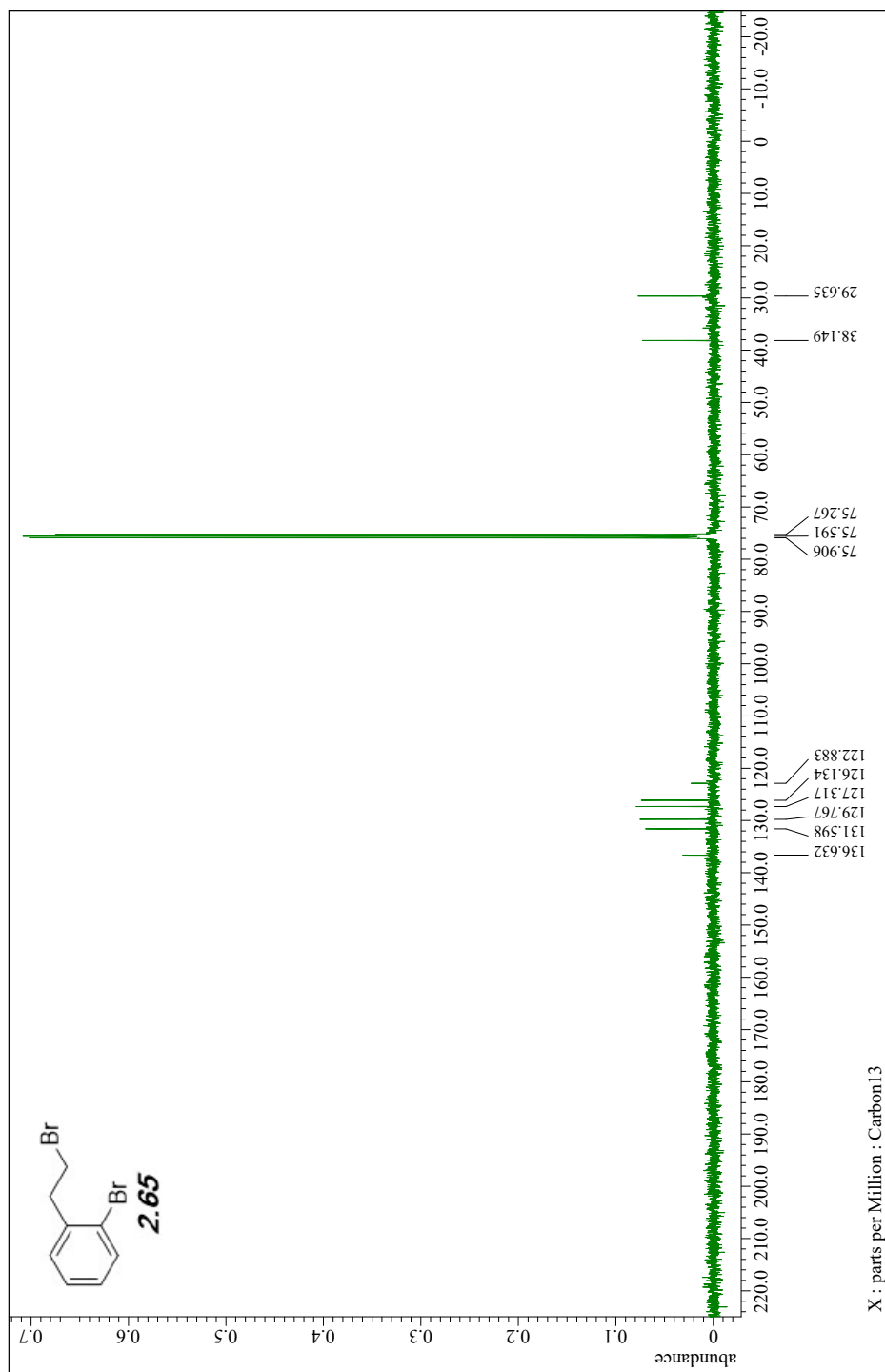


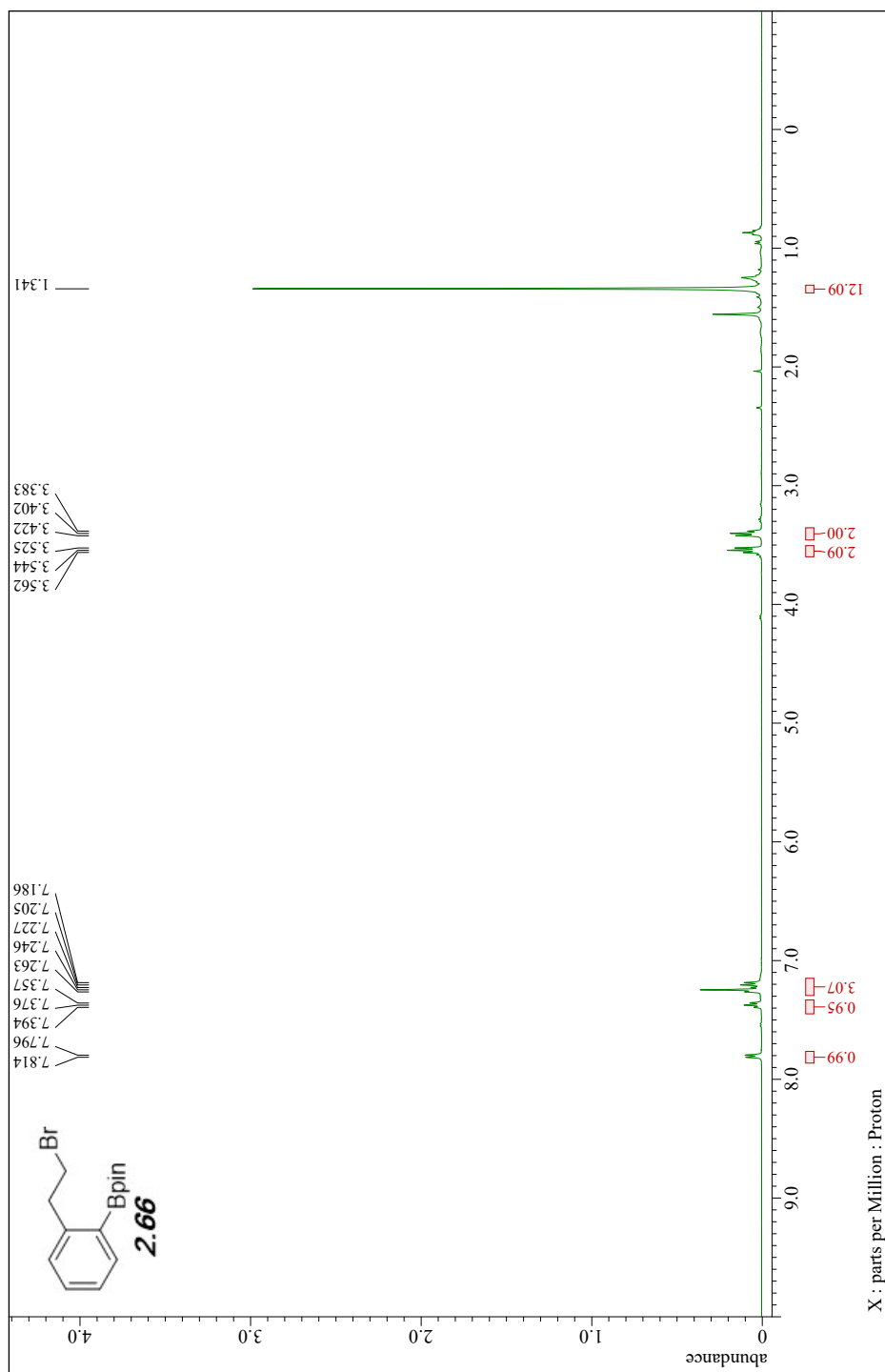


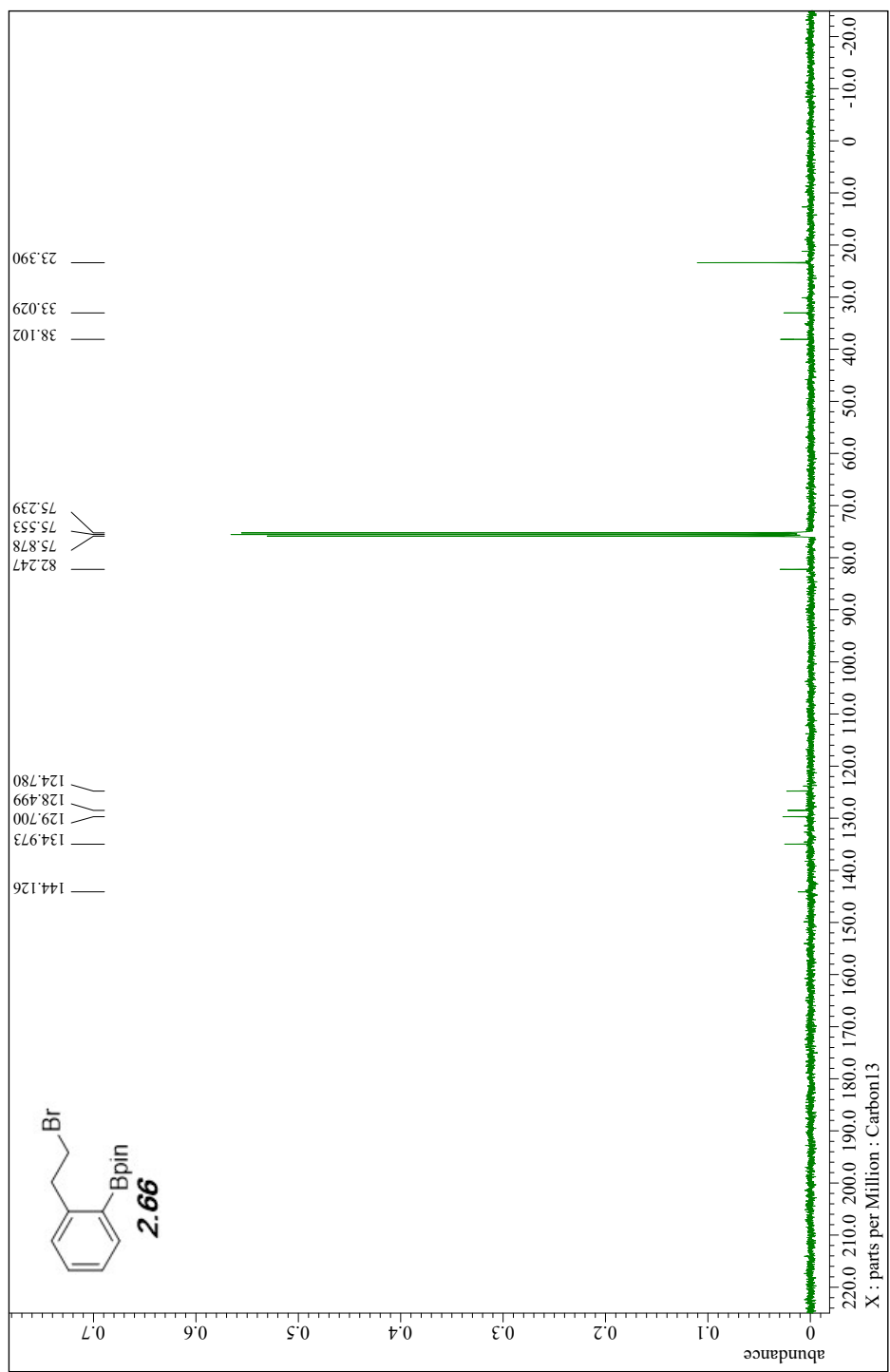


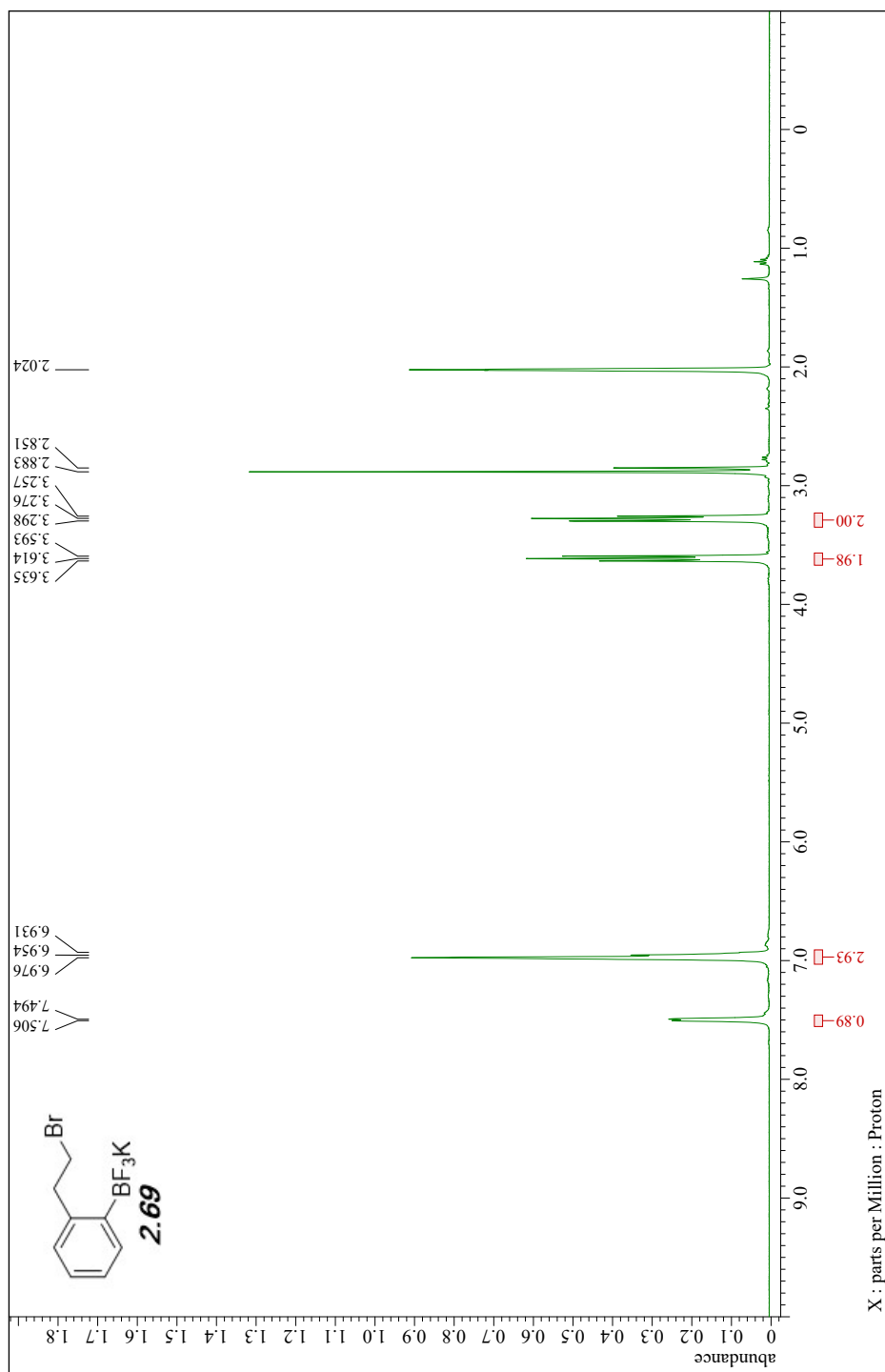


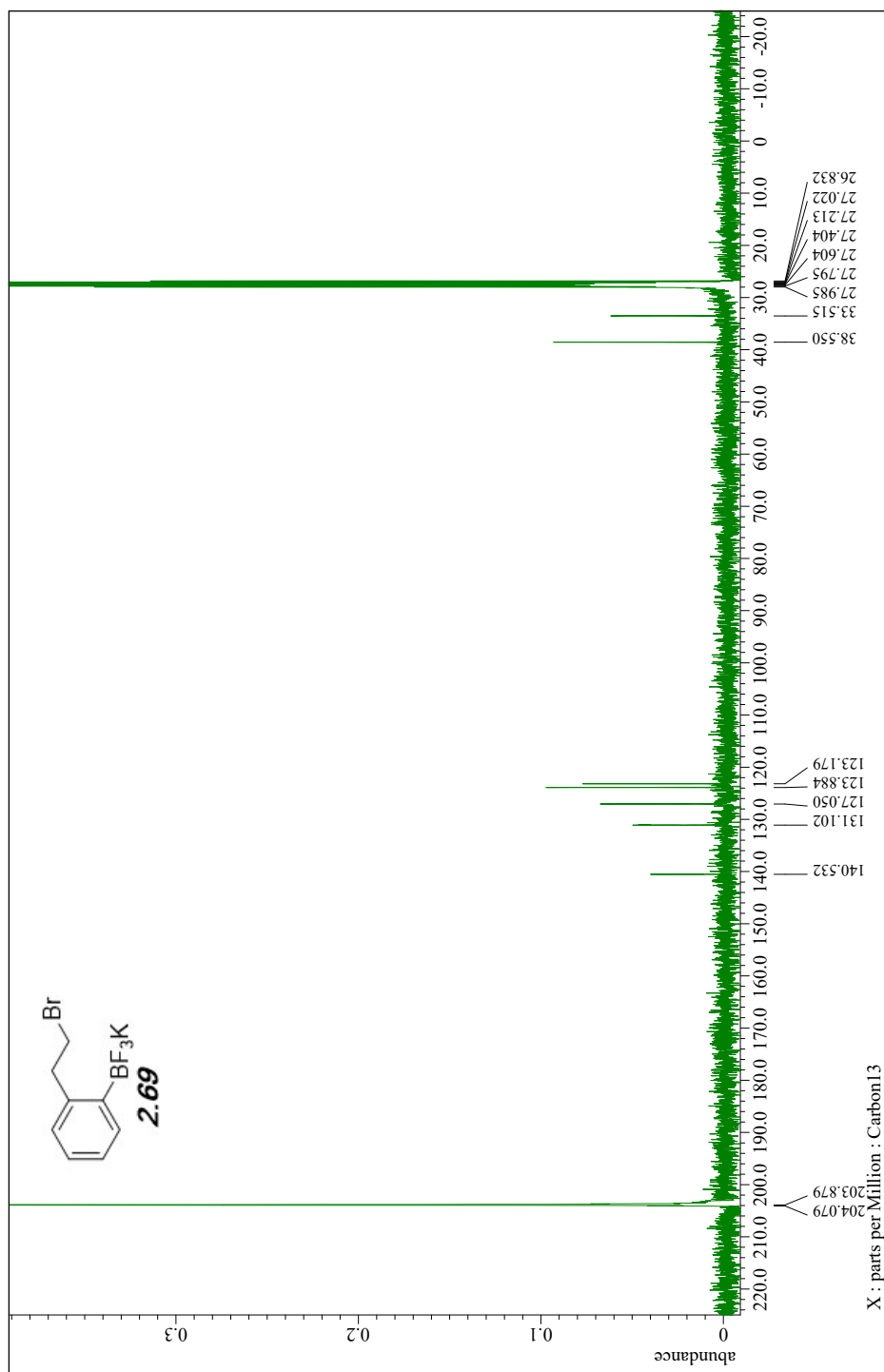


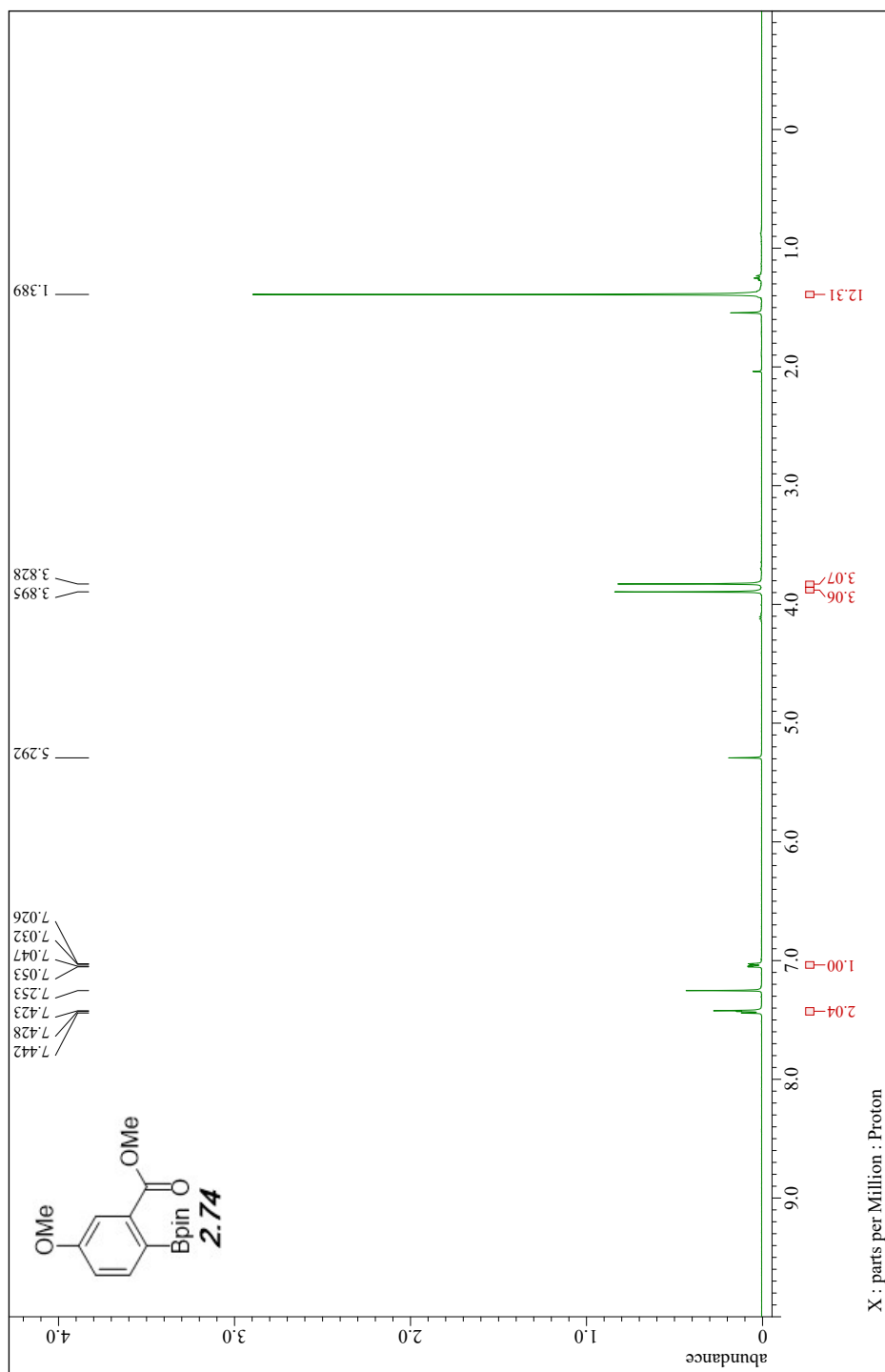


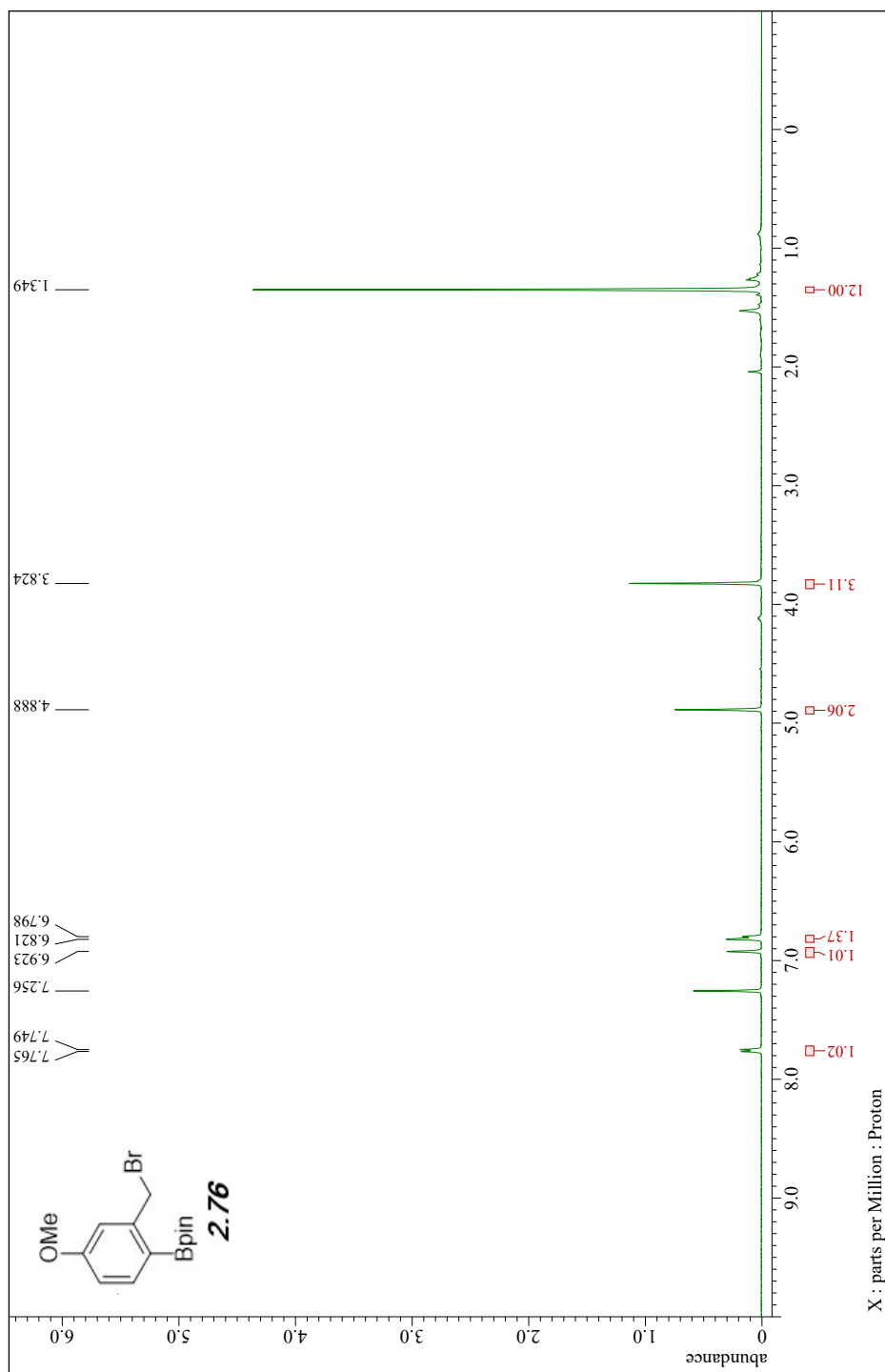


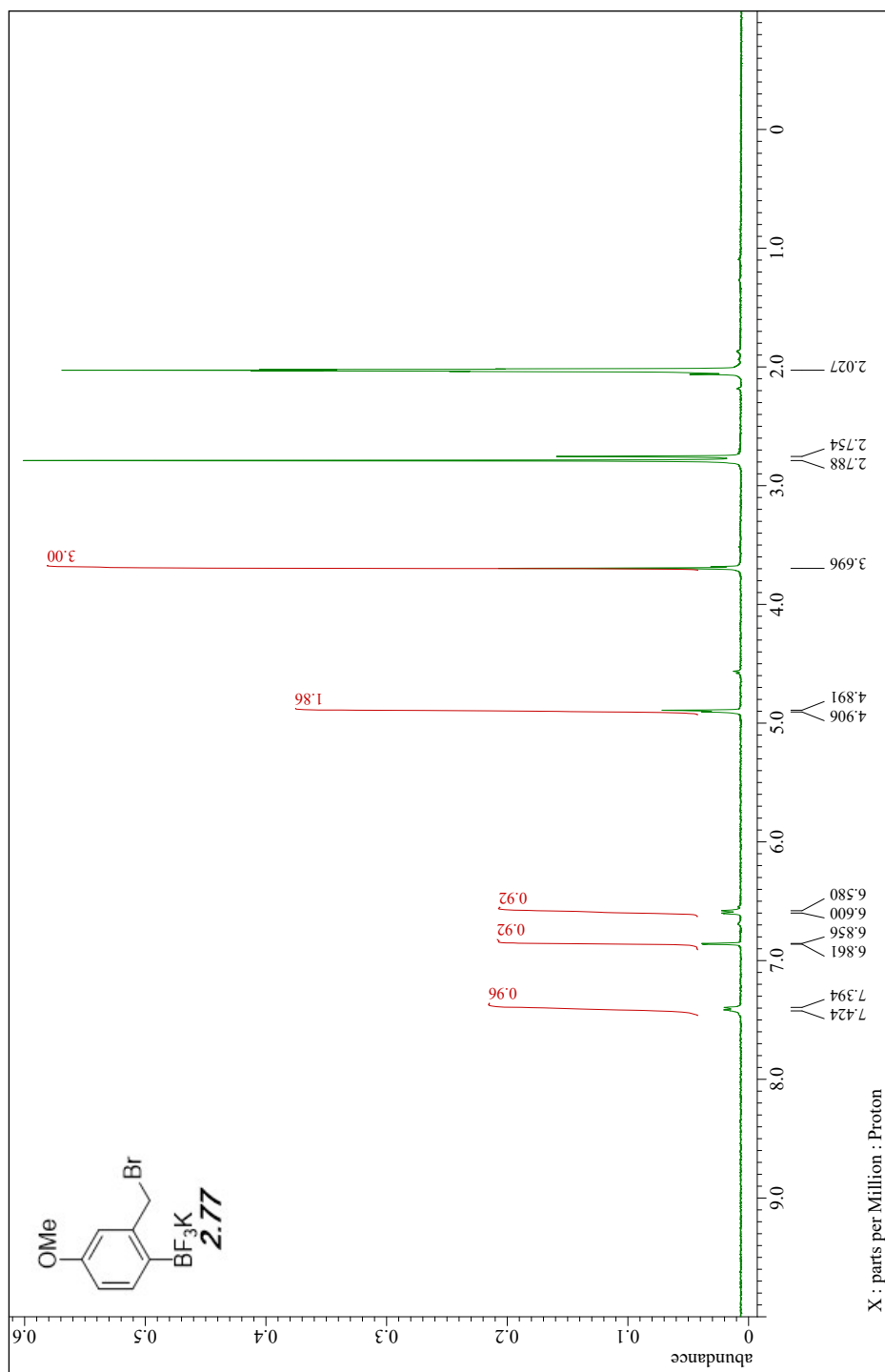






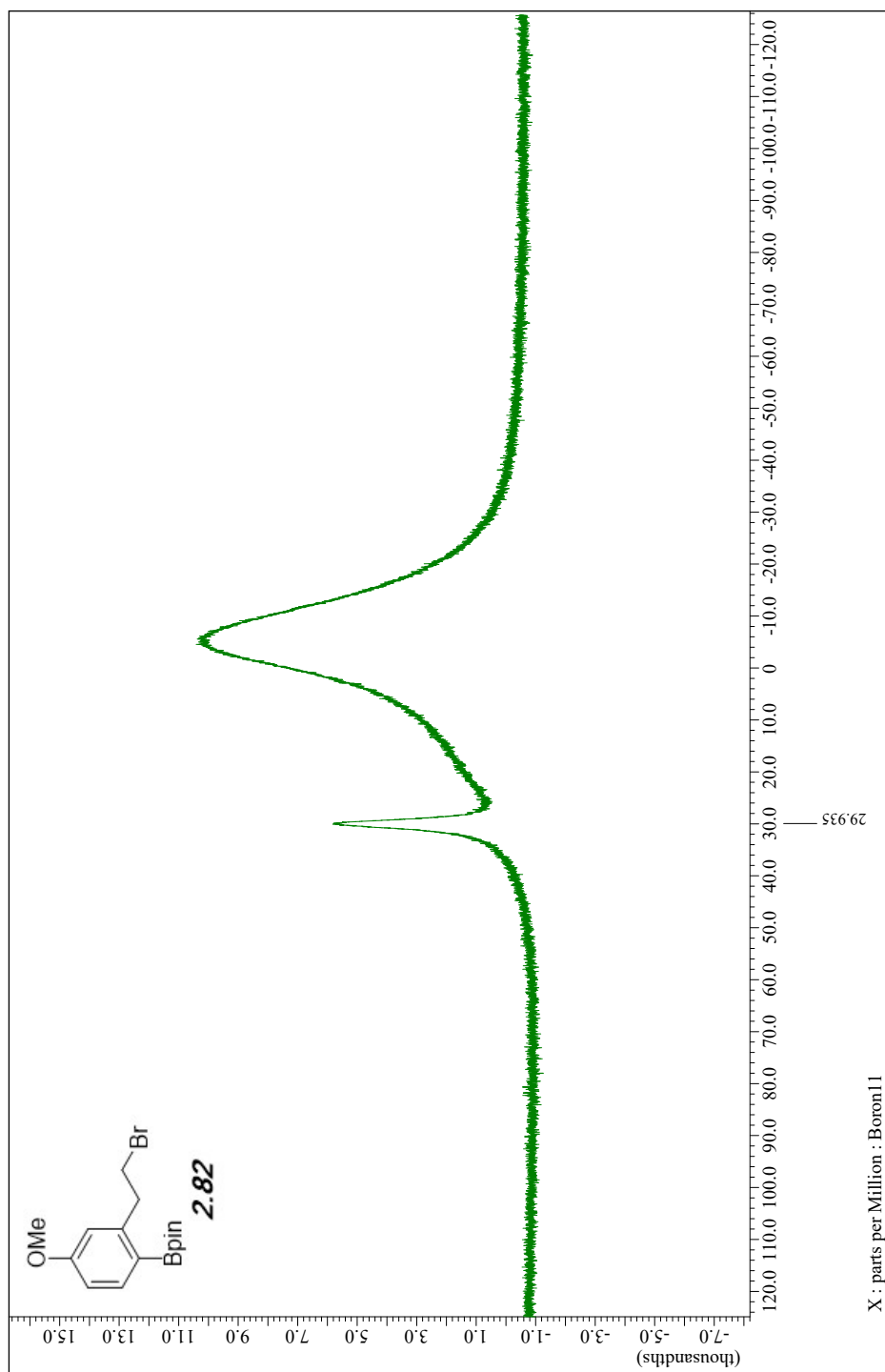


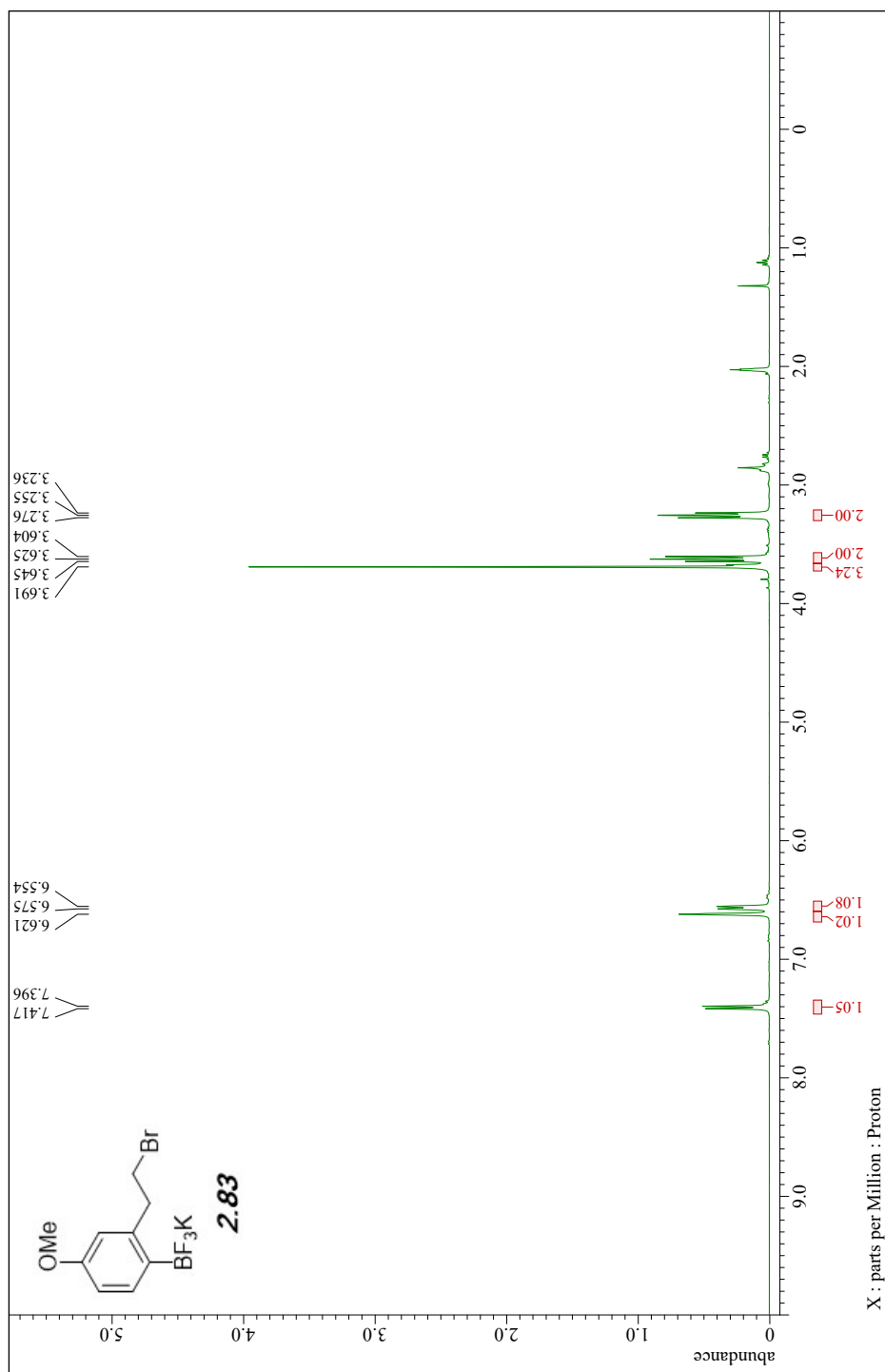


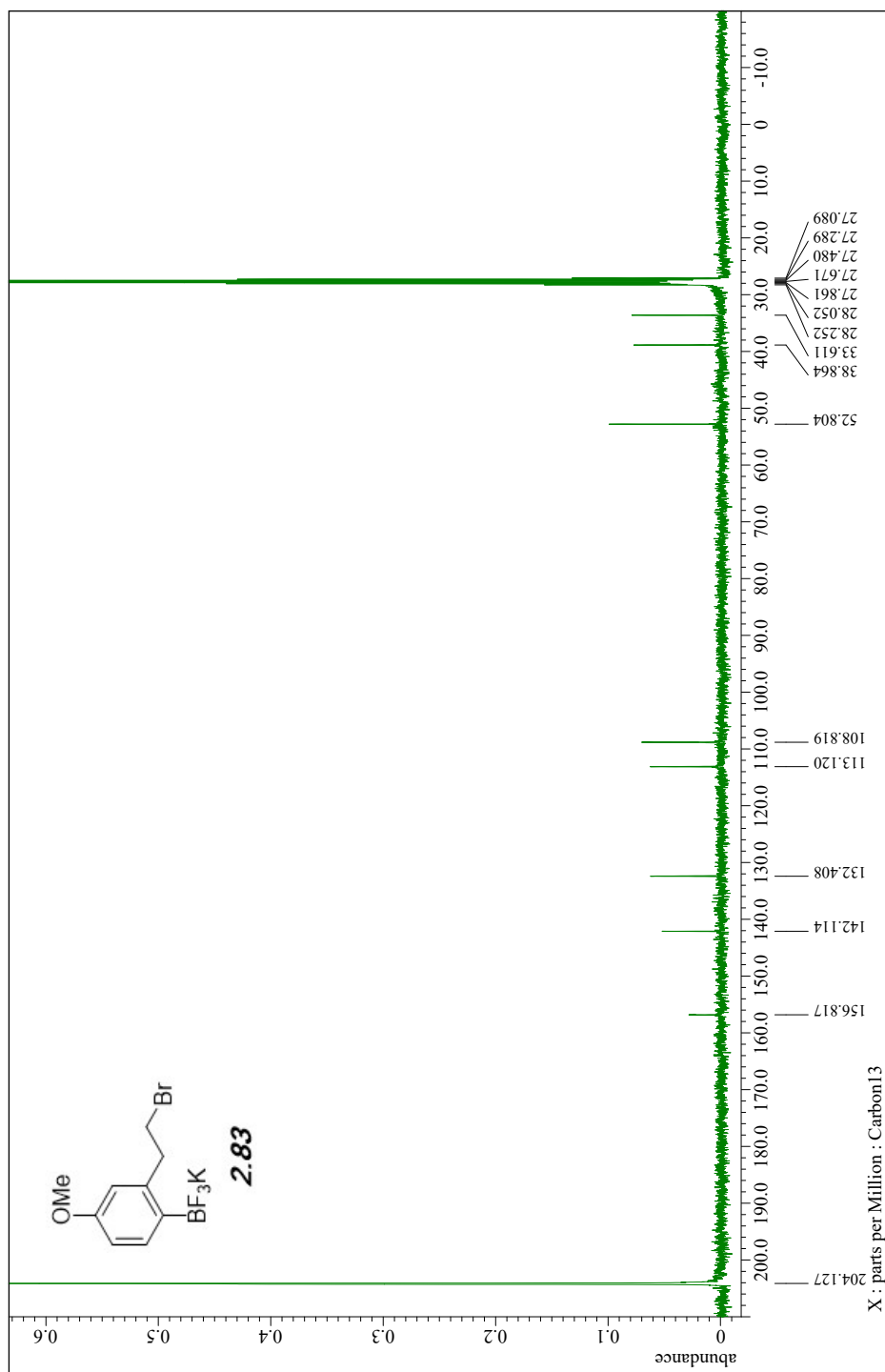


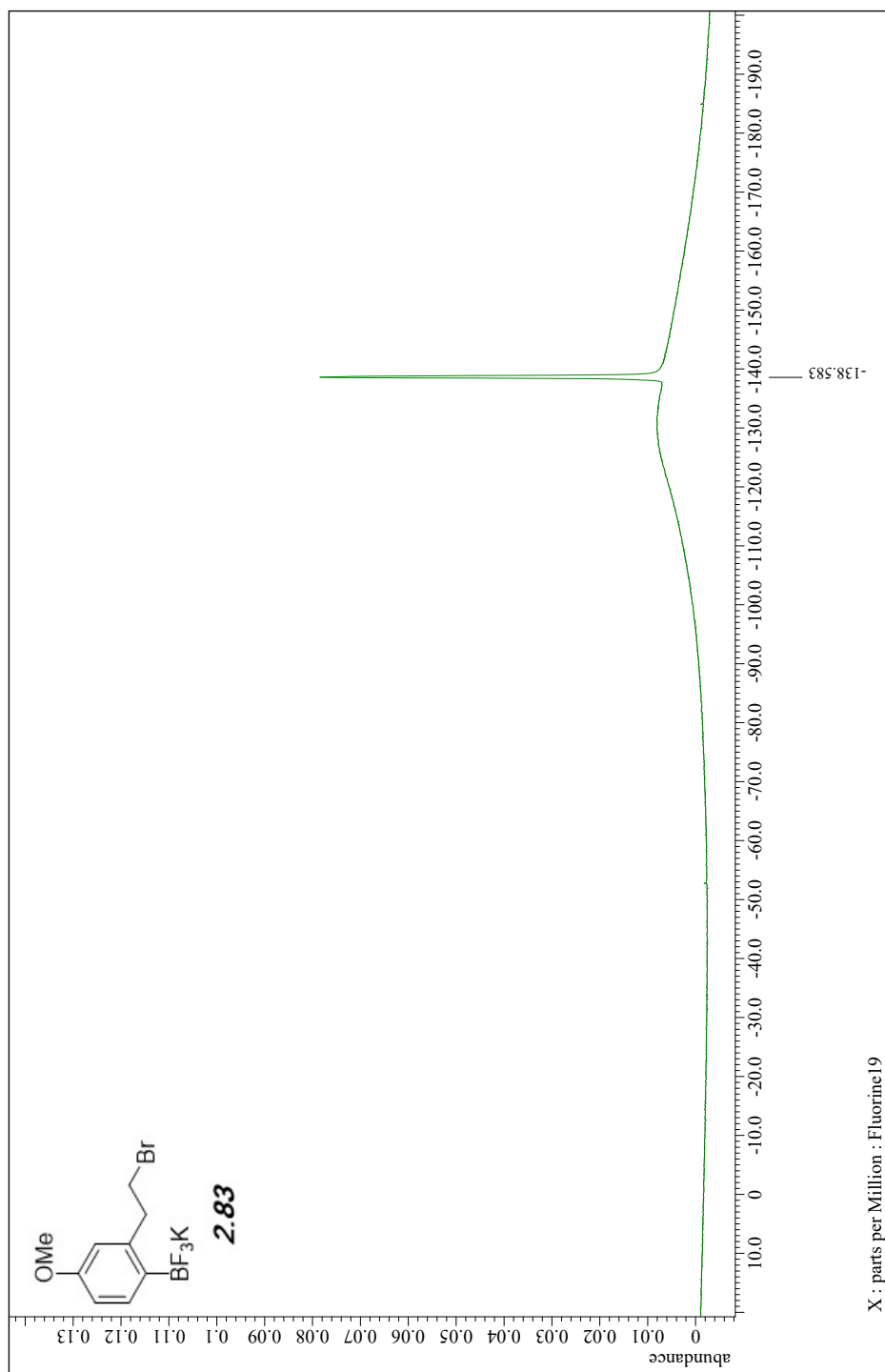


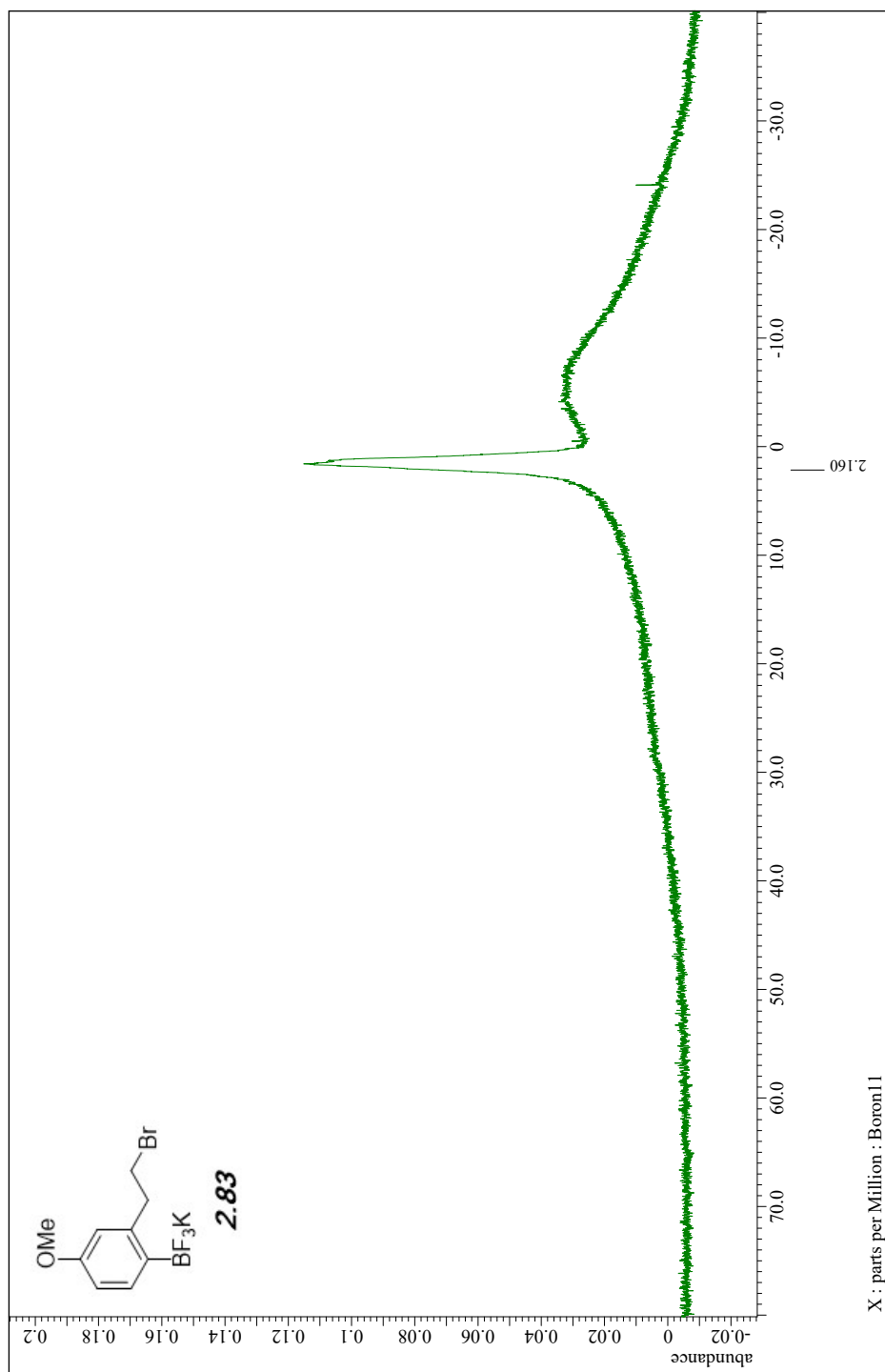










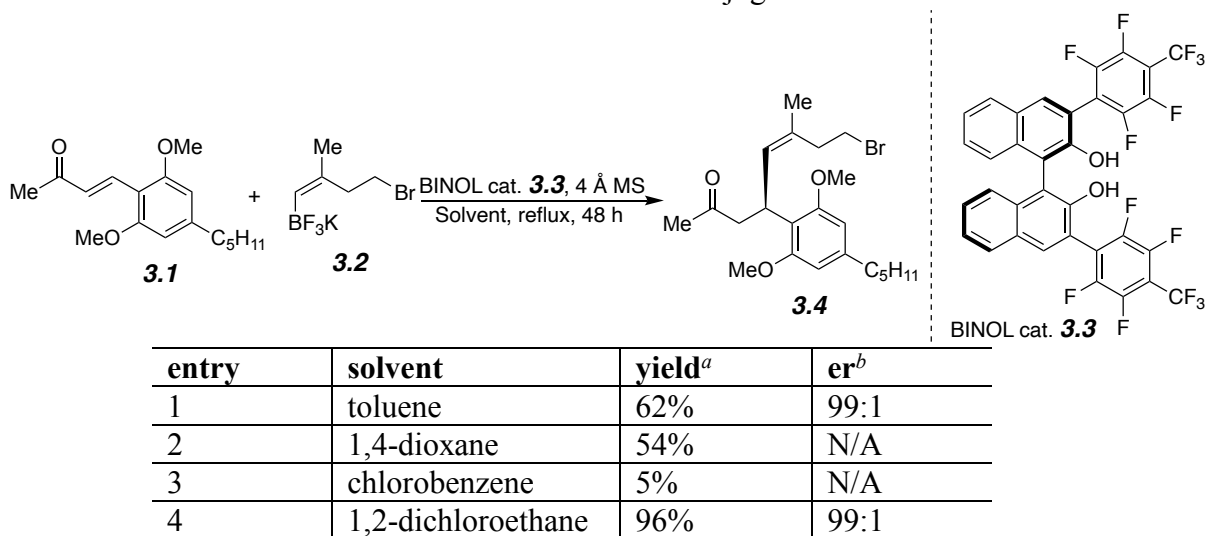


## Chapter 3 Conjugate Addition Enolate Alkylation Reaction Development

### 3.1 Reaction Discovery and Optimization

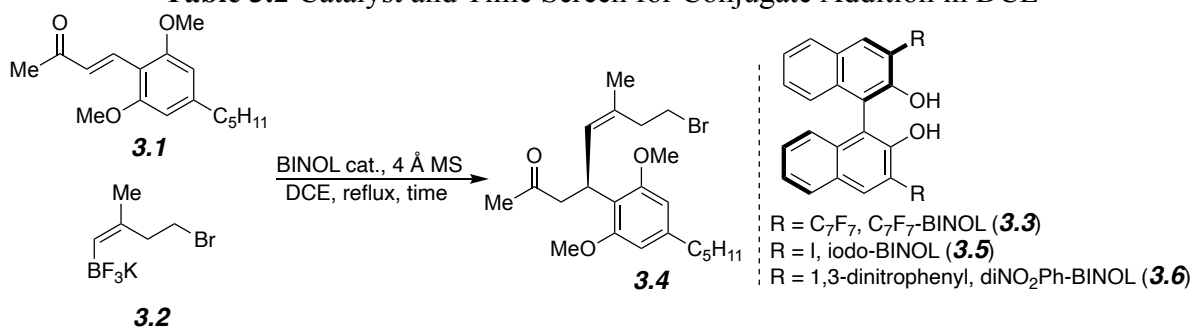
With the ambiphilic vinyl trifluoroborate **3.2** in hand, we started to explore the annulation reaction we designed for THC synthesis (Table 3.1). The enone **3.1** and 3,3'-perfluorotoluy-BINOL catalyst **3.3** could be synthesized in high yield following literature reported procedures.<sup>1,2</sup> After screening several commonly used solvents in organocatalyzed conjugate additions with catalyst loadings similar to those previously reported by our group,<sup>2</sup> 1,2-dichloroethane (DCE) was found to be the most effective solvent for this specific system. The conjugate addition in DCE gave 96% yield of **3.4** with 99:1 er, which were excellent results.

**Table 3.1** Solvent Screen for Conjugate Addition



<sup>a</sup>Yields determined by integrating <sup>1</sup>H NMR peaks relative to 1 equiv of methyl(4-nitrophenyl) carboxylate as an internal standard. <sup>b</sup>er determined by HPLC with chiral stationary phase

After finding an effective solvent, we evaluated the performance of several BINOL-derived catalysts under similar conditions (Table 3.2). It was found that the original catalyst **3** was the most effective catalyst for this reaction. It not only gave the highest yield for a given reaction time, but also had the fastest reaction rate comparing to other catalysts.

**Table 3.2** Catalyst and Time Screen for Conjugate Addition in DCE

entry	catalyst	time (h)	yield <sup>a</sup>
1	<b>3</b>	2	72%
2	<b>3</b>	5	87%
3	<b>3</b>	10	100%
4	<b>3</b>	24	95%
5	<b>5</b>	2	59%
6	<b>5</b>	5	77%
7	<b>5</b>	10	89%
8	<b>5</b>	24	87%
9	<b>6</b>	2	46%
10	<b>6</b>	5	63%
11	<b>6</b>	10	78%
12	<b>6</b>	24	85%

<sup>a</sup>Yields determined by integrating <sup>1</sup>H NMR peaks relative to 1 equiv of methyl(4-nitrophenyl) carboxylate as an internal standard.

Based on our proposed reaction mechanism (Figure 1), it was hypothesized that the transient boron enolate could be trapped by intramolecular alkylation with an electrophilic carbon bearing a good leaving group (see **3.10** to **3.11**). However, such a cyclization was not observed during our rigorous screening for the optimal conjugate addition solvent and catalyst. We attributed this to the boron enolate not being strong enough for the enolate alkylation to take place. On the other hand, loss of the bromide was not observed, which indicated a Finkelstein reaction with fluoride was not competitive. With the bromide leaving group still present, the reaction could proceed after completion of conjugate addition by using additional base to activate the enolate for cyclization.

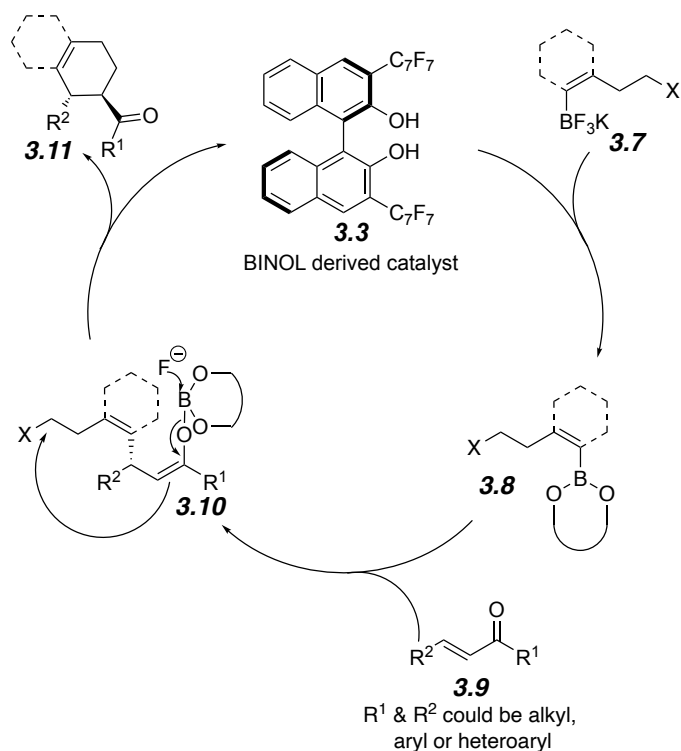
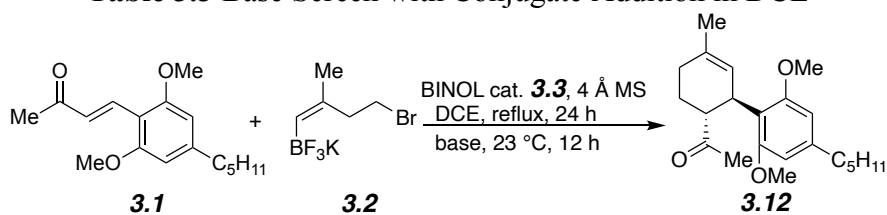


**Figure 3.1** Proposed Conjugate Addition Enolate Alkylation Mechanism

Several bases were screened for activation of the enolate by their addition to the solution after completion of the conjugate addition (Table 3.3). For the alkylation to take place and form a 6-membered ring, a thermodynamic enolate had to be generated on the more substituted side of the ketone. Typical strong kinetic bases such as LDA and *n*-BuLi were tested under thermodynamic conditions, namely adding less than 1 equivalent of base to the conjugate addition mixture at low temperature (entries 1 and 2). No cyclization was observed in those attempts. Using an excess amount of relatively weak bases such as triethylamine and cesium carbonate did not lead to a reactive enolate (entries 3 and 4). KHMDS was examined via direct addition to the reaction mixture at room temperature, and no cyclization product was observed by NMR (Entry 5). A typical thermodynamic base for enolate formation, potassium *tert*-butoxide, was also examined. However, no desired product was observed with or without 18-crown-6 to amplify the basicity via potassium sequestration (entries 6 and 7). We realized that the solubility of these bases in DCE

might not be good enough for effective enolate activation. Potassium *tert*-amylate, which was known to be more soluble in non-polar solvents, was examined to address this potential problem, but it still failed to generate the desired product (entry 8). We hypothesized that DCE might have poor compatibility with these bases because halogenated solvents could react with bases. It led us to the testing of other solvents that could allow alkylation.

**Table 3.3** Base Screen with Conjugate Addition in DCE



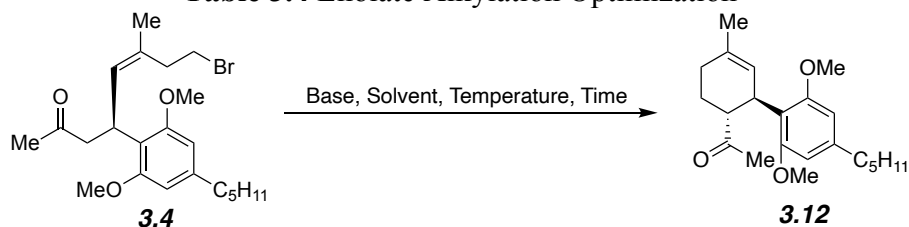
entry	base (equiv)	yield <sup>a</sup>
1 <sup>b</sup>	LDA (0.95)	0%
2 <sup>b</sup>	<i>n</i> -BuLi (0.95)	0%
3	Et <sub>3</sub> N (3)	0%
4	Cs <sub>2</sub> CO <sub>3</sub> (3)	0%
5	KHMDS (3)	0%
6	K <i>Ot</i> -Bu (3)	0%
7 <sup>c</sup>	K <i>Ot</i> -Bu (3)	0%
8	K <i>Ot</i> -amyl (3)	0%

<sup>a</sup>Yields determined by integrating <sup>1</sup>H NMR peaks relative to 1 equiv of methyl(4-nitrophenyl) carboxylate as an internal standard. ; <sup>b</sup>reaction was cooled to -78 °C before addition of base then warmed up to room temperature; <sup>c</sup>3 equiv 18-crown-6 was added.

To assess potential conditions for enolate alkylation, the isolated conjugate addition product was dissolved in THF, and several bases were examined (Table 3.4). Using a strong kinetic base under thermodynamic conditions was not effective in producing the desired product (entries 1 and 2). Interestingly, when KHMDS was used at room temperature with a prolonged reaction time (entries 3 and 4), the cyclization product was isolated in 50% yield with a diastereomeric ratio greater than 20:1. A thermodynamic condition could thus favor this enolate alkylation. An excess of K*Ot*-Bu gave almost quantitative yield after the reaction mixture was stirred for 12 hours at room temperature with full retention of enantiopurity and an outstanding diastereomeric ratio

(entry 5). We were then eager to combine the conjugate addition and enolate alkylation into a single reaction. Due to DCE's poor compatibility with bases, *KOt*-Bu would not promote the reactivity of the enolate, either in pure DCE or a 1:1 mixture of DCE and THF (entries 6 and 7). Meanwhile, THF would not allow the conjugate addition to take place. Based on our experience with these two process, an ideal solvent would replicate the polar aprotic properties of THF for the enolate alkylation while having the non-coordinating nature and elevated boiling point of DCE or toluene to ensure a good performance in the conjugate addition. 2-Methyl-terahydrofuran (2-MeTHF), an ecologically friendly solvent,<sup>3</sup> was identified to be the perfect bridge between these two solvent characteristics. It proved to be excellent for the enolate alkylation annulation (entry 8) and provided a high yield and enantioselectivity in the conjugate addition (Table 3.5).

**Table 3.4** Enolate Alkylation Optimization

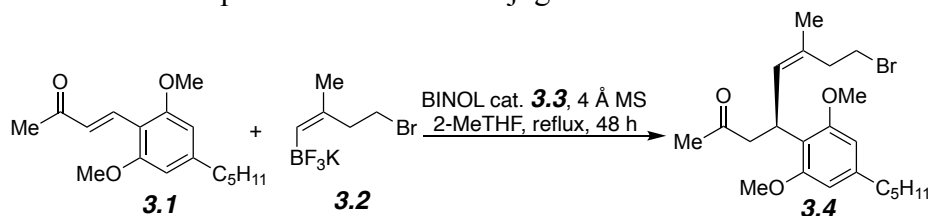


entry	base (equiv)	solvent	temperature	time (h)	result
1	LiHMDS (1.1)	THF	-78 °C to 23 °C	2	0% <sup>a</sup>
2	LDA (0.9)	THF	-78 °C to 0 °C	10	0% <sup>a</sup>
3	KHMDS (0.9)	THF	23 °C	8	0% <sup>a</sup>
4	KHMDS (0.9)	THF	23 °C	36	50% <sup>b</sup> dr > 20:1
5	<i>KOt</i> -Bu (3.0)	THF	23 °C	12	98% <sup>b</sup> (99:1 er) <sup>c</sup> dr > 20:1
6	<i>KOt</i> -Bu (3.0)	DCE	23 °C	12	0% <sup>a</sup>
7	<i>KOt</i> -Bu (3.0)	THF/DCE (1:1)	23 °C	12	0% <sup>a</sup>
8	<i>KOt</i> -Bu (3.0)	2-MeTHF	23 °C	12	98% <sup>b</sup> (99:1 er) <sup>c</sup> dr > 20:1

<sup>a</sup>Yields determined by integrating <sup>1</sup>H NMR peaks relative to 1 equiv *trans*-stilbene as an internal standard. ; <sup>b</sup>isolated yield; <sup>c</sup>er determined by HPLC with chiral stationary phase.

While screening various conjugate addition conditions for reaction optimization,<sup>4</sup> we noticed that the yield would often significantly decrease if the number of equivalents of the nucleophile was lowered (Table 3.5, entries 3 to 11). The potassium trifluoroborate salt had very limited solubility in 2-MeTHF, and molecular sieves were not soluble at. We observed that the amount of insoluble solid in the mixture would also affect the overall yield (entries 12 and 13). We hypothesized that the stirring efficacy of the stirring bar was affected by the presence of the insoluble particles. Meanwhile, a certain amount of molecule sieves must be included to absorb the fluoride salt from reaction (entry 1 and 2). After optimization, the conjugate addition could be conducted at 1 mmol scale with a 1 M concentration with only 1.2 equivalents of the trifluoroborate while consistently delivering high yield (98%) and outstanding enantioselectivity (99:1).

**Table 3.5** Optimization of the Conjugate Addition in 2-MeTHF

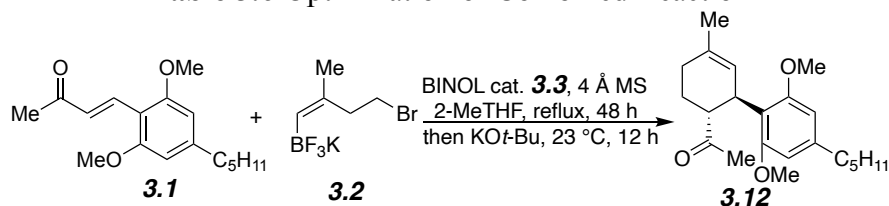


entry	loading of <b>2</b> (equiv)	concentration	molecular sieves/ 0.2 mmol enone	result
1	3.0	0.05 M	250 mg	98% <sup>a</sup> (99:1 er) <sup>c</sup>
2	3.0	0.05 M	50 mg	90% <sup>a</sup>
3	3.0	0.1 M	50 mg	98% <sup>a</sup>
4	2.5	0.1 M	50 mg	92% <sup>a</sup>
5	2.0	0.1 M	50 mg	89% <sup>a</sup>
6	1.5	0.1 M	50 mg	34% <sup>a</sup>
7	1.2	0.1 M	50 mg	53% <sup>a</sup>
8	2.0	0.2 M	50 mg	85% <sup>a</sup>
9	2.0	0.4 M	50 mg	98% <sup>a</sup>
10	2.0	0.8 M	25 mg	98% <sup>b</sup> (99:1 er) <sup>c</sup>
11	1.5	0.8 M	50 mg	75% <sup>a</sup>
12	1.2	1.0 M	50 mg	86% <sup>a</sup>
13	1.2	1.0 M	25 mg	98% <sup>b</sup> (99:1 er) <sup>c</sup>

<sup>a</sup>Yields determined by integrating <sup>1</sup>H NMR peaks relative to 1 equiv of methyl(4-nitrophenyl) carboxylate as an internal standard. ; <sup>b</sup>isolated yield; <sup>c</sup>er determined by HPLC with chiral stationary phase.

After securing the optimal conjugate addition conditions, we searched for the most effective way to combine it with the enolate alkylation reaction (Table 3.6). A correlation between the equivalents of trifluoroborate and of base was observed. As the equivalents of trifluoroborate increased, more base was needed for full conversion of the conjugate addition product to the alkylation product (entries 1–6). We hypothesized that the base was partially saturated by the Lewis acidic boron species in the reaction (entry 5). However, those boron species could not be sequestered by Lewis basic additives such as HMPA and DMPU (entries 7 and 8). The reaction still required 2 additional equivalents of base to fully react. Nonetheless, the optimal conditions for the conjugate addition enolate alkylation annulation were successfully defined (entry 6).

**Table 3.6** Optimization of Combined Reaction



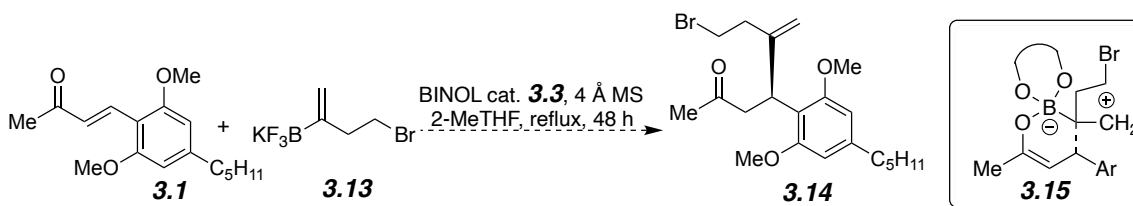
entry	loading of 2 (equiv)	loading of KO <sup>t</sup> -Bu (equiv)	additive	result
1	3.0	6.0	N/A	98% <sup>a</sup> (99:1 er) <sup>c</sup> dr > 20:1
2	2.0	5.0	N/A	98% <sup>a</sup> (99:1 er) <sup>c</sup> dr > 20:1
3	1.5	4.0	N/A	99% <sup>b</sup>
4	1.5	3.0	N/A	98% <sup>b</sup>
5	1.2	2.5	N/A	80% <sup>b</sup>
6	1.2	3.0	N/A	98% <sup>a</sup> (99:1 er) <sup>c</sup> dr > 20:1
7	1.2	1.0	HMPA <sup>d</sup>	30% <sup>b, e</sup>
8	1.2	1.0	DMPU <sup>d</sup>	30% <sup>b, e</sup>

<sup>a</sup>Isolated yield. <sup>b</sup>Yields determined by integrating <sup>1</sup>H NMR peaks relative to 1 equiv of *trans*-stilbene as an internal standard. <sup>c</sup>er determined by HPLC with chiral stationary phase. <sup>d</sup>2.4 equiv of each additive was used respectively. <sup>e</sup>Reaction went to full completion after adding 2 more equivalents of base and stirring for 12 hours.

Satisfyingly, 2-MeTHF produced amazing results for the combined tandem reaction. The key THC intermediate **3.12** was obtained using enone **3.1** and ambiphilic vinyl trifluoroborate **3.2** as a single diastereomer in almost quantitative yield (98%) with an outstanding er (99:1). Ideally, modification of the enone and the trifluoroborate precursors could access analogs bearing various substituents, including those containing aryl or heteroaryl groups.

### 3.2 Conjugate Addition Scope

With the optimal conditions in hand, various ambiphilic trifluoroborates were tested to potentially modify on the cyclohexene ring of THC. The geminal ambiphilic trifluoroborate **3.13** was first tested in the reaction due to the similarity in its structure compared to trifluoroborate **3.2** (Scheme 1). However, no reactivity was observed with the optimal conditions, and the enone **3.1** was recovered. The reaction was considered in the light of a series of mechanistic study conducted by Thien Nguyen, Michelle Yang, Bailey Brooks, and Neomi Hiller in the May lab.<sup>5,6</sup> According to the proposed mechanism, partial positive charge will form on the terminal sp<sup>2</sup> carbon during the C–C bond formation step (Scheme 3.1, **3.15**). The reactivity of this trifluoroborate was thus reduced because there was no substituent to stabilize this developing partial positive charge.



**Scheme 3.1** Conjugate Addition with Geminal Trifluoroborate **13**

The conjugate addition with a series of aryl trifluoroborates was examined next (Figure 3.2). Trifluoroborates **3.16** and **3.17** were first assessed; however, they did not produce any of the corresponding product. In the reaction with trifluoroborate **3.17**, significant protodeboronation was observed, indicating that protodeboronation was competing with conjugate addition. This problem

could potentially be addressed by incorporation of an electron donating substituent, such as methoxy group on the aryl ring, to increase the reactivity of the trifluoroborate. Based on this hypothesis, trifluoroborates **3.18** and **3.19** were synthesized and used in the conjugate addition. While the boronate nucleophile **3.19** gave the conjugate addition product **3.23** in 90% yield and 98:2 er, the trifluoroborate **3.18** did not show any sign of reaction in the same reaction setup, presumably due to the electron withdrawing benzylic bromide pulling electron density away from the nucleophilic carbon.

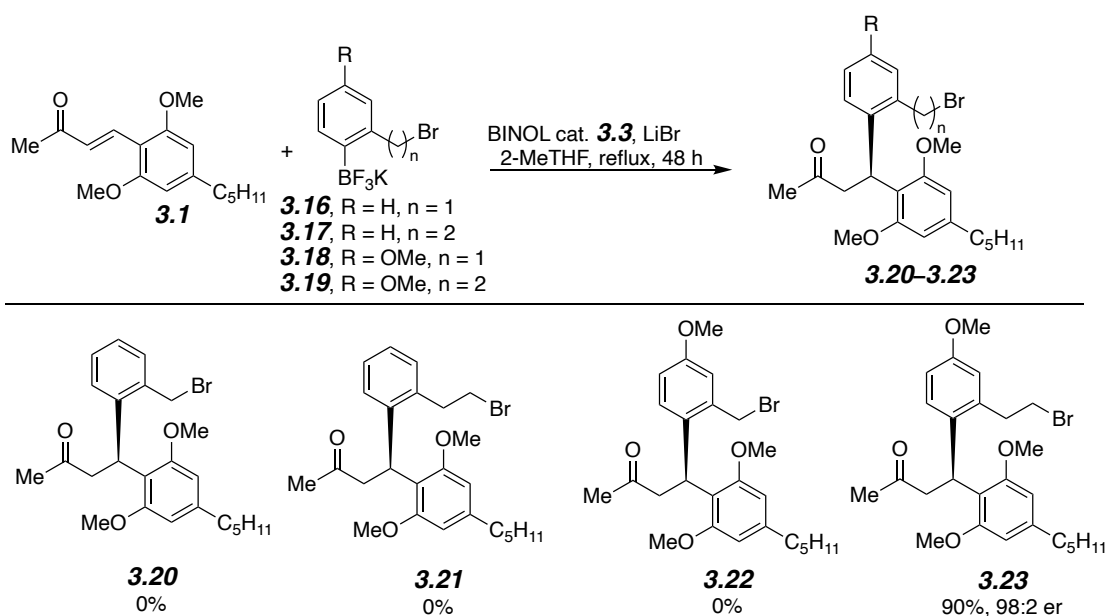
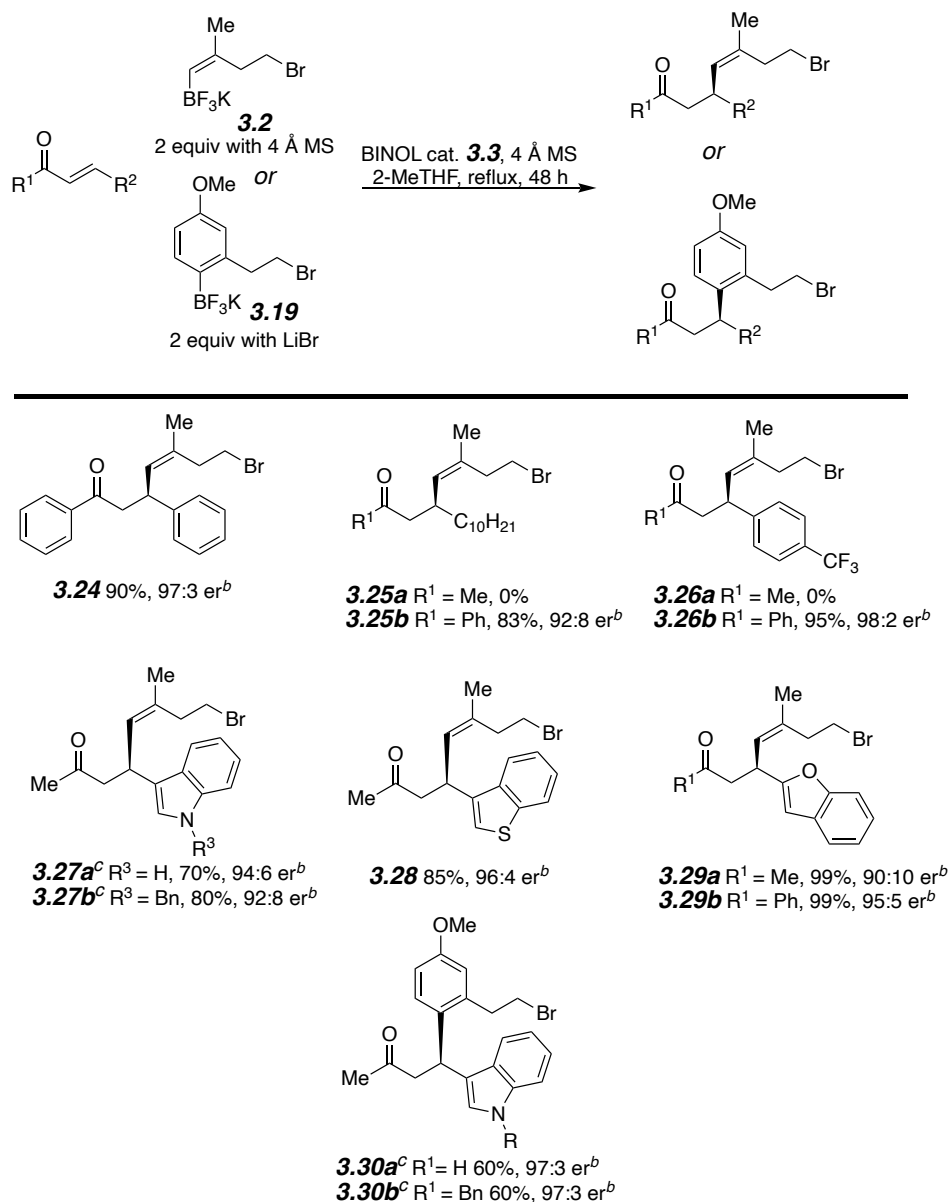


**Figure 3.2** Conjugate Addition with Ambiphilic Aryl Trifluoroborates

Various enones were also synthesized and tested to show that these ambiphilic trifluoroborates would enable cannabinoid analog development (Figure 3.3). The conjugate addition worked very well with phenyl and alkyl substituents (**3.24** and **3.25b**). Changing the enone electronics with an electron-withdrawing group on the  $\beta$ -aryl ring to produce ketone **3.26b** did not cause deviation from a high yield and enantioselectivity. The conjugate addition also showed great tolerance with heteroaryl substituted enones (**27–29**). Both unprotected and benzyl protected indolyl enones had fast reaction rates, with similar yields and ers (**3.27a** and **3.27b**), which

demonstrated that heteroaryls will be tolerated for analog synthesis. Notably, sufficient stabilization must be provided for the partial positive charge on the  $\beta$  position of the enone, otherwise the reaction would not take place as shown in **3.25a** and **3.26a**. The aryl trifluoroborate **3.19** also showed promising compatibility with electrophiles containing heteroaryl substituents (**3.30a** and **3.30b**).

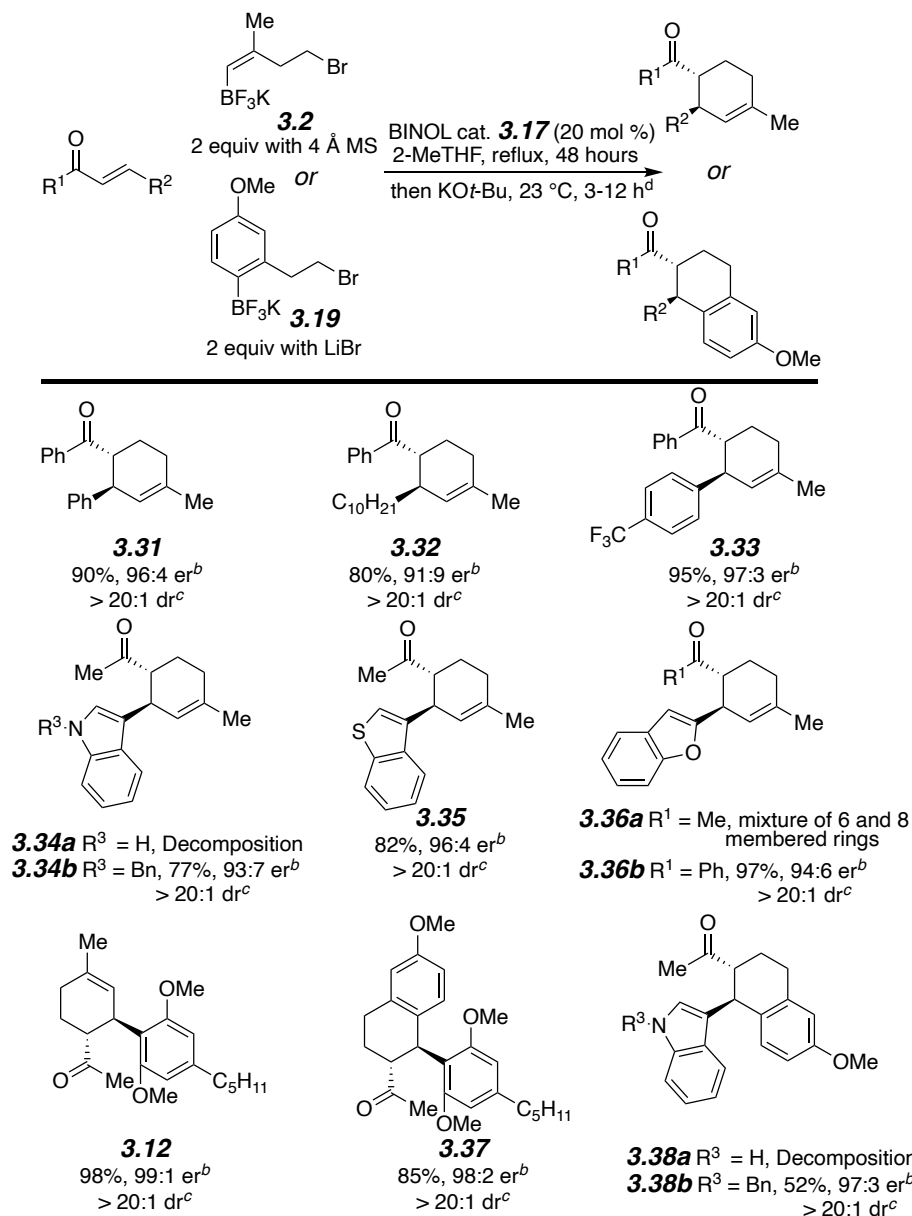


<sup>a</sup>All yields are average of at least two trials. <sup>b</sup>*er* was determined by HPLC with chiral stationary phase. <sup>c</sup>Reaction completed in 2 hours.

**Figure 3.3** Conjugate Addition Scope with Ambiphilic Vinyl Trifluoroborate **2**

### 3.3 Conjugate Addition Enolate Alkylation Scope

The tandem conjugate addition/enolate alkylation annulation conditions were applied to the same array of substrates presented previously, resulting in high stereoselectivity while maintaining compatibility with various functional groups (Figure 3.4).



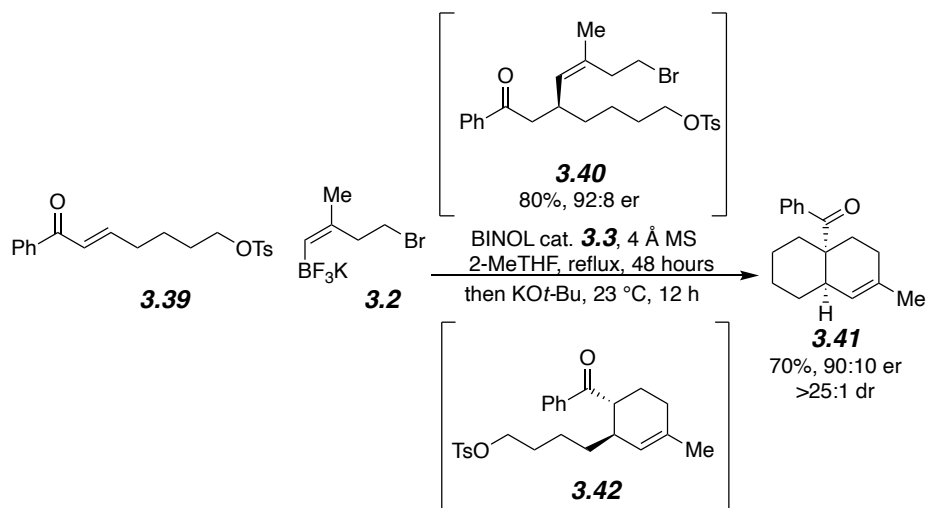
<sup>a</sup>all yields are average of at least 2 trials; <sup>b</sup>er was determined by HPLC with chiral stationary phase; <sup>c</sup>dr was determined by crude <sup>1</sup>H-NMR; <sup>d</sup>reaction times differ due to sensitivity of different substrates under basic conditions.

**Figure 3.4** Conjugate Addition/Enolate Alkylation Annulation Tandem Reaction

For the Alkyl, aryl, and electron-poor aryl substrates, the tandem yield and enantioselectivity did not deviate from those obtained in the isolated conjugate addition, even though an additional transformation was incorporated (**3.31–3.33**). Consequently, the efficiency of this annulation was greatly enhanced in the combined, single-reaction approach. On the other hand, two of the heteroaryl substrates provided additional challenges for the alkylation stage of the annulation. The use of unprotected indolyl and benzofuranyl substrates gave a complex mixture after being treated with base (see **3.34a**, **3.36a**, and **3.38a**). For indolyl substrates, this problem was easily addressed by using a protecting group to prevent deprotonation at the indole N–H, and both products **3.34b** and **3.38b** were obtained successfully with good yield and er. Notably, product **3.34b** resembles recently developed synthetic cannabinoids in literature<sup>7,8</sup> but has the THC cyclohexenyl ring incorporated with high enantiopurity. In the case of the benzofuranyl substrate, some formation of an 8-membered ring product was observed, presumably due to kinetic enolate formation on the methyl side of the ketone. Indeed, a phenyl ketone derivative prevented competing enolate formation and **3.36b** was obtained in 97% yield and 94:6 er as a single diastereomer. The benzothiophene substrate also gave a consistent yield and enantioselectivity for the tandem reaction (see **3.35**). A precursor for a THC analog that would be inaccessible by prior enantioselective catalysis routes, **3.37**, was obtained in 85% yield and 98:2 er.

Given that the addition of excess KO*t*-Bu could enable additional enolate formation, subsequent alkylation could occur to furnish polycyclic products containing all-carbon quaternary centers from an enone like **3.39** with a pendent alkyl halide or tosylate (Scheme 3.2). Again, the success of this strategy depended on the compatibility of nucleophilic organoboronates with traditional electrophiles. Conjugate addition in isolation gave  $\beta$ -branched **3.40** in 80% yield and 92:8 er. In the tandem conjugate addition/enolate alkylation, the *cis*-decalin **3.41** was obtained in

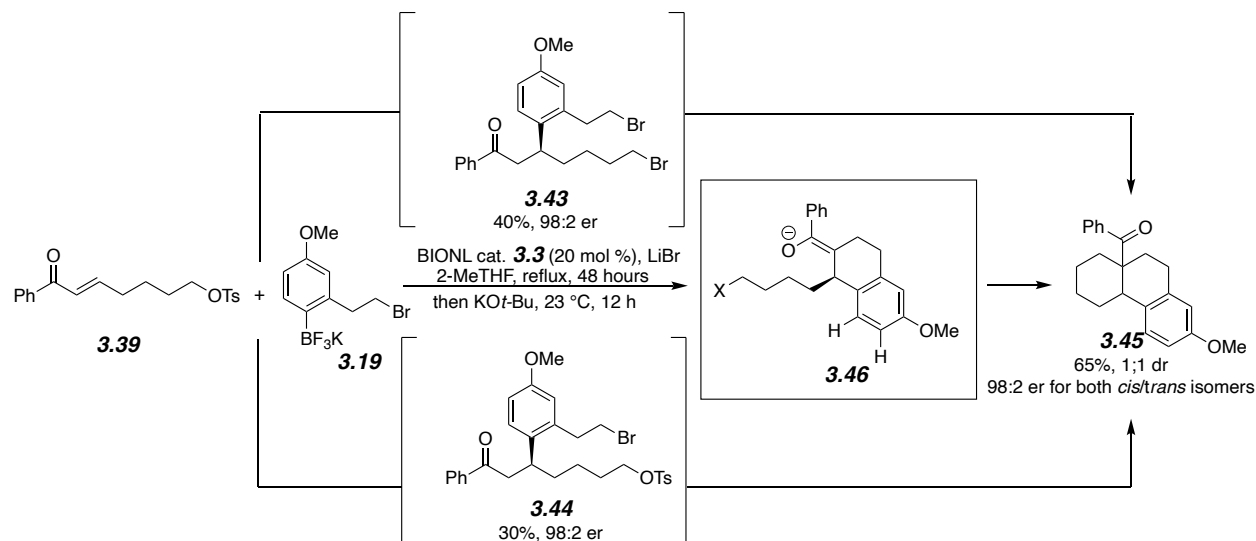
70% yield and 90:10 er with an outstanding dr that was higher than 25:1. The initial stereocenter set by conjugate addition effectively controlled the subsequent alkylations. Apparently, the enolate derived from **3.40** reacts faster with the alkyl bromide than the alkyl tosylate, since the resulting intermediate **3.42** could be isolated in small quantities and identified via  $^1\text{H}$  NMR.



**Scheme 3.2** Double Alkylation to Form a *cis*-Decalin with Quaternary Carbon

Interestingly, in the reaction between aryl nucleophile **3.19** and enone **3.39** (Scheme 3.3), two arylated products, **3.43** and **3.44** were isolated from the conjugate addition, presumably due to a competing Finkelstein reaction by the bromide in the system. Surprisingly, this Finkelstein reactivity was not observed from the fluoride generated during the reaction, presumably due to the sequestration of fluoride by boron. The annulation afforded benzo-fused decalin **3.45** in a 1:1 ratio of diastereomers in 65% overall yield and 98:2 er for each diastereomer. After the tandem annulation and deprotonation to access the putative enolate intermediate **3.46**, we hypothesized that the low diastereoselectivity resulted from the similar conformational energies of positioning the flexible alkyl chain in either a pseudoaxial or pseudoequatorial position. The additional steric hinderance from the fused aryl ring and the accompanying allylic strain compared to its vinyl counterpart is likely responsible for the similar conformational energies, leading to a 50/50 chance of electrophilic attack on either the top or the bottom face of the enolate. This steric effect was also

observed in the  $^1\text{H}$  NMR spectrum of **3.37**. The limited rotation of the dimethoxyaryl ring resulted in significant broadening of the methyl ether peaks instead of the sharp peaks observed in the less crowded congener **3.12**.



**Scheme 3.3** Double Alkylation to Form a Decalin with Aryl Trifluoroborate

### 3.4 Conclusion

After rigorous exploration, we successfully developed a novel conjugate addition/enolate alkylation annulation reaction enabled by sophisticated ambiphilic organoborate alkyl halides, which selectively set two adjacent stereocenter in a single reaction. By simple modification of trifluoroborate ambiphiles, analogs can be obtained that were inaccessible with prior enantioselective catalytic routes. All-carbon quaternary centers can even be generated with high enantioselectivity. This metal-free method shows high compatibility with various functional groups, including heteroaryl substituents, and its modularity will allow access to novel cannabinoid analogs, such as those with benzo-fused rings. We will conduct further investigation for conditions that would allow outstanding performance from more ambiphilic organoboronates in this type of transformation.

## 3.5 Experimental

### 3.5.1 Material and Methods

All reactions were carried out in flame- or oven-dried glassware under a positive pressure of argon unless the reaction contained water as a solvent. Dichloromethane, toluene, THF and acetonitrile were purged with argon and dried over activated alumina columns. 1,2-dichloroethane was freshly distilled from CaH<sub>2</sub> before use. 2-Methyl-tetrahydrofuran (2-MeTHF) was purchased from Acros Organics MS as “extra dry 99%+ stabilizer free” in an AcroSeal bottle. Flash chromatography was performed using 60 Å silica gel (Sigma Aldrich). Preparative and analytical plate chromatography was performed on Sigma Aldrich silica gel plates, 250 µm thickness, 60 Å pore size, with UV light at 254 nm used to visualize the plates. Chemical names were generated using Cambridge Soft ChemBioDraw Ultra 12.0. Analysis by HPLC was performed on a Shimadzu Prominence LC (LC-20AB) equipped with an SPD-20A UV-Vis detector (190 nm–400 nm) and a Chiralpak or Chiralcel (250 mm x 4.6 mm) column (see below for column details). The <sup>1</sup>H, <sup>13</sup>C, <sup>11</sup>B, and <sup>19</sup>F NMR spectra were recorded on a JEOL ECA-600, ECA-500, or ECX-400P spectrometer using the residual solvent peak as an internal standard (CDCl<sub>3</sub>: 7.25 ppm for <sup>1</sup>H NMR and 77.00 ppm for <sup>13</sup>C NMR). NMR yields were determined by addition of 1 equivalent of methyl (4-nitrophenyl) carboxylate or *trans*-stilbene as an internal standard to the crude reaction mixture. IR spectra were obtained using a ThermoNicolet Avatar 370 FT-IR instrument. HRMS analyses were performed under contract by UT Austin’s mass spectrometric facility via an Agilent 6546 Q-TOF LC/MS (high res ESI), Agilent 6530 Q-TOP LC/MS (high resolution CI, APCI or APPI), or Waters Autospec GC/MS (high resolution CI) instrument.

Commercially available compounds were purchased from Sigma Aldrich, Acros, Combi-Blocks, Oakwood Chemical, Alfa Aesar, Ambeed, ArkPharm, Beantown Chemical, TCI, and Cambridge Isotope Laboratories and were used without further purification.

### 3.5.2 HPLC Columns

Chiralpak AY-3: Amylose tris-(5-chloro-2-methylphenylcarbamate) coated on 3  $\mu\text{m}$  silica gel

Chiralpak AD-H: Amylose tris-(3,5-dimethylphenylcarbamate) coated on 5  $\mu\text{m}$  silica gel

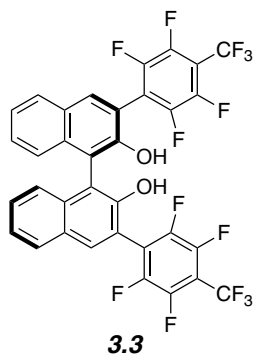
Chiralpak ID: Amylose tris-(3-chlorophenylcarbamate) immobilized on 5  $\mu\text{m}$  silica gel

Chiralcel OJ-H: Cellulose tris-(4-methylbenzoate) coated on 5  $\mu\text{m}$  silica gel

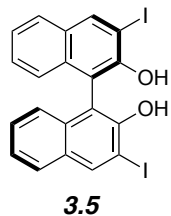
Chiralcel OD-H: Cellulose tris-(3,5-dimethylphenylcarbamate) coated on 5  $\mu\text{m}$  silica gel

Chiralpak AS-H: Amylose tris-[(S)- $\alpha$ -methylbenzylcarbamate] coated on 5  $\mu\text{m}$  silica gel

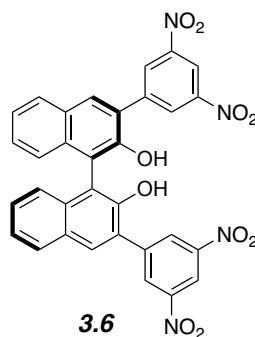
### 3.5.3 Synthesis of the Catalysts



Both (*R*)- and racemic 3,3'-(C<sub>7</sub>F<sub>7</sub>)<sub>2</sub>-BINOL catalysts (**3.3**) were synthesized following a reported procedure from our group.<sup>2</sup> All data matched the literature report.

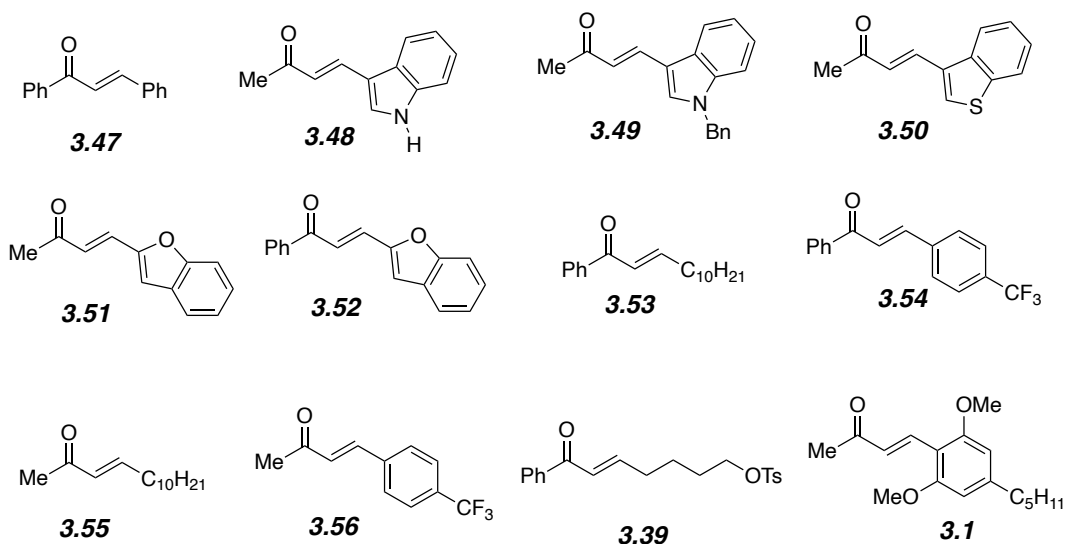


Racemic 3,3'-iodo-BINOL catalysts (**3.5**) were synthesized following a reported procedure from our group.<sup>1</sup> All data matched the literature report.



Racemic 3,3'-bis(1,3-dinitrophenyl)BINOL catalysts (**3.6**) were from a batch synthesized by our group alumni Truong N. Nguyen.

### 3.5.4 Synthesis of Enones



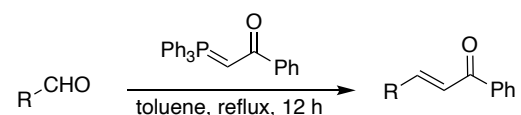
**3.47** is commercially available from Sigma Aldrich.

**3.48, 3.50, 3.51, and 3.56** were prepared following a literature procedure, and all spectral data matched literature reports.<sup>2</sup>

**3.55** was prepared following a literature procedure, and all spectral data matched literature reports.<sup>9</sup>

**3.49** was prepared following a literature procedure, and all spectral data matched literature reports.<sup>10</sup>

### General Procedure for phenyl enone synthesis via Wittig Reaction

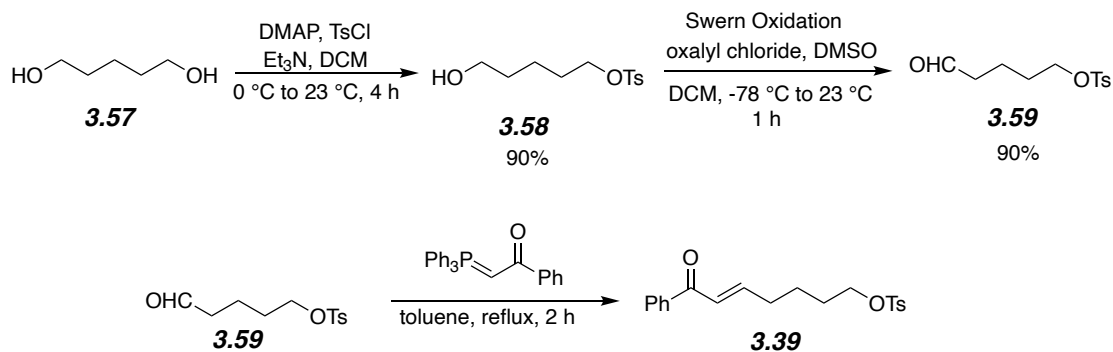


To a flask equipped with a stir bar and a condenser was added the carboxaldehyde (2.0 mmol, 1 equiv), (benzoylmethylene)triphenylphosphorane (456.5 mg, 2.4 mmol, 1.2 equiv), and toluene (4 mL). The reaction mixture was heated to reflux for 12 hours. After completion, the reaction mixture was concentrated under reduced pressure. The crude mixture was purified via flash column chromatography with an appropriate eluent on silica gel.

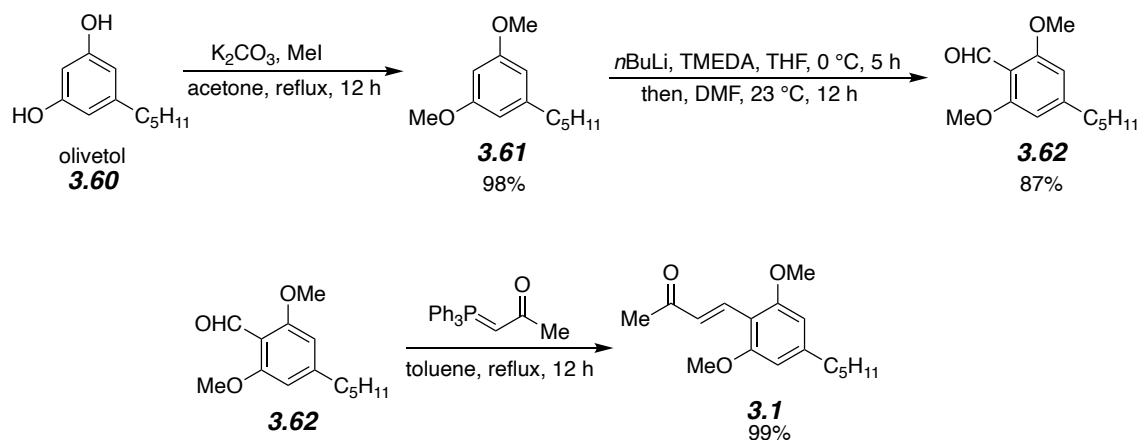
**3.52** was prepared following the general procedure using the corresponding alkyl aldehyde. It is a known compound.<sup>11</sup>

**3.53** was prepared following the general procedure using the corresponding alkyl aldehyde. It is a known compound.<sup>12</sup>

**3.54** was prepared following the general procedure using the corresponding alkyl aldehyde. It is a known compound.<sup>13</sup>

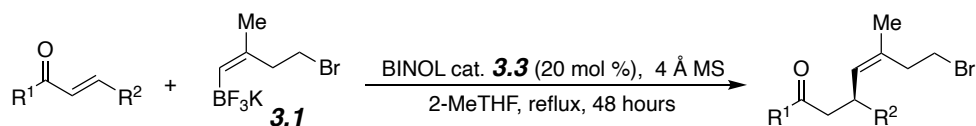


**(E)-7-oxo-7-phenylhept-5-en-1-yl 4-methylbenzenesulfonate (3.39).** Aldehyde **3.59** was prepared following a literature procedure from diol **3.57** and all data matched literature reports.<sup>14</sup> Compound **3.39** was prepared from aldehyde **3.59** (5 mmol) following the general procedure but requiring a shorter amount of time (2 hours). After silica gel chromatography using 20% ethyl acetate in hexanes as eluent, the title compound was obtained in 99% yield (1.77 g) as a sticky yellow oil at room temperature (it becomes solid in a -20 °C freezer, returning to liquid form after warming back to room temperature). **<sup>1</sup>H-NMR** (600 MHz, chloroform-d)  $\delta$  7.91 (d,  $J = 7.6$  Hz, 2H), 7.78 (d,  $J = 7.6$  Hz, 2H), 7.56 (t,  $J = 7.2$  Hz, 1H), 7.47 (t,  $J = 7.6$  Hz, 2H), 7.33 (d,  $J = 7.6$  Hz, 2H), 6.98-6.94 (m, 1H), 6.85 (d,  $J = 15.1$  Hz, 1H), 4.04 (t,  $J = 6.2$  Hz, 2H), 2.43 (s, 3H), 2.28 (q,  $J = 7.1$  Hz, 2H), 1.73-1.68 (m, 2H), 1.55-1.55 (m, 2H). **<sup>13</sup>C-NMR** (101 MHz, chloroform-d)  $\delta$  189.2, 147.0, 143.4, 136.3, 131.5, 131.3, 128.4, 127.1, 127.1, 126.4, 124.9, 68.6, 30.5, 26.9, 22.6, 20.2 **IR** 2925, 1669, 1596, 1352, 1172, 1096, 923, 661, 553  $\text{cm}^{-1}$  **HRMS-ESI m/z** calcd. for  $\text{C}_{20}\text{H}_{22}\text{O}_4\text{S}$   $[\text{M}+\text{H}]^+$  359.1312, found 359.1312



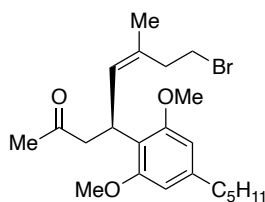
**(E)-4-(2,6-dimethoxy-4-pentylphenyl)but-3-en-2-one (3.1).** Aldehyde **3.62** was prepared following a literature procedure.<sup>15</sup> To a flask equipped with a stir bar and a condenser was added **3.62** (1.18g, 5 mmol), 1-triphenylphosphoranylidene-2-propanone (1.91 g, 6 mmol, 1.2 equiv), and toluene (20 ml). The reaction mixture was heated to 110 °C for 12 hours. After completion, the reaction mixture was concentrated under reduced pressure. The crude mixture was purified via flash column chromatography with 20% ethyl acetate in hexanes on silica gel. The product was obtained in 99% yield (1.38 g) as a white to pale yellow solid, and all spectral data matched literature reports.<sup>16</sup>

### 3.5.5 General procedure of the BINOL-catalyzed conjugate addition reactions between (*Z*)-(4-bromo-2-methylbut-1-en-1-yl)trifluoro- $\lambda^4$ -borane, potassium salt (**3.2**) and various enones (0.2 mmol scale)



To a 2-dram vial equipped with a stir bar were added 4 Å powdered molecular sieves (25 mg), and the vial was flamed-dried under high vacuum. The vial was allowed to cool to room temperature and backfilled with argon. The corresponding enone (0.2 mmol, 1 equiv), (*R*)-3,3'-(C<sub>7</sub>F<sub>7</sub>)<sub>2</sub>-BINOL (28.7 mg, 0.04 mmol, 0.2 equiv), (*Z*)-(4-bromo-2-methylbut-1-en-1-yl)trifluoro-

$\lambda^4$ -borane, potassium salt (**3.1**) (102.7 mg, 0.4 mmol, 2 equiv) were then added. Anhydrous 2-MeTHF (0.25 mL) was added. The mixture was stirred for 2 minutes at room temperature to form a suspension of fine particulates. The vial was well sealed with Teflon thread tape, and the reaction was heated to 81 °C in a sand bath. The reaction was monitored by TLC. After the reaction was complete, the solution was filtered through a short celite pad and concentrated. The crude reaction mixture was purified via column chromatography on silica gel with appropriate eluent.



**(*S,Z*)-8-bromo-4-(2,6-dimethoxy-4-pentylphenyl)-6-methyloct-5-en-2-one (3.4).** The crude reaction mixture was purified via flash column chromatography with 2-5% ethyl acetate in hexanes as the eluent. HPLC Chiralpak AD-H (hexane/*i*-PrOH = 99:1, 0.5 mL/min, UV-190 detector)

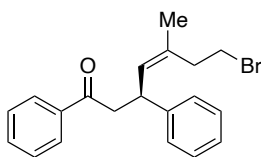
**Result** 83.4 mg, 98% yield; 99:1 er

**<sup>1</sup>H-NMR** (500 MHz, chloroform-*d*)  $\delta$  6.34 (s, 2H), 5.67 (d,  $J = 9.2$  Hz, 1H), 4.71 (td,  $J = 8.9, 6.1$  Hz, 1H), 3.83 (s, 6H), 3.36-3.31 (m, 1H), 3.16-3.11 (m, 1H), 3.01 (q,  $J = 8.2$  Hz, 1H), 2.87-2.75 (m, 2H), 2.62-2.51 (m, 3H), 2.06 (s, 3H), 1.65 (s, 3H), 1.62-1.56 (m, 2H), 1.36-1.30 (m, 4H), 0.90 (t,  $J = 6.9$  Hz, 3H) **<sup>13</sup>C-NMR** (126 MHz, chloroform-*d*)  $\delta$  208.9, 157.6, 142.9, 132.1, 130.6, 117.1, 104.5, 55.7, 48.2, 36.6, 36.4, 31.8, 31.2, 31.0, 30.2, 29.6, 23.5, 22.7, 14.2 **IR** 2929, 2856, 1712, 1606, 1580, 1453, 1418, 1353, 1226, 1188, 1146, 1113, 1024, 973, 823, 651, 594, 533  $\text{cm}^{-1}$  **HRMS-ESI**  $m/z$  calcd. for  $\text{C}_{22}\text{H}_{33}^{79}\text{BrO}_3$  [ $\text{M}+\text{H}$ ]<sup>+</sup> 425.1686, found 425.1688; calcd. for  $\text{C}_{22}\text{H}_{33}^{81}\text{BrO}_3$  [ $\text{M}+\text{H}$ ]<sup>+</sup> 427.1668, found 427.1671

**This reaction could also be conducted at 1 mmol scale following the procedure below.**

To a 2-dram vial equipped with a stir bar was added 4 Å powdered molecular sieves (125 mg), and the vial was flamed-dried under high vacuum. The vial was cooled to room temperature and backfilled with Argon. The enone **3.1** (276.4 mg, 1 mmol, 1 equiv), (*R*)-3,3'-(C<sub>7</sub>F<sub>7</sub>)<sub>2</sub>-BINOL (143.5 mg, 0.2 mmol, 0.2 equiv), (*Z*)-(4-bromo-2-methylbut-1-en-1-yl)trifluoro-λ<sup>4</sup>-borane, potassium salt (**3.2**, 306 mg, 1.2 mmol, 1.2 equiv) were then added. Anhydrous 2-MeTHF (1 mL) was added. The mixture was stirred for 2 minutes at room temperature to form a suspension of fine particulates. The vial was well sealed by Teflon thread tape, and the reaction was heated to 81 °C in a sand bath. The reaction was monitored by TLC analysis. After the reaction was complete, the solution was filtered through a short celite pad and concentrated. The crude reaction mixture was purified via flash column chromatography with 2-5% ethyl acetate in hexanes as the eluent. HPLC Chiralpak AD-H (hexane/*i*-PrOH = 99:1, 0.5 mL/min, UV-190 detector)

**Result** 415.7 mg, 98% yield; 99:1 er

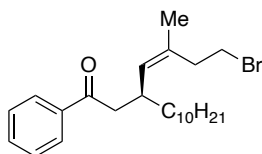


**(*S,Z*)-7-bromo-5-methyl-1,3-diphenylhept-4-en-1-one (3.24)** The crude reaction mixture was purified via flash column chromatography with 10-30% dichloromethane in hexanes as the eluent. HPLC Chiralpak ID (hexane/*i*-PrOH = 90:10, 1.0 mL/min, UV-254 detector)

**Result** 64.5 mg, 90% yield; 97:3 er

**<sup>1</sup>H-NMR** (500 MHz, chloroform-*d*) δ 7.92 (d, *J* = 7.4 Hz, 2H), 7.55 (t, *J* = 7.4 Hz, 1H), 7.45 (t, *J* = 7.7 Hz, 2H), 7.32-7.28 (m, 4H), 7.21-7.18 (m, 1H), 5.49 (d, *J* = 9.7 Hz, 1H), 4.29 (dd,

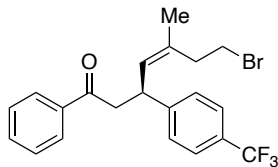
$J = 16.7, 7.1$  Hz, 1H), 3.41-3.25 (m, 4H), 2.76-2.65 (m, 2H), 1.70 (s, 3H)  $^{13}\text{C-NMR}$  (126 MHz, chloroform- $d$ )  $\delta$  198.4, 144.6, 137.1, 133.2, 133.1, 130.8, 128.8, 128.7, 128.2, 127.3, 126.5, 46.1, 39.7, 35.9, 30.6, 23.2 **IR** 3059, 3325, 2967, 1684, 1588, 1493, 1447, 1355, 1255, 1200, 1022, 1001, 979, 841, 747, 689, 548  $\text{cm}^{-1}$  **HRMS-ESI**  $m/z$  calcd. for  $\text{C}_{20}\text{H}_{21}^{79}\text{BrO}$   $[\text{M}+\text{H}]^+$  357.0849, found 357.0853; calcd. for  $\text{C}_{20}\text{H}_{21}^{81}\text{BrO}$   $[\text{M}+\text{H}]^+$  359.0830, found 359.0834



**(*S,Z*)-3-(4-bromo-2-methylbut-1-en-1-yl)-1-phenyltridecan-1-one (3.25b).** The crude reaction mixture was purified via flash column chromatography with 20-30% dichloromethane in hexanes as the eluent. HPLC Chiralpak AD-H (hexane/*i*-PrOH = 99:1, 0.5 mL/min, UV-254 detector)

**Result** 70.1 mg, 83% yield; 92:8 er

$^1\text{H-NMR}$  (400 MHz, chloroform- $d$ )  $\delta$  7.91 (d,  $J = 7.1$  Hz, 2H), 7.56-7.52 (m, 1H), 7.45 (t,  $J = 7.6$  Hz, 2H), 5.03 (d,  $J = 8.5$  Hz, 1H), 3.33 (t,  $J = 7.8$  Hz, 2H), 2.95-2.86 (m, 3H), 2.60-2.52 (m, 2H), 1.65 (d,  $J = 1.1$  Hz, 3H), 1.26 (broad, 18H), 0.86 (t,  $J = 6.8$  Hz, 3H)  $^{13}\text{C-NMR}$  (126 MHz, chloroform- $d$ )  $\delta$  199.7, 137.4, 133.0, 132.4, 132.2, 128.7, 128.2, 44.9, 35.9, 35.8, 34.6, 32.0, 30.9, 29.9, 29.8, 29.7, 29.4, 27.5, 23.0, 22.8, 14.2 **IR** 3186, 2921, 2851, 2259, 1683, 1596, 1580, 1448, 1402, 1377, 1272, 1209, 750, 689, 647, 608, 504  $\text{cm}^{-1}$  **HRMS-ESI**  $m/z$  calcd. for  $\text{C}_{24}\text{H}_{37}^{79}\text{BrO}$   $[\text{M}+\text{H}]^+$  421.2101, found 421.2101; calcd. for  $\text{C}_{24}\text{H}_{37}^{81}\text{BrO}$   $[\text{M}+\text{H}]^+$  423.2083, found 423.2083

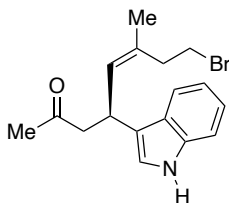


**(S,Z)-7-bromo-5-methyl-1-phenyl-3-(4-(trifluoromethyl)phenyl)hept-4-en-1-one**

**(3.26b).** The crude reaction mixture was purified via flash column chromatography with 20-30% dichloromethane in hexanes as the eluent. HPLC Chiralpak ID (hexane/i-PrOH = 95:5, 1.0 mL/min, UV-254 detector)

**Result** 80.5 mg, 95% yield; 98:2 er

**<sup>1</sup>H-NMR** (500 MHz, chloroform-d)  $\delta$  7.91 (d,  $J$  = 7.4 Hz, 2H), 7.58-7.54 (m, 3H), 7.45 (t,  $J$  = 7.4 Hz, 2H), 7.40 (d,  $J$  = 8.0 Hz, 2H), 5.48 (d,  $J$  = 9.7 Hz, 1H), 4.37 (dd,  $J$  = 16.0, 6.9 Hz, 1H), 3.45-3.29 (m, 4H), 2.71 (q,  $J$  = 6.5 Hz, 2H), 1.71 (s, 3H) **<sup>13</sup>C-NMR** (126 MHz, chloroform-d)  $\delta$  197.8, 148.6, 136.9, 133.8, 133.4, 130.0, 128.8, 128.1, 127.8, 125.8, 125.7, 125.7, 125.7, 45.6, 39.4, 35.7, 30.4, 23.0 **IR** 2970, 1684, 1617, 1596, 1448, 1419, 1314, 1256, 1161, 1108, 1066, 1023, 822, 779, 757, 607, 543  $\text{cm}^{-1}$  **HRMS-ESI m/z** calcd. for  $\text{C}_{21}\text{H}_{20}^{79}\text{BrF}_3\text{O}$  [M+H]<sup>+</sup> 425.0722, found 425.0723; calcd. for  $\text{C}_{21}\text{H}_{20}^{81}\text{BrF}_3\text{O}$  [M+H]<sup>+</sup> 427.0704, found 427.0708

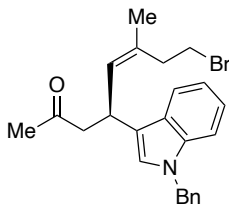


**(S,Z)-8-bromo-4-(1H-indol-3-yl)-6-methyloct-5-en-2-one (3.27a).** The reaction was quenched and worked up after 2 hours, since decomposition was observed with prolonged reaction time. The crude reaction mixture was purified via flash column chromatography with 5-10% ethyl

acetate in hexanes as the eluent. HPLC Chiralpak ID (hexane/i-PrOH = 95:5, 1.0 mL/min, UV-254 detector).

**Result** 46.5 mg, 70% yield; 94:6 er

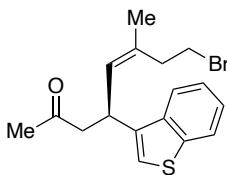
**<sup>1</sup>H-NMR** (500 MHz, chloroform-d)  $\delta$  8.01 (s, 1H), 7.64 (d,  $J$  = 7.4 Hz, 1H), 7.35 (d,  $J$  = 8.0 Hz, 1H), 7.19 (t,  $J$  = 7.4 Hz, 1H), 7.12 (t,  $J$  = 7.4 Hz, 1H), 6.99 (d,  $J$  = 1.7 Hz, 1H), 5.56 (d,  $J$  = 9.7 Hz, 1H), 4.38 (dd,  $J$  = 16.3, 7.2 Hz, 1H), 3.40 (ddd,  $J$  = 44.8, 17.3, 7.9 Hz, 2H), 3.01-2.77 (m, 4H), 2.09 (s, 3H), 1.73 (s, 3H) **<sup>13</sup>C-NMR** (126 MHz, chloroform-d)  $\delta$  208.0, 136.6, 132.5, 130.5, 126.1, 122.2, 121.0, 119.5, 119.4, 118.8, 111.5, 50.3, 35.8, 31.7, 30.8, 30.8, 23.1 **IR** 3407, 2966, 1700, 1456, 1419, 1354, 1338, 1258, 1243, 1157, 1125, 1095, 1010, 739, 653, 493  $\text{cm}^{-1}$  **HRMS-ESI**  $m/z$  calcd. for  $\text{C}_{17}\text{H}_{20}^{79}\text{BrNO}$   $[\text{M}+\text{H}]^+$  334.0810, found 334.0801; calcd. for  $\text{C}_{17}\text{H}_{20}^{81}\text{BrNO}$   $[\text{M}+\text{H}]^+$  336.0782, found 336.0792



**(S,Z)-4-(1-benzyl-1H-indol-3-yl)-8-bromo-6-methyloct-5-en-2-one (3.27b).** The reaction was quenched and worked up after 2 hours, since decomposition was observed with prolonged reaction time. The crude reaction mixture was purified via flash column chromatography with 5-10% ethyl acetate in hexanes as the eluent. HPLC Chiralcel OD-H (hexane/i-PrOH = 90:10, 1.0 mL/min, UV-254 detector)

**Result** 67.7 mg, 80% yield; 92:8 er

**<sup>1</sup>H-NMR** (500 MHz, chloroform-d)  $\delta$  7.66 (d,  $J = 7.7$  Hz, 1H), 7.31-7.24 (m, 4H), 7.19-7.08 (m, 4H), 6.94 (s, 1H), 5.56 (d,  $J = 9.6$  Hz, 1H), 5.26 (s, 2H), 4.42-4.37 (m, 1H), 3.48-3.33 (m, 2H), 3.02-2.79 (m, 4H), 2.09 (s, 3H), 1.74 (s, 3H) **<sup>13</sup>C-NMR** (126 MHz, chloroform-d)  $\delta$  207.9, 137.7, 137.0, 132.6, 130.6, 128.9, 127.7, 126.8, 126.8, 125.2, 122.0, 119.6, 119.2, 118.0, 110.1, 50.4, 50.0, 35.8, 31.7, 30.9, 30.8, 23.2 **IR** 3028, 2910, 2886, 1707, 1611, 1559, 1495, 1465, 1354, 1331, 1267, 1212, 1154, 1028, 846, 740, 700, 552  $\text{cm}^{-1}$  **HRMS-ESI m/z** calcd. for  $\text{C}_{24}\text{H}_{26}^{79}\text{BrNO}$   $[\text{M}+\text{Na}]^+$  446.1090, found 446.1098; calcd. for  $\text{C}_{24}\text{H}_{26}^{81}\text{BrNO}$   $[\text{M}+\text{Na}]^+$  448.1073, found 448.1079

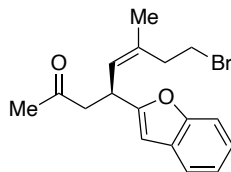


**(*S,Z*)-4-(benzo[*b*]thiophen-3-yl)-8-bromo-6-methyloct-5-en-2-one (3.28).** The crude reaction mixture was purified via flash column chromatography with 2-5% ethyl acetate in hexanes as the eluent. HPLC Chiralcel OD-H (hexane/*i*-PrOH = 90:10, 1.0 mL/min, UV-254 detector)

**Result** 59.7 mg, 85% yield; 96:4 er

**<sup>1</sup>H-NMR** (500 MHz, chloroform-d)  $\delta$  7.84 (d,  $J = 7.9$  Hz, 1H), 7.80 (d,  $J = 7.9$  Hz, 1H), 7.39 (t,  $J = 7.1$  Hz, 1H), 7.34 (t,  $J = 7.2$  Hz, 1H), 7.13 (s, 1H), 5.51 (d,  $J = 9.6$  Hz, 1H), 4.52 (td,  $J = 8.8, 5.5$  Hz, 1H), 3.46-3.29 (m, 2H), 2.97-2.82 (m, 2H), 2.79-2.76 (m, 2H), 2.11 (s, 3H), 1.74 (s, 3H) **<sup>13</sup>C-NMR** (126 MHz, chloroform-d)  $\delta$  206.9, 140.8, 138.9, 137.8, 134.0, 129.4, 124.5, 124.1, 123.2, 122.0, 121.5, 49.8, 35.8, 33.5, 30.8, 30.5, 23.1 **IR** 2966, 2873, 1711, 1425, 1355, 1268, 1212, 1155, 1020, 989, 833, 759, 730, 711, 656, 558  $\text{cm}^{-1}$  **HRMS-ESI m/z** calcd. for

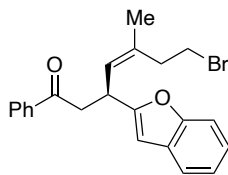
$C_{17}H_{19}^{79}BrOS$   $[M+H]^+$  351.0413, found 351.0403; calcd. for  $C_{17}H_{19}^{81}BrOS$   $[M+H]^+$  353.0393, found 353.0397



**(S,Z)-4-(benzofuran-2-yl)-8-bromo-6-methyloct-5-en-2-one (3.29a).** The crude reaction mixture was purified via flash column chromatography with 2-5% ethyl acetate in hexanes as the eluent. HPLC Chiralpak ID (hexane/i-PrOH = 90:10, 1.0 mL/min, UV-254 detector)

**Result** 66.1 mg, 99% yield; 90:10 er

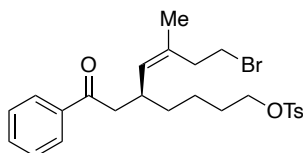
**$^1H$ -NMR** (500 MHz, chloroform- $d$ )  $\delta$  7.46 (d,  $J$  = 7.3 Hz, 1H), 7.39 (d,  $J$  = 7.9 Hz, 1H), 7.22-7.15 (m, 2H), 6.39 (s, 1H), 5.36 (d,  $J$  = 9.9 Hz, 1H), 4.32 (dd,  $J$  = 16.4, 6.9 Hz, 1H), 3.51-3.41 (m, 2H), 3.03 (dd,  $J$  = 16.9, 6.0 Hz, 1H), 2.85-2.70 (m, 3H), 2.12-2.20 (3H), 1.76 (d,  $J$  = 1.3 Hz, 3H)  **$^{13}C$ -NMR** (126 MHz, chloroform- $d$ )  $\delta$  206.3, 159.5, 154.7, 135.2, 128.6, 126.8, 123.6, 122.7, 120.7, 111.0, 102.0, 47.6, 35.7, 33.7, 30.7, 30.5, 23.2 **IR** 2967, 2855, 1715, 1539, 1453, 1358, 1252, 1213, 1157, 1027, 936, 871, 799, 750, 741, 556  $cm^{-1}$  **HRMS-ESI  $m/z$**  calcd. for  $C_{17}H_{19}^{79}BrO_2$   $[M+H]^+$  335.0641, found 335.0633; calcd. for  $C_{17}H_{19}^{81}BrO_2$   $[M+H]^+$  337.0622, found 337.0623



**(*S,Z*)-3-(benzofuran-2-yl)-7-bromo-5-methyl-1-phenylhept-4-en-1-one (3.29b).** The crude reaction mixture was purified via flash column chromatography with 2-5% ethyl acetate in hexanes as the eluent. HPLC Chiralpak ID (hexane/*i*-PrOH = 90:10, 1.0 mL/min, UV-254 detector) Note: It was observed with this example that thoroughly drying the trifluoroborate helped improve the er, presumably due to the competing coordination from any acetone residue retained from before the recrystallization step.

**Result** 78.2 mg, 99% yield; 95:5 er

**<sup>1</sup>H-NMR** (600 MHz, chloroform-*d*)  $\delta$  7.96 (d,  $J$  = 7.6 Hz, 2H), 7.56 (t,  $J$  = 7.2 Hz, 1H), 7.46 (t,  $J$  = 7.6 Hz, 3H), 7.39 (d,  $J$  = 8.2 Hz, 1H), 7.18 (dt,  $J$  = 23.8, 7.0 Hz, 2H), 6.44 (s, 1H), 5.44 (d,  $J$  = 9.6 Hz, 1H), 4.52 (dd,  $J$  = 14.1, 8.6 Hz, 1H), 3.61-3.34 (m, 4H), 2.86-2.71 (m, 2H), 1.75 (s, 3H) **<sup>13</sup>C-NMR** (101 MHz, chloroform-*d*)  $\delta$  197.6, 159.8, 154.8, 136.9, 135.2, 133.4, 128.8, 128.7, 128.2, 127.0, 123.6, 122.7, 120.7, 111.0, 102.1, 42.9, 35.9, 34.1, 30.6, 23.3 **IR** 3057, 2967, 2880, 1684, 1596, 1580, 1453, 1355, 1252, 1217, 1178, 1001, 979, 797, 755, 698, 646, 612  $\text{cm}^{-1}$  **HRMS-ESI**  $m/z$  calcd. for  $\text{C}_{22}\text{H}_{21}^{79}\text{BrO}_2$   $[\text{M}+\text{Na}]^+$  419.0617, found 419.0619; calcd. for  $\text{C}_{22}\text{H}_{21}^{81}\text{BrO}_2$   $[\text{M}+\text{Na}]^+$  421.0599, found 421.0601



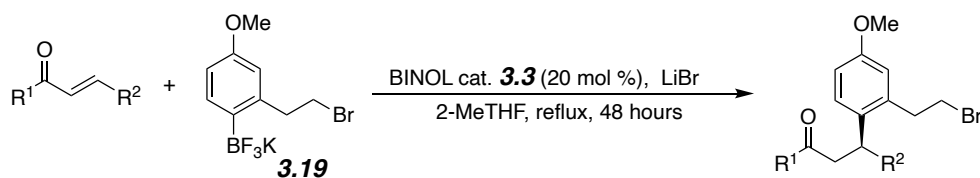
**(*S,Z*)-9-bromo-7-methyl-5-(2-oxo-2-phenylethyl)non-6-en-1-yl 4-methylbenzenesulfonate (3.40).** The crude reaction mixture was purified via flash column chromatography with 5-

15% ethyl acetate in hexanes as the eluent. HPLC Chiralpak ID (hexane/*i*-PrOH = 90:10, 1.0 mL/min, UV-254 detector)

**Result** 81.0 mg, 80% yield; 92:8 er

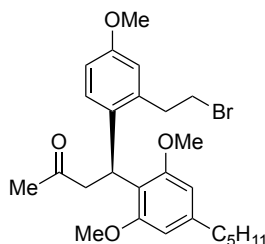
**<sup>1</sup>H-NMR** (400 MHz, chloroform-*d*)  $\delta$  7.90 (d, *J* = 7.1 Hz, 2H), 7.77 (d, *J* = 8.3 Hz, 2H), 7.55 (t, *J* = 7.5 Hz, 1H), 7.45 (t, *J* = 7.6 Hz, 2H), 7.33 (d, *J* = 8.0 Hz, 2H), 5.00 (d, *J* = 8.7 Hz, 1H), 3.99 (t, *J* = 6.4 Hz, 2H), 3.33 (t, *J* = 7.5 Hz, 2H), 2.89 (s, 3H), 2.55 (t, *J* = 7.6 Hz, 2H), 2.43 (s, 3H), 1.65-1.58 (m, 5H), 1.44-1.16 (m, 4H) **<sup>13</sup>C-NMR** (126 MHz, chloroform-*d*)  $\delta$  199.4, 144.8, 137.2, 133.1, 132.9, 131.6, 129.9, 128.7, 128.2, 128.0, 70.6, 44.6, 35.6, 35.0, 34.1, 30.9, 29.0, 23.3, 22.8, 21.7 **IR** 3060, 2920, 2859, 1672, 1596, 1495, 1470, 1448, 1396, 1375, 1343, 1307, 1298, 1269, 1235, 1219, 1204, 1190, 1168, 1119, 1107, 1097, 1074, 1046, 1021, 989, 971, 949, 842, 833, 746, 664, 590, 563, 552, 533, 490, 463 cm<sup>-1</sup> **HRMS-ESI m/z** calcd. for C<sub>25</sub>H<sub>31</sub><sup>79</sup>BrO<sub>4</sub>S [M+H]<sup>+</sup> 507.1199, found 507.1209; calcd. for C<sub>25</sub>H<sub>31</sub><sup>81</sup>BrO<sub>4</sub>S [M+H]<sup>+</sup> 509.1181, found 509.1191

**3.5.6 General procedure of the BINOL-catalyzed conjugate addition reactions between (2-(2-bromoethyl)-4-methoxyphenyl)trifluoro- $\lambda^4$ -borane, potassium salt (3.19) and various enones (0.2 mmol scale).**



To a 2-dram vial equipped with a stir bar was added LiBr (17.4 mg, 0.2 mmol, 1 equiv), and the vial and salt were flame dried under high vacuum. The vial was allowed to cool to room temperature and backfilled with argon. The corresponding enone (0.2 mmol, 1 equiv), (*R*)-3,3'-(C<sub>7</sub>F<sub>7</sub>)<sub>2</sub>-BINOL (28.7 mg, 0.04 mmol, 0.2 equiv), (2-(2-bromoethyl)-4-methoxyphenyl)trifluoro- $\lambda^4$ -borane, potassium salt (**3.19**, 128.4 mg, 0.4 mmol, 2 equiv) were then added. Anhydrous 2-MeTHF (0.25 mL) was added unless otherwise stated. The mixture was stirred for 2 minutes at

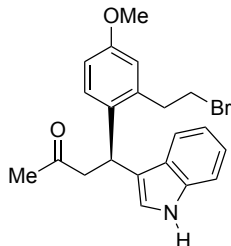
room temperature to form a suspension of fine particulates. The vial was well sealed by Teflon tape, and the reaction was heated to 81 °C in a sand bath. The reaction was monitored by TLC analysis. After the reaction was complete, the solution was filtered through a short celite pad and concentrated. The crude reaction mixture was purified via column chromatography on silica gel with appropriate eluents.



**(S)-4-(2-(2-bromoethyl)-4-methoxyphenyl)-4-(2,6-dimethoxy-4-pentylphenyl)butan-2-one (3.23).** The crude reaction mixture was purified via flash column chromatography with 5-15% ethyl acetate in hexanes as the eluent. HPLC Chiralcel OD-H (hexane/*i*-PrOH = 90:10, 1.0 mL/min, UV-254 detector)

**Result** 88.3 mg, 90% yield; 98:2 er

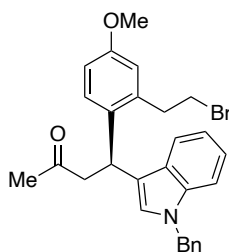
**<sup>1</sup>H-NMR** (500 MHz, chloroform-*d*) δ 7.35 (d, *J* = 8.7 Hz, 1H), 6.71 (dd, *J* = 8.7, 2.8 Hz, 1H), 6.59 (d, *J* = 2.7 Hz, 1H), 6.31 (s, 2H), 5.18-5.15 (m, 1H), 3.74 (s, 3H), 3.72 (s, 6H), 3.40-3.35 (m, 2H), 3.15 (t, *J* = 8.6 Hz, 2H), 3.04 (dd, *J* = 16.0, 7.0 Hz, 1H), 2.92-2.87 (m, 1H), 2.50 (t, *J* = 7.8 Hz, 2H), 2.08 (s, 3H), 1.59-1.54 (m, 2H), 1.34-1.24 (m, 4H), 0.87 (t, *J* = 7.0 Hz, 3H) **<sup>13</sup>C-NMR** (126 MHz, chloroform-*d*) δ 208.5, 157.8, 157.5, 143.3, 138.8, 133.8, 129.7, 116.8, 115.2, 111.6, 104.8, 55.6, 55.2, 47.2, 36.9, 36.5, 32.4, 31.7, 31.7, 31.2, 30.0, 22.7, 14.2 **IR** 2929, 2855, 1711, 1605, 1576, 1449, 1453, 1303, 1226, 1114, 1042, 973, 821, 661 cm<sup>-1</sup> **HRMS-ESI m/z** calcd. for C<sub>26</sub>H<sub>35</sub><sup>79</sup>BrO<sub>4</sub> [M+Na]<sup>+</sup> 513.1611, found 513.1624; calcd. for C<sub>26</sub>H<sub>35</sub><sup>81</sup>BrO<sub>4</sub> [M+Na]<sup>+</sup> 515.1594, found 515.1608



**(S)-4-(2-(2-bromoethyl)-4-methoxyphenyl)-4-(1H-indol-3-yl)butan-2-one (3.30a).** The reaction was quenched and worked up after 2 hours, since decomposition was observed with prolonged reaction time. The crude reaction mixture was purified via flash column chromatography with 5-15% ethyl acetate in hexanes as the eluent. HPLC Chiralpak ID (hexane/i-PrOH = 90:10, 0.5 mL/min, UV-254 detector)

**Result** 48.1 mg, 60% yield; 97:3 er

**<sup>1</sup>H-NMR** (400 MHz, chloroform-d)  $\delta$  7.95 (s, 1H), 7.46 (d,  $J$  = 8.0 Hz, 1H), 7.32 (d,  $J$  = 4.4 Hz, 1H), 7.24 (d,  $J$  = 7.1 Hz, 1H, overlapping with chloroform-H), 7.19-7.15 (m, 1H), 7.07 (t,  $J$  = 7.9 Hz, 1H), 6.79-6.72 (m, 3H), 4.95 (t,  $J$  = 7.3 Hz, 1H), 3.78 (s, 3H), 3.53-3.15 (m, 6H), 2.09 (s, 3H) **<sup>13</sup>C-NMR** (126 MHz, chloroform-d)  $\delta$  207.7, 158.0, 138.4, 136.7, 133.6, 128.1, 126.2, 122.4, 122.3, 119.6, 119.3, 119.2, 116.0, 112.5, 111.4, 55.3, 50.1, 36.9, 33.0, 32.3, 30.7 **IR** 3407, 2934, 1706, 1607, 1499, 1456, 1419, 1355, 1338, 1292, 1247, 1157, 1094, 1042, 907, 818, 734  $\text{cm}^{-1}$  **HRMS-ESI m/z** calcd. for  $\text{C}_{21}\text{H}_{22}^{79}\text{BrNO}_2$   $[\text{M}+\text{Na}]^+$  422.0726, found 422.0732; calcd. for  $\text{C}_{21}\text{H}_{22}^{81}\text{BrNO}_2$   $[\text{M}+\text{Na}]^+$  424.0708, found 424.071

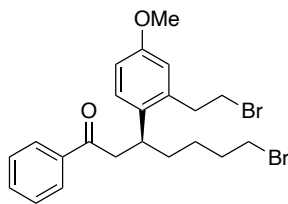


**(S)-4-(1-benzyl-1H-indol-3-yl)-4-(2-(2-bromoethyl)-4-methoxyphenyl)butan-2-one**

**(3.30b).** The reaction was quenched and worked up after 2 hours, since decomposition was observed with prolonged reaction time. The crude reaction mixture was purified via flash column chromatography with 5-15% ethyl acetate in hexanes as the eluent. HPLC Chiralcel OD-H (hexane/*i*-PrOH = 90:10, 1.0 mL/min, UV-254 detector)

**Result** 59.1 mg, 60% yield; 97:3 er

**<sup>1</sup>H-NMR** (500 MHz, chloroform-*d*)  $\delta$  7.48 (d,  $J = 7.9$  Hz, 1H), 7.29-7.20 (m, 5H), 7.16-7.13 (m, 1H), 7.08-7.02 (m, 3H), 6.79 (dd,  $J = 8.5, 2.8$  Hz, 1H), 6.75 (d,  $J = 2.7$  Hz, 1H), 6.67 (s, 1H), 5.22 (s, 2H), 4.99-4.96 (m, 1H), 3.79 (s, 3H), 3.53-3.40 (m, 2H), 3.36-3.17 (m, 4H), 2.09 (s, 3H) **<sup>13</sup>C-NMR** (101 MHz, chloroform-*d*)  $\delta$  207.6, 158.0, 138.4, 137.6, 137.1, 133.6, 128.8, 128.1, 127.6, 126.9, 126.6, 126.6, 122.2, 119.4, 119.4, 118.5, 116.0, 112.5, 110.1, 55.3, 50.2, 50.0, 36.9, 33.1, 32.3, 30.7 **IR** 2927, 1710, 1635, 1466, 1452, 1355, 1296, 1154, 1094, 1041, 1028, 1013, 966, 803, 738, 423  $\text{cm}^{-1}$  **HRMS-ESI  $m/z$**  calcd. for  $\text{C}_{28}\text{H}_{28}^{79}\text{BrNO}_2$   $[\text{M}+\text{Na}]^+$  512.1196, found 512.1196; calcd. for  $\text{C}_{28}\text{H}_{28}^{81}\text{BrNO}_2$   $[\text{M}+\text{Na}]^+$  514.1179, found 514.1180



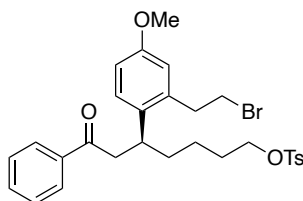
**(S)-7-bromo-3-(2-(2-bromoethyl)-4-methoxyphenyl)-1-phenylheptan-1-one (3.43).**

This product was isolated from the same reaction that produced **3.44**. The crude reaction mixture was purified via flash column chromatography with 5-15% ethyl acetate in hexanes as the eluent.

HPLC Chiralpak ID (hexane/*i*-PrOH = 90:10, 1.0 mL/min, UV-254 detector)

**Result** 38.5 mg, 40% yield; 98:2 er

**<sup>1</sup>H-NMR** (500 MHz, chloroform-*d*)  $\delta$  7.88 (d,  $J$  = 7.4 Hz, 2H), 7.53 (t,  $J$  = 7.3 Hz, 1H), 7.43 (t,  $J$  = 7.7 Hz, 2H), 7.15 (d,  $J$  = 8.6 Hz, 1H), 6.78 (dd,  $J$  = 8.6, 2.6 Hz, 1H), 6.69 (d,  $J$  = 2.6 Hz, 1H), 3.76 (s, 3H), 3.63-3.48 (m, 3H), 3.35-3.31 (m, 2H), 3.25-3.22 (m, 4H), 1.82-1.70 (m, 3H), 1.62-1.21 (m, 3H) **<sup>13</sup>C-NMR** (126 MHz, chloroform-*d*)  $\delta$  199.0, 157.7, 138.3, 137.1, 134.9, 133.2, 128.7, 128.1, 127.2, 115.3, 113.2, 55.3, 45.8, 36.7, 36.2, 34.7, 33.6, 32.9, 32.3, 26.2 **IR** 2932, 2855, 1700, 1684, 1607, 1596, 1576, 1501, 1447, 1248, 1161, 1001, 457, 428, 417  $\text{cm}^{-1}$  **HRMS-ESI  $m/z$**  calcd. for  $\text{C}_{22}\text{H}_{26}^{79}\text{Br}_2\text{O}_2$  [ $\text{M}+\text{Na}$ ]<sup>+</sup> 503.0192, found 503.0198; calcd. for  $\text{C}_{22}\text{H}_{26}^{79}\text{Br}^{81}\text{Br}$   $\text{O}_2$  [ $\text{M}+\text{Na}$ ]<sup>+</sup> 505.0173, found 505.0184; calcd. for  $\text{C}_{22}\text{H}_{26}^{81}\text{Br}_2\text{O}_2$  [ $\text{M}+\text{Na}$ ]<sup>+</sup> 507.0156, found 507.0163



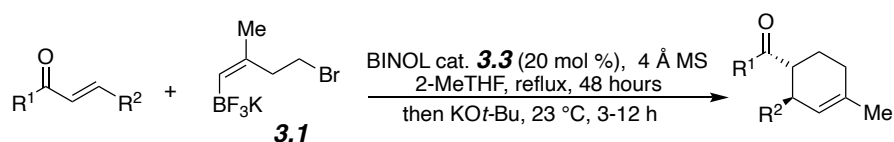
**(S)-5-(2-(2-bromoethyl)-4-methoxyphenyl)-7-oxo-7-phenylheptyl 4-methylbenzenesulfonate (3.44).** This product was isolated from the same reaction that produced **3.43**. The crude

reaction mixture was purified via flash column chromatography with 5-15% ethyl acetate in hexanes as the eluent. HPLC Chiralpak ID (hexane/i-PrOH = 90:10, 1.0 mL/min, UV-254 detector)

**Result** 34.5 mg, 30% yield; 98:2 er

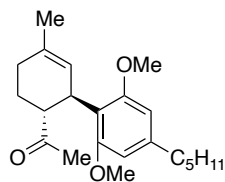
**<sup>1</sup>H-NMR** (500 MHz, chloroform-*d*)  $\delta$  7.88-7.86 (m, 2H), 7.73 (d,  $J = 8.3$  Hz, 2H), 7.55-7.52 (m, 1H), 7.43 (t,  $J = 7.7$  Hz, 2H), 7.31 (d,  $J = 8.0$  Hz, 2H), 7.07-7.13 (1H), 6.76 (dd,  $J = 8.6, 2.7$  Hz, 1H), 6.67 (d,  $J = 2.7$  Hz, 1H), 3.94 (t,  $J = 6.4$  Hz, 2H), 3.76 (s, 3H), 3.61-3.55 (m, 1H), 3.51-3.44 (m, 2H), 3.21-3.16 (m, 4H), 2.42 (s, 3H), 1.69-1.49 (m, 4H), 1.29-1.09 (m, 2H) **<sup>13</sup>C-NMR** (101 MHz, chloroform-*d*)  $\delta$  198.9, 157.7, 144.8, 138.2, 137.0, 134.8, 133.3, 133.1, 129.9, 128.7, 128.1, 128.0, 115.3, 113.1, 70.4, 55.3, 45.7, 36.7, 36.5, 32.3, 29.0, 23.5, 21.8 **IR** 2935, 1684, 1596, 1495, 1447, 1354, 1267, 1248, 1210, 1187, 1173, 1039, 1081, 1096, 1039, 1018, 1001, 815, 755, 662, 574, 553 $\text{cm}^{-1}$  **HRMS-ESI m/z** calcd. for  $\text{C}_{29}\text{H}_{33}^{79}\text{BrO}_5\text{S}$   $[\text{M}+\text{Na}]^+$  595.1124, found 595.1134; calcd. for  $\text{C}_{29}\text{H}_{33}^{81}\text{BrO}_5\text{S}$   $[\text{M}+\text{Na}]^+$  597.1108, found 597.1120

### 3.5.7 General procedure of the tandem BINOL-catalyzed conjugate addition enolate alkylation annulation between (*Z*)-(4-bromo-2-methylbut-1-en-1-yl)trifluoro- $\lambda^4$ -borane, potassium salt (**3.2**) and various enones (0.2 mmol scale)



To a 2-dram vial equipped with a stir bar was added 4 Å powdered molecular sieves (25 mg), and the vial was flame-dried under high vacuum. The vial was cooled to room temperature and backfilled with Argon. The corresponding enone (0.2 mmol, 1 equiv), (*R*)-3,3'-( $\text{C}_7\text{F}_7$ )<sub>2</sub>-BINOL (28.7 mg, 0.04 mmol, 0.2 equiv), (*Z*)-(4-bromo-2-methylbut-1-en-1-yl)trifluoro- $\lambda^4$ -borane, potassium salt (**3.2**, 102.7 mg, 0.4 mmol, 2 equiv) were then added. Anhydrous 2-MeTHF (0.25 mL) was added unless otherwise stated. The mixture was stirred for 2 minutes at room temperature

to form a suspension of fine particulates. The vial was well sealed by Teflon thread tape, and the reaction was heated to 81 °C in a sand bath. The reaction was monitored by TLC. After the reaction was complete, the solution was allowed to cool back to room temperature. Potassium *tert*-butoxide (112 mg, 1 mmol, 5 equiv) was added in several portions (1 equiv at a time, stirred thoroughly before adding the next portion) unless otherwise stated. The reaction was stirred at room temperature for an additional 3-12 hours. The reaction was diluted with diethyl ether (2 mL), then quenched by adding diluted hydrochloric acid (0.2 M) dropwise until both layers turned clear. The aqueous layer was extracted with diethyl ether (3 mL x 3). The combined organic layer was washed with brine and dried with MgSO<sub>4</sub> and the solvent was removed under reduced pressure. The crude reaction mixture was purified via column chromatography on silica gel with appropriate eluents.



**1-((1R,2R)-2',6'-dimethoxy-5-methyl-4'-pentyl-1,2,3,4-tetrahydro-[1,1'-biphenyl]-2-yl)ethan-1-one (3.12).** This reaction was allowed to stir for 12 hours after adding potassium *tert*-butoxide (112 mg, 1 mmol, 5 equiv). The crude reaction mixture was purified via flash column chromatography with 2-5% ethyl acetate in hexanes as the eluent. HPLC Chiralpak AD-H (hexane/*i*-PrOH = 99:1, 0.5 mL/min, UV-190 detector)

**Result** 67.3 mg, 98% yield; 99:1 er; single diastereomer

**<sup>1</sup>H-NMR** (400 MHz, chloroform-*d*)  $\delta$  6.33 (s, 2H), 5.14 (s, 1H), 4.18-4.13 (m, 1H), 3.73 (s, 6H), 3.30-3.24 (m, 1H), 2.52 (t,  $J = 7.9$  Hz, 2H), 2.16-2.09 (m, 1H), 2.00-1.95 (m, 1H), 1.92-1.86 (m, 4H), 1.83-1.72 (m, 1H), 1.65 (s, 3H), 1.62-1.56 (m, 1H), 1.35-1.29 (m, 4H), 0.88 (t,  $J =$

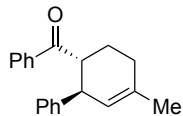
6.9 Hz, 3H) <sup>13</sup>C-NMR (101 MHz, chloroform-d) δ 213.8, 158.5, 142.9, 131.2, 124.9, 117.2, 104.9, 56.0, 51.2, 36.5, 34.7, 31.8, 31.2, 29.6, 28.7, 26.7, 23.4, 22.7, 14.2

All spectral data match literature report.<sup>17</sup>

**This reaction could also be conducted at 1 mmol scale following the procedure below.**

To a 2-dram vial equipped with a stir bar were added 4 Å powdered molecular sieves (125 mg), and the vial was flamed-dried under high vacuum. The vial was cooled to room temperature and backfilled with Argon. The enone **3.1** (276.4 mg, 1 mmol, 1 equiv), (*R*)-3,3'-(C<sub>7</sub>F<sub>7</sub>)<sub>2</sub>-BINOL (143.5 mg, 0.2 mmol, 0.2 equiv), (*Z*)-(4-bromo-2-methylbut-1-en-1-yl)trifluoro-λ<sup>4</sup>-borane potassium salt (**3.2**, 306 mg, 1.2 mmol, 1.2 equiv) were then added. Anhydrous 2-MeTHF (1 mL) was added. The mixture was stirred for 2 minutes at room temperature to form a suspension of fine particulates. The vial was well sealed by Teflon tape, and the reaction was heated to 81 °C in a sand bath. The reaction was monitored by TLC analysis. After the reaction was complete, the solution was cooled back to room temperature. Potassium *tert*-butoxide (336 mg, 3 mmol, 3 equiv) was added in several portions (1 equiv at a time, stirred thoroughly before adding the next portion). The reaction was stirred at room temperature for an additional 12 hours. Then the reaction was first diluted with diethyl ether (5 mL) and then quenched by adding diluted hydrochloric acid (0.2 M) dropwise until both layers turned clear. The aqueous layer was extracted with diethyl ether (10 mL x 3). The combined organic layer was washed with brine then dried with MgSO<sub>4</sub> and the solvent was removed under reduced pressure. The crude reaction mixture was purified via flash column chromatography with 2-5% ethyl acetate in hexanes as the eluent. HPLC Chiralpak AD-H (hexane/*i*-PrOH = 99:1, 0.5 mL/min, UV-190 detector)

**Result** 336.4 mg, 98% yield; 99:1 er; single diastereomer

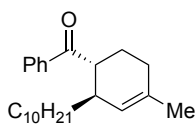


**((1R,2R)-5-methyl-1,2,3,4-tetrahydro-[1,1'-biphenyl]-2-yl)(phenyl)methanone (3.31).**

Reaction was allowed to stir for 5 hours after adding potassium *tert*-butoxide (112 mg, 1 mmol, 5 equiv). The crude reaction mixture was purified via flash column chromatography with 20-30% dichloromethane in hexanes as the eluent. HPLC Chiralpak ID (hexane/*i*-PrOH = 99:1, 1.0 mL/min, UV-254 detector)

**Result** 49.7 mg, 90%; 96:4 er; single diastereomer

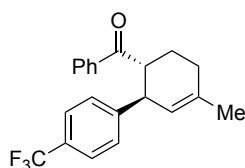
**<sup>1</sup>H-NMR** (500 MHz, chloroform-*d*)  $\delta$  7.69 (d,  $J = 8.4$  Hz, 2H), 7.46-7.43 (m, 1H), 7.32 (t,  $J = 7.7$  Hz, 2H), 7.21-7.17 (m, 4H), 7.11-7.08 (m, 1H), 5.46 (s, 1H), 3.95 (td,  $J = 5.5, 3.2$  Hz, 1H), 3.56-3.51 (m, 1H), 2.27-1.80 (m, 4H), 1.78 (s, 3H) **<sup>13</sup>C-NMR** (126 MHz, chloroform-*d*)  $\delta$  203.6, 145.1, 137.0, 133.9, 132.8, 128.5, 128.4, 128.3, 128.1, 126.4, 124.8, 50.0, 44.2, 29.6, 27.2, 23.7 **IR** 3025, 2925, 1671, 1598, 1447, 1340, 1247, 1075. 817. 799, 779, 756, 705, 694, 671, 628, 540, 521, 504  $\text{cm}^{-1}$  **HRMS-ESI m/z** calcd. for  $\text{C}_{20}\text{H}_{20}\text{O}$   $[\text{M}+\text{Na}]^+$  299.1406, found 299.1404



**((1R,2R)-2-decyl-4-methylcyclohex-3-en-1-yl)(phenyl)methanone (3.32).** The reaction was allowed to stir for 12 hours after the addition of potassium *tert*-butoxide (112 mg, 1 mmol, 5 equiv). The crude reaction mixture was purified via flash column chromatography with 20-30% dichloromethane in hexanes as the eluent. HPLC Chiralcel OJ-H (hexane/*i*-PrOH = 99:1, 1.0 mL/min, UV-254 detector)

**Result** 54.3 mg, 80%; 91:9 er; single diastereomer

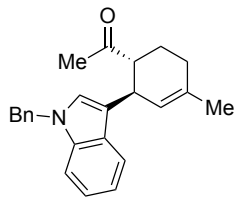
**<sup>1</sup>H-NMR** (600 MHz, chloroform-d)  $\delta$  7.96 (d,  $J = 7.6$  Hz, 2H), 7.55 (t,  $J = 6.9$  Hz, 1H), 7.46 (t,  $J = 7.9$  Hz, 2H), 5.41 (s, 1H), 3.25-3.21 (m, 1H), 2.68 (s, 1H), 2.11-1.63 (m, 7H), 1.33-1.15 (m, 18H), 0.86 (t,  $J = 7.2$  Hz, 3H) **<sup>13</sup>C-NMR** (126 MHz, chloroform-d)  $\delta$  204.3, 137.2, 133.0, 132.8, 128.7, 128.3, 125.1, 47.2, 37.2, 35.1, 32.0, 29.9, 29.9, 29.7, 29.4, 27.5, 26.8, 23.7, 22.8, 14.2 **IR** 2921, 2852, 1680, 1597, 1580, 1446, 1377, 1203, 1001, 950, 840, 806, 779, 699, 672  $\text{cm}^{-1}$  **HRMS-ESI m/z** calcd. for  $\text{C}_{24}\text{H}_{36}\text{O}$   $[\text{M}+\text{H}]^+$  341.2839, found 341.2842



**((1R,2R)-5-methyl-4'-(trifluoromethyl)-1,2,3,4-tetrahydro-[1,1'-biphenyl]-2-yl)(phenyl)met- hanone (3.33).** The reaction was allowed to stir for 8 hours after adding potassium *tert*-butoxide (112 mg, 1 mmol, 5 equiv). The crude reaction mixture was purified via flash column chromatography with 20-30% dichloromethane in hexanes as the eluent. HPLC Chiralcel OD-H (hexane/*i*-PrOH = 90:10, 1.0 mL/min, UV-254 detector)

**Result** 65.0 mg, 95% yield; 97:3 er; single diastereomer

**<sup>1</sup>H-NMR** (400 MHz, chloroform-d)  $\delta$  7.71 (d,  $J = 7.6$  Hz, 2H), 7.49-7.42 (m, 3H), 7.33 (q,  $J = 7.6$  Hz, 4H), 5.40 (s, 1H), 4.04 (d,  $J = 7.6$  Hz, 1H), 3.54-3.49 (m, 1H), 2.29-1.78 (m, 7H) **<sup>13</sup>C-NMR** (101 MHz, chloroform-d)  $\delta$  202.7, 136.5, 134.7, 133.1, 128.7, 128.6, 128.1, 125.4, 125.3, 123.9, 77.4, 77.1, 76.8, 49.9, 43.8, 29.7, 27.3, 23.6 **IR** 2927, 1674, 1617, 1596, 1448, 1423, 1380, 1323, 1163, 1151, 1111, 1068, 979, 837, 796, 775., 758, 701, 680, 610, 536  $\text{cm}^{-1}$  **HRMS-ESI m/z** calcd. for  $\text{C}_{21}\text{H}_{19}\text{F}_3\text{O}$   $[\text{M}+\text{H}]^+$  345.1461, found 345.1465

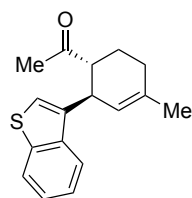


**1-((1R,2R)-2-(1-benzyl-1H-indol-3-yl)-4-methylcyclohex-3-en-1-yl)ethan-1-one**

**(3.34b).** Conjugate addition completed in 2 hours. Reaction was allowed to stir for 12 hours after adding potassium *tert*-butoxide (112 mg, 1 mmol, 5 equiv). The crude reaction mixture was purified via flash column chromatography with 5-15% ethyl acetate in hexanes as the eluent. HPLC Chiralcel OD-H (hexane/*i*-PrOH = 90:10, 1.0 mL/min, UV-254 detector)

**Result** 52.6 mg, 77% yield; 93:7 er; single diastereomer

**<sup>1</sup>H-NMR** (500 MHz, chloroform-*d*)  $\delta$  7.60 (d,  $J = 7.9$  Hz, 1H), 7.29-7.26 (m, 2H), 7.22 (d,  $J = 7.9$  Hz, 2H), 7.16-7.11 (m, 1H), 7.08-7.05 (m, 3H), 6.90 (s, 1H), 5.52 (s, 1H), 5.25 (s, 2H), 3.95 (d,  $J = 8.3$  Hz, 1H), 2.98-2.94 (m, 1H), 2.18-1.93 (m, 6H), 1.86-1.73 (m, 4H) **<sup>13</sup>C-NMR** (126 MHz, chloroform-*d*)  $\delta$  212.7, 137.8, 137.1, 133.1, 128.8, 127.6, 127.0, 126.7, 126.4, 124.6, 121.8, 119.8, 119.0, 118.1, 109.9, 77.4, 77.1, 76.9, 53.6, 50.0, 35.5, 29.8, 29.3, 25.3, 23.5 **IR** 3029, 2922, 1706, 1611, 1559, 1465, 1452, 1354, 1330, 1160, 1014, 954, 908, 804, 747, 694  $\text{cm}^{-1}$  **HRMS-ESI**  $m/z$  calcd. for  $\text{C}_{24}\text{H}_{25}\text{NO}$   $[\text{M}+\text{H}]^+$  344.2009, found 344.2008



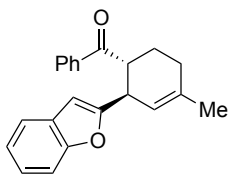
**1-((1R,2R)-2-(benzo[b]thiophen-3-yl)-4-methylcyclohex-3-en-1-yl)ethan-1-one (3.35).**

The reaction was allowed to stir for 12 hours after adding potassium *tert*-butoxide (112 mg, 1 mmol, 5 equiv). The crude reaction mixture was purified via flash column chromatography with

2-5% ethyl acetate in hexanes as the eluent. HPLC Chiralpak ID (hexane/*i*-PrOH = 95:5, 1.0 mL/min, UV-254 detector)

**Result** 44.1 mg, 82% yield; 96:4 er; single diastereomer

**<sup>1</sup>H-NMR** (500 MHz, chloroform-*d*)  $\delta$  7.85-7.83 (m, 1H), 7.75 (dd,  $J = 6.9, 1.9$  Hz, 1H), 7.36-7.31 (m, 2H), 7.10 (s, 1H), 5.46 (q,  $J = 1.4$  Hz, 1H), 4.16 (td,  $J = 4.7, 2.2$  Hz, 1H), 2.96-2.92 (m, 1H), 2.17-1.82 (m, 7H), 1.74 (s, 3H) **<sup>13</sup>C-NMR** (126 MHz, chloroform-*d*)  $\delta$  211.4, 141.1, 139.0, 137.9, 134.1, 124.3, 124.0, 123.1, 123.1, 122.8, 122.2, 52.3, 37.4, 29.3, 28.9, 24.6, 23.6 **IR** 3392, 2922, 1700, 1496, 1457, 1426, 1352, 1253, 1150, 836, 815, 759, 717, 652  $\text{cm}^{-1}$  **HRMS-ESI *m/z*** calcd. for C<sub>17</sub>H<sub>18</sub>OS [M+Na]<sup>+</sup> 293.0971, found 293.0968



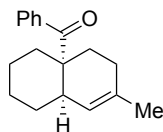
**((1*R*,2*R*)-2-(benzofuran-2-yl)-4-methylcyclohex-3-en-1-yl)(phenyl)methanone (3.36b).**

The reaction was allowed to stir for 3 hours after adding potassium *tert*-butoxide (112 mg, 1 mmol, 5 equiv). Decomposition was observed for a prolonged reaction time. The crude reaction mixture was purified via flash column chromatography with 2-10% ethyl acetate in hexanes as the eluent. HPLC Chiralpak ID (hexane/*i*-PrOH = 90:10, 1.0 mL/min, UV-254 detector)

**Result** 61.0 mg, 97% yield; 94:6 er; single diastereomer

**<sup>1</sup>H-NMR** (500 MHz, chloroform-*d*)  $\delta$  7.90 (d,  $J = 7.3$  Hz, 2H), 7.49 (t,  $J = 7.4$  Hz, 1H), 7.39 (t,  $J = 7.7$  Hz, 3H), 7.33 (d,  $J = 8.0$  Hz, 1H), 7.17-7.10 (m, 2H), 6.38 (s, 1H), 5.59 (s, 1H), 4.22 (d,  $J = 7.7$  Hz, 1H), 3.89-3.85 (m, 1H), 2.24-1.79 (m, 7H) **<sup>13</sup>C-NMR** (126 MHz, chloroform-*d*)  $\delta$  202.4, 160.5, 154.7, 136.4, 135.2, 133.1, 128.7, 128.7, 128.3, 123.4, 122.5, 120.7, 120.5, 111.0, 102.8, 77.4, 77.1, 76.9, 45.7, 37.8, 29.2, 26.4, 23.7 **IR** 3057, 2926, 1676, 1596, 1580, 1472, 1446,

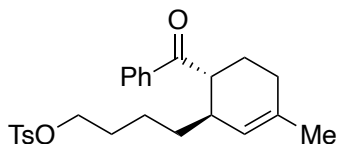
1363, 1290, 1255, 1200, 1159, 1006, 960, 880, 855, 801, 750, 739, 697, 668, 612  $\text{cm}^{-1}$  **HRMS-ESI**  $m/z$  calcd. for  $\text{C}_{22}\text{H}_{20}\text{O}_2$   $[\text{M}+\text{Na}]^+$  339.1356, found 339.1356



**((4aR,8aR)-7-methyl-1,3,4,5,6,8a-hexahydronaphthalen-4a(2H)-yl)(phenyl)methanone (3.41)**. The reaction was allowed to stir for 12 hours after adding potassium *tert*-butoxide (134.4 mg, 1.2 mmol, 6 equiv). The crude reaction mixture was purified via flash column chromatography with 2-5% ethyl acetate in hexanes as the eluent. HPLC Chiralcel OJ-H (hexane/*i*-PrOH = 99:1, 1.0 mL/min, UV-254 detector)

**Result** 35.4 mg, 70%; 90:10 er; dr greater than 25:1. A trace amount of the diastereomer could also be isolated.

**$^1\text{H-NMR}$**  (500 MHz, chloroform-*d*)  $\delta$  7.54 (d,  $J$  = 8.0 Hz, 2H), 7.43 (d,  $J$  = 8.0 Hz, 1H), 7.36 (t,  $J$  = 7.4 Hz, 2H), 5.27 (s, 1H), 2.77 (s, 1H), 2.05-1.72 (m, 6H), 1.63 (d,  $J$  = 14.3 Hz, 4H), 1.50-1.25 (m, 5H)  **$^{13}\text{C-NMR}$**  (126 MHz, chloroform-*d*)  $\delta$  211.1, 140.3, 132.8, 130.2, 128.5, 128.2, 127.9, 127.2, 126.4, 51.0, 36.8, 30.2, 27.8, 23.4, 22.4 **IR** 2924, 2853, 1669, 1596, 1443, 1232, 1176, 1018, 1001, 968, 905, 778, 700, 688, 624  $\text{cm}^{-1}$  **HRMS-ESI**  $m/z$  calcd. for  $\text{C}_{18}\text{H}_{22}\text{O}$   $[\text{M}+\text{H}]^+$  225.1743, found 225.1743

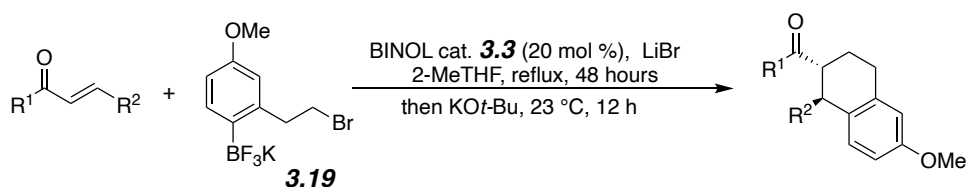


Less than 10 mg of single alkylation product **3.42** was isolated in a control experiment after adding base to the reaction to synthesis **3.41** and stirring for 3 hours.  **$^1\text{H-NMR}$**  (400 MHz,

chloroform-d)  $\delta$  7.93 (d,  $J = 7.1$  Hz, 2H), 7.74 (d,  $J = 8.5$  Hz, 2H), 7.56 (t,  $J = 7.3$  Hz, 1H), 7.47 (t,  $J = 7.6$  Hz, 2H), 7.30 (d,  $J = 8.0$  Hz, 2H), 5.32 (s, 1H), 3.95 (td,  $J = 6.4, 1.1$  Hz, 2H), 3.20-3.14 (m, 1H), 2.69-2.59 (m, 1H), 2.42 (s, 3H), 2.13-2.03 (m, 1H), 1.96-1.88 (m, 2H), 1.67-1.73 (3H), 1.65-1.07 (m, 7H)

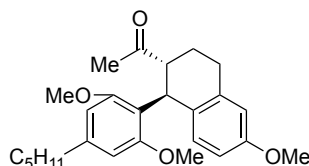
3.5.8

**3.5.8 General procedure of the BINOL-catalyzed conjugate addition tandem enolate alkylation annulation between (2-(2-bromoethyl)-4-methoxyphenyl)trifluoro- $\lambda^4$ -borane, potassium salt (30) and various enones (0.2 mmol scale)**



To a 2-dram vial equipped with a stir bar was added 4 Å powdered molecular sieves (25 mg), and the vial was flamed-dried under high vacuum. The vial was cooled to room temperature and back-filled with Argon. The corresponding enone (0.2 mmol, 1 equiv), (*R*)-3,3'-(C<sub>7</sub>F<sub>7</sub>)<sub>2</sub>-BINOL (28.7 mg, 0.04 mmol, 0.2 equiv), (2-(2-bromoethyl)-4-methoxyphenyl)trifluoro- $\lambda^4$ -borane, and potassium salt (**3.19**, 128.4 mg, 0.4 mmol, 2 equiv) were then added. Anhydrous 2-methyl-THF (0.25 mL) was added unless otherwise stated. The mixture was stirred for 2 minutes at room temperature to form a suspension of fine particulates. The vial was well sealed by Teflon thread tape, and the reaction was heated to 81 °C in a sand bath. The reaction was monitored by TLC analysis. After the reaction was complete, the solution was cooled to room temperature. Potassium *tert*-butoxide (112 mg, 1 mmol, 5 equiv) was added in several portions (1 equiv at a time, stirred thoroughly before adding the next portion) unless otherwise stated. The reaction was stirred at room temperature for an additional 12 hours. The reaction was diluted with diethyl ether (2 mL),

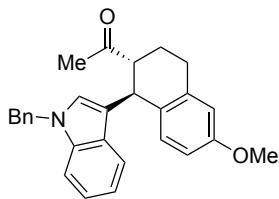
then quenched by adding diluted hydrochloric acid (0.2 M) dropwise until both layers turned clear. The aqueous layer was extracted with diethyl ether (3 mL x 3). The combined organic layer was washed with brine and dried with MgSO<sub>4</sub> and the solvent was removed under reduced pressure. The crude reaction mixture was purified via column chromatography on silica gel with appropriate eluents.



**1-((1S,2R)-1-(2,6-dimethoxy-4-pentylphenyl)-6-methoxy-1,2,3,4-tetrahydronaphthalen-2-yl)-ethan-1-one (3.37).** Reaction was allowed to stir for 12 hours after adding potassium *tert*-butoxide (112 mg, 1 mmol, 5 equiv). The crude reaction mixture was purified via flash column chromatography with 5-20% ethyl acetate in hexanes as the eluent. HPLC Chiralcel OD-H (hexane/*i*-PrOH = 90:10, 1.0 mL/min, UV-254 detector)

**Result** 70.1 mg, 85%; 98:2 er; single diastereomer

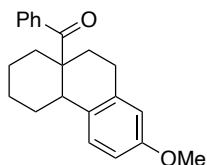
**<sup>1</sup>H-NMR** (400 MHz, chloroform-*d*) δ 6.59-6.58 (m, 2H), 6.50 (dd, *J* = 8.5, 2.8 Hz, 1H), 6.35 (s, 2H), 4.80 (d, *J* = 10.8 Hz, 1H), 3.86-3.44 (m, 10H), 2.99-2.80 (m, 2H), 2.49-2.59 (2H), 2.07-2.01 (m, 1H), 1.94-1.84 (m, 4H), 1.62 (t, *J* = 7.6 Hz, 2H), 1.36-1.30 (m, 4H), 0.89 (t, *J* = 6.9 Hz, 3H) **<sup>13</sup>C-NMR** (126 MHz, chloroform-*d*) δ 212.9, 158.4, 156.9, 143.3, 137.1, 132.3, 128.3, 118.1, 112.7, 111.8, 56.0, 55.2, 52.7, 36.6, 36.4, 31.8, 31.1, 29.8, 28.7, 26.9, 22.7, 14.2 **IR** 2928, 2855, 1707, 1606, 1576, 1498, 1349, 1276, 1254, 1231, 1202, 1114, 1039, 972, 806, 786, 723 cm<sup>-1</sup> **HRMS-ESI m/z** calcd. for C<sub>26</sub>H<sub>34</sub>O<sub>4</sub> [M+Na]<sup>+</sup> 433.2349, found 433.2348



**1-((1S,2R)-1-(1-benzyl-1H-indol-3-yl)-6-methoxy-1,2,3,4-tetrahydronaphthalen-2-yl)ethan-1-one (3.38b).** Conjugate addition completed in 2 hours. Reaction was allowed to stir for 12 hours after adding potassium *tert*-butoxide (112 mg, 1 mmol, 5 equiv). The crude reaction mixture was purified via flash column chromatography with 5-15% ethyl acetate in hexanes as the eluent. HPLC Chiralcel OD-H (hexane/*i*-PrOH = 90:10, 1.0 mL/min, UV-254 detector)

**Result** 42.7 mg, 52% yield; 97:3 er; single diastereomer

**<sup>1</sup>H-NMR** (500 MHz, chloroform-*d*)  $\delta$  7.29-7.24 (m, 2H), 7.20 (dd,  $J = 23.0, 8.1$  Hz, 3H), 7.15-7.09 (m, 1H), 7.05 (d,  $J = 6.9$  Hz, 2H), 6.96 (t,  $J = 7.9$  Hz, 1H), 6.89 (d,  $J = 6.9$  Hz, 2H), 6.66 (d,  $J = 2.6$  Hz, 1H), 6.56 (dd,  $J = 8.6, 2.7$  Hz, 1H), 5.25 (d,  $J = 3.0$  Hz, 2H), 4.56 (d,  $J = 9.3$  Hz, 1H), 3.75 (s, 3H), 3.29-3.24 (m, 1H), 3.05-2.89 (m, 2H), 2.11-1.93 (m, 2H), 1.90 (s, 3H) **<sup>13</sup>C-NMR** (126 MHz, chloroform-*d*)  $\delta$  212.0, 157.6, 137.7, 137.2, 136.7, 130.7, 130.6, 128.8, 127.8, 127.6, 126.7, 126.6, 121.8, 120.1, 119.1, 118.1, 113.0, 112.4, 110.0, 55.2, 54.6, 50.0, 38.3, 30.2, 29.3, 25.5 **IR** 2924, 1706, 1608, 1545, 1464, 1452, 1355, 1330, 1254, 1232, 1154, 1029, 965, 909, 856, 811, 784, 726, 698, 643, 559, 523  $\text{cm}^{-1}$  **HRMS-ESI**  $m/z$  calcd. for  $\text{C}_{28}\text{H}_{27}\text{NO}_2$   $[\text{M}+\text{Na}]^+$  432.1934, found 432.1937



**(2-methoxy-5,6,7,8,9,10-hexahydrophenanthren-8a(4bH)-yl)(phenyl)methanone**

( **mixture of *cis/trans*, 3.45**). The reaction was allowed to stir for 12 hours after adding potassium *tert*-butoxide (134.4 mg, 1.2 mmol, 6 equiv). The crude reaction mixture was purified via flash column chromatography with 5-15% ethyl acetate in hexanes as the eluent. HPLC Chiralpak ID (hexane/*i*-PrOH = 95:5, 1.0 mL/min, UV-254 detector). Diastereomers could be separated effectively using this HPLC condition.

**Result** 41.4 mg, 65% yield; 1:1 dr; 98:2 er for each diastereomer

**NMR** contains a pair of diastereomers. Spectra attached in appendix. **IR** 2925, 2851, 1700, 1606, 1569, 1497, 1463, 1446, 1287, 1268, 1254, 1231, 1196, 1116, 1070, 1031, 911, 872, 770, 700 cm<sup>-1</sup> **HRMS-ESI m/z** calcd. for C<sub>22</sub>H<sub>24</sub>O<sub>2</sub> [M+Na]<sup>+</sup> 343.1669, found 343.1670

### 3.6 Bibliography

1. Le, P. Q.; Nguyen, T. S.; May, J. A. A General Method for the Enantioselective Synthesis of Chiral Heterocycles. *Org. Lett.* **2012**, *14*, 6104-6107.
2. Shih, J.-L.; Nguyen, T. S.; May, J. A. Organocatalyzed Asymmetric Conjugate Addition of Heteroaryl and Aryl Trifluoroborates: a Synthetic Strategy for Discoipyrrole D. *Angew. Chem. Int. Ed.* **2015**, *54*, 9931-9935
3. a) Pace, V.; Hoyos, P.; Castoldi, L.; de María, P. D.; Alcántara, A. R. 2-Methyltetrahydrofuran (2-MeTHF): A Biomass-Derived Solvent with Broad Application in Organic Chemistry. *ChemSusChem*, **2012**, *5*, 1396–1379; b) Pellis, A.; Byrne, F. P.; Sherwood, J.; Vastano, M.;

Comerford, J. W.; Farmer, T. J. Safer bio-based solvents to replace toluene and tetrahydrofuran for the biocatalyzed synthesis of polyesters. *Green Chem*, **2019**, *21*, 1686–1694

4. Please see Experimental Section of time screen.

5. Nguyen, T. S.; Yang, M. S.; May, J. A. Experimental Mechanistic Insight Into The BINOL-catalyzed Enantioselective Conjugate Addition of Boronates to Enones. *Tetrahedron Lett.* **2015**, *56*, 3337–3341.

6. Brooks, B.; Hiller, N.; May, J. A. Reaction Rate Differences Between Organotrifluoroborates And Boronic Acids in BINOL-catalyzed Conjugate Addition to Enones. *Tetrahedron Lett.* **2021**, *83*, 153412.

7. Worob, A.; Wenthur, C. DARK Classics in Chemical Neuroscience: Synthetic Cannabinoids (Spice/K2). *ACS Chem. Neurosci.* **2020**, *11*, 3881–3892.

8. Banister, S. D.; Moir, M.; Stuart, J.; Kevin, R. C.; Wood, K. E.; Longworth, M.; Wilkinson, S. M.; Beinat, C.; Buchanan, A. S.; Glass, M.; Connor, M.; McGregor, I. S.; Kassiou, M. Pharmacology of Indole and Indazole Synthetic Cannabinoid Designer Drugs AB-FUBINACA, ADB-FUBINACA, AB-PINACA, ADB-PINACA, 5F-AB-PINACA, 5F-ADB-PINACA, ADBICA, and 5F-ADBICA. *ACS Chem. Neurosci.* **2015**, *6*, 1546–1559.

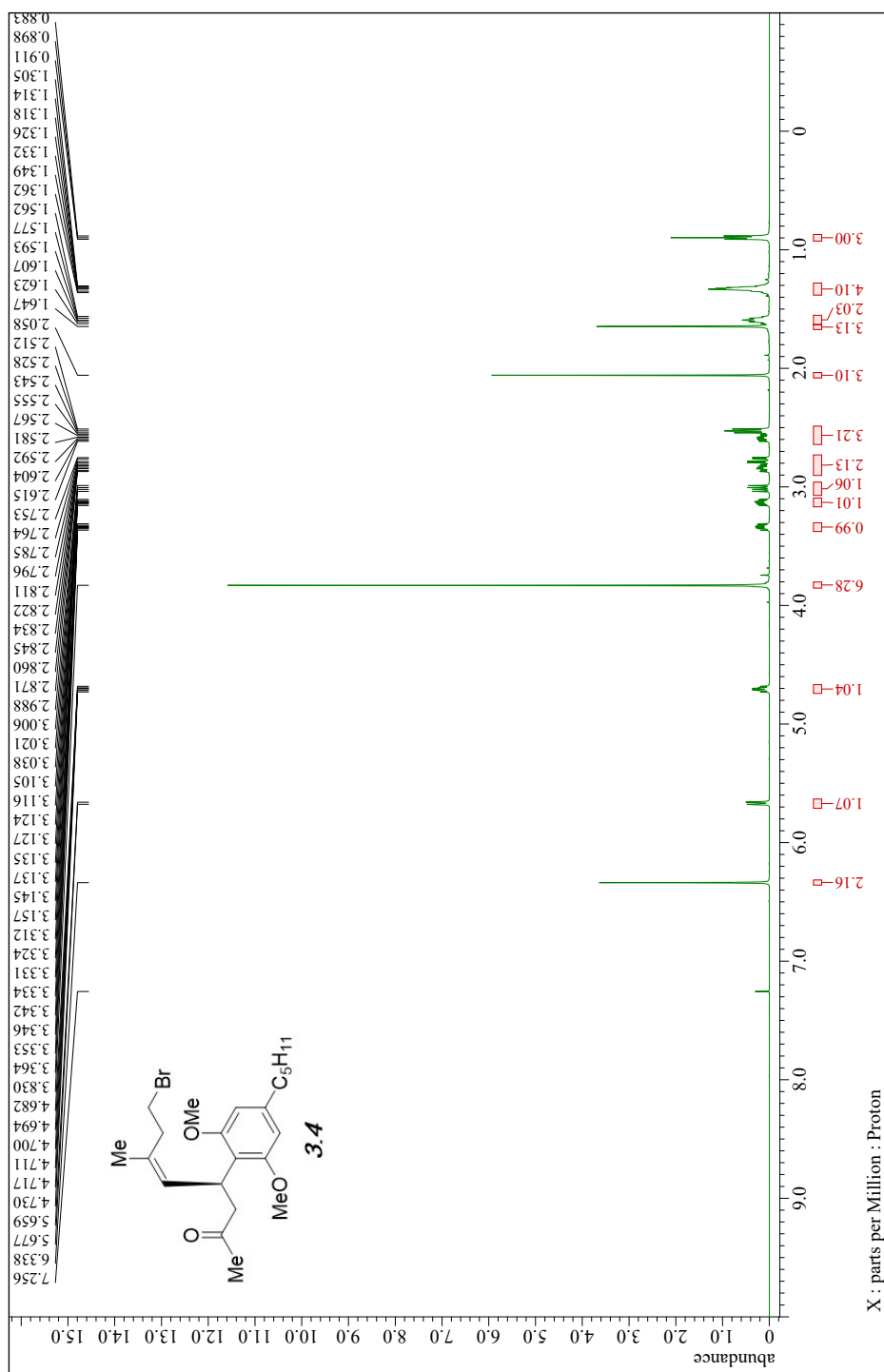
9. Wube, A. A.; Bucar, F.; Hochfellner, C.; Blunder, M.; Bauer, R. Synthesis of *N*-substituted 2-[(1*E*)-alkenyl]-4-(1*H*)-quinone Derivatives as Antimycobacterial Agents Against Non-tubercular Mycobacteria. *Eur. J. Med. Chem.* **2011**, *46*, 2091–2101.

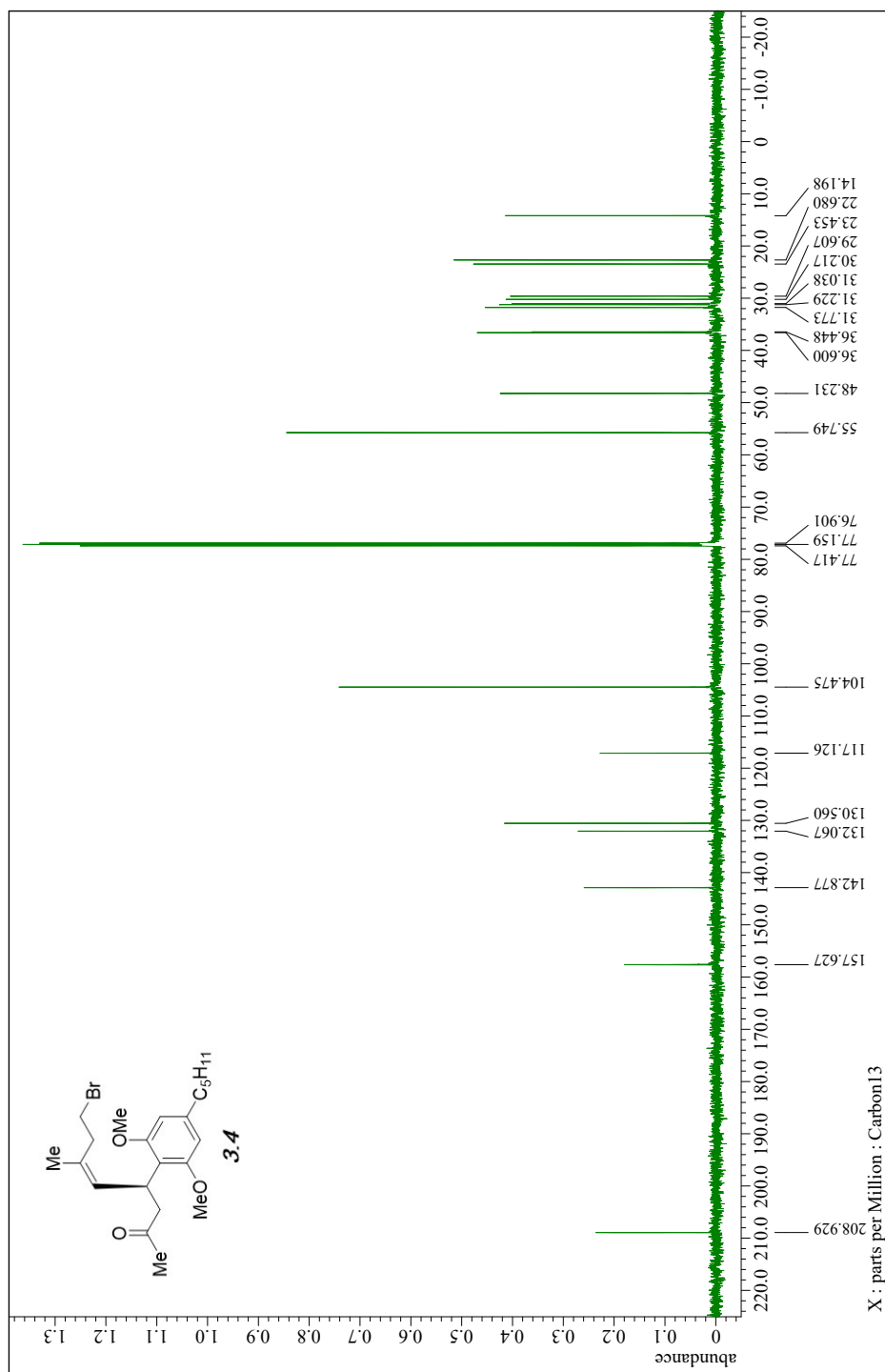
10. Nguyen, T. N.; Nguyen, T. S.; May, J. A. Bronsted Acid Catalyzed Homoconjugate Addition of Organotrifluoroborates to Arylated Cyclopropyl Ketones. *Org. Lett.* **2016**, *18*, 3786–3789.

11. Altowyan, M. S.; Barakat, A.; Al-Majid, A. M.; Al-Ghulikah, H. A. Spiroindolone Analogues as Potential Hypoglycemic with Dual Inhibitory Activity on  $\alpha$ -Amylase and  $\alpha$ -Glucosidase. *Molecules* **2019**, *24*, 2342.
12. Tan, Y.; Luo, S.; Li, D.; Zhang, N.; Jia, S.; Liu, Y.; Qin, W.; Song, C. E.; Yan, H. Enantioselective Synthesis of anti-syn-Trihalides and anti-syn-anti-Tetrahalides via Asymmetric  $\beta$ -Elimination. *J. Am. Chem. Soc.* **2017**, *139*, 6431–6436.
13. Jiang, Q.; Jia, J.; Xu, B.; Zhao, A.; Guo, C.-C. Iron-Facilitated Oxidative Radical Decarboxylative Cross-Coupling between  $\alpha$ -Oxocarboxylic Acids and Acrylic Acides: An Approach to  $\alpha,\beta$ -Unsaturated Carbonyls. *J. Org. Chem.* **2015**, *80*, 3586–3596.
14. Borjesson, L.; Welch, C. J. Synthesis of 2-Hydroxymethyl-1-oxaquinolizidine. *Tetrahedron*, **1992**, *48*, 6325–6334.
15. Trost, B. M.; Dogra, K. Synthesis of (–)- $\Delta^9$ -trans-Tetrahydrocannabinol: Stereocontrol via Mo-Catalyzed Asymmetric Allylic Alkylation Reaction. *Org. Lett.* **2007**, *9*, 861–863.
16. Ballerini, E.; Minuti, L.; Piermatti, O. High-Pressure Diels-Alder Cycloadditions between Benzylideneacetones and 1,3-Butadienes: Application to the Synthesis of (R,R)-(–)- and (S,S)-(+)- $\Delta^8$ -Tetrahydrocannabinol. *J. Org. Chem.* **2020**, *75*, 4251–4260.
17. Shultz, Z. P.; Lawrence, G. A.; Jacobson, J. M.; Cruz, E. J.; Leahy, J. W. Enantioselective Total Synthesis of Cannabinoids—A Route for Analogue Development. *Org. Lett.* **2018**, *20*, 381–384.

## **Chapter 3**

## **Appendix**

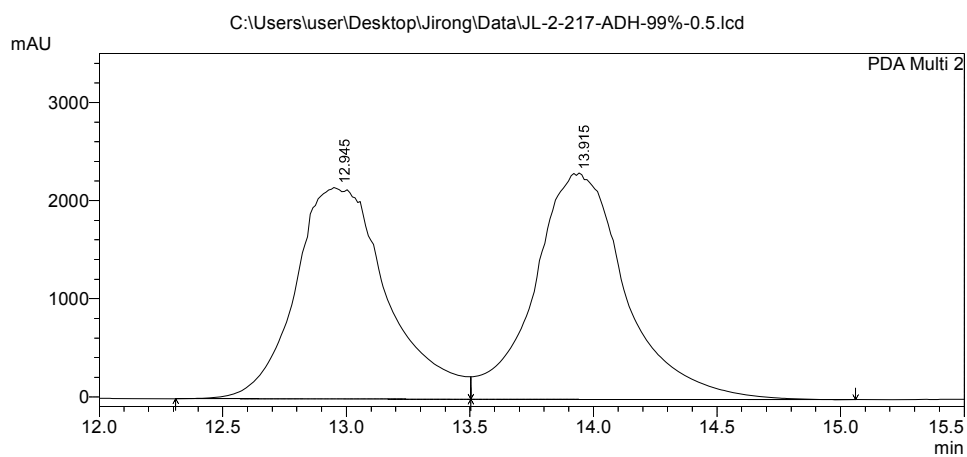




## ==== Shimadzu LcSolution Analysis Report ====

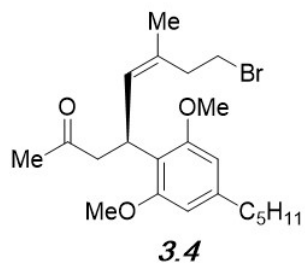
C:\Users\user\Desktop\Jirong\Data\JL-2-217-ADH-99%-0.5.lcd  
Acquired by : Admin  
Sample Name : JL-2-217-ADH-99%-0.5  
Sample ID : JL-2-217-ADH-99%-0.5  
Tray# : 1  
Vial # : 8  
Injection Volume : 5 uL  
Data File Name : JL-2-217-ADH-99%-0.5.lcd  
Method File Name : pos2-99%\_20min\_0.5\_D2.lcm  
Batch File Name : Batch table C2\_99%\_20min\_0.5\_D2.lcb  
Report File Name : Default.lcr  
Data Acquired : 6/23/2020 2:05:04 PM  
Data Processed : 7/19/2021 2:49:56 PM

### <Chromatogram>



PeakTable

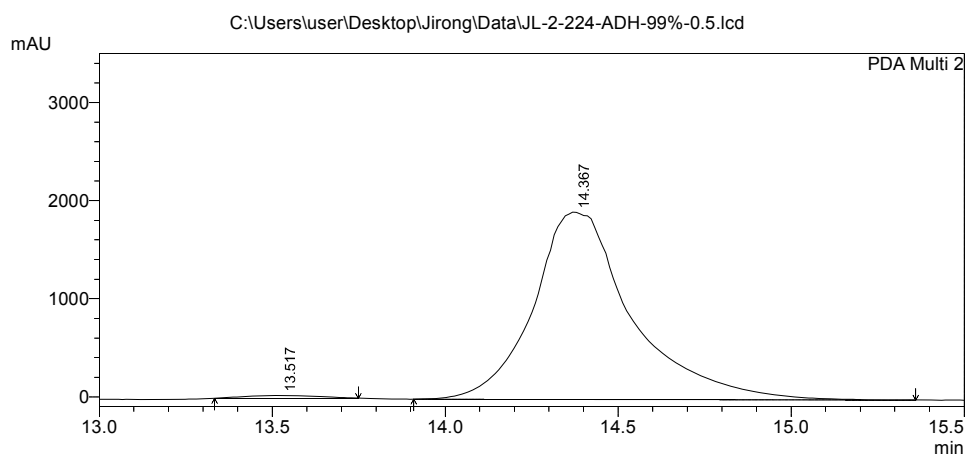
Peak#	Ret. Time	Area	Height	Area %	Height %
1	12.945	56167812	2156526	48.623	48.366
2	13.915	59348233	2302212	51.377	51.634
Total		115516045	4458738	100.000	100.000



## ==== Shimadzu LCsolution Analysis Report ====

C:\Users\user\Desktop\Jirong\Data\JL-2-224-ADH-99%-0.5.lcd  
Acquired by : Admin  
Sample Name : JL-2-224-ADH-99%-0.5  
Sample ID : JL-2-224-ADH-99%-0.5  
Tray# : 1  
Vial # : 9  
Injection Volume : 5 uL  
Data File Name : JL-2-224-ADH-99%-0.5.lcd  
Method File Name : pos2-99%\_20min\_0.5\_D2.lcm  
Batch File Name : Batch table C2\_99%\_20min\_0.5\_D2.lcb  
Report File Name : Default.lcr  
Data Acquired : 6/24/2020 10:09:43 AM  
Data Processed : 7/19/2021 2:47:04 PM

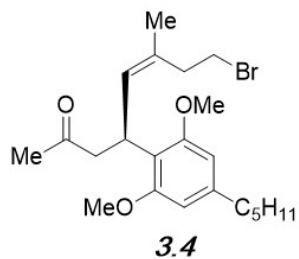
### <Chromatogram>

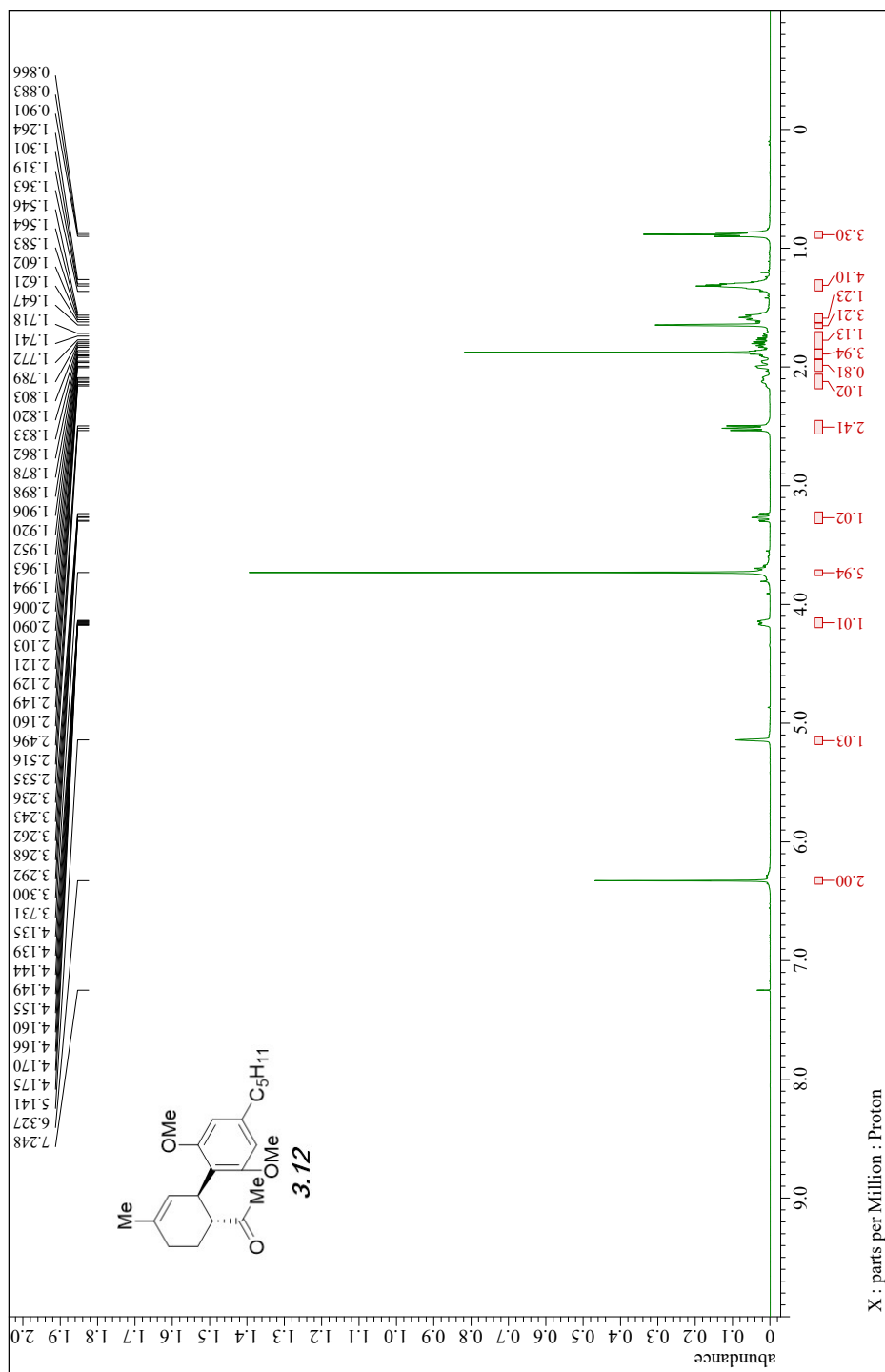


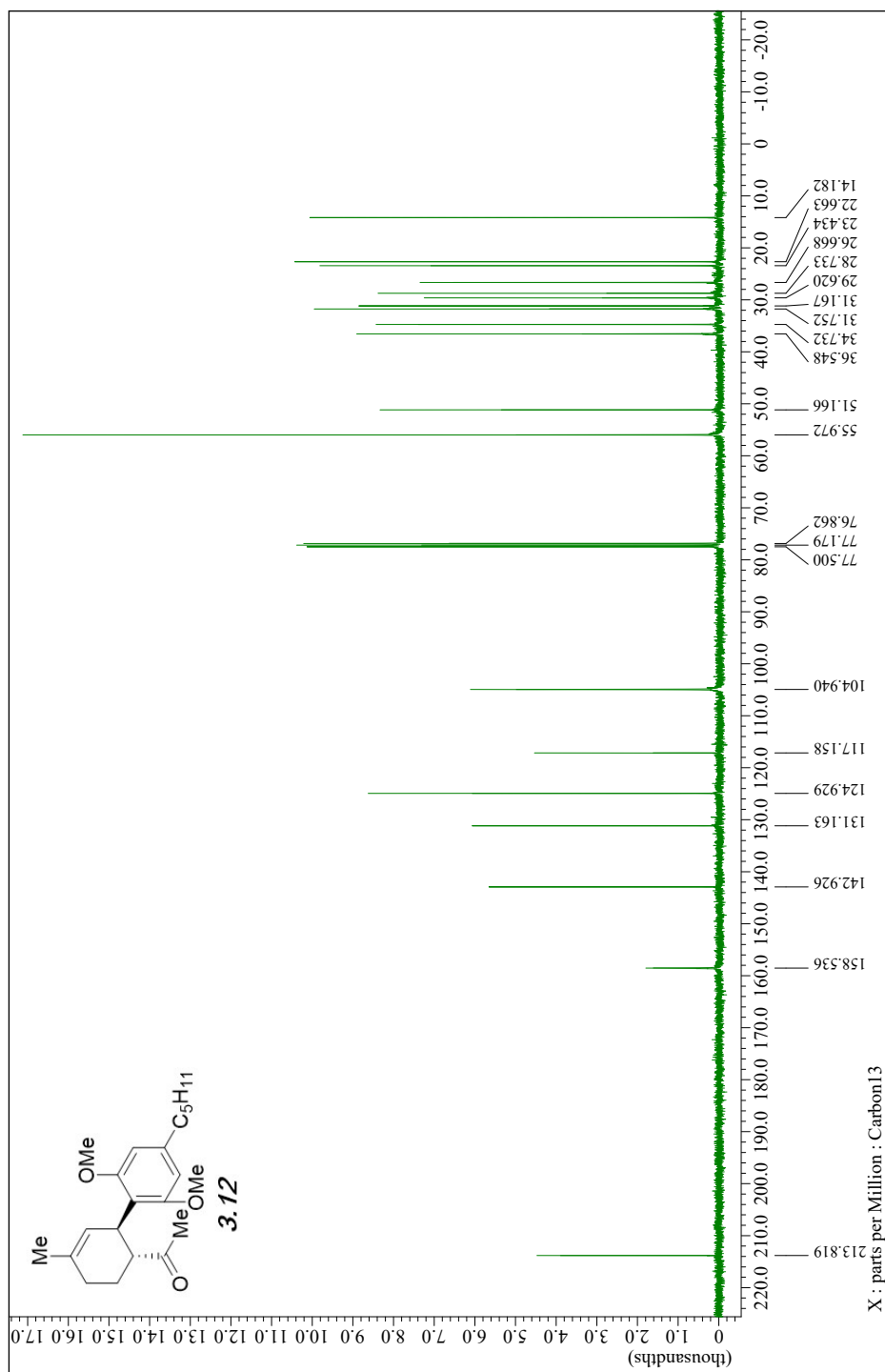
PeakTable

PDA Ch2 190nm 4nm

Peak#	Ret. Time	Area	Height	Area %	Height %
1	13.517	404778	27954	1.057	1.442
2	14.367	37897677	1910273	98.943	98.558
Total		38302455	1938227	100.000	100.000



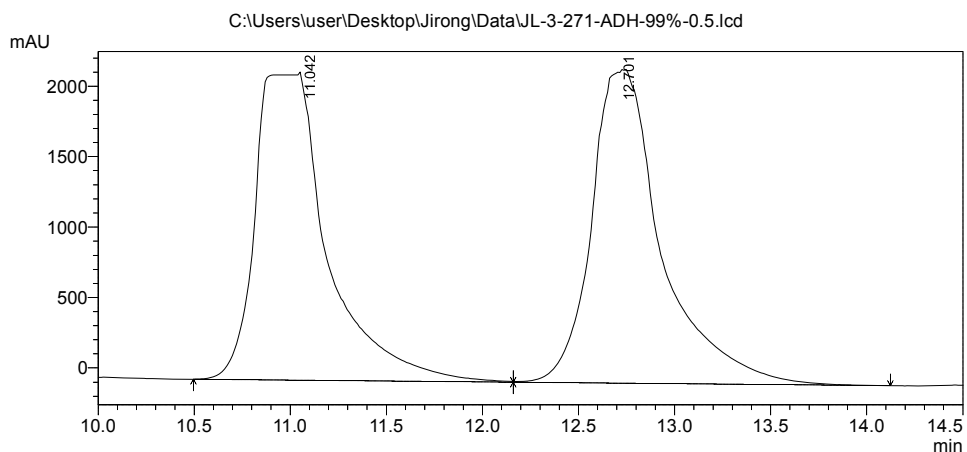




## ==== Shimadzu LcSolution Analysis Report ====

C:\Users\user\Desktop\Jirong\Data\JL-3-271-ADH-99%-0.5.lcd  
 Acquired by : Admin  
 Sample Name : JL-3-271-ADH-99%-0.5  
 Sample ID : JL-3-271-ADH-99%-0.5  
 Tray# : 1  
 Vial # : 15  
 Injection Volume : 5 uL  
 Data File Name : JL-3-271-ADH-99%-0.5.lcd  
 Method File Name : pos2-99%\_20min\_0.5\_D2.lcm  
 Batch File Name : Batch table C2\_99%\_20min\_0.5\_D2.lcb  
 Report File Name : Default.lcr  
 Data Acquired : 7/1/2021 10:40:35 AM  
 Data Processed : 7/2/2021 11:04:52 AM

### <Chromatogram>

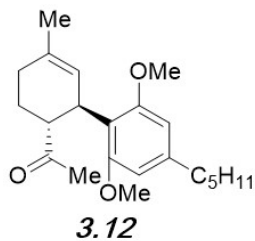


1 PDA Multi 2/190nm 4nm

PeakTable

PDA Ch2 190nm 4nm

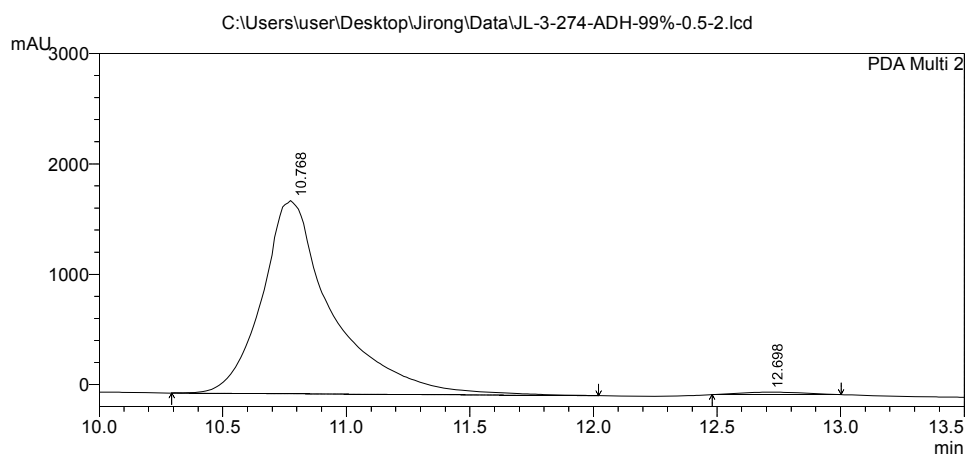
Peak#	Ret. Time	Area	Height	Area %	Height %
1	11.042	56791413	2187254	50.104	49.765
2	12.701	56555028	2207935	49.896	50.235
Total		113346441	4395189	100.000	100.000



## ==== Shimadzu LCsolution Analysis Report ====

C:\Users\user\Desktop\Jirong\Data\JL-3-274-ADH-99%-0.5-2.lcd  
 Acquired by : Admin  
 Sample Name : JL-3-274-ADH-99%-0.5  
 Sample ID : JL-3-274-ADH-99%-0.5  
 Tray# : 1  
 Vial # : 15  
 Injection Volume : 5 uL  
 Data File Name : JL-3-274-ADH-99%-0.5-2.lcd  
 Method File Name : pos2-99%\_20min\_0.5\_D2.lcm  
 Batch File Name : Batch table C2\_99%\_20min\_0.5\_D2.lcb  
 Report File Name : Default.lcr  
 Data Acquired : 7/9/2021 3:55:16 PM  
 Data Processed : 7/9/2021 4:15:55 PM

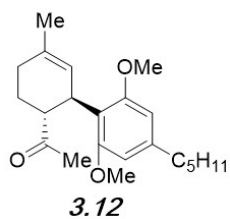
### <Chromatogram>

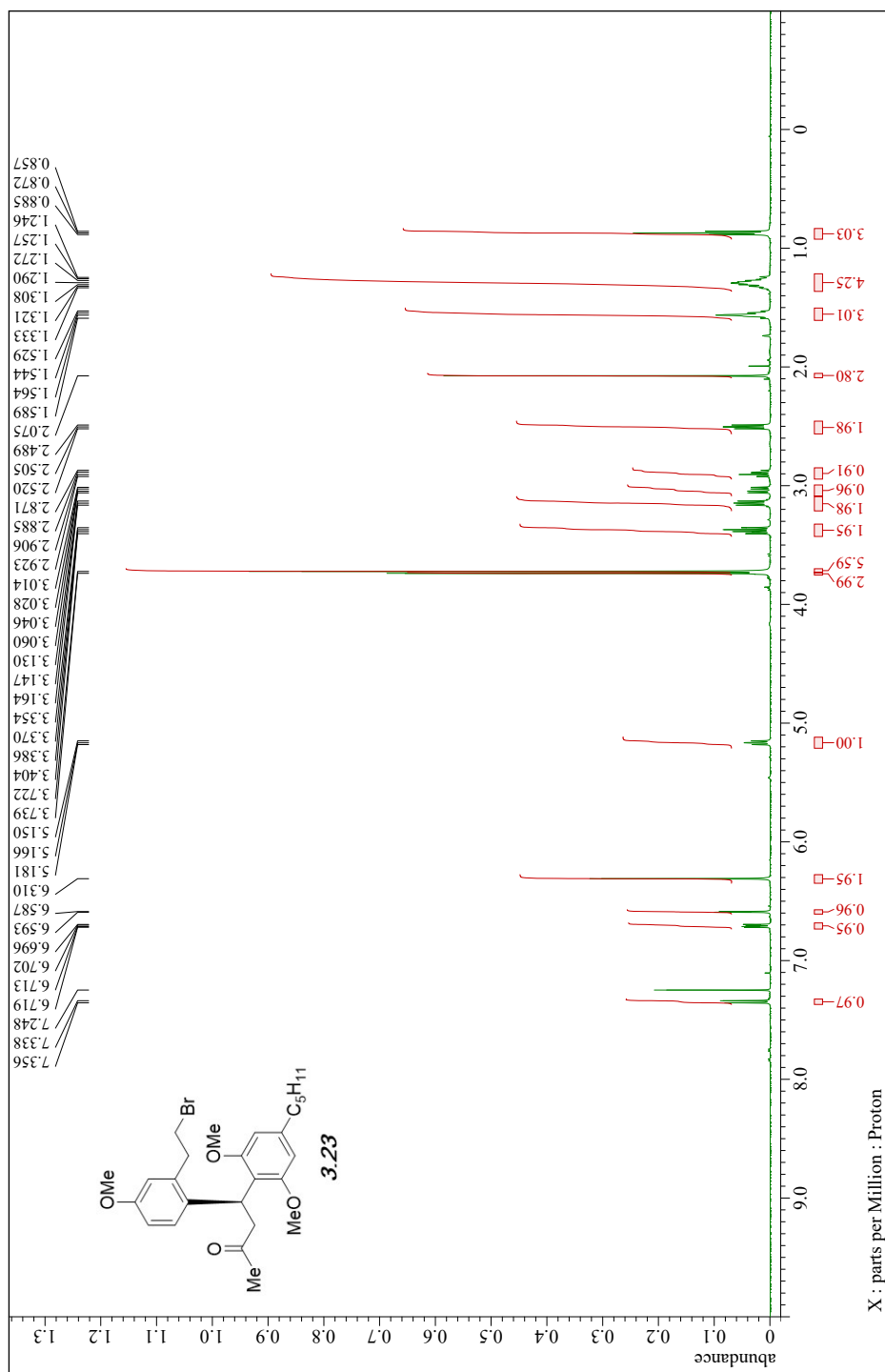


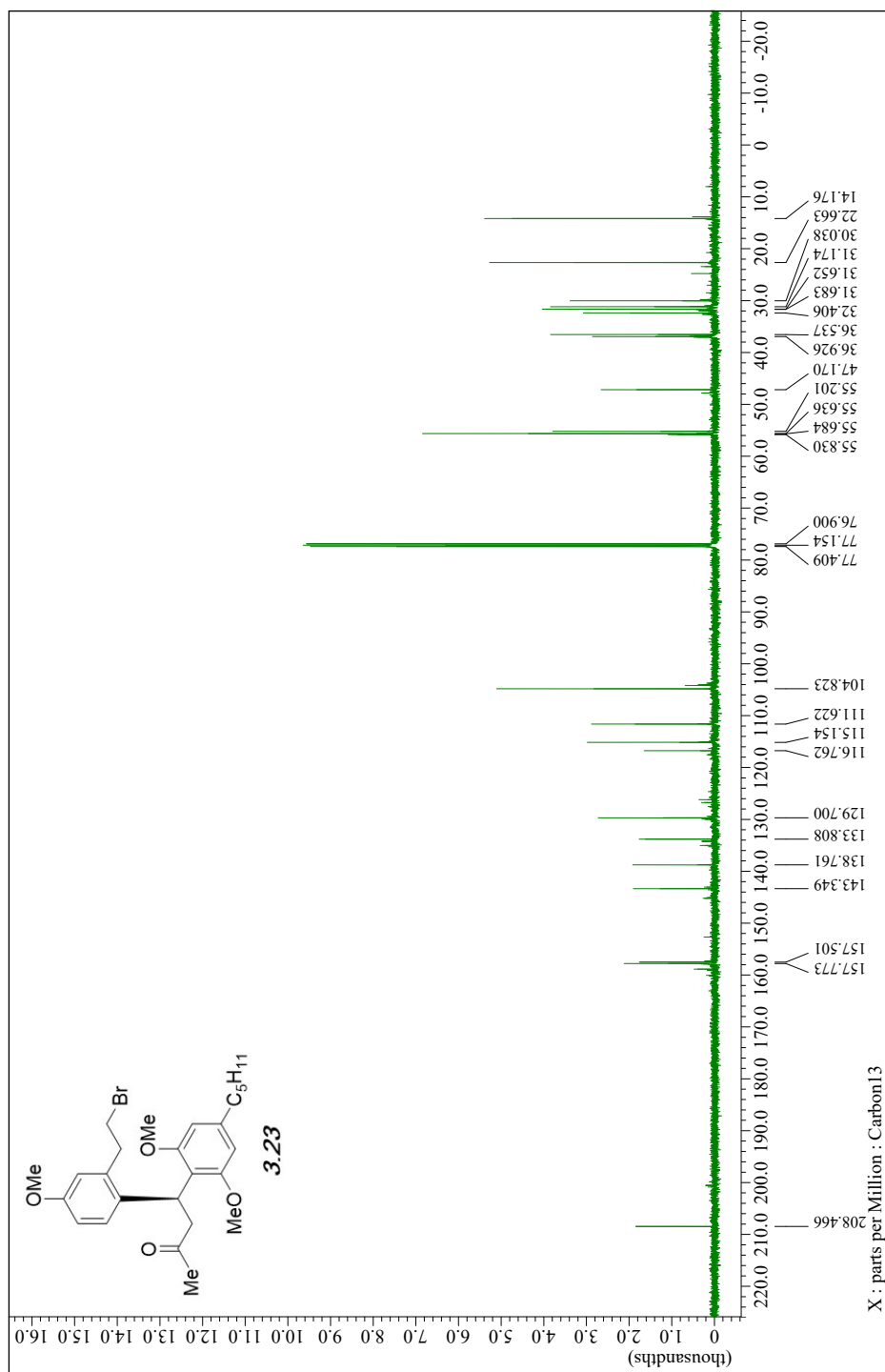
PeakTable

PDA Ch2 190nm 4nm

Peak#	Ret. Time	Area	Height	Area %	Height %
1	10.768	34950486	1751437	98.823	98.733
2	12.698	416217	22482	1.177	1.267
Total		35366703	1773919	100.000	100.000



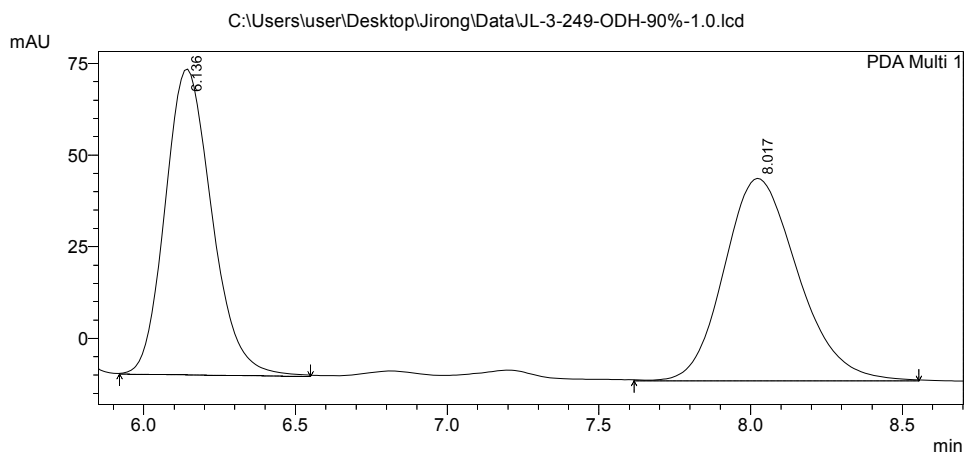




## ==== Shimadzu LCsolution Analysis Report ====

C:\Users\user\Desktop\Jirong\Data\JL-3-249-ODH-90%-1.0.lcd  
 Acquired by : Admin  
 Sample Name : JL-3-249-ODH-90%-1.0  
 Sample ID : JL-3-249-ODH-90%-1.0  
 Tray# : 1  
 Vial # : 15  
 Injection Volume : 10 uL  
 Data File Name : JL-3-249-ODH-90%-1.0.lcd  
 Method File Name : pos5\_90%\_60min\_1.0\_D2.lcm  
 Batch File Name : Batch\_table\_C5-90\_60min\_1.0\_d2.lcb  
 Report File Name : Default.lcr  
 Data Acquired : 6/5/2021 12:37:57 PM  
 Data Processed : 8/12/2021 11:33:29 AM

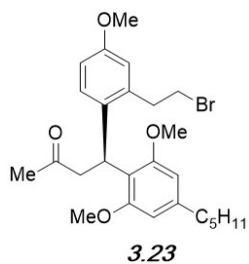
### <Chromatogram>



1 PDA Multi 1/254nm 4nm

PeakTable

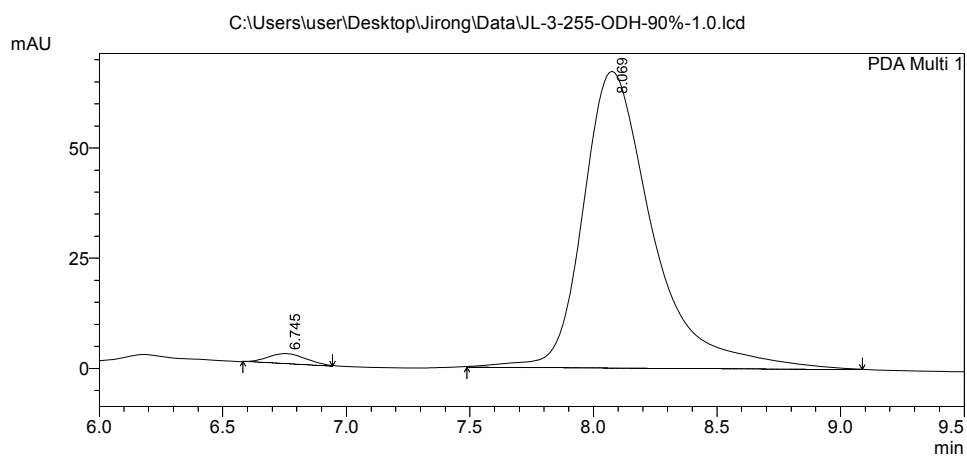
Peak#	Ret. Time	Area	Height	Area %	Height %
1	6.136	894323	83367	48.905	60.170
2	8.017	934384	55187	51.095	39.830
Total		1828707	138554	100.000	100.000



## ==== Shimadzu LCsolution Analysis Report ====

C:\Users\user\Desktop\Jirong\Data\JL-3-255-ODH-90%-1.0.lcd  
 Acquired by : Admin  
 Sample Name : JL-3-255-ODH-90%-1.0  
 Sample ID : JL-3-255-ODH-90%-1.0  
 Tray# : 1  
 Vial # : 15  
 Injection Volume : 10 uL  
 Data File Name : JL-3-255-ODH-90%-1.0.lcd  
 Method File Name : pos5\_90%\_60min\_1.0\_D2.lcm  
 Batch File Name : Batch\_table\_C5-90\_60min\_1.0\_d2.lcb  
 Report File Name : Default.lcr  
 Data Acquired : 6/23/2021 1:13:13 PM  
 Data Processed : 6/23/2021 2:01:05 PM

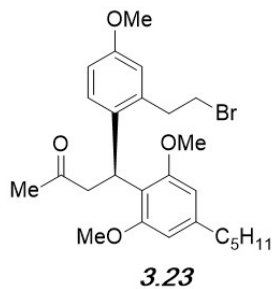
### <Chromatogram>

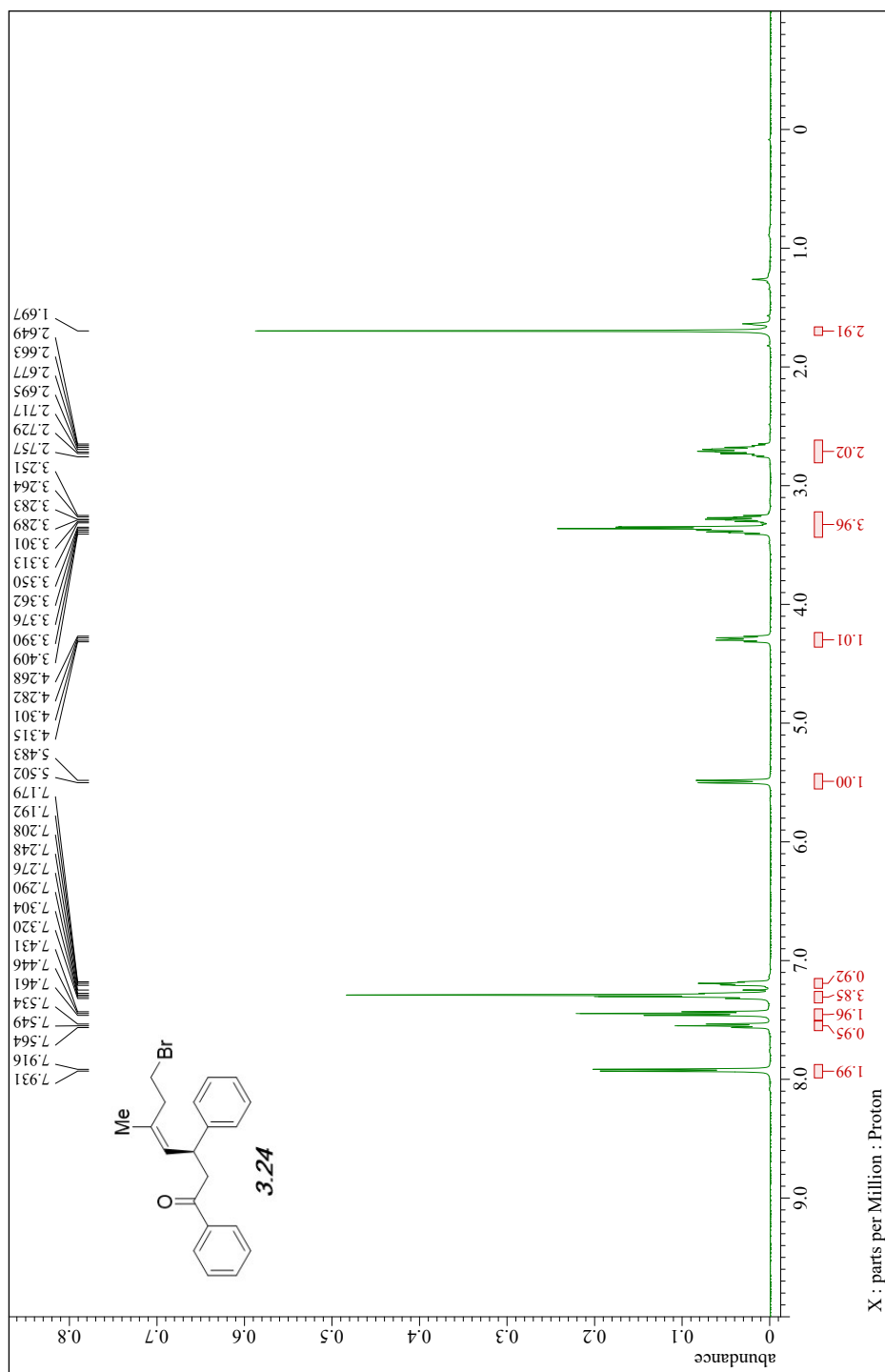


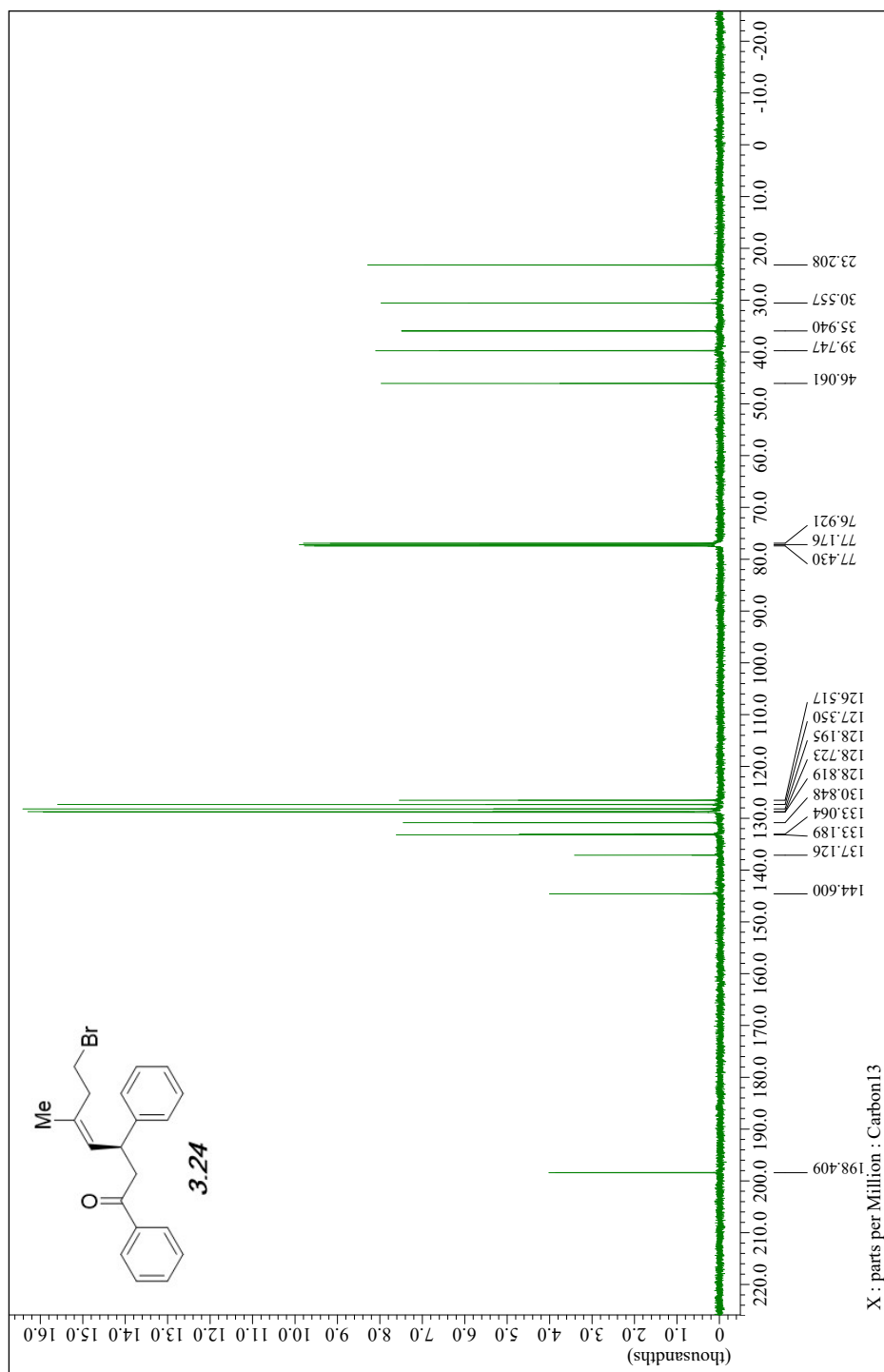
PeakTable

PDA Ch1 254nm 4nm

Peak#	Ret. Time	Area	Height	Area %	Height %
1	6.745	23071	2209	1.715	3.174
2	8.069	1322128	67381	98.285	96.826
Total		1345199	69590	100.000	100.000



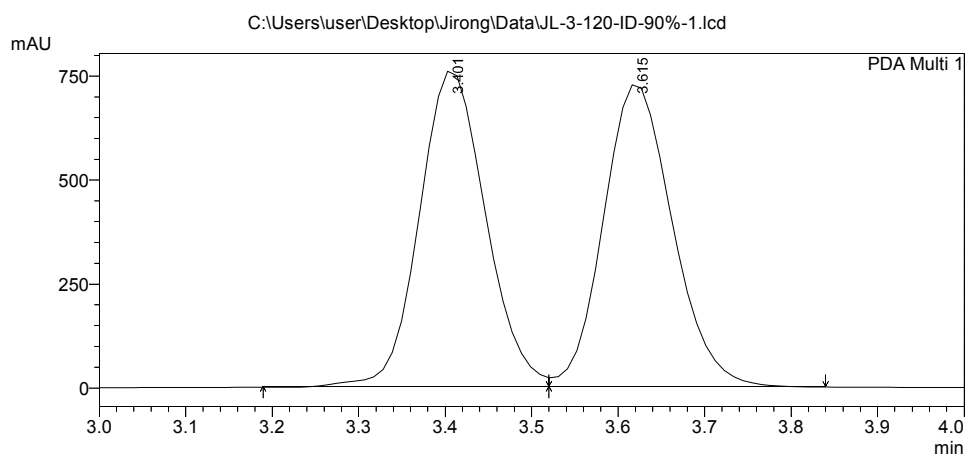




# ==== Shimadzu LcSolution Analysis Report ====

C:\Users\user\Desktop\Jirong\Data\JL-3-120-ID-90%-1.lcd  
Acquired by : Admin  
Sample Name : JL-3-120-ID-90%-1  
Sample ID : JL-3-120-ID-90%-1  
Tray# : 1  
Vial # : 1  
Injection Volume : 10 uL  
Data File Name : JL-3-120-ID-90%-1.lcd  
Method File Name : pos3-90%\_60MIN\_1.0\_D2.lcm  
Batch File Name : Batch table C3\_90%\_60min\_1.0\_D2.lcb  
Report File Name : Default.lcr  
Data Acquired : 4/16/2021 11:17:47 AM  
Data Processed : 9/1/2021 1:47:40 PM

## <Chromatogram>

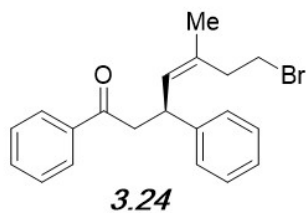


1 PDA Multi 1/254nm 4nm

PeakTable

PDA Ch1 254nm 4nm

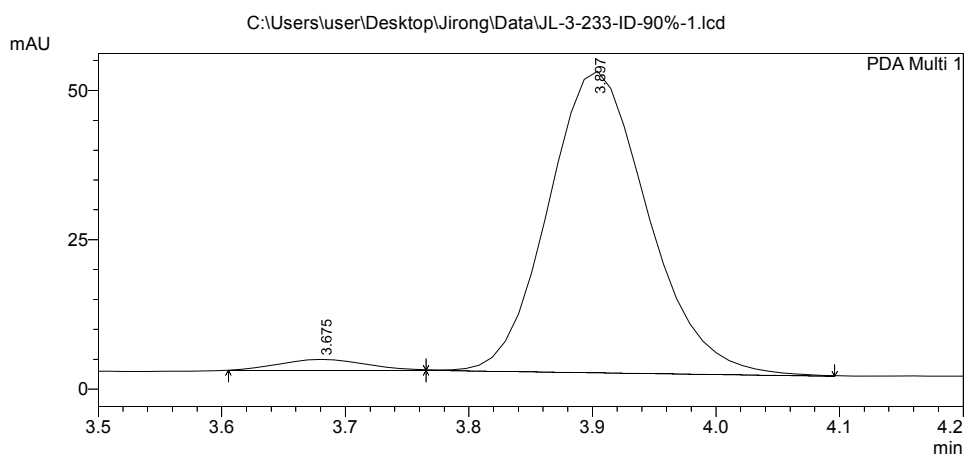
Peak#	Ret. Time	Area	Height	Area %	Height %
1	3.401	4036802	757744	50.104	51.100
2	3.615	4020024	725117	49.896	48.900
Total		8056826	1482862	100.000	100.000



# ==== Shimadzu LCsolution Analysis Report ====

C:\Users\user\Desktop\Jirong\Data\JL-3-233-ID-90%-1.lcd  
Acquired by : Admin  
Sample Name : JL-3-233-ID-90%-1  
Sample ID : JL-3-233-ID-90%-1  
Tray# : 1  
Vial # : 15  
Injection Volume : 10 uL  
Data File Name : JL-3-233-ID-90%-1.lcd  
Method File Name : pos3-90%\_10MIN\_1\_d2.lcm  
Batch File Name : Batch table C3\_90%\_10min\_1.0\_D2.lcb  
Report File Name : Default.lcr  
Data Acquired : 5/12/2021 3:53:45 PM  
Data Processed : 5/27/2021 2:36:22 PM

## <Chromatogram>

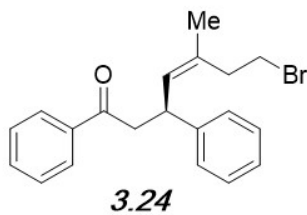


1 PDA Multi 1/254nm 4nm

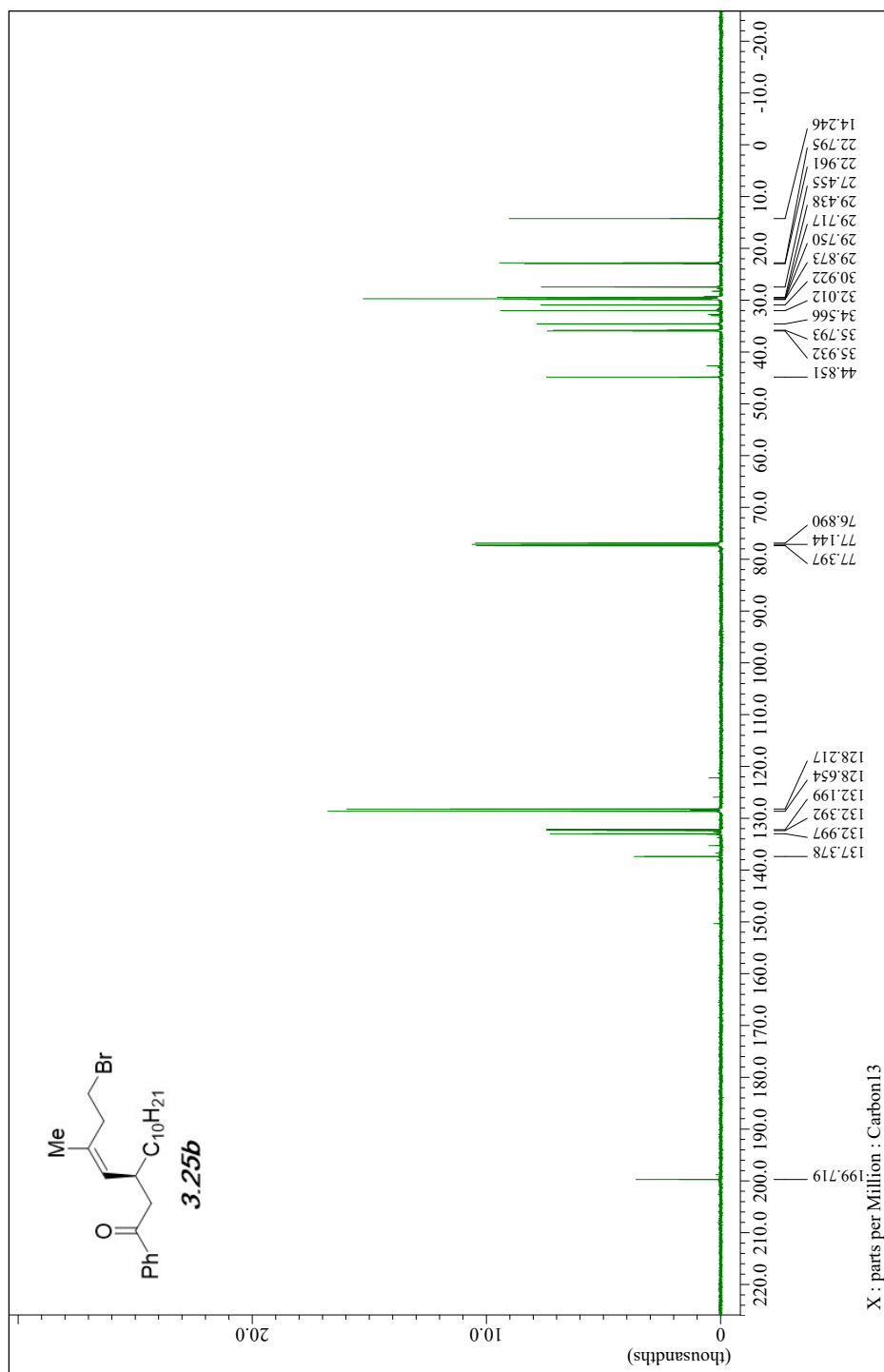
PeakTable

PDA Ch1 254nm 4nm

Peak#	Ret. Time	Area	Height	Area %	Height %
1	3.675	9143	1867	3.127	3.565
2	3.897	283212	50494	96.873	96.435
Total		292356	52361	100.000	100.000



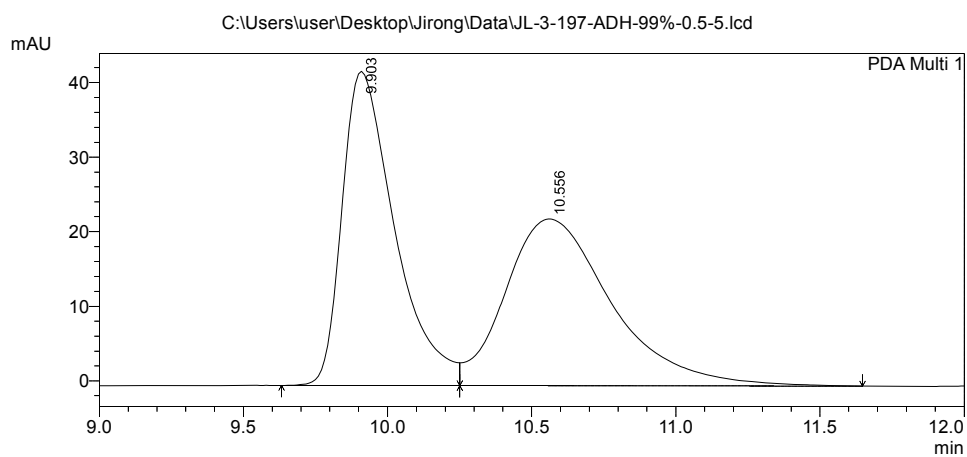




## ==== Shimadzu LCsolution Analysis Report ====

C:\Users\user\Desktop\Jirong\Data\JL-3-197-ADH-99%-0.5-5.lcd  
 Acquired by : Admin  
 Sample Name : JL-3-197-ADH-99%-0.5  
 Sample ID : JL-3-197-ADH-99%-0.5  
 Tray# : 1  
 Vial # : 15  
 Injection Volume : 5 uL  
 Data File Name : JL-3-197-ADH-99%-0.5-5.lcd  
 Method File Name : pos2-99%\_20min\_0.5\_D2.lcm  
 Batch File Name : Batch table C2\_99%\_20min\_0.5\_D2.lcb  
 Report File Name : Default.lcr  
 Data Acquired : 5/26/2021 12:04:09 PM  
 Data Processed : 6/16/2021 12:13:44 PM

### <Chromatogram>

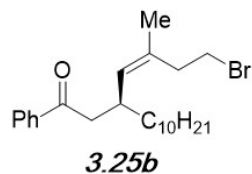


1 PDA Multi 1/254nm 4nm

PeakTable

PDA Ch1 254nm 4nm

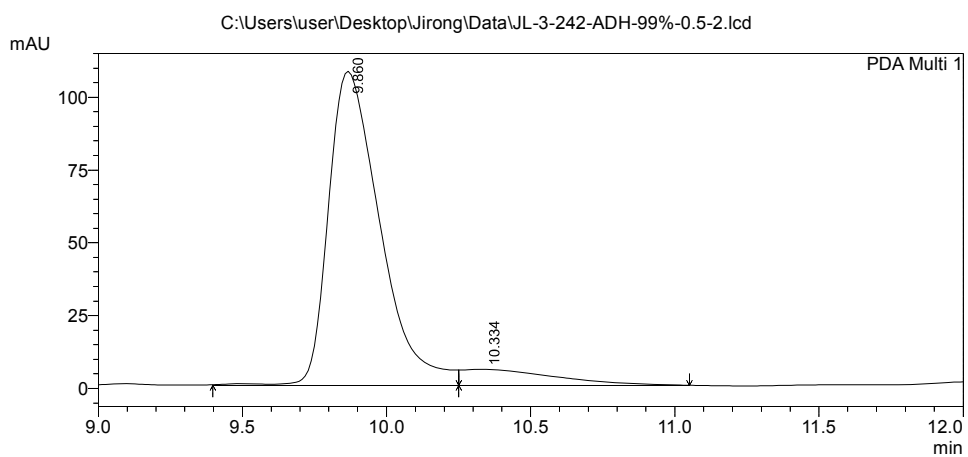
Peak#	Ret. Time	Area	Height	Area %	Height %
1	9.903	535413	42140	48.316	65.326
2	10.556	572740	22367	51.684	34.674
Total		1108154	64506	100.000	100.000



## ==== Shimadzu LCsolution Analysis Report ====

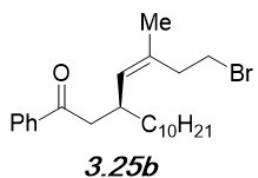
C:\Users\user\Desktop\Jirong\Data\JL-3-242-ADH-99%-0.5-2.lcd  
 Acquired by : Admin  
 Sample Name : JL-3-242-ADH-99%-0.5  
 Sample ID : JL-3-242-ADH-99%-0.5  
 Tray# : 1  
 Vial # : 15  
 Injection Volume : 5 uL  
 Data File Name : JL-3-242-ADH-99%-0.5-2.lcd  
 Method File Name : pos2-99%\_20min\_0.5\_D2.lcm  
 Batch File Name : Batch table C2\_99%\_20min\_0.5\_D2.lcb  
 Report File Name : Default.lcr  
 Data Acquired : 5/26/2021 2:45:46 PM  
 Data Processed : 5/26/2021 3:05:51 PM

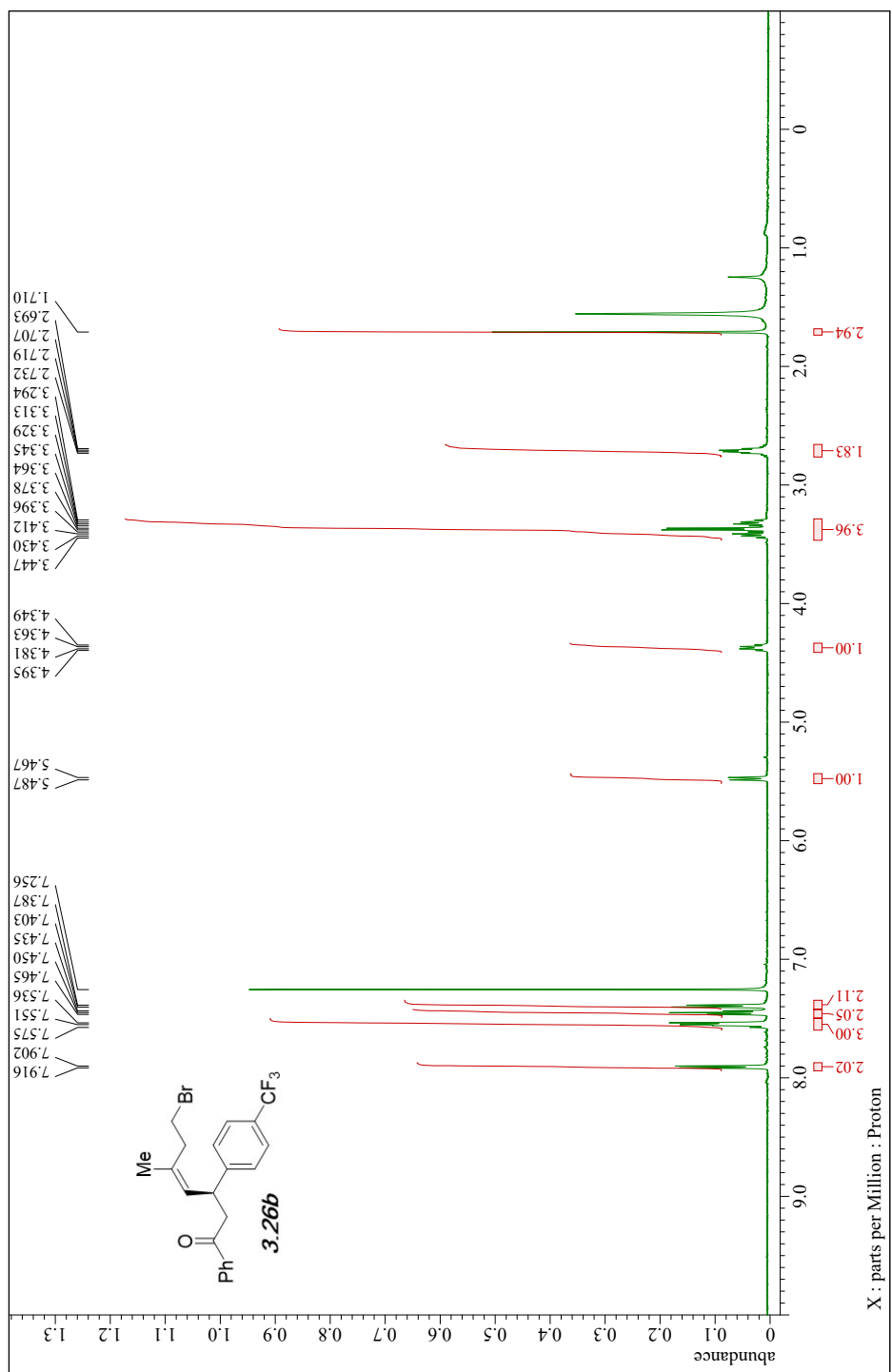
### <Chromatogram>

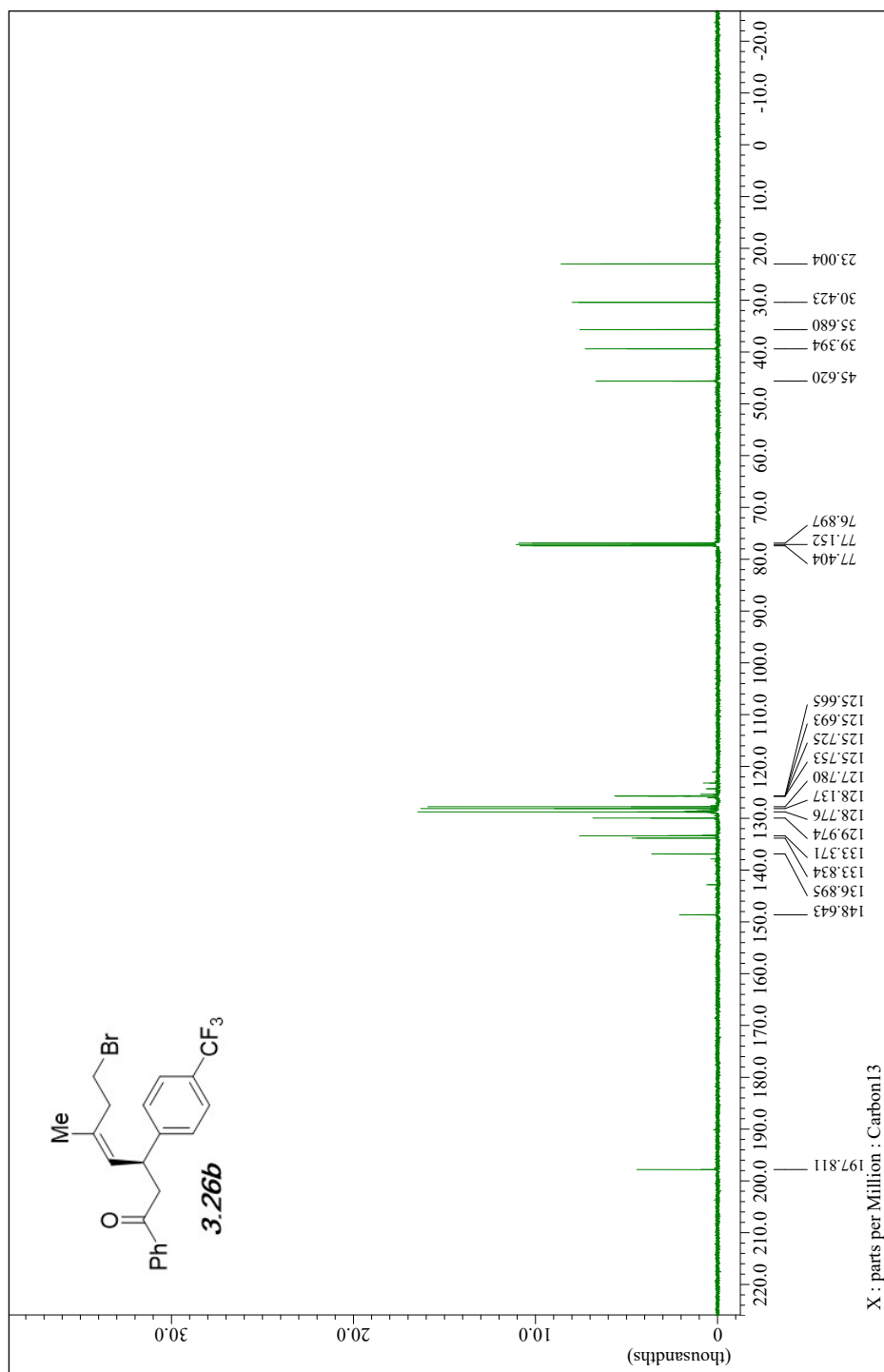


PeakTable

Peak#	Ret. Time	Area	Height	Area %	Height %
1	9.860	1346141	107928	91.473	95.080
2	10.334	125489	5585	8.527	4.920
Total		1471630	113513	100.000	100.000



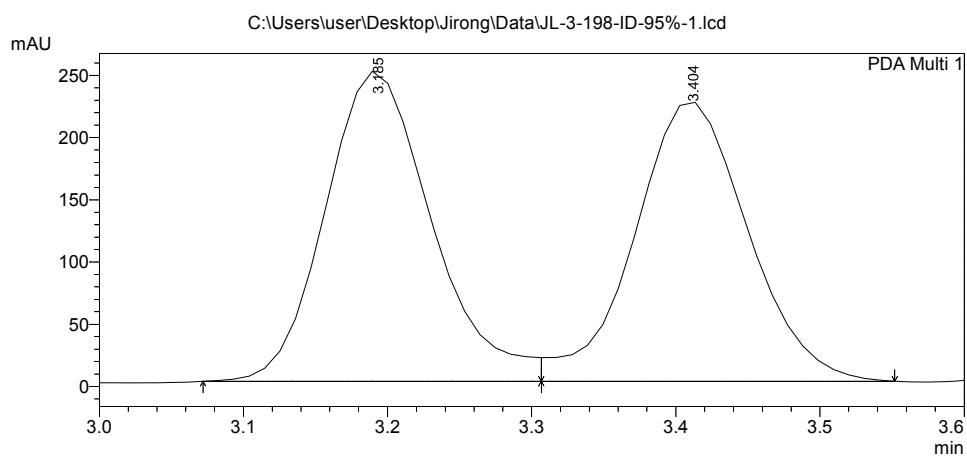




## ==== Shimadzu LCsolution Analysis Report ====

C:\Users\user\Desktop\Jirong\Data\JL-3-198-ID-95%-1.lcd  
Acquired by : Admin  
Sample Name : JL-3-198-ID-95%-1  
Sample ID : JL-3-198-ID-95%-1  
Tray# : 1  
Vial # : 14  
Injection Volume : 10 uL  
Data File Name : JL-3-198-ID-95%-1.lcd  
Method File Name : pos3-95%\_20min\_1.0\_D2.lcm  
Batch File Name : Batch table C3\_95%\_20min\_1.0\_D2.lcb  
Report File Name : Default.lcr  
Data Acquired : 4/19/2021 6:04:21 PM  
Data Processed : 4/19/2021 6:24:22 PM

### <Chromatogram>

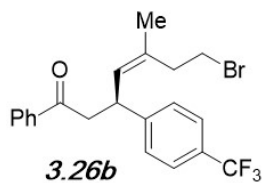


1 PDA Multi 1/254nm 4nm

PeakTable

PDA Ch1 254nm 4nm

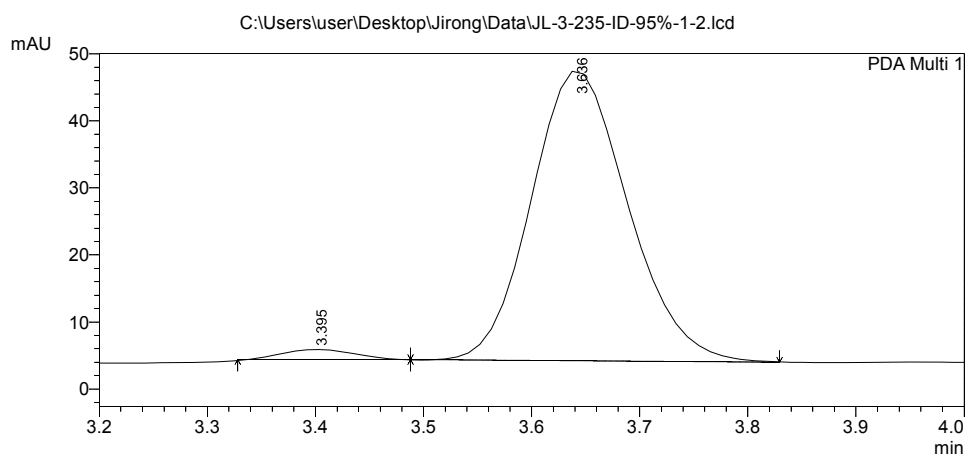
Peak#	Ret. Time	Area	Height	Area %	Height %
1	3.185	1281281	249169	51.217	52.637
2	3.404	1220395	224204	48.783	47.363
Total		2501676	473373	100.000	100.000



## ==== Shimadzu LCsolution Analysis Report ====

C:\Users\user\Desktop\Jirong\Data\JL-3-235-ID-95%-1-2.lcd  
 Acquired by : Admin  
 Sample Name : JL-3-235-ID-95%-1  
 Sample ID : JL-3-235-ID-95%-1  
 Tray# : 1  
 Vial # : 15  
 Injection Volume : 10 uL  
 Data File Name : JL-3-235-ID-95%-1-2.lcd  
 Method File Name : pos3-95%\_20min\_1.0\_D2.lcm  
 Batch File Name : Batch table C3\_95%\_20min\_1.0\_D2.lcb  
 Report File Name : Default.lcr  
 Data Acquired : 5/19/2021 4:29:23 PM  
 Data Processed : 5/27/2021 2:38:44 PM

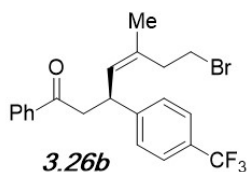
### <Chromatogram>

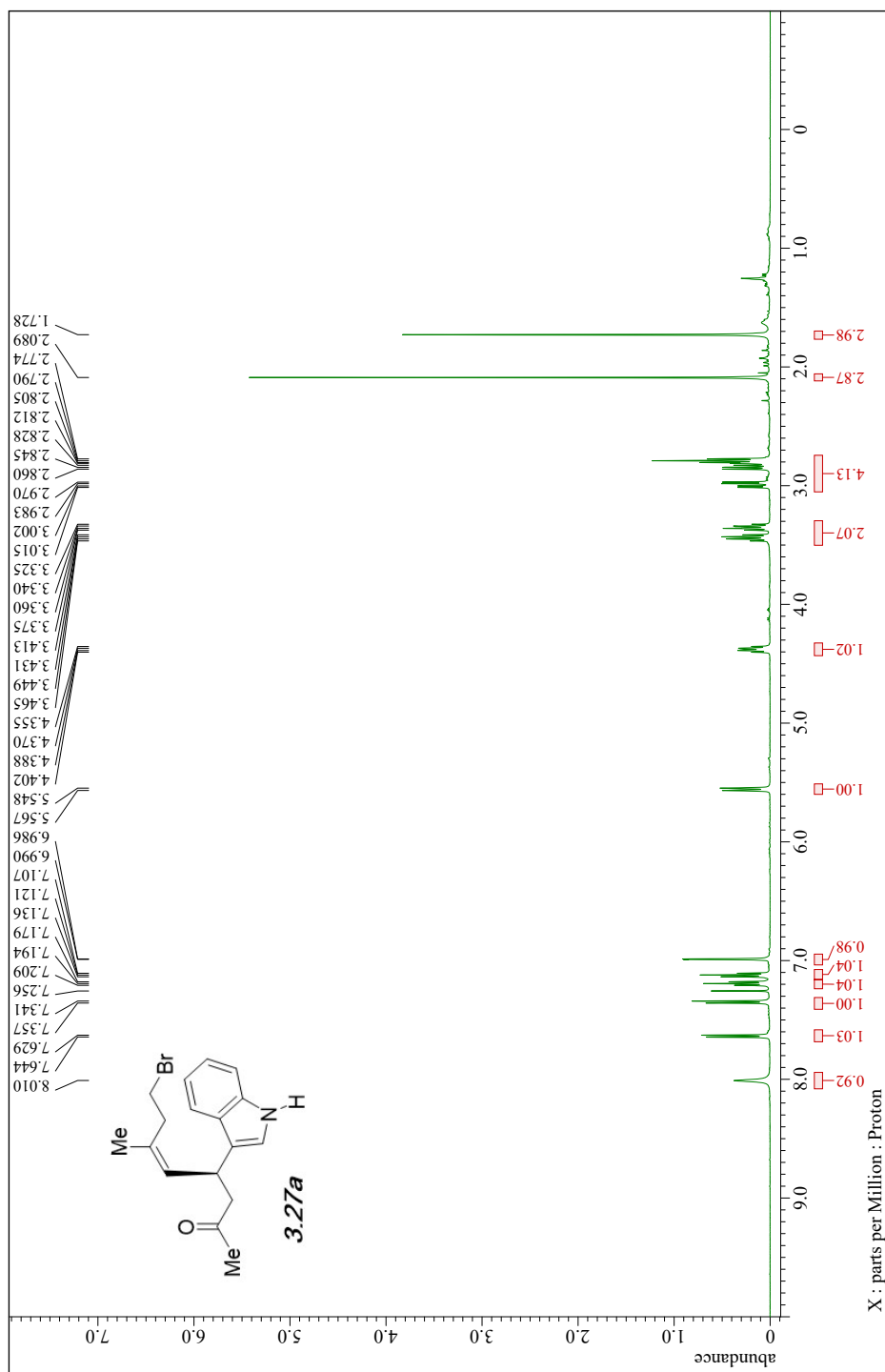


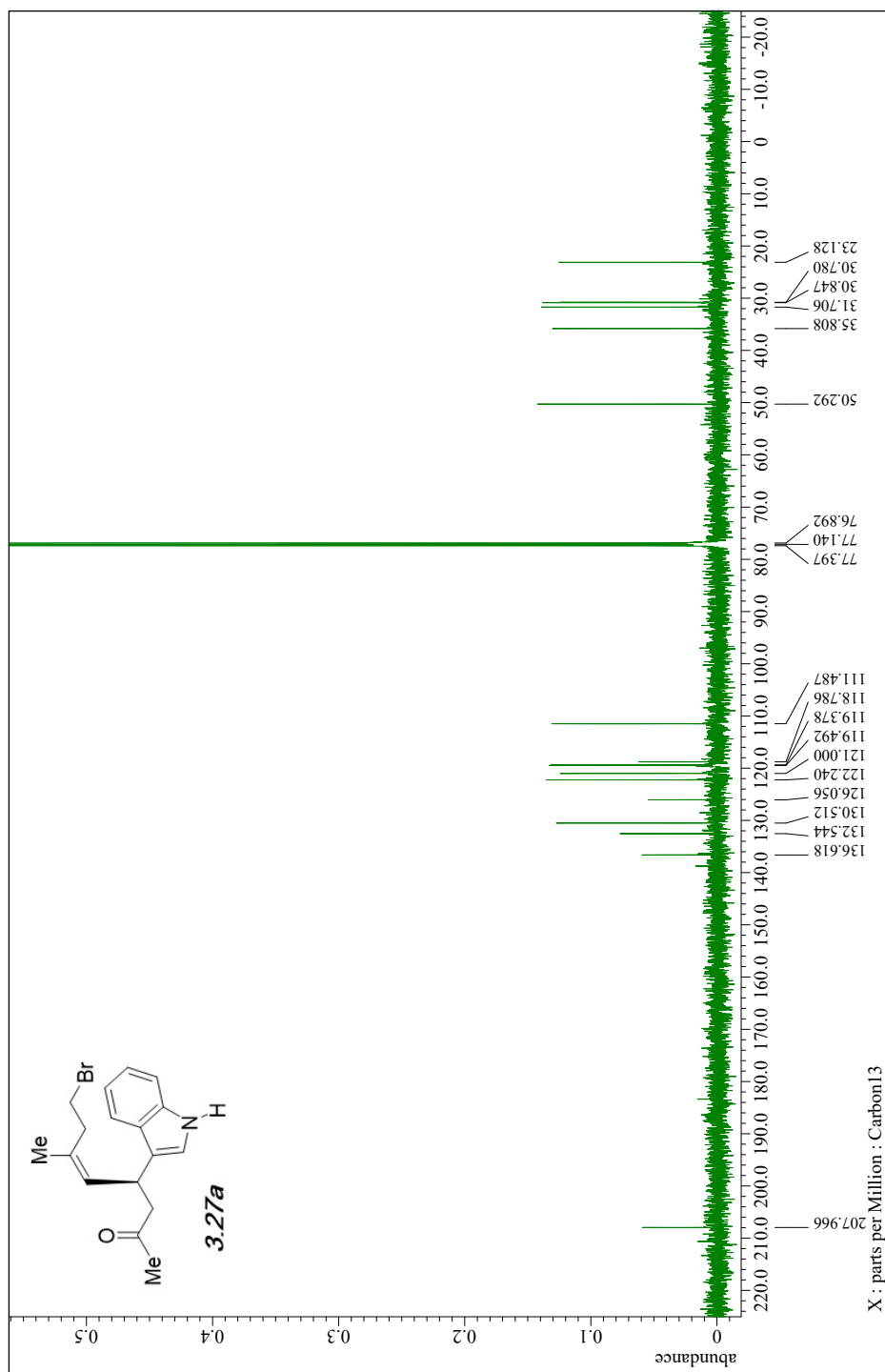
PDA Ch1 254nm 4nm

PeakTable

Peak#	Ret. Time	Area	Height	Area %	Height %
1	3.395	6916	1515	2.513	3.389
2	3.636	268309	43180	97.487	96.611
Total		275225	44694	100.000	100.000





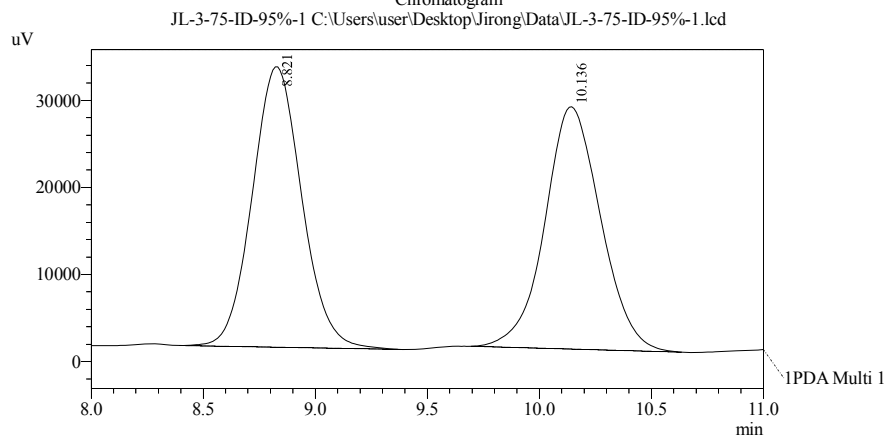


## ==== Shimadzu LCsolution Analysis Report ====

### Sample Information

Acquired by : Admin  
 Sample Name : JL-3-75-ID-95%-1  
 Sample ID : JL-3-75-ID-95%-1  
 Tray# : 1  
 Vial# : 2  
 Injection Volume : 10 uL  
 Data Filename : JL-3-75-ID-95%-1.lcd  
 Method Filename : pos3-95%\_60min\_1.0\_D2.lcm  
 Batch Filename :  
 Report Filename :  
 Date Acquired : 12/1/2020 3:56:27 PM  
 Data Processed : 4/8/2021 11:36:57 AM

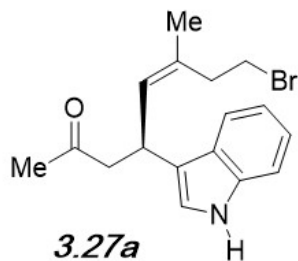
### Chromatogram



### PeakTable

PDA Ch1 254nm 4nm

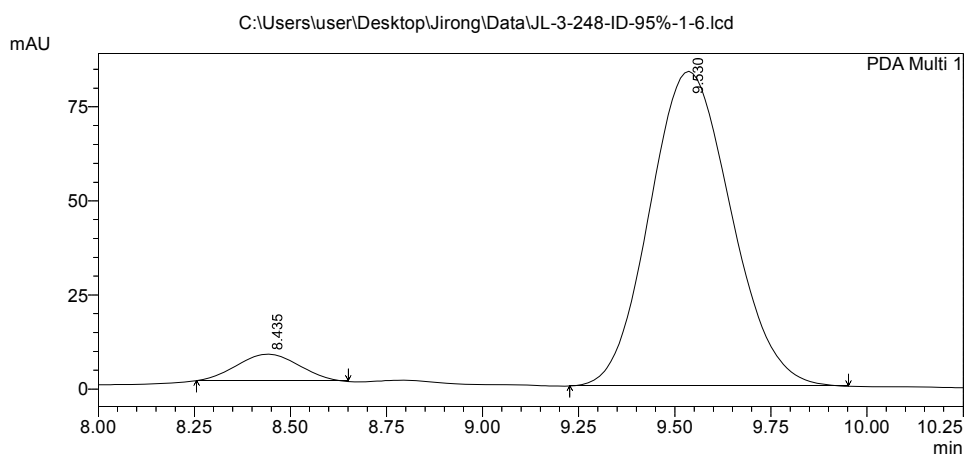
Peak#	Ret. Time	Area	Height	Area %	Height %
1	8.821	495454	32197	50.631	53.624
2	10.136	483104	27845	49.369	46.376
Total		978559	60042	100.000	100.000



## ==== Shimadzu LCsolution Analysis Report ====

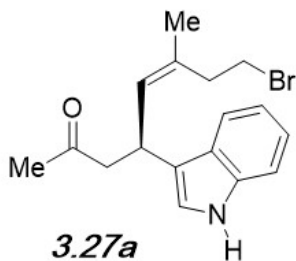
C:\Users\user\Desktop\Jirong\Data\JL-3-248-ID-95%-1-6.lcd  
 Acquired by : Admin  
 Sample Name : JL-3-248-ID-95%-1  
 Sample ID : JL-3-248-ID-95%-1  
 Tray# : 1  
 Vial # : 15  
 Injection Volume : 10 uL  
 Data File Name : JL-3-248-ID-95%-1-6.lcd  
 Method File Name : pos3-95%\_20min\_1.0\_D2.lcm  
 Batch File Name : Batch table C3\_95%\_20min\_1.0\_D2.lcb  
 Report File Name : Default.lcr  
 Data Acquired : 5/31/2021 5:19:51 PM  
 Data Processed : 6/1/2021 4:45:38 PM

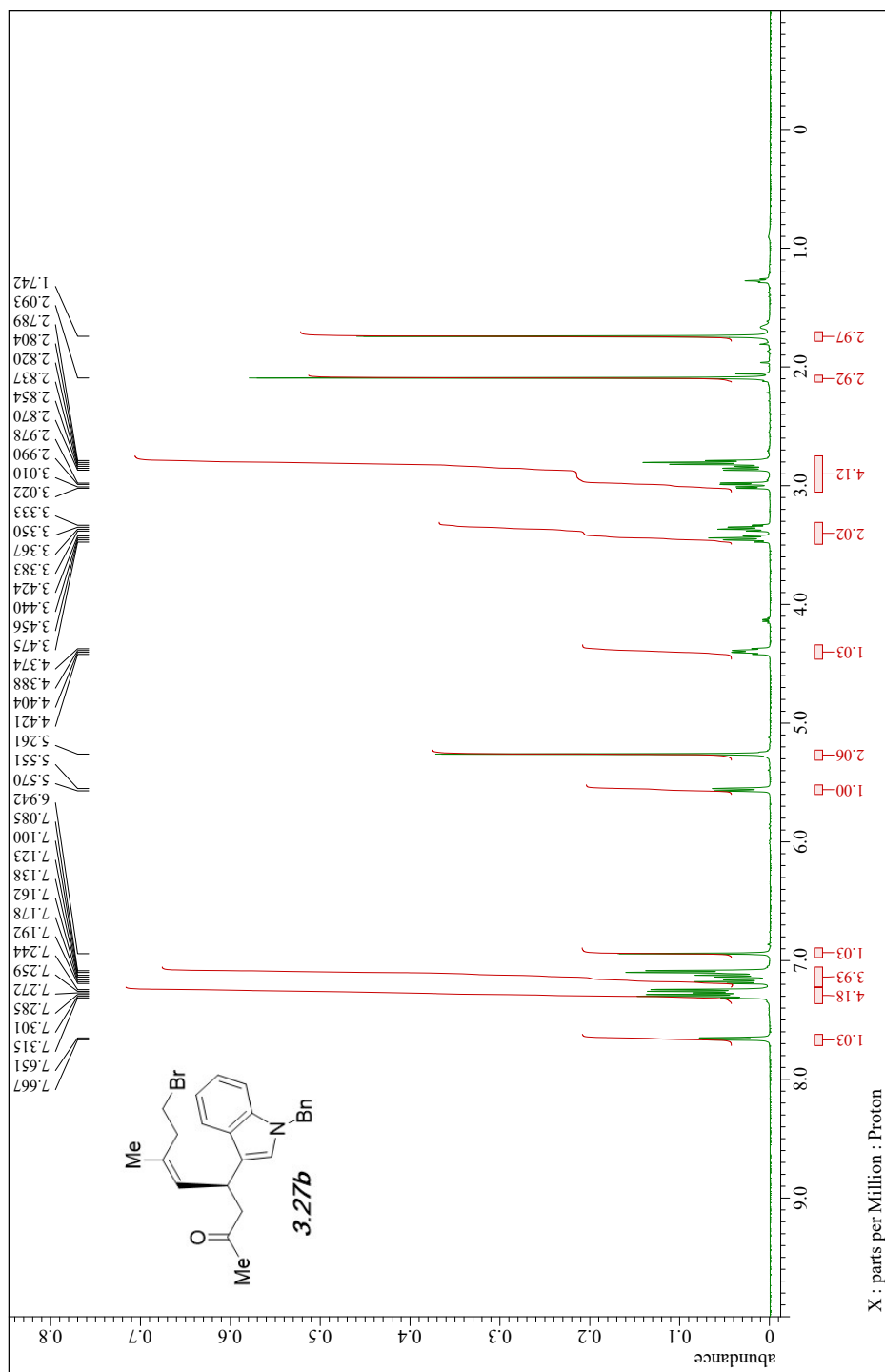
### <Chromatogram>

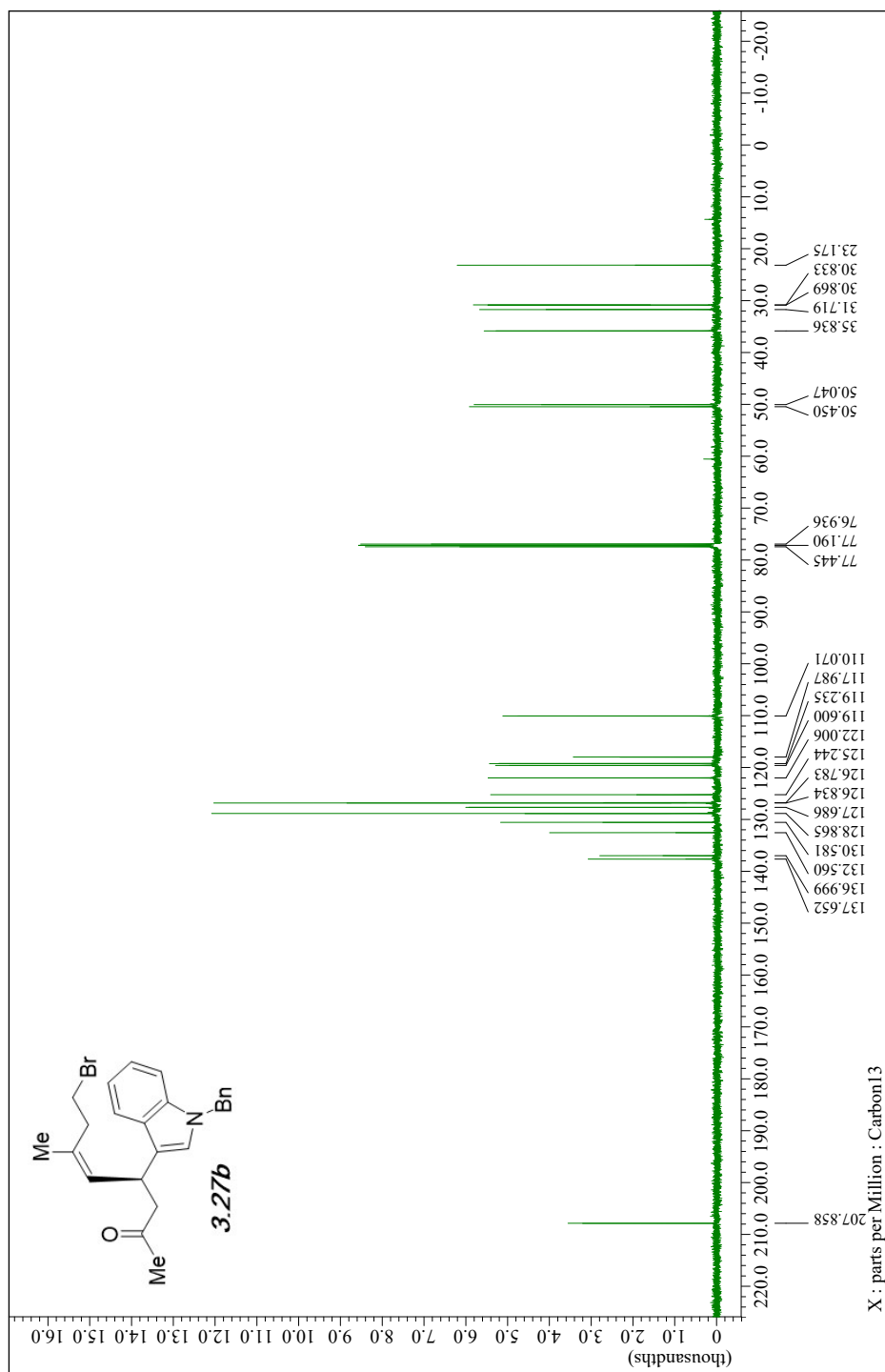


PeakTable

Peak#	Ret. Time	Area	Height	Area %	Height %
1	8.435	77588	7004	5.943	7.733
2	9.530	1228030	83572	94.057	92.267
Total		1305618	90577	100.000	100.000



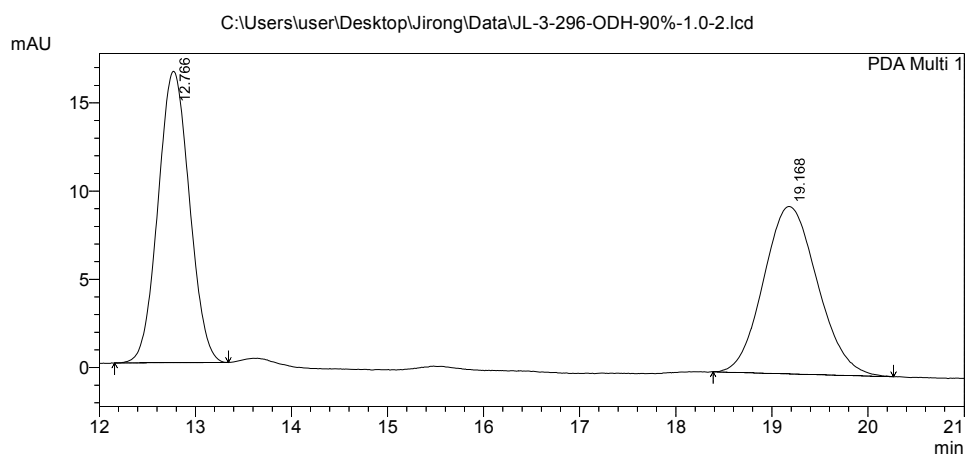




## ==== Shimadzu LCsolution Analysis Report ====

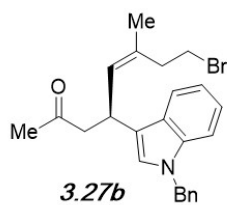
C:\Users\user\Desktop\Jirong\Data\JL-3-296-ODH-90%-1.0-2.lcd  
 Acquired by : Admin  
 Sample Name : JL-3-296-ODH-90%-1.0  
 Sample ID : JL-3-296-ODH-90%-1.0  
 Tray# : 1  
 Vial # : 15  
 Injection Volume : 10 uL  
 Data File Name : JL-3-296-ODH-90%-1.0-2.lcd  
 Method File Name : pos5\_90%\_60min\_1.0\_D2.lcm  
 Batch File Name : Batch\_table\_C5-90\_60min\_1.0\_d2.lcb  
 Report File Name : Default.lcr  
 Data Acquired : 8/9/2021 3:15:59 PM  
 Data Processed : 8/9/2021 3:51:06 PM

### <Chromatogram>



PeakTable

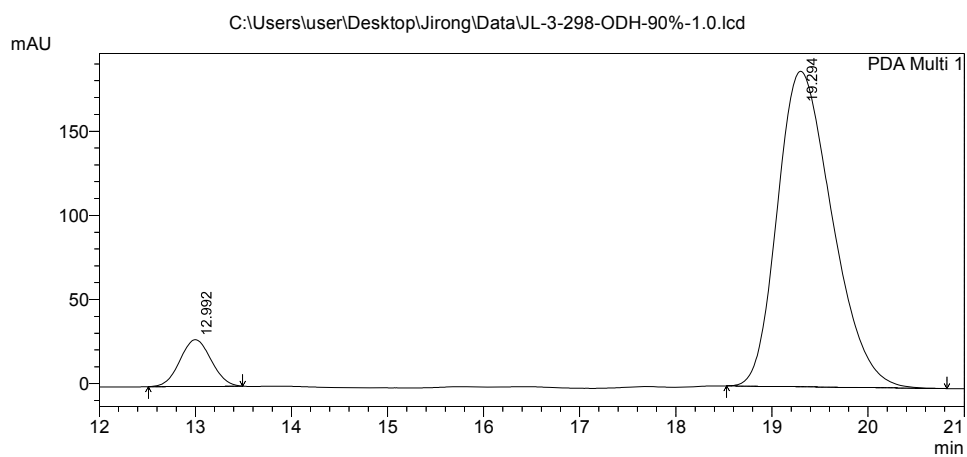
Peak#	Ret. Time	Area	Height	Area %	Height %
1	12.766	375461	16526	50.327	63.495
2	19.168	370580	9502	49.673	36.505
Total		746042	26028	100.000	100.000



## ==== Shimadzu LCsolution Analysis Report ====

C:\Users\user\Desktop\Jirong\Data\JL-3-298-ODH-90%-1.0.lcd  
 Acquired by : Admin  
 Sample Name : JL-3-298-ODH-90%-1.0  
 Sample ID : JL-3-298-ODH-90%-1.0  
 Tray# : 1  
 Vial # : 15  
 Injection Volume : 10 uL  
 Data File Name : JL-3-298-ODH-90%-1.0.lcd  
 Method File Name : pos5\_90%\_60min\_1.0\_D2.lcm  
 Batch File Name : Batch\_table\_C5-90\_60min\_1.0\_d2.lcb  
 Report File Name : Default.lcr  
 Data Acquired : 8/14/2021 3:11:42 PM  
 Data Processed : 8/17/2021 4:18:17 PM

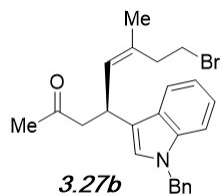
### <Chromatogram>

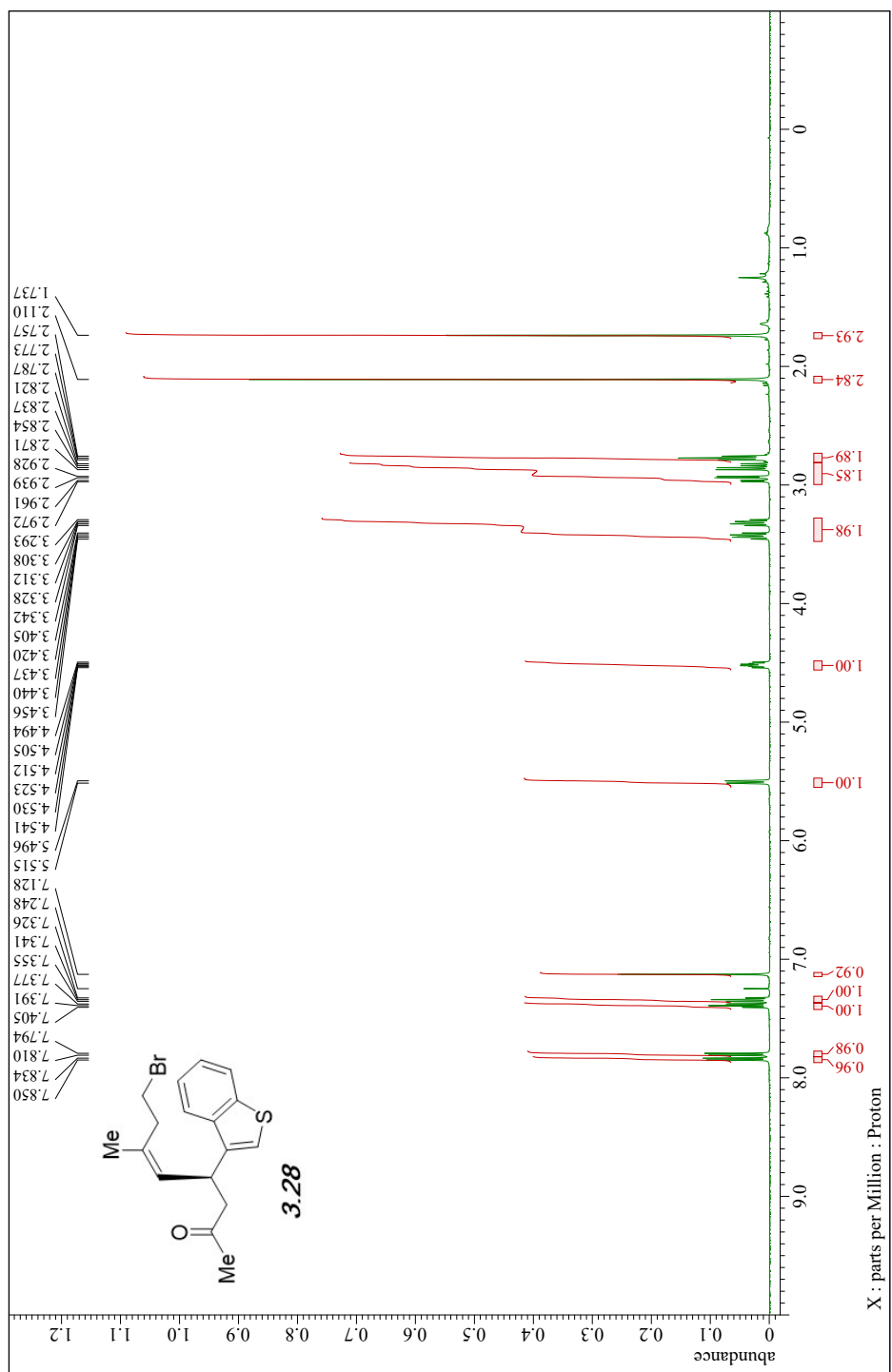


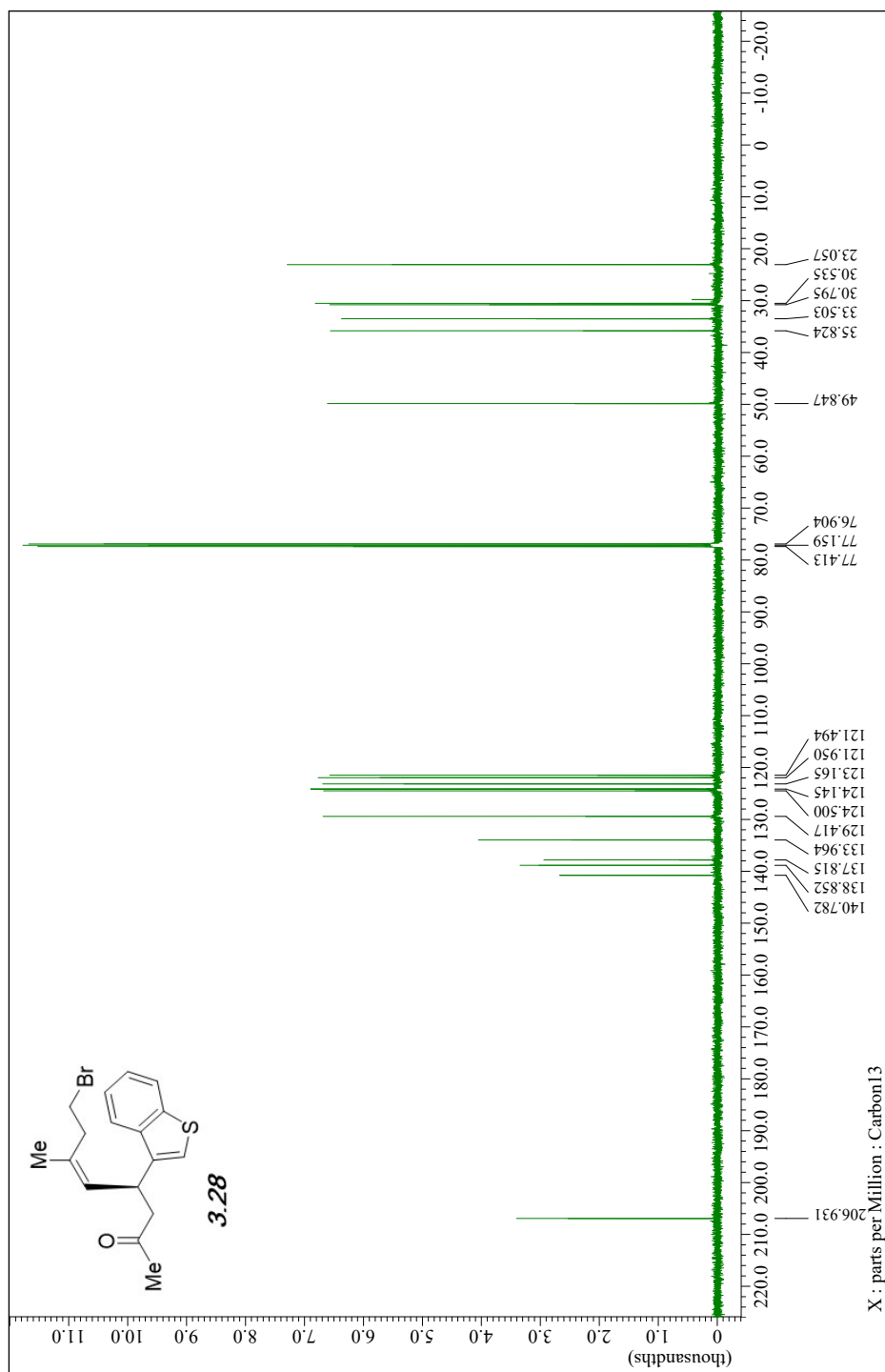
PeakTable

PDA Ch1 254nm 4nm

Peak#	Ret. Time	Area	Height	Area %	Height %
1	12.992	637955	27960	7.920	12.979
2	19.294	7417520	187467	92.080	87.021
Total		8055475	215427	100.000	100.000



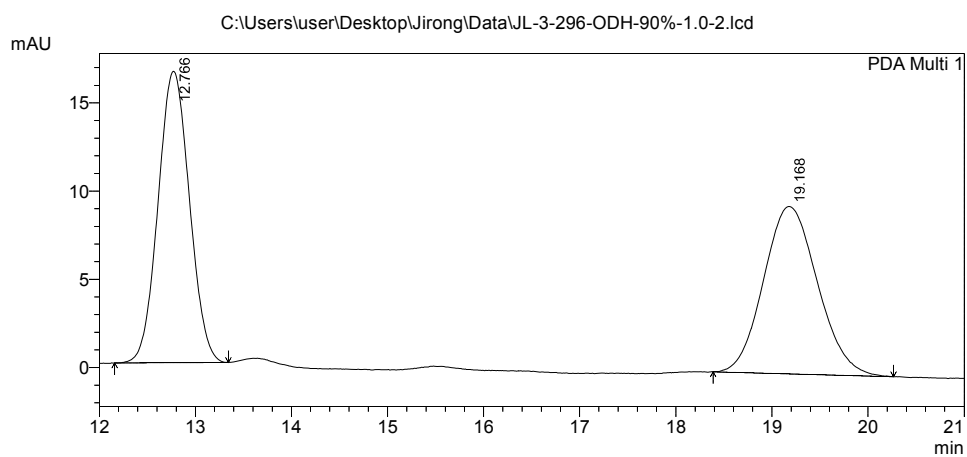




## ==== Shimadzu LCsolution Analysis Report ====

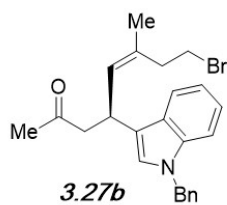
C:\Users\user\Desktop\Jirong\Data\JL-3-296-ODH-90%-1.0-2.lcd  
 Acquired by : Admin  
 Sample Name : JL-3-296-ODH-90%-1.0  
 Sample ID : JL-3-296-ODH-90%-1.0  
 Tray# : 1  
 Vial # : 15  
 Injection Volume : 10 uL  
 Data File Name : JL-3-296-ODH-90%-1.0-2.lcd  
 Method File Name : pos5\_90%\_60min\_1.0\_D2.lcm  
 Batch File Name : Batch\_table\_C5-90\_60min\_1.0\_d2.lcb  
 Report File Name : Default.lcr  
 Data Acquired : 8/9/2021 3:15:59 PM  
 Data Processed : 8/9/2021 3:51:06 PM

### <Chromatogram>



PeakTable

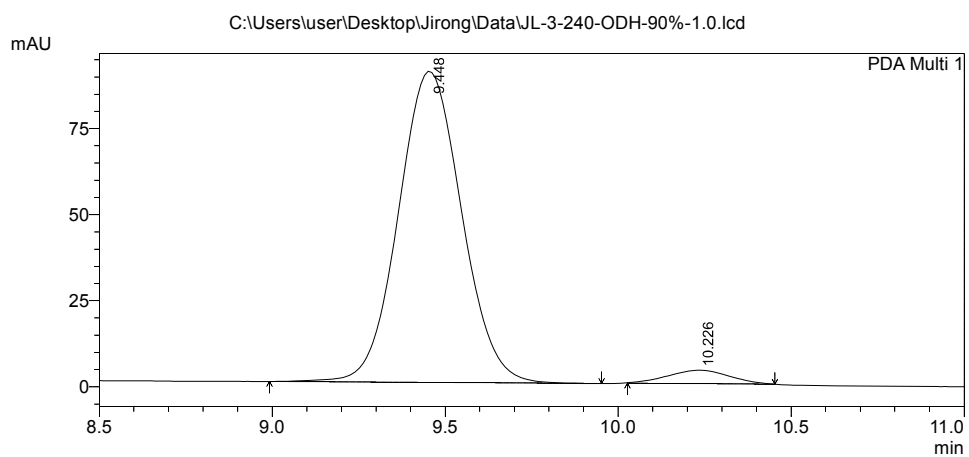
Peak#	Ret. Time	Area	Height	Area %	Height %
1	12.766	375461	16526	50.327	63.495
2	19.168	370580	9502	49.673	36.505
Total		746042	26028	100.000	100.000



## ==== Shimadzu LCsolution Analysis Report ====

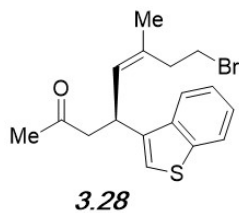
C:\Users\user\Desktop\Jirong\Data\JL-3-240-ODH-90%-1.0.lcd  
 Acquired by : Admin  
 Sample Name : JL-3-240-ODH-90%-1.0  
 Sample ID : JL-3-240-ODH-90%-1.0  
 Tray# : 1  
 Vial # : 15  
 Injection Volume : 10 uL  
 Data File Name : JL-3-240-ODH-90%-1.0.lcd  
 Method File Name : pos5\_90%\_60min\_1.0\_D2.lcm  
 Batch File Name : Batch\_table\_C5-90\_60min\_1.0\_d2.lcb  
 Report File Name : Default.lcr  
 Data Acquired : 5/21/2021 4:09:16 PM  
 Data Processed : 5/21/2021 4:24:46 PM

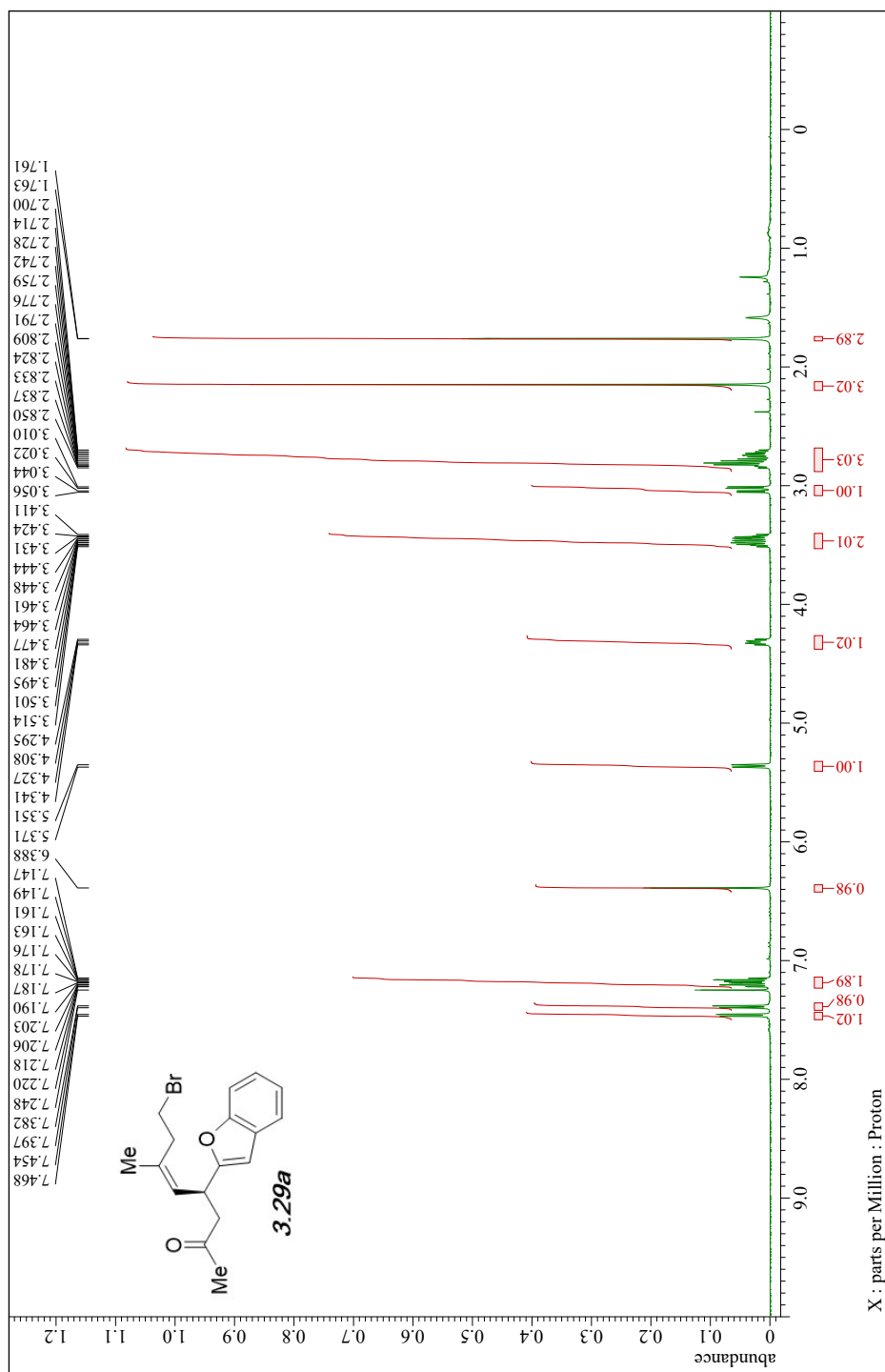
### <Chromatogram>

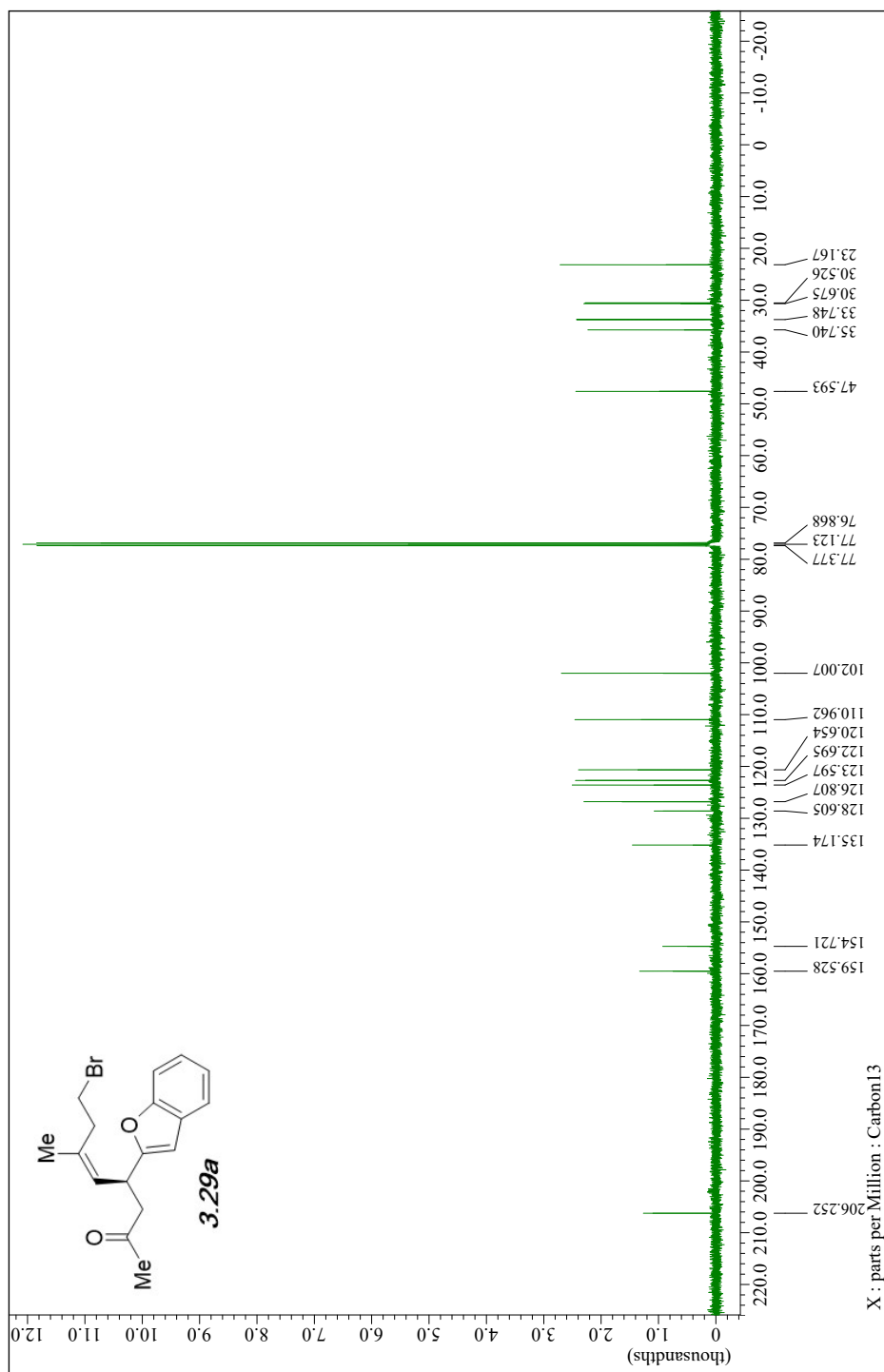


PeakTable

PDA Ch1 254nm 4nm					
Peak#	Ret. Time	Area	Height	Area %	Height %
1	9.448	1150046	90399	95.958	95.862
2	10.226	48449	3902	4.042	4.138
Total		1198495	94301	100.000	100.000



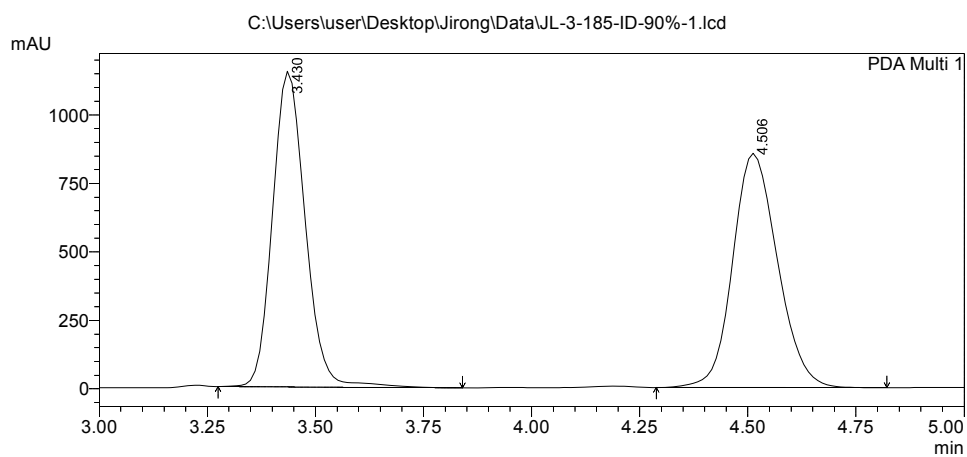




# ==== Shimadzu LcSolution Analysis Report ====

C:\Users\user\Desktop\Jirong\Data\JL-3-185-ID-90%-1.lcd  
Acquired by : Admin  
Sample Name : JL-3-185-ID-90%-1  
Sample ID : JL-3-185-ID-90%-1  
Tray# : 1  
Vial # : 8  
Injection Volume : 10 uL  
Data File Name : JL-3-185-ID-90%-1.lcd  
Method File Name : pos3-90%\_60MIN\_1.0\_D2.lcm  
Batch File Name : Batch table C3\_90%\_60min\_1.0\_D2.lcb  
Report File Name : Default.lcr  
Data Acquired : 4/10/2021 12:34:18 PM  
Data Processed : 4/10/2021 1:36:39 PM

## <Chromatogram>

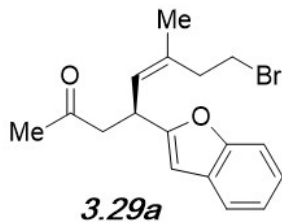


1 PDA Multi 1/254nm 4nm

PeakTable

PDA Ch1 254nm 4nm

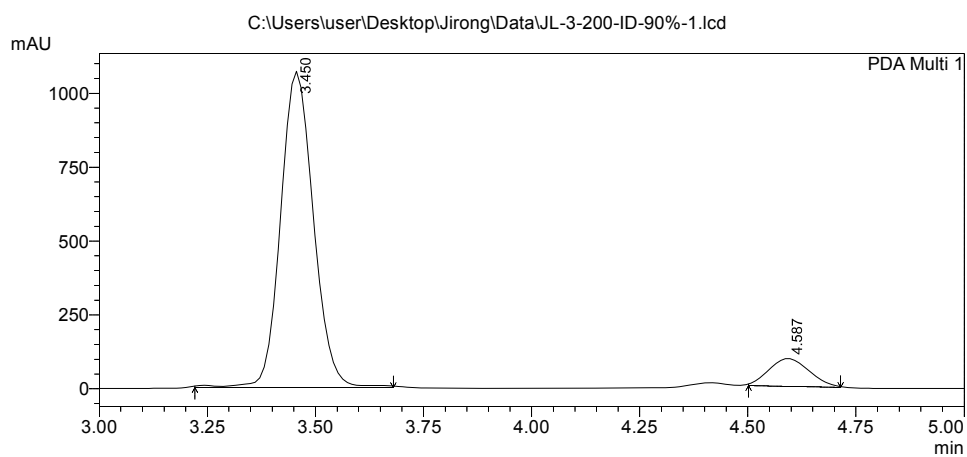
Peak#	Ret. Time	Area	Height	Area %	Height %
1	3.430	6073878	1152132	49.628	57.389
2	4.506	6164872	855440	50.372	42.611
Total		12238751	2007572	100.000	100.000



# ==== Shimadzu LCsolution Analysis Report ====

C:\Users\user\Desktop\Jirong\Data\JL-3-200-ID-90%-1.lcd  
Acquired by : Admin  
Sample Name : JL-3-200-ID-90%-1  
Sample ID : JL-3-200-ID-90%-1  
Tray# : 1  
Vial # : 12  
Injection Volume : 10 uL  
Data File Name : JL-3-200-ID-90%-1.lcd  
Method File Name : pos3-90%\_10MIN\_1\_d2.lcm  
Batch File Name : Batch table C3\_90%\_10min\_1.0\_D2.lcb  
Report File Name : Default.lcr  
Data Acquired : 4/22/2021 5:57:42 PM  
Data Processed : 5/17/2021 12:17:40 PM

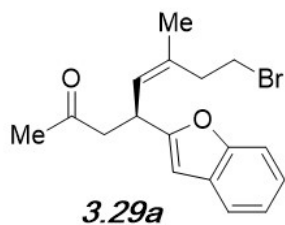
## <Chromatogram>



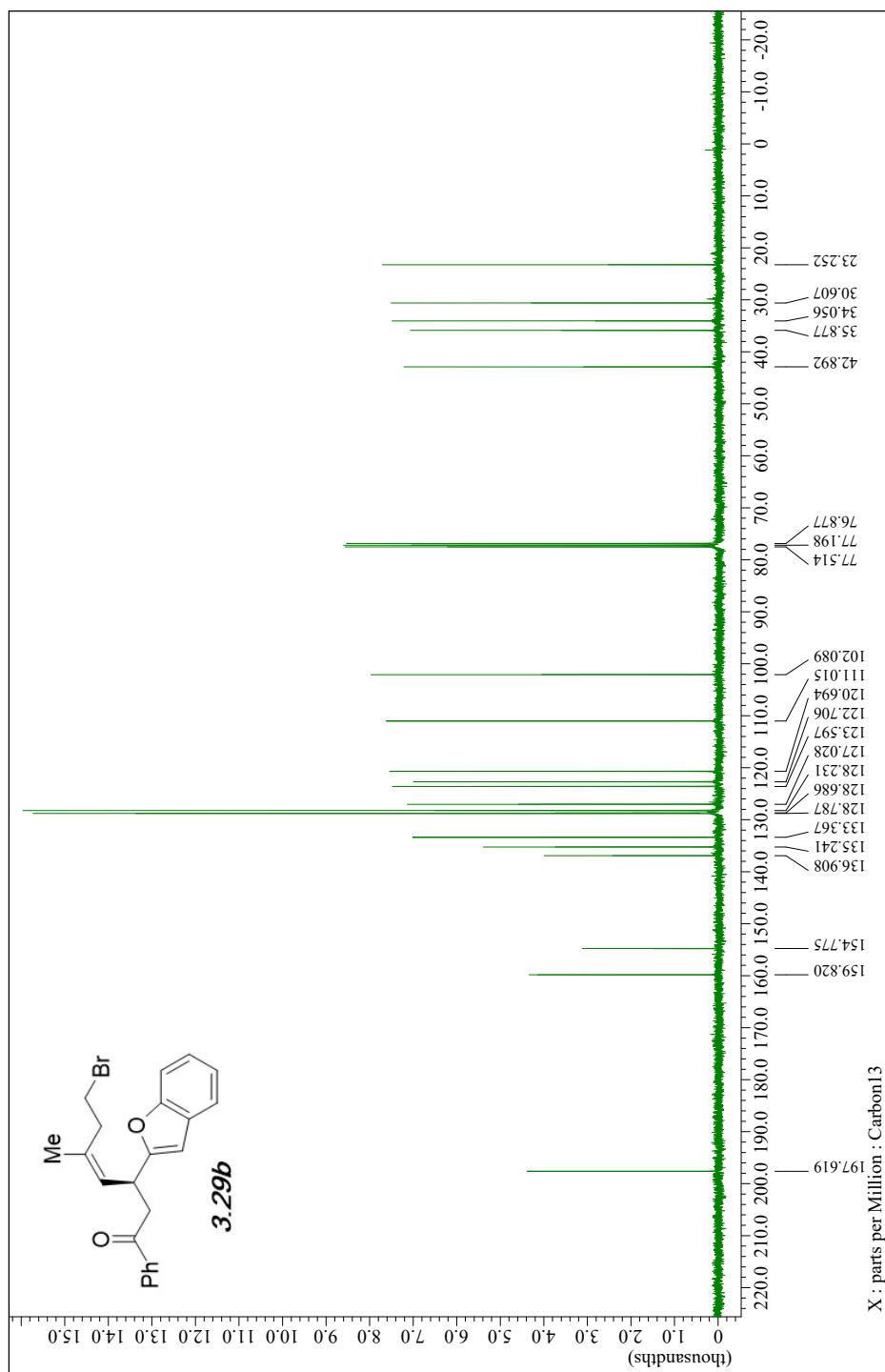
1 PDA Multi 1/254nm 4nm

PeakTable

Peak#	Ret. Time	Area	Height	Area %	Height %
1	3.450	5678363	1070461	90.252	91.947
2	4.587	613340	93757	9.748	8.053
Total		6291703	1164218	100.000	100.000



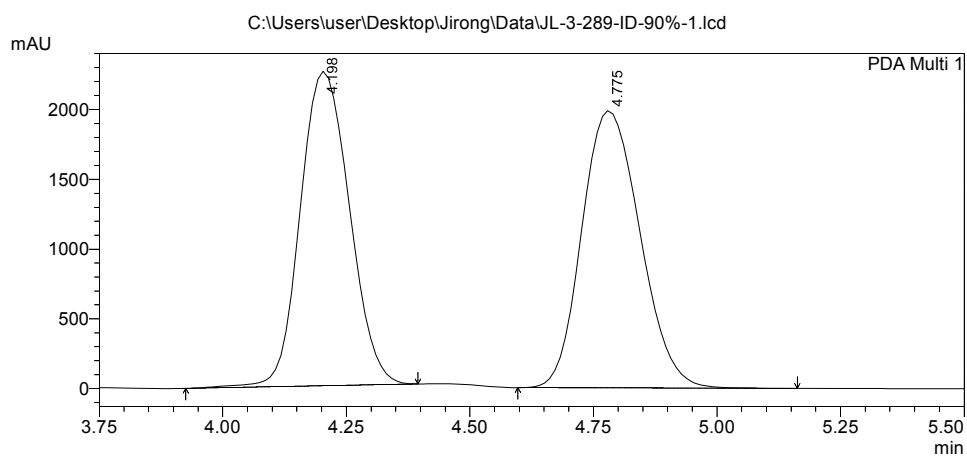




## ==== Shimadzu LcSolution Analysis Report ====

Acquired by : Admin  
Sample Name : JL-3-289-ID-90%-1  
Sample ID : JL-3-289-ID-90%-1  
Tray# : 1  
Vial # : 15  
Injection Volume : 10 uL  
Data File Name : JL-3-289-ID-90%-1.lcd  
Method File Name : pos3-90%\_60MIN\_1.0\_D2.lcm  
Batch File Name : Batch table C3\_90%\_60min\_1.0\_D2.lcb  
Report File Name : Default.lcr  
Data Acquired : 8/3/2021 2:00:24 PM  
Data Processed : 8/27/2021 4:03:55 PM

### <Chromatogram>

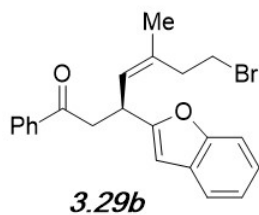


1 PDA Multi 1/254nm 4nm

PeakTable

PDA Ch1 254nm 4nm

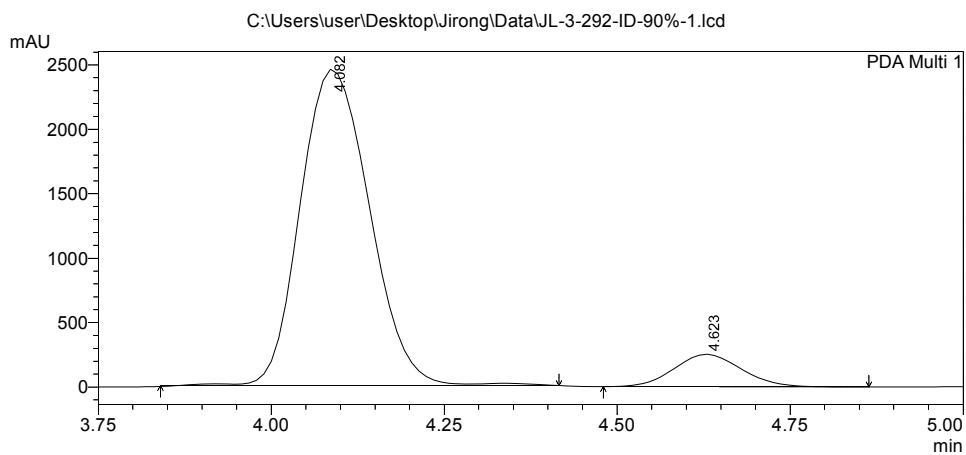
Peak#	Ret. Time	Area	Height	Area %	Height %
1	4.198	15628009	2253424	49.012	53.150
2	4.775	16258085	1986282	50.988	46.850
Total		31886094	4239706	100.000	100.000



# ==== Shimadzu LCsolution Analysis Report ====

C:\Users\user\Desktop\Jirong\Data\JL-3-292-ID-90%-1.lcd  
Acquired by : Admin  
Sample Name : JL-3-292-ID-90%-1  
Sample ID : JL-3-292-ID-90%-1  
Tray# : 1  
Vial # : 15  
Injection Volume : 10 uL  
Data File Name : JL-3-292-ID-90%-1.lcd  
Method File Name : pos3-90%\_10MIN\_1\_d2.lcm  
Batch File Name : Batch table C3\_90%\_10min\_1.0\_D2.lcb  
Report File Name : Default.lcr  
Data Acquired : 8/6/2021 10:16:43 AM  
Data Processed : 8/6/2021 10:24:03 AM

## <Chromatogram>

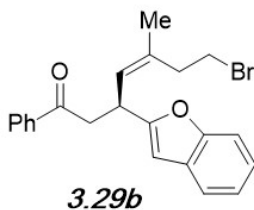


1 PDA Multi 1/254nm 4nm

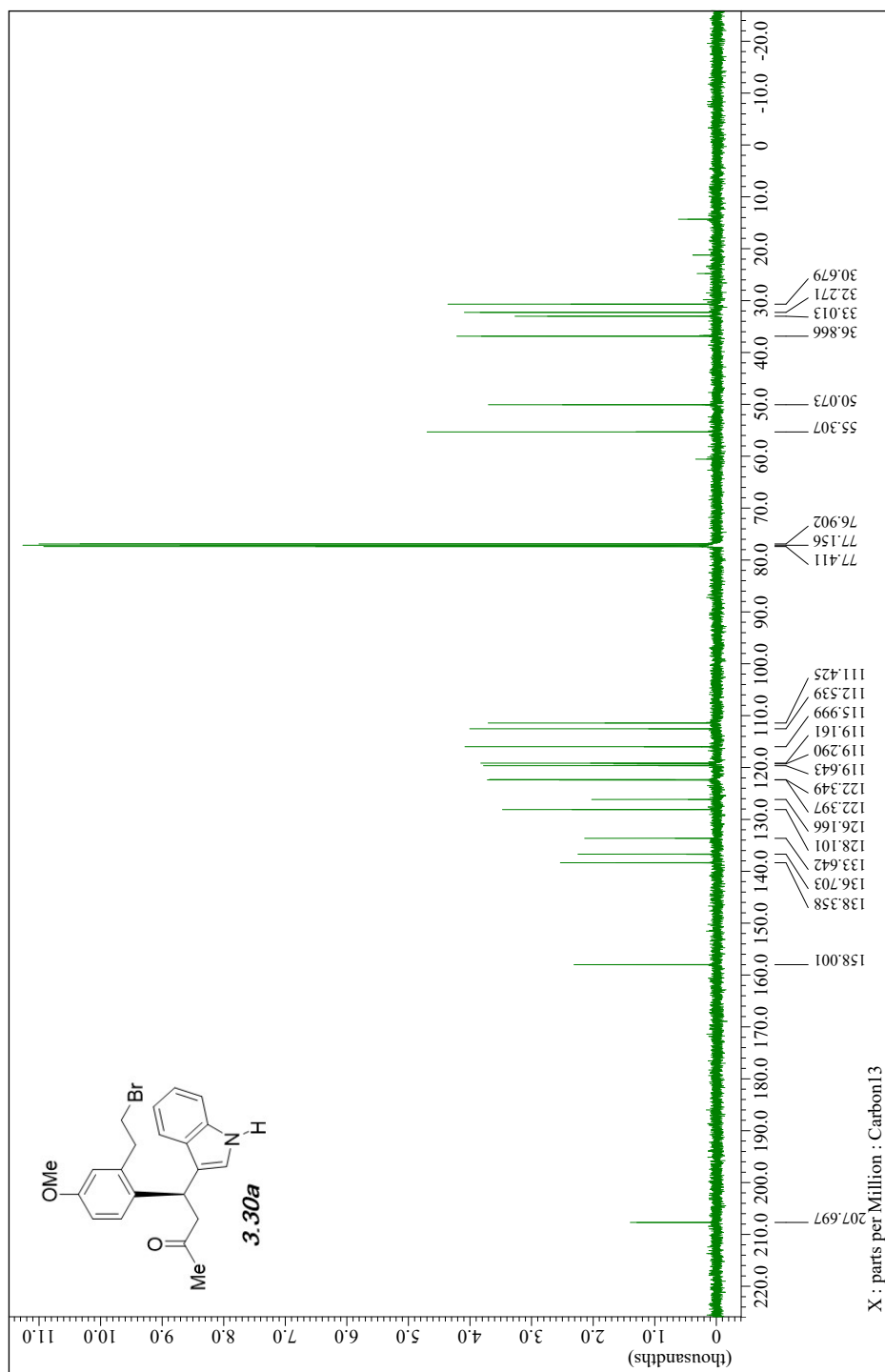
PeakTable

PDA Ch1 254nm 4nm

Peak#	Ret. Time	Area	Height	Area %	Height %
1	4.082	17169541	2456308	90.974	90.703
2	4.623	1703537	251780	9.026	9.297
Total		18873078	2708088	100.000	100.000



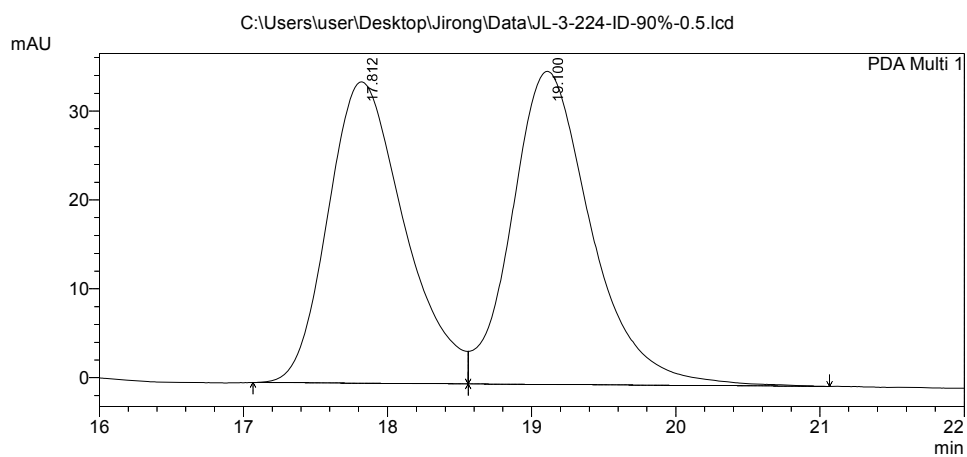




## ==== Shimadzu LcSolution Analysis Report ====

C:\Users\user\Desktop\Jirong\Data\JL-3-224-ID-90%-0.5.lcd  
Acquired by : Admin  
Sample Name : JL-3-224-ID-90%-0.5  
Sample ID : JL-3-224-ID-90%-0.5  
Tray# : 1  
Vial # : 15  
Injection Volume : 10 uL  
Data File Name : JL-3-224-ID-90%-0.5.lcd  
Method File Name : pos3-90%\_60MIN\_0.5\_d2.lcm  
Batch File Name : Batch table C3\_90%\_60min\_0.5\_D2.lcb  
Report File Name : Default.lcr  
Data Acquired : 5/5/2021 2:53:24 PM  
Data Processed : 5/5/2021 3:16:15 PM

### <Chromatogram>

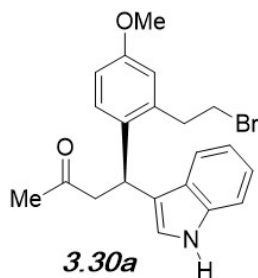


1 PDA Multi 1/254nm 4nm

PeakTable

PDA Ch1 254nm 4nm

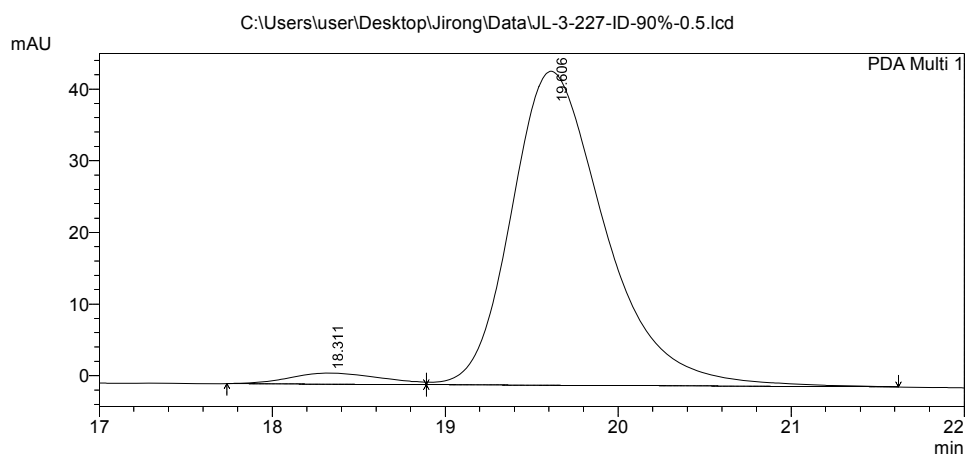
Peak#	Ret. Time	Area	Height	Area %	Height %
1	17.812	1253359	33891	48.233	49.038
2	19.100	1345182	35222	51.767	50.962
Total		2598541	69113	100.000	100.000



## ==== Shimadzu LcSolution Analysis Report ====

C:\Users\user\Desktop\Jirong\Data\JL-3-227-ID-90%-0.5.lcd  
Acquired by : Admin  
Sample Name : JL-3-227-ID-90%-0.5  
Sample ID : JL-3-227-ID-90%-0.5  
Tray# : 1  
Vial # : 15  
Injection Volume : 10 uL  
Data File Name : JL-3-227-ID-90%-0.5.lcd  
Method File Name : pos3-90%\_60MIN\_0.5\_d2.lcm  
Batch File Name : Batch table C3\_90%\_60min\_0.5\_D2.lcb  
Report File Name : Default.lcr  
Data Acquired : 5/7/2021 11:08:16 AM  
Data Processed : 5/7/2021 11:32:40 AM

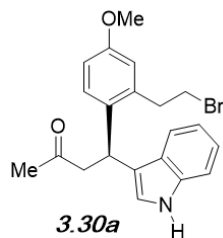
### <Chromatogram>

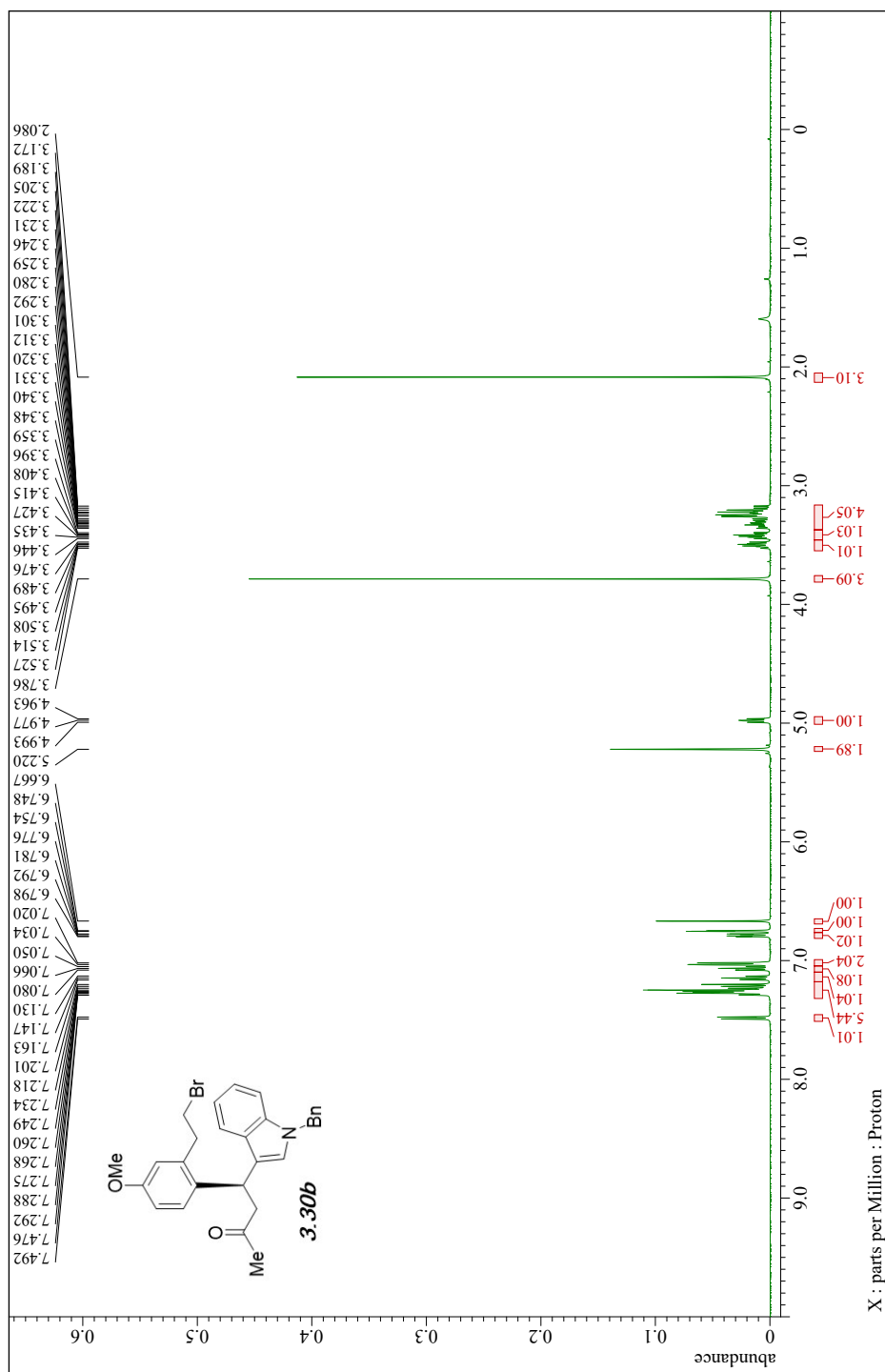


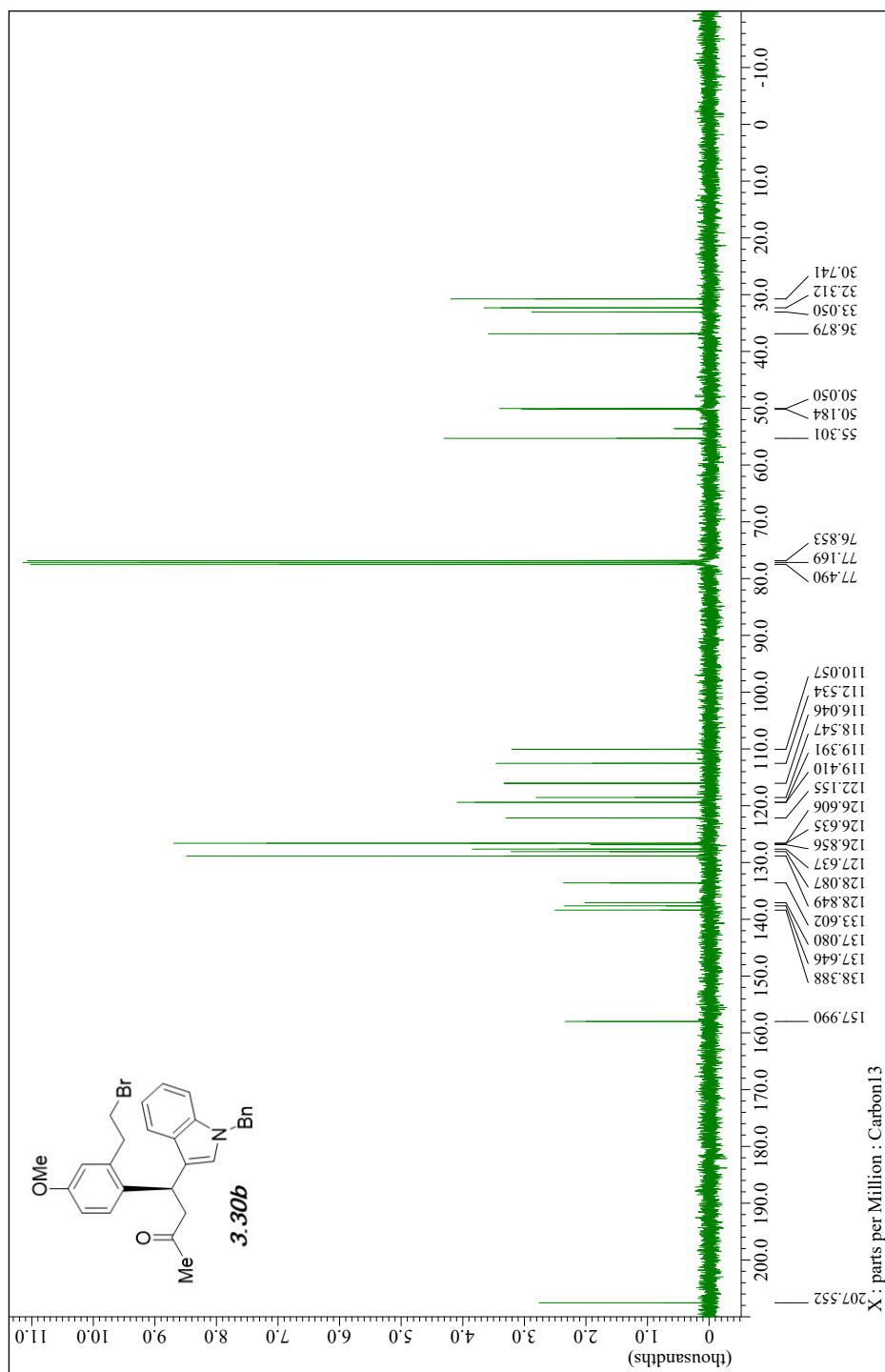
PeakTable

PDA Ch1 254nm 4nm

Peak#	Ret. Time	Area	Height	Area %	Height %
1	18.311	55152	1522	3.235	3.357
2	19.606	1649700	43819	96.765	96.643
Total		1704852	45341	100.000	100.000



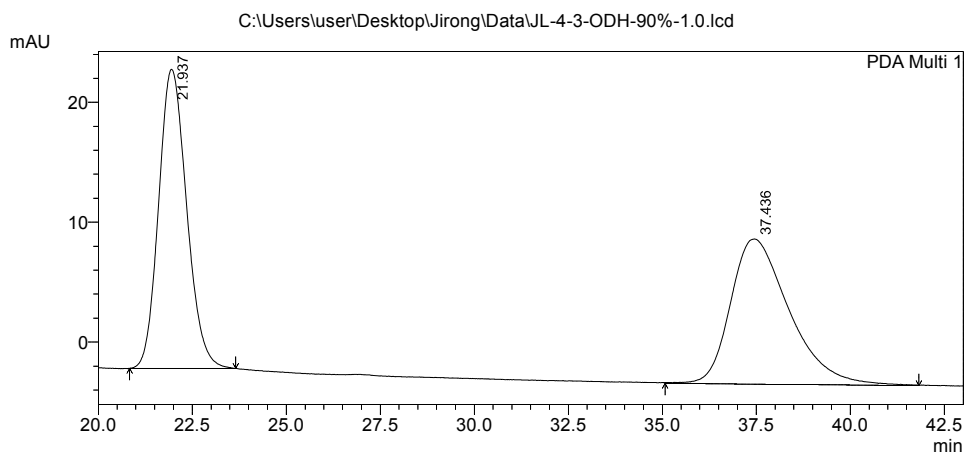




## ==== Shimadzu LCsolution Analysis Report ====

C:\Users\user\Desktop\Jirong\Data\JL-4-3-ODH-90%-1.0.lcd  
 Acquired by : Admin  
 Sample Name : JL-4-3-ODH-90%-1.0  
 Sample ID : JL-4-3-ODH-90%-1.0  
 Tray# : 1  
 Vial # : 15  
 Injection Volume : 10 uL  
 Data File Name : JL-4-3-ODH-90%-1.0.lcd  
 Method File Name : pos5\_90%\_60min\_1.0\_D2.lcm  
 Batch File Name : Batch\_table\_C5-90\_60min\_1.0\_d2.lcb  
 Report File Name : Default.lcr  
 Data Acquired : 8/17/2021 3:31:45 PM  
 Data Processed : 8/17/2021 4:20:06 PM

### <Chromatogram>

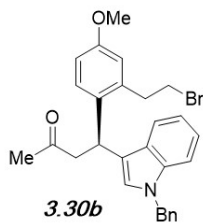


1 PDA Multi 1/254nm 4nm

PeakTable

PDA Ch1 254nm 4nm

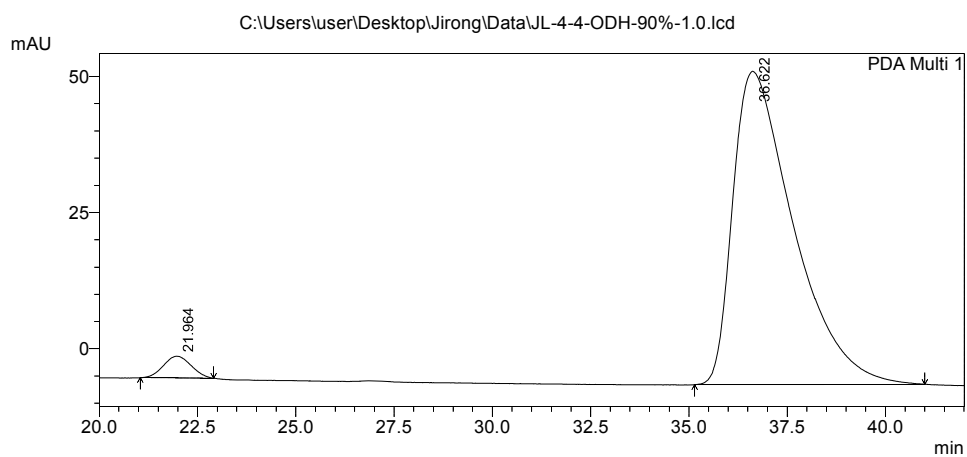
Peak#	Ret. Time	Area	Height	Area %	Height %
1	21.937	1293667	24944	49.456	67.296
2	37.436	1322101	12122	50.544	32.704
Total		2615768	37065	100.000	100.000



## ==== Shimadzu LcSolution Analysis Report ====

C:\Users\user\Desktop\Jirong\Data\JL-4-4-ODH-90%-1.0.lcd  
 Acquired by : Admin  
 Sample Name : JL-4-4-ODH-90%-1.0  
 Sample ID : JL-4-4-ODH-90%-1.0  
 Tray# : 1  
 Vial # : 15  
 Injection Volume : 10 uL  
 Data File Name : JL-4-4-ODH-90%-1.0.lcd  
 Method File Name : pos5\_90%\_60min\_1.0\_D2.lcm  
 Batch File Name : Batch\_table\_C5-90\_60min\_1.0\_d2.lcb  
 Report File Name : Default.lcr  
 Data Acquired : 8/20/2021 10:48:30 AM  
 Data Processed : 8/20/2021 12:39:05 PM

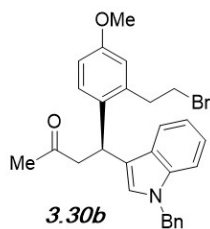
### <Chromatogram>

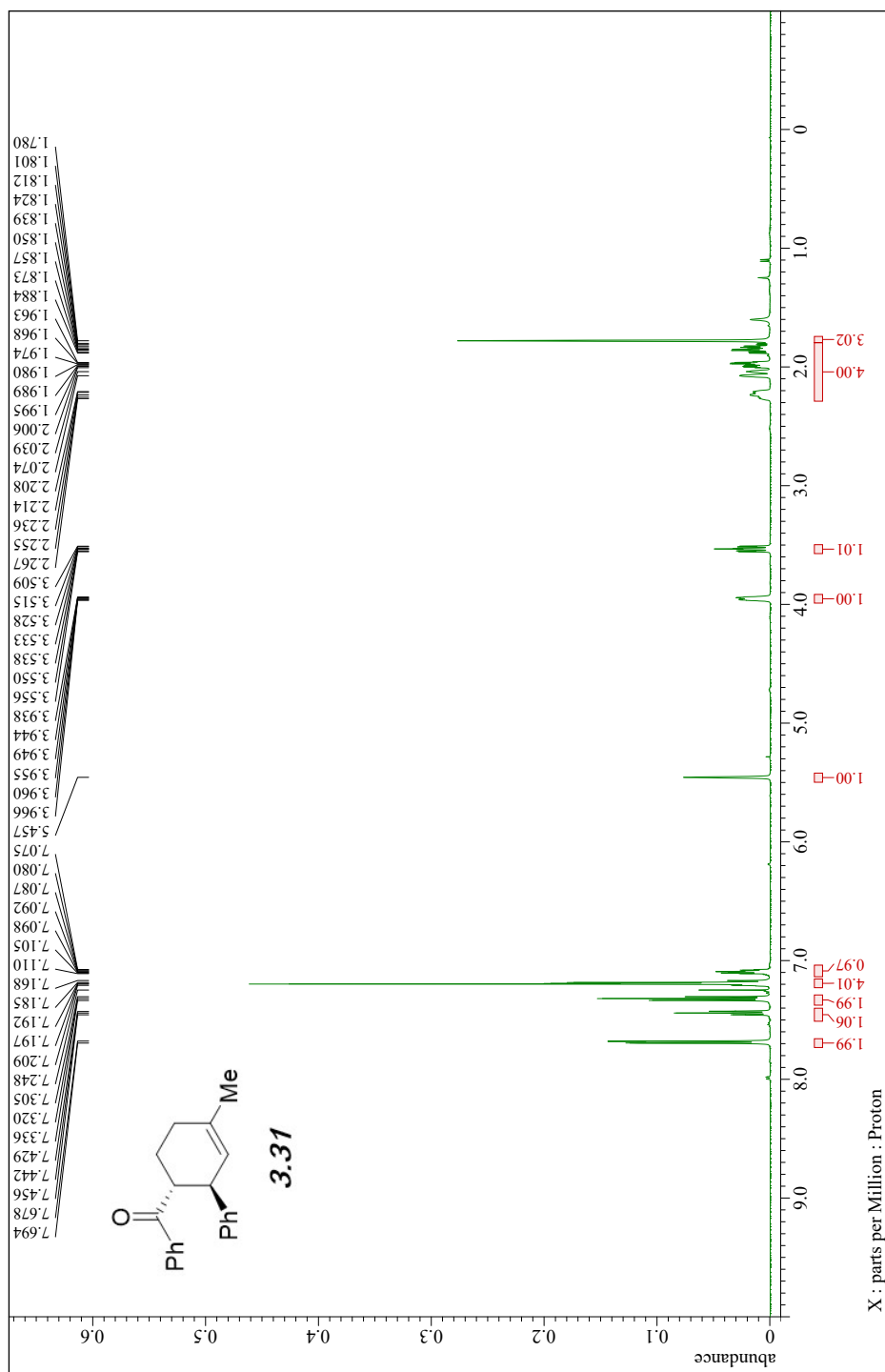


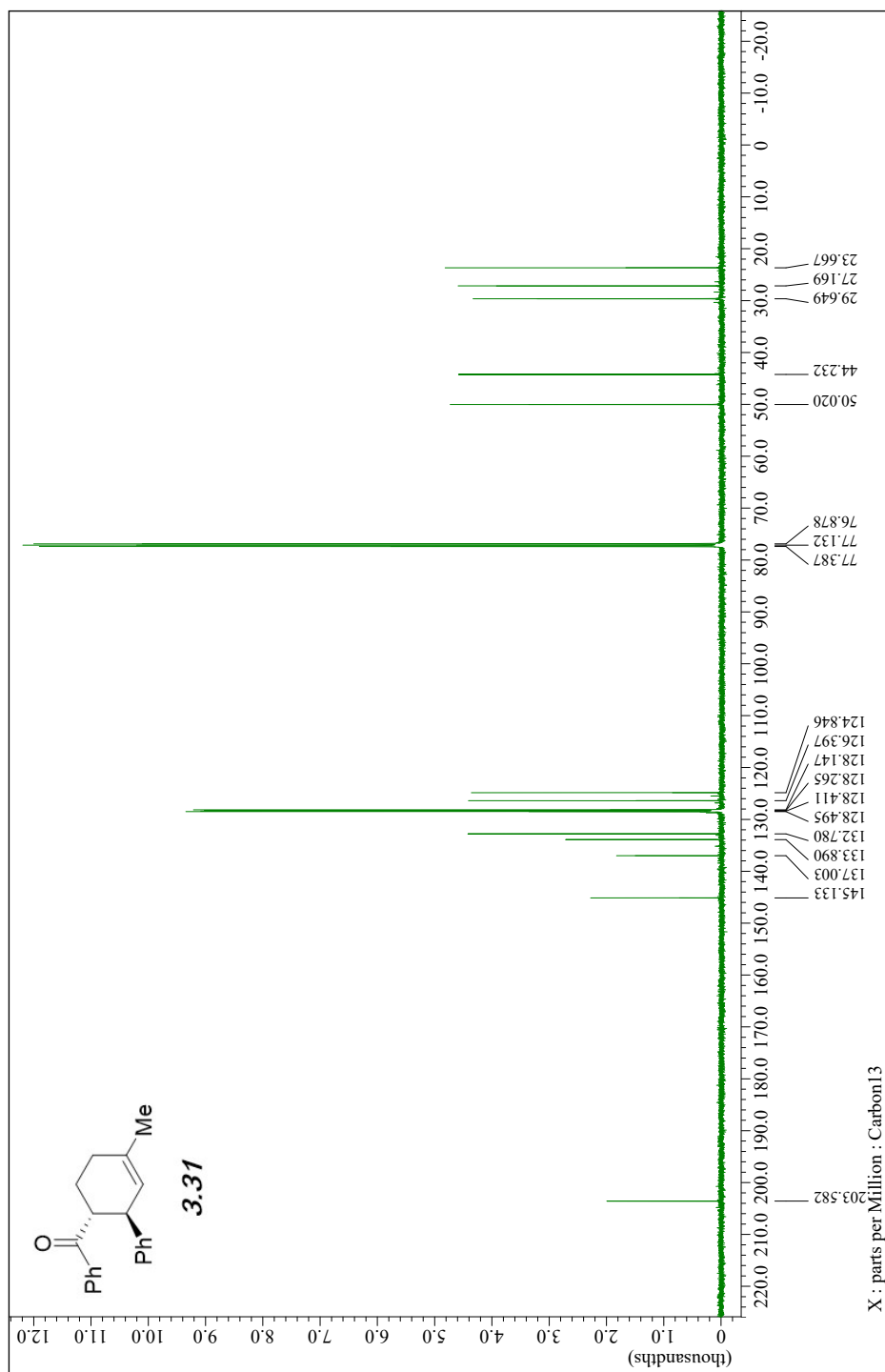
1 PDA Multi 1/254nm 4nm

PeakTable

Peak#	Ret. Time	Area	Height	Area %	Height %
1	21.964	197939	4006	3.113	6.508
2	36.622	6161330	57552	96.887	93.492
Total		6359269	61559	100.000	100.000



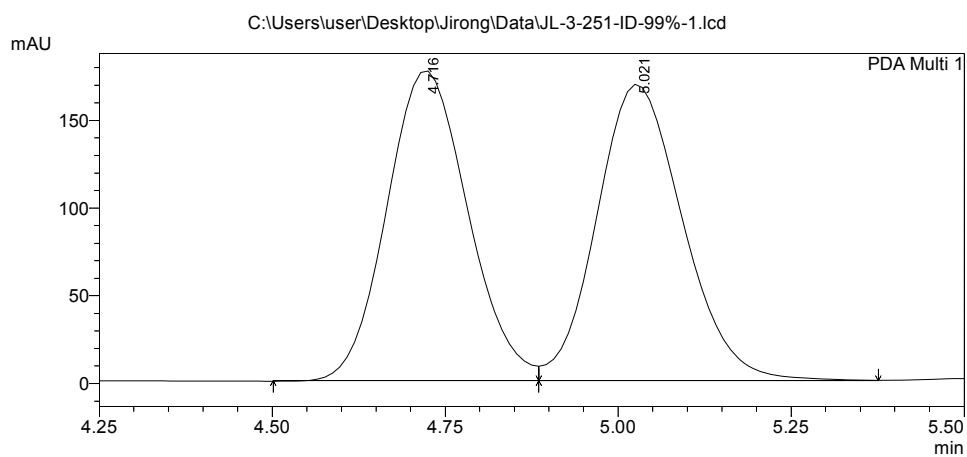




# ==== Shimadzu LCsolution Analysis Report ====

C:\Users\user\Desktop\Jirong\Data\JL-3-251-ID-99%-1.lcd  
Acquired by : Admin  
Sample Name : JL-3-251-ID-99%-1  
Sample ID : JL-3-251-ID-99%-1  
Tray# : 1  
Vial # : 15  
Injection Volume : 10 uL  
Data File Name : JL-3-251-ID-99%-1.lcd  
Method File Name : pos3-99%\_60min\_1.0\_D2.lcm  
Batch File Name : Batch table C3\_99%\_60min\_1.0\_D2.lcb  
Report File Name : Default.lcr  
Data Acquired : 6/7/2021 12:53:42 PM  
Data Processed : 6/7/2021 2:00:24 PM

## <Chromatogram>

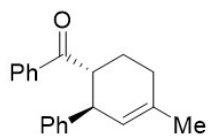


1 PDA Multi 1/254nm 4nm

PeakTable

PDA Ch1 254nm 4nm

Peak#	Ret. Time	Area	Height	Area %	Height %
1	4.716	1439951	176415	49.716	51.084
2	5.021	1456396	168931	50.284	48.916
Total		2896348	345347	100.000	100.000

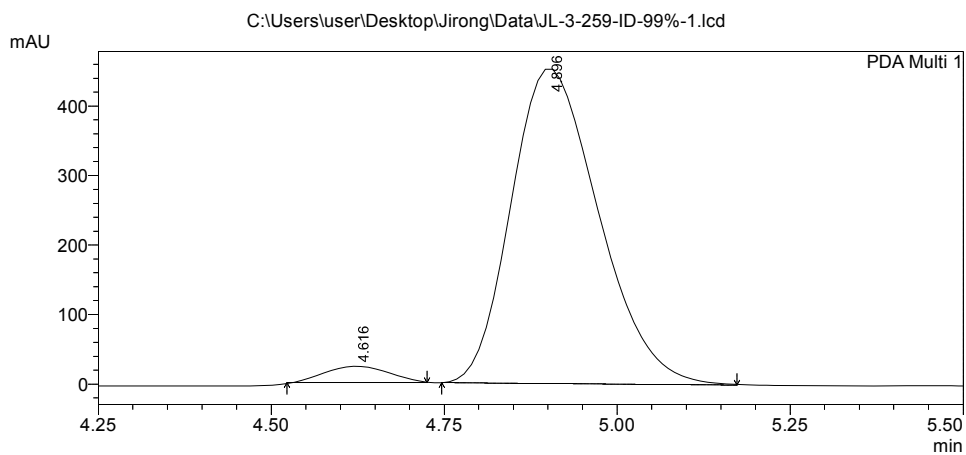


**3.31**

# ==== Shimadzu LcSolution Analysis Report ====

C:\Users\user\Desktop\Jirong\Data\JL-3-259-ID-99%-1.lcd  
Acquired by : Admin  
Sample Name : JL-3-259-ID-99%-1  
Sample ID : JL-3-259-ID-99%-1  
Tray# : 1  
Vial # : 15  
Injection Volume : 10 uL  
Data File Name : JL-3-259-ID-99%-1.lcd  
Method File Name : pos3-99%\_10min\_1.0\_D2.lcm  
Batch File Name : Batch table C3\_99%\_10min\_1.0\_D2.lcb  
Report File Name : Default.lcr  
Data Acquired : 6/14/2021 10:34:56 AM  
Data Processed : 6/17/2021 11:26:00 AM

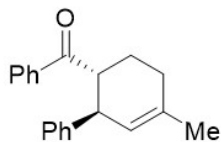
## <Chromatogram>



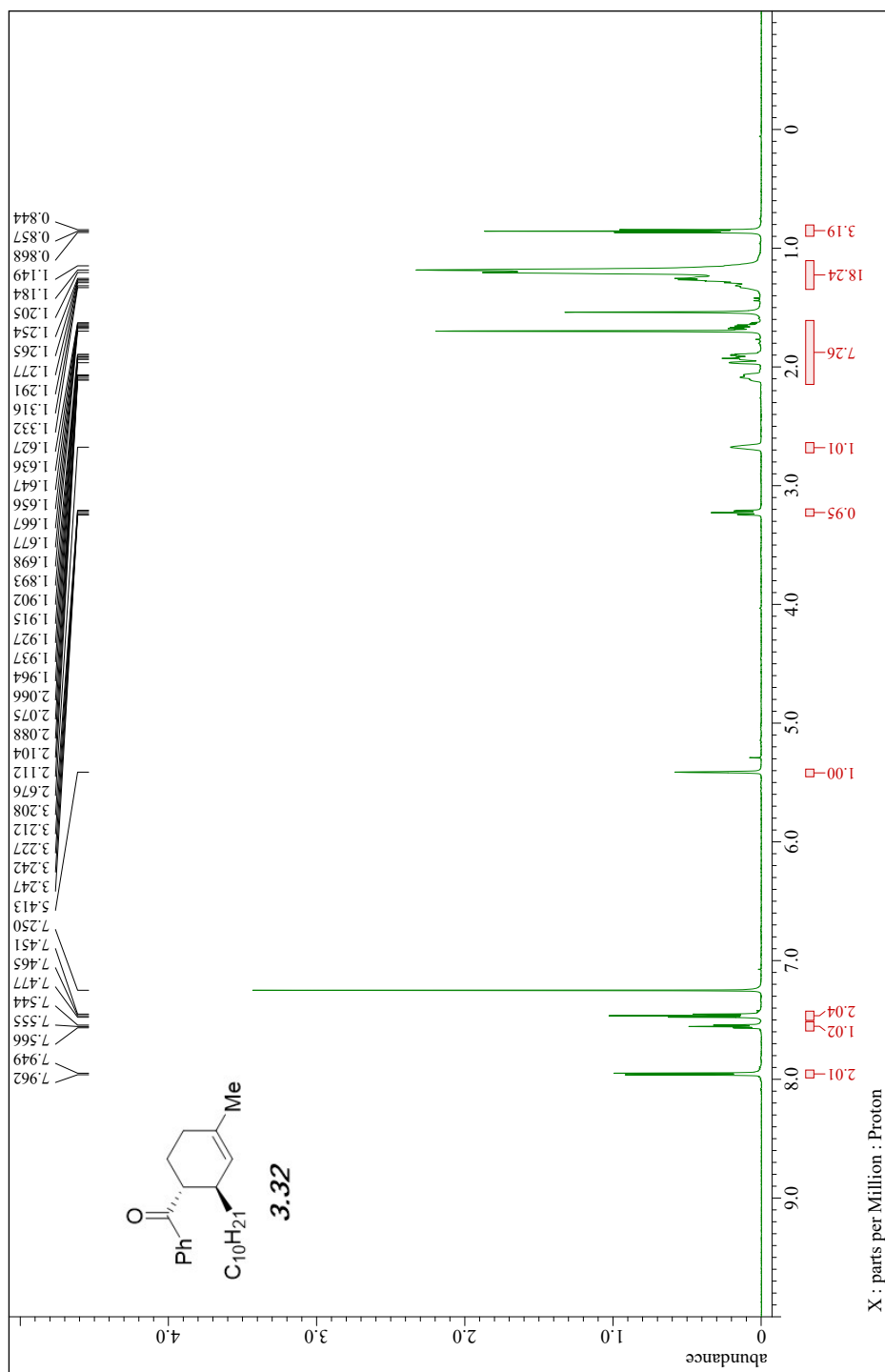
PeakTable

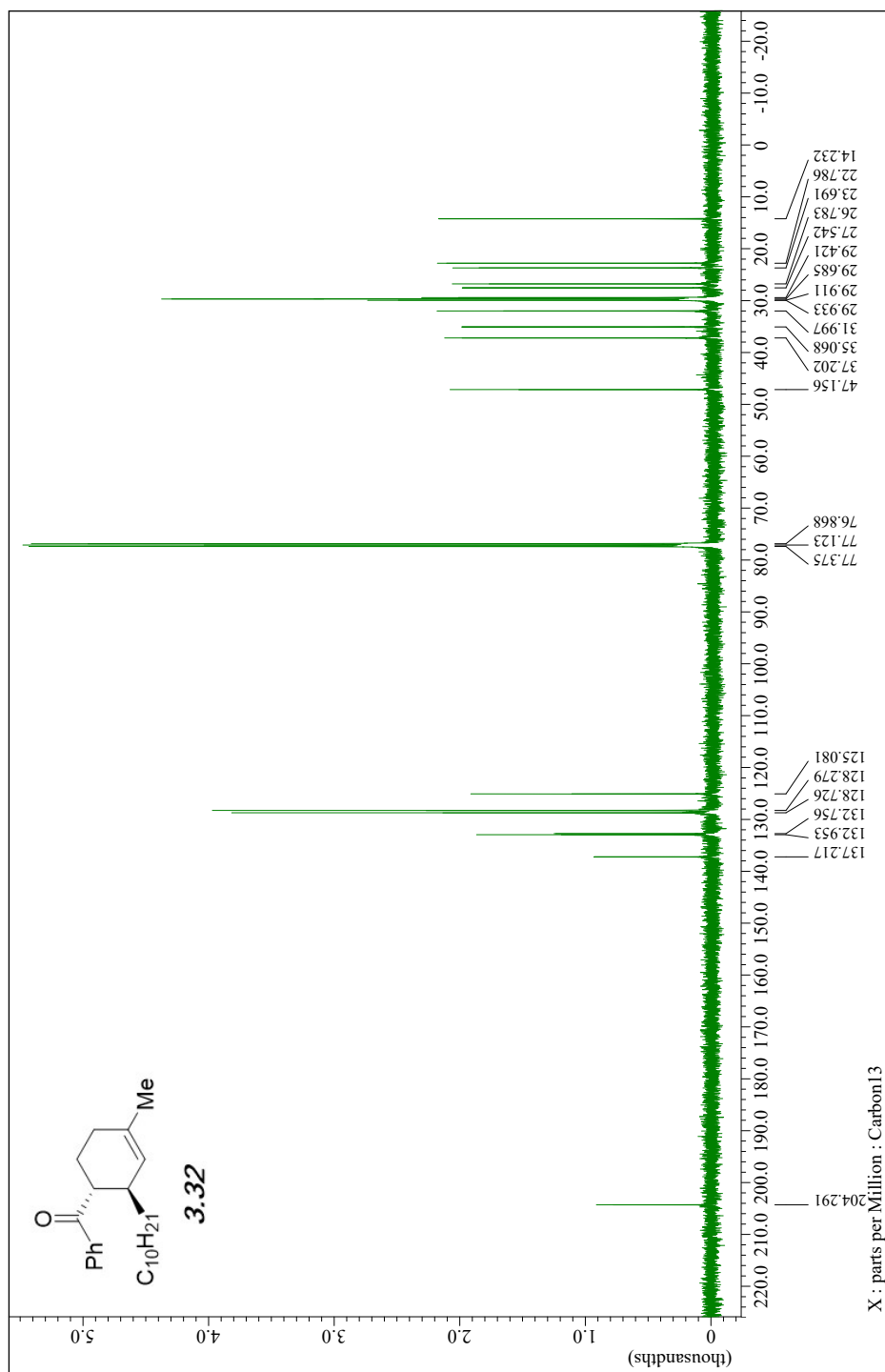
PDA Ch1 254nm 4nm

Peak#	Ret. Time	Area	Height	Area %	Height %
1	4.616	155391	23804	3.751	5.002
2	4.896	3987702	452117	96.249	94.998
Total		4143093	475922	100.000	100.000



**3.31**

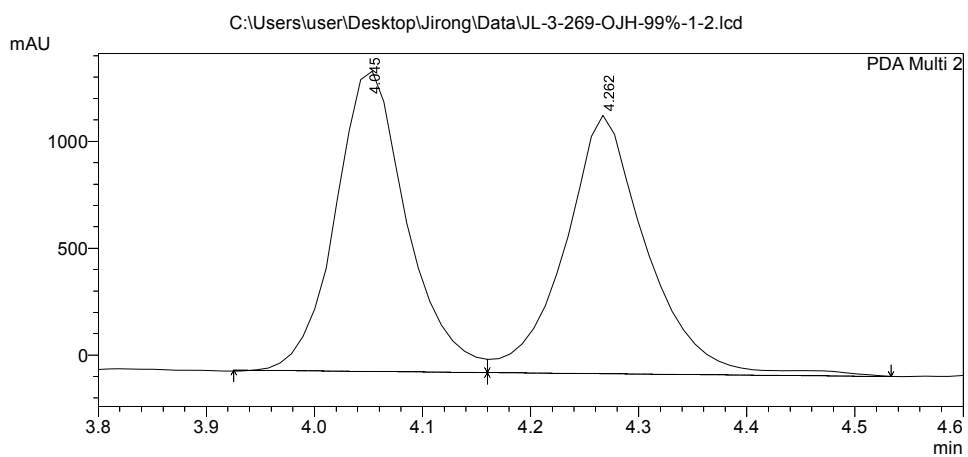




## ==== Shimadzu LCsolution Analysis Report ====

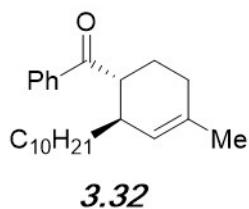
C:\Users\user\Desktop\Jirong\Data\JL-3-269-OJH-99%-1-2.lcd  
 Acquired by : Admin  
 Sample Name : JL-3-269-OJH-99%-1  
 Sample ID : JL-3-269-OJH-99%-1  
 Tray# : 1  
 Vial # : 15  
 Injection Volume : 10 uL  
 Data File Name : JL-3-269-OJH-99%-1-2.lcd  
 Method File Name : pos4\_99%\_30min\_1\_D2.lcm  
 Batch File Name : Batch\_table\_C4-99\_30min\_1\_D2.lcb  
 Report File Name : Default.lcr  
 Data Acquired : 7/6/2021 1:57:53 PM  
 Data Processed : 7/8/2021 6:17:40 PM

### <Chromatogram>



PeakTable

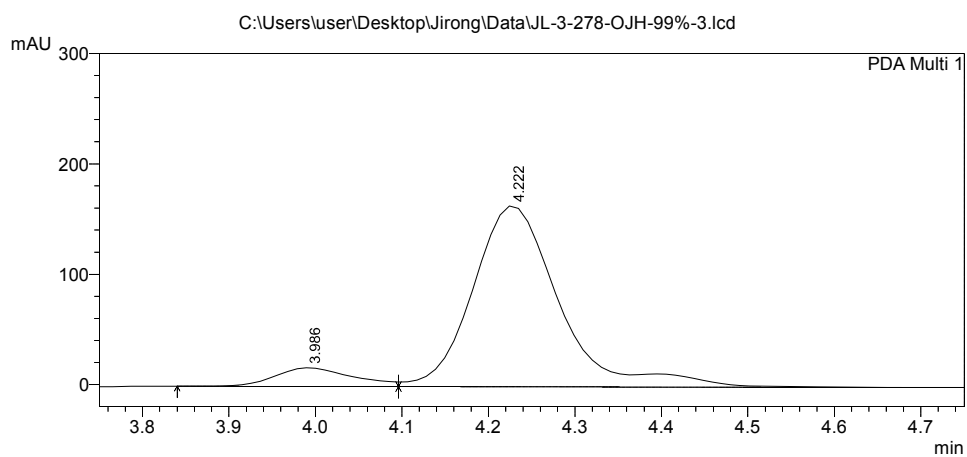
Peak#	Ret. Time	Area	Height	Area %	Height %
1	4.045	6469478	1403895	50.380	53.730
2	4.262	6371948	1208957	49.620	46.270
Total		12841425	2612852	100.000	100.000



## ==== Shimadzu LCsolution Analysis Report ====

C:\Users\user\Desktop\Jirong\Data\JL-3-278-OJH-99%-3.lcd  
 Acquired by : Admin  
 Sample Name : JL-3-278-OJH-99%-1  
 Sample ID : JL-3-278-OJH-99%-1  
 Tray# : 1  
 Vial # : 15  
 Injection Volume : 10 uL  
 Data File Name : JL-3-278-OJH-99%-3.lcd  
 Method File Name : pos4\_99%\_30min\_1\_D2.lcm  
 Batch File Name : Batch\_table\_C4-99\_30min\_1\_D2.lcb  
 Report File Name : Default.lcr  
 Data Acquired : 9/27/2021 10:41:55 AM  
 Data Processed : 9/27/2021 12:00:00 PM

### <Chromatogram>

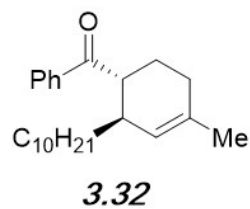


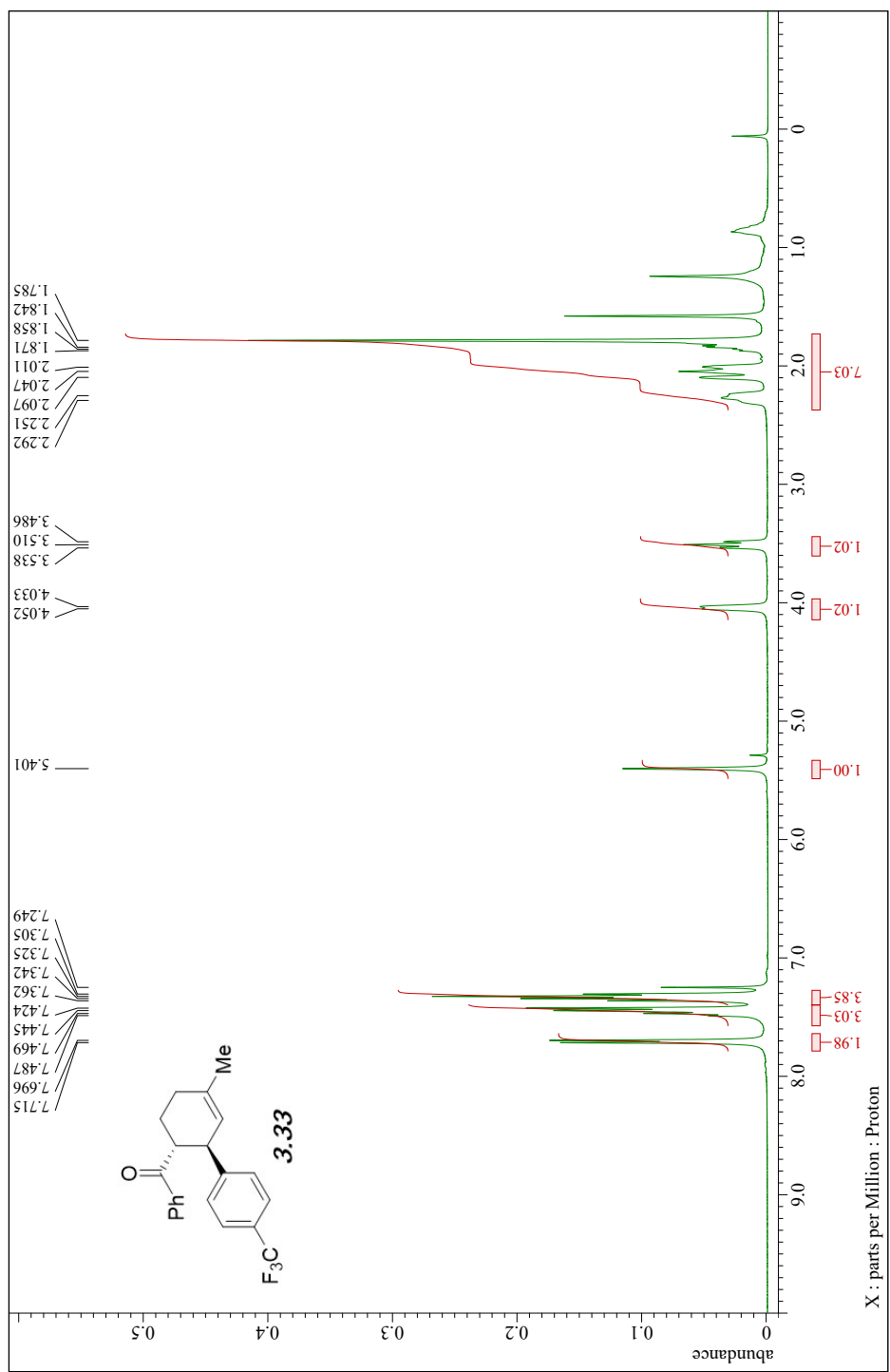
1 PDA Multi 1/254nm 4nm

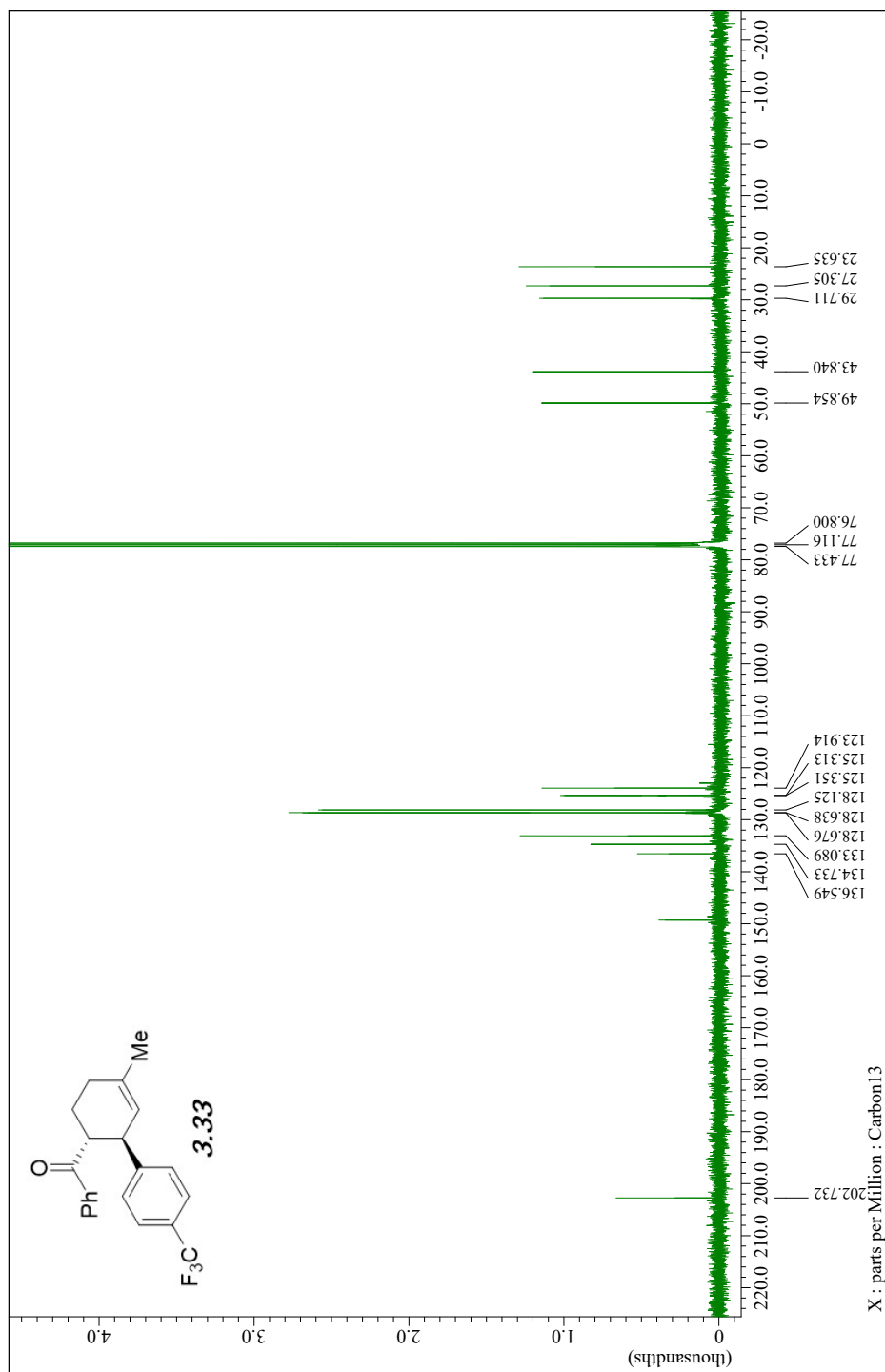
PeakTable

PDA Ch1 254nm 4nm

Peak#	Ret. Time	Area	Height	Area %	Height %
1	3.986	107124	16950	8.568	9.366
2	4.222	1143183	164019	91.432	90.634
Total		1250307	180969	100.000	100.000



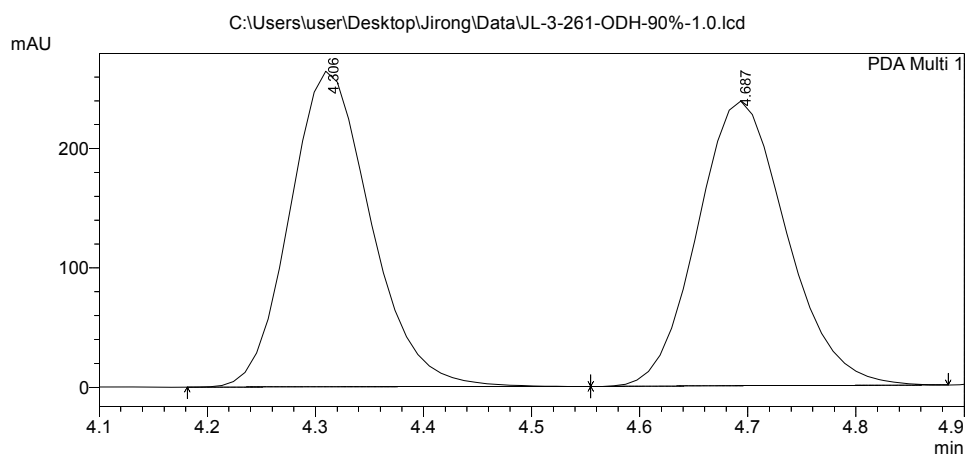




# ==== Shimadzu LCsolution Analysis Report ====

C:\Users\user\Desktop\Jirong\Data\JL-3-261-ODH-90%-1.0.lcd  
Acquired by : Admin  
Sample Name : JL-3-261-ODH-90%-1.0  
Sample ID : JL-3-261-ODH-90%-1.0  
Tray# : 1  
Vial # : 15  
Injection Volume : 10 uL  
Data File Name : JL-3-261-ODH-90%-1.0.lcd  
Method File Name : pos5\_90%\_60min\_1.0\_D2.lcm  
Batch File Name : Batch\_table\_C5-90\_60min\_1.0\_d2.lcb  
Report File Name : Default.lcr  
Data Acquired : 7/12/2021 2:17:31 PM  
Data Processed : 7/13/2021 12:48:35 PM

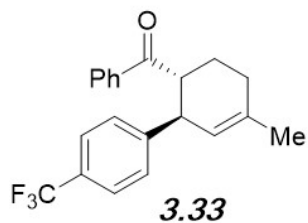
## <Chromatogram>



1 PDA Multi 1/254nm 4nm

PeakTable

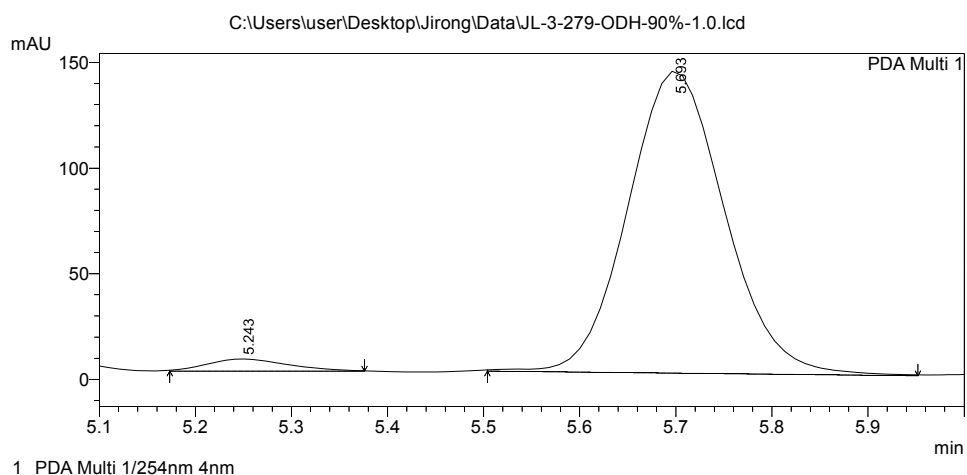
Peak#	Ret. Time	Area	Height	Area %	Height %
1	4.306	1378201	264395	50.164	52.559
2	4.687	1369181	238646	49.836	47.441
Total		2747381	503042	100.000	100.000



## ==== Shimadzu LCsolution Analysis Report ====

C:\Users\user\Desktop\Jirong\Data\JL-3-279-ODH-90%-1.0.lcd  
 Acquired by : Admin  
 Sample Name : JL-3-279-ODH-90%-1.0  
 Sample ID : JL-3-279-ODH-90%-1.0  
 Tray# : 1  
 Vial # : 15  
 Injection Volume : 10 uL  
 Data File Name : JL-3-279-ODH-90%-1.0.lcd  
 Method File Name : pos5\_90%\_60min\_1.0\_D2.lcm  
 Batch File Name : Batch\_table\_C5-90\_60min\_1.0\_d2.lcb  
 Report File Name : Default.lcr  
 Data Acquired : 7/13/2021 12:36:27 PM  
 Data Processed : 7/13/2021 12:48:52 PM

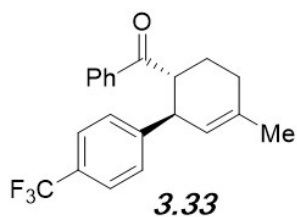
### <Chromatogram>

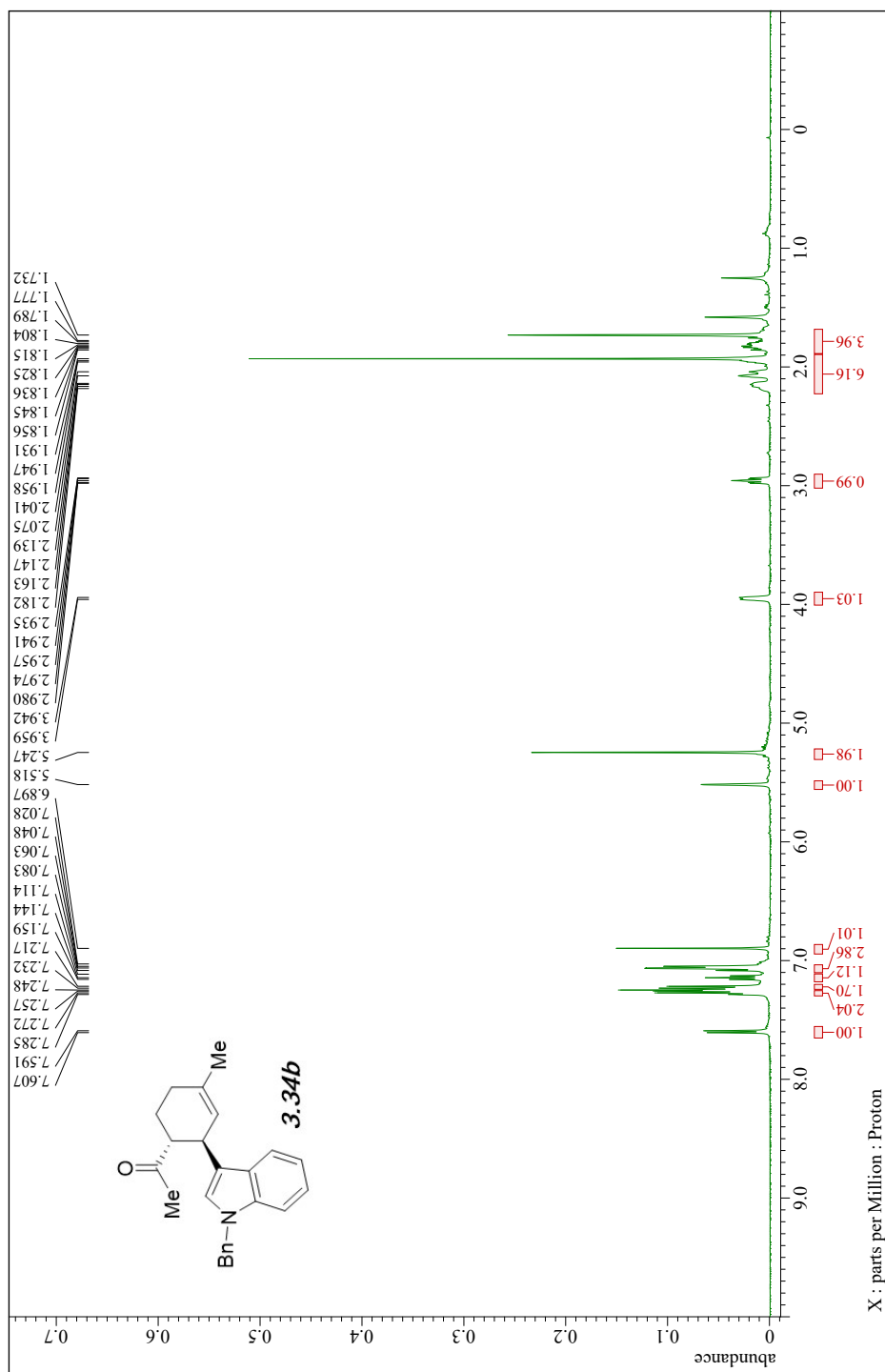


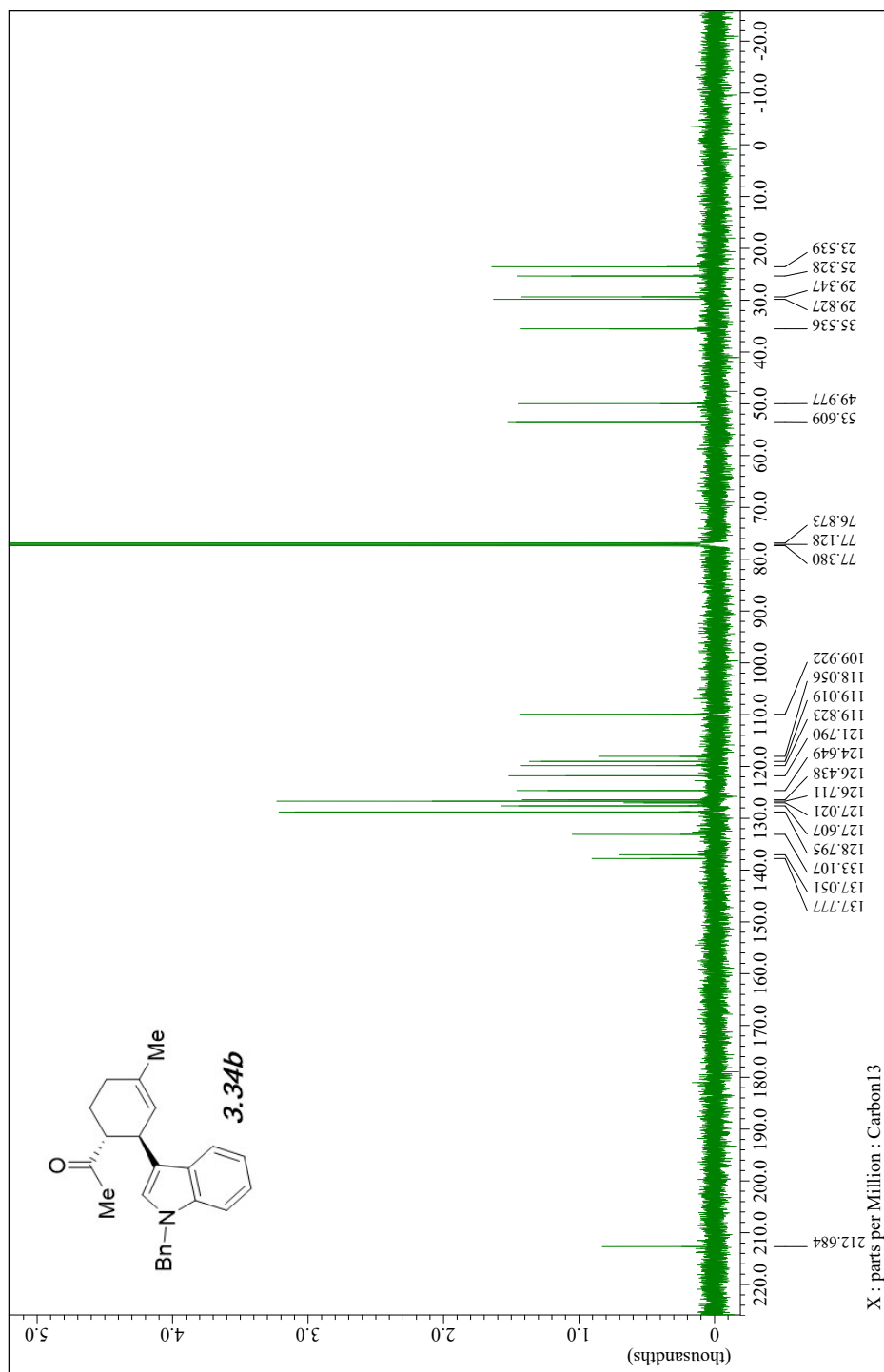
PeakTable

PDA Ch1 254nm 4nm

Peak#	Ret. Time	Area	Height	Area %	Height %
1	5.243	33507	5746	3.232	3.867
2	5.693	1003229	142856	96.768	96.133
Total		1036736	148603	100.000	100.000



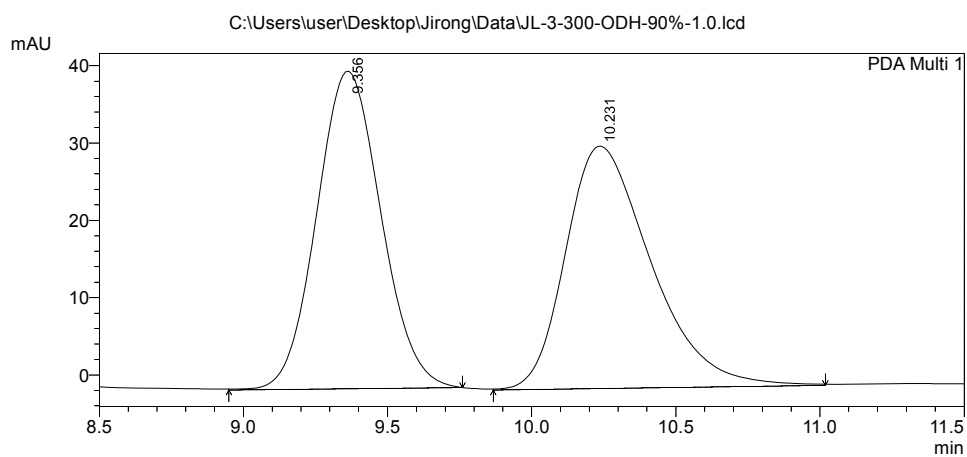




## ==== Shimadzu LCsolution Analysis Report ====

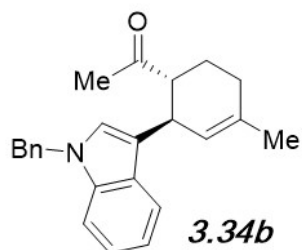
Acquired by : Admin  
Sample Name : JL-3-300-ODH-90%-1.0  
Sample ID : JL-3-300-ODH-90%-1.0  
Tray# : 1  
Vial # : 15  
Injection Volume : 10 uL  
Data File Name : JL-3-300-ODH-90%-1.0.lcd  
Method File Name : pos5\_90%\_60min\_1.0\_D2.lcm  
Batch File Name : Batch\_table\_C5-90\_60min\_1.0\_d2.lcb  
Report File Name : Default.lcr  
Data Acquired : 8/12/2021 10:28:50 AM  
Data Processed : 8/27/2021 11:25:19 AM

### <Chromatogram>



PeakTable

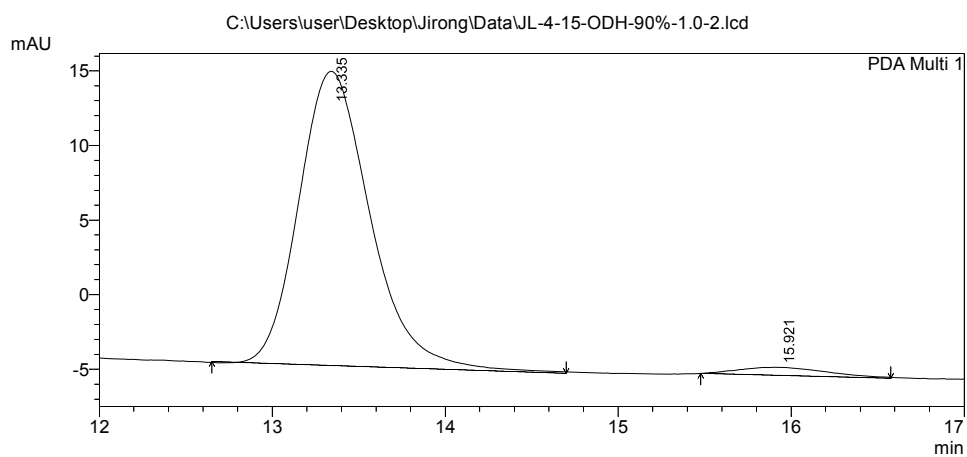
Peak#	Ret. Time	Area	Height	Area %	Height %
1	9.356	637922	41073	49.598	56.705
2	10.231	648256	31360	50.402	43.295
Total		1286179	72433	100.000	100.000



## ==== Shimadzu LCsolution Analysis Report ====

C:\Users\user\Desktop\Jirong\Data\JL-4-15-ODH-90%-1.0-2.lcd  
 Acquired by : Admin  
 Sample Name : JL-4-15-ODH-90%-1.0  
 Sample ID : JL-4-15-ODH-90%-1.0  
 Tray# : 1  
 Vial # : 15  
 Injection Volume : 10 uL  
 Data File Name : JL-4-15-ODH-90%-1.0-2.lcd  
 Method File Name : pos5\_90%\_60min\_1.0\_D2.lcm  
 Batch File Name : Batch\_table\_C5-90\_60min\_1.0\_d2.lcb  
 Report File Name : Default.lcr  
 Data Acquired : 9/2/2021 3:03:12 PM  
 Data Processed : 9/2/2021 3:24:12 PM

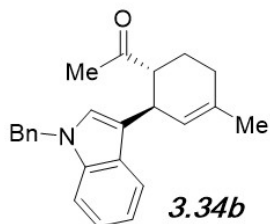
### <Chromatogram>

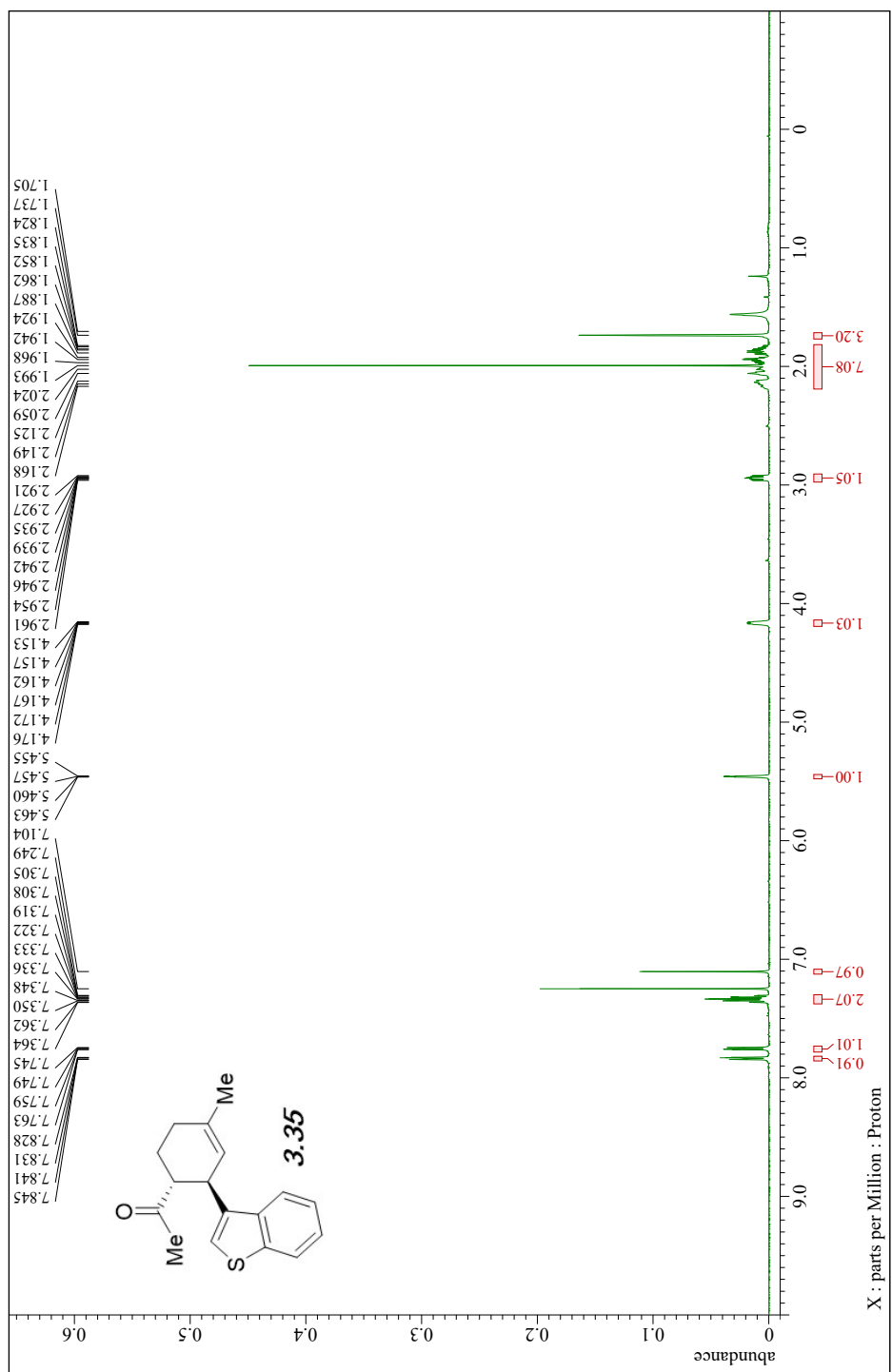


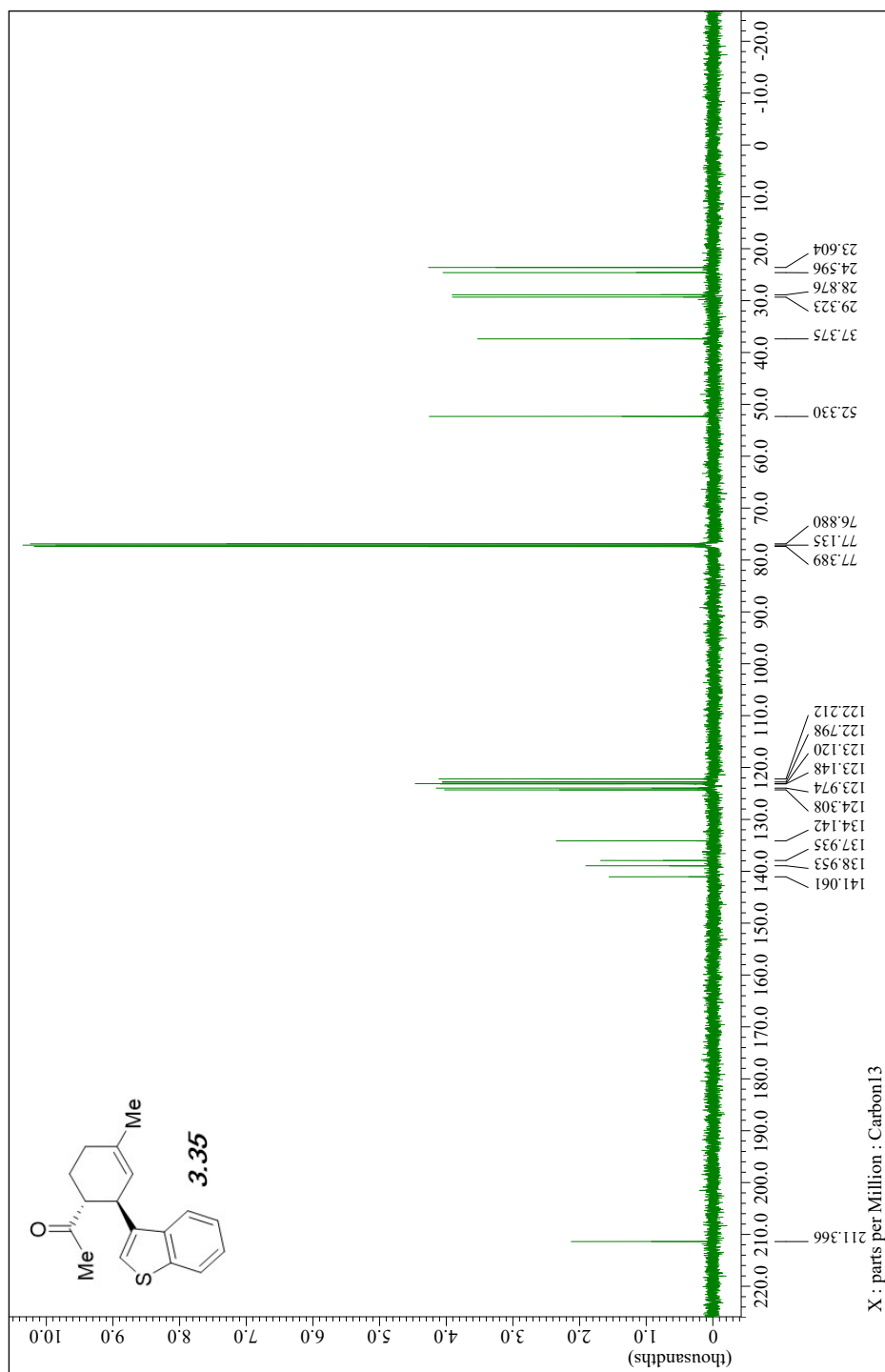
1 PDA Multi 1/254nm 4nm

PeakTable

PDA Ch1 254nm 4nm					
Peak#	Ret. Time	Area	Height	Area %	Height %
1	13.335	566163	19732	96.710	97.275
2	15.921	19262	553	3.290	2.725
Total		585425	20285	100.000	100.000



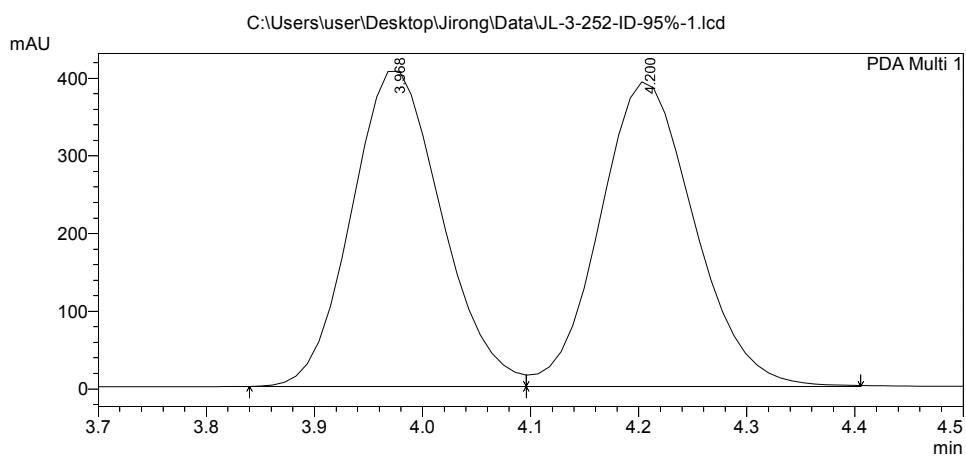




# ==== Shimadzu LcSolution Analysis Report ====

C:\Users\user\Desktop\Jirong\Data\JL-3-252-ID-95%-1.lcd  
Acquired by : Admin  
Sample Name : JL-3-252-ID-95%-1  
Sample ID : JL-3-252-ID-95%-1  
Tray# : 1  
Vial # : 15  
Injection Volume : 10 uL  
Data File Name : JL-3-252-ID-95%-1.lcd  
Method File Name : pos3-95%\_20min\_1.0\_D2.lcm  
Batch File Name : Batch table C3\_95%\_20min\_1.0\_D2.lcb  
Report File Name : Default.lcr  
Data Acquired : 6/5/2021 1:04:17 PM  
Data Processed : 6/5/2021 2:13:00 PM

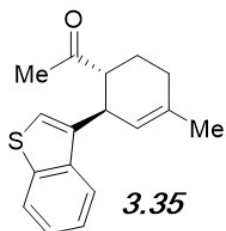
## <Chromatogram>



PeakTable

PDA Ch1 254nm 4nm

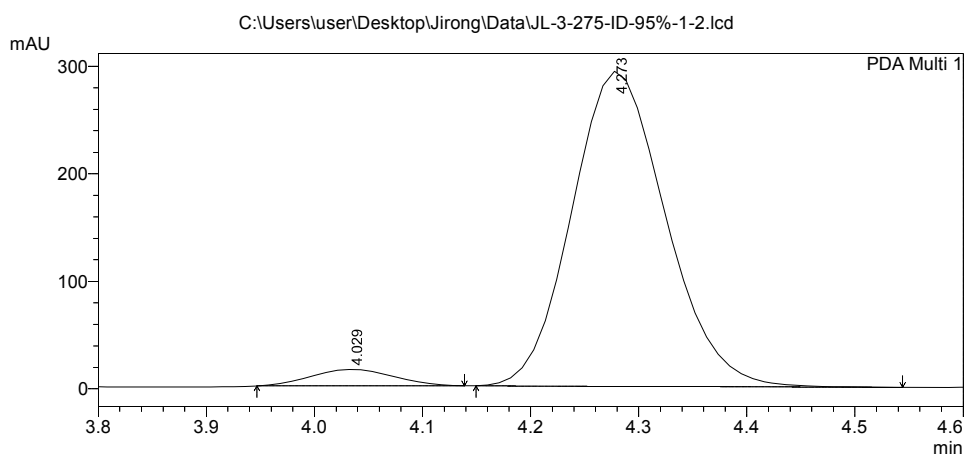
Peak#	Ret. Time	Area	Height	Area %	Height %
1	3.968	2357209	405350	49.802	50.826
2	4.200	2375908	392170	50.198	49.174
Total		4733117	797520	100.000	100.000



## ==== Shimadzu LcSolution Analysis Report ====

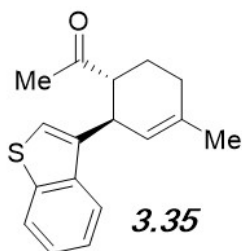
C:\Users\user\Desktop\Jirong\Data\JL-3-275-ID-95%-1-2.lcd  
 Acquired by : Admin  
 Sample Name : JL-3-275-ID-95%-1  
 Sample ID : JL-3-275-ID-95%-1  
 Tray# : 1  
 Vial # : 15  
 Injection Volume : 10 uL  
 Data File Name : JL-3-275-ID-95%-1-2.lcd  
 Method File Name : pos3-95%\_20min\_1.0\_D2.lcm  
 Batch File Name : Batch table C3\_95%\_20min\_1.0\_D2.lcb  
 Report File Name : Default.lcr  
 Data Acquired : 7/6/2021 4:21:56 PM  
 Data Processed : 7/6/2021 4:34:53 PM

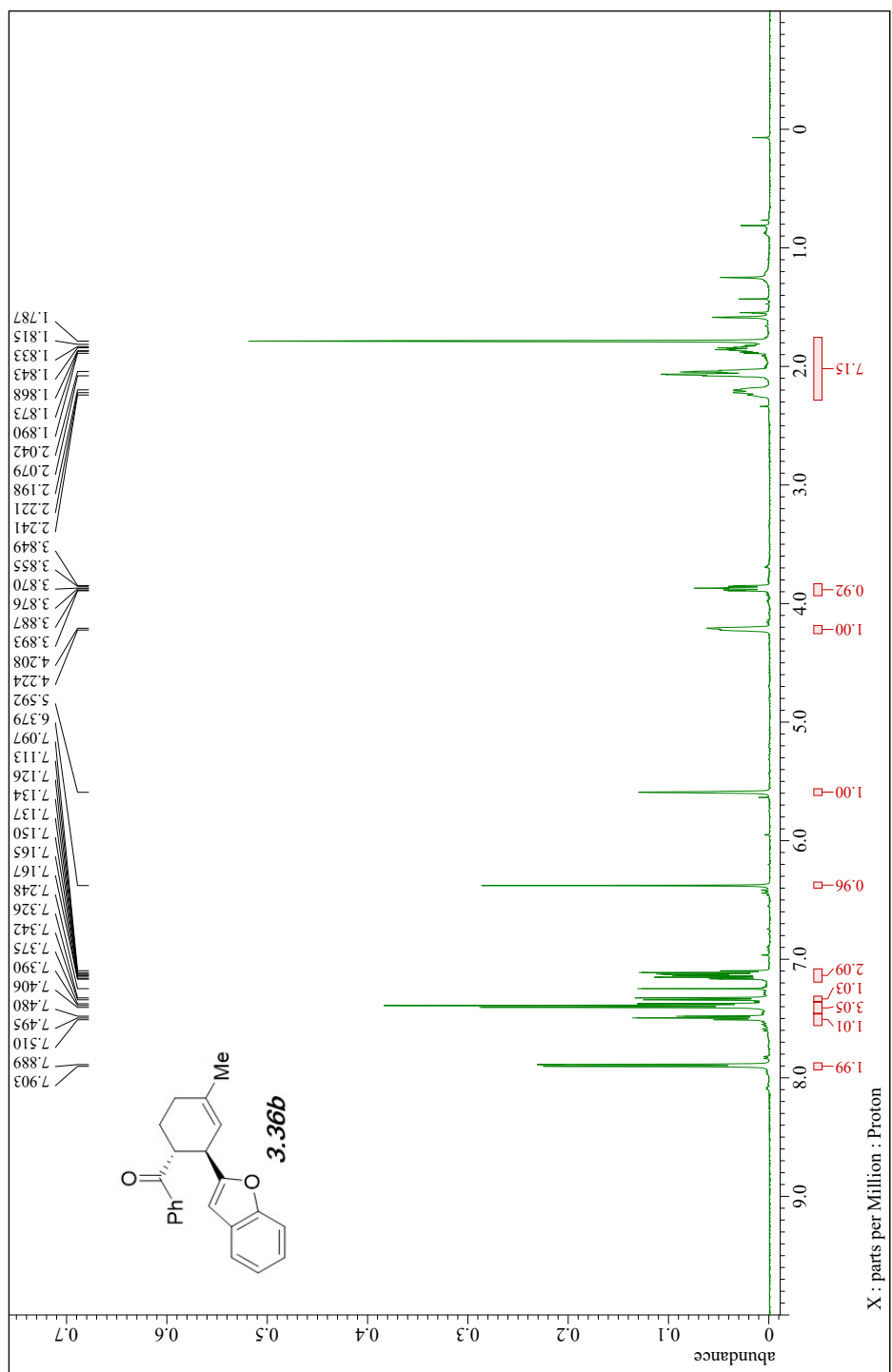
### <Chromatogram>

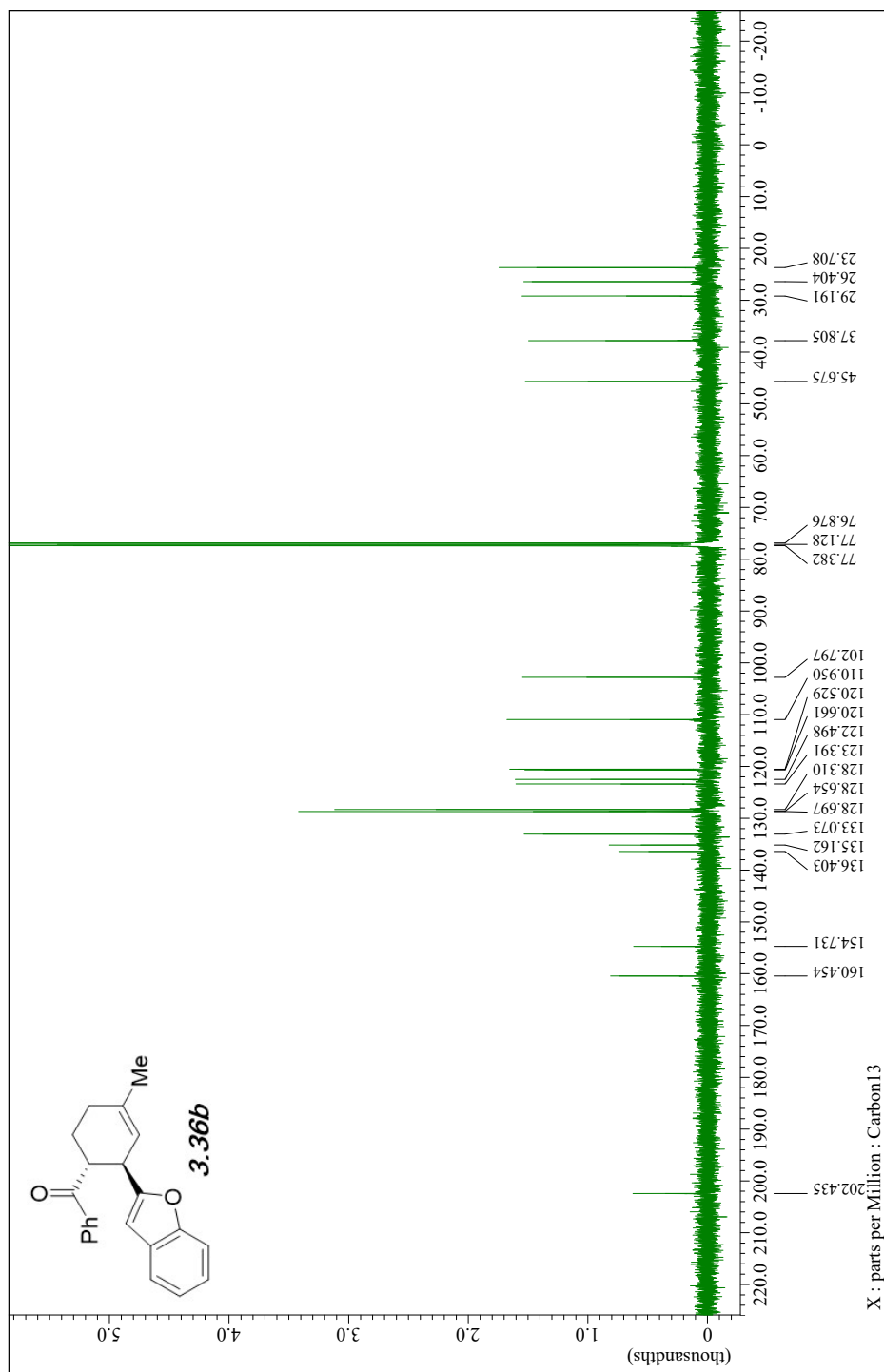


PeakTable

Peak#	Ret. Time	Area	Height	Area %	Height %
1	4.029	82001	15406	4.435	4.996
2	4.273	1767012	292973	95.565	95.004
Total		1849013	308379	100.000	100.000



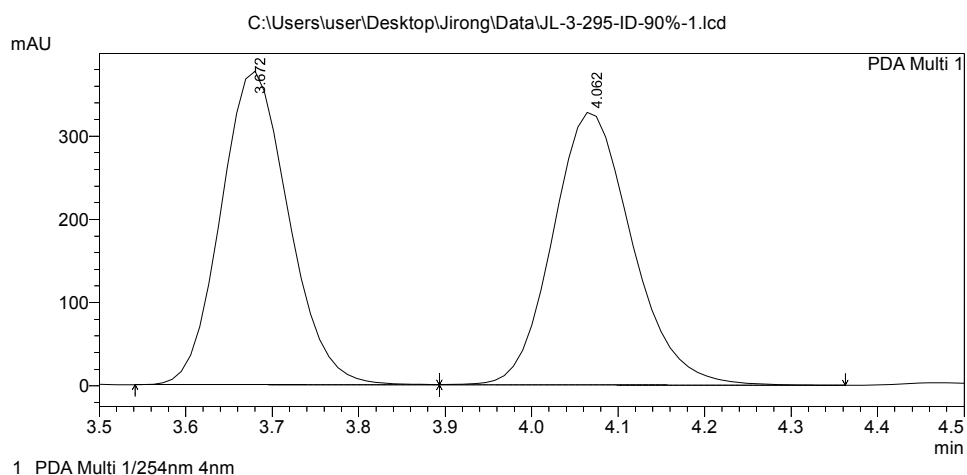




## ==== Shimadzu LCsolution Analysis Report ====

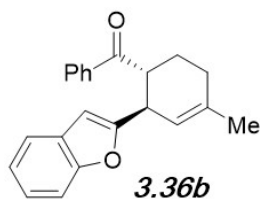
C:\Users\user\Desktop\Jirong\Data\JL-3-295-ID-90%-1.lcd  
 Acquired by : Admin  
 Sample Name : JL-3-295-ID-90%-1  
 Sample ID : JL-3-295-ID-90%-1  
 Tray# : 1  
 Vial # : 15  
 Injection Volume : 10 uL  
 Data File Name : JL-3-295-ID-90%-1.lcd  
 Method File Name : pos3-90%\_60MIN\_1.0\_D2.lcm  
 Batch File Name : Batch table C3\_90%\_60min\_1.0\_D2.lcb  
 Report File Name : Default.lcr  
 Data Acquired : 8/5/2021 11:14:17 AM  
 Data Processed : 8/5/2021 11:29:57 AM

### <Chromatogram>



PeakTable

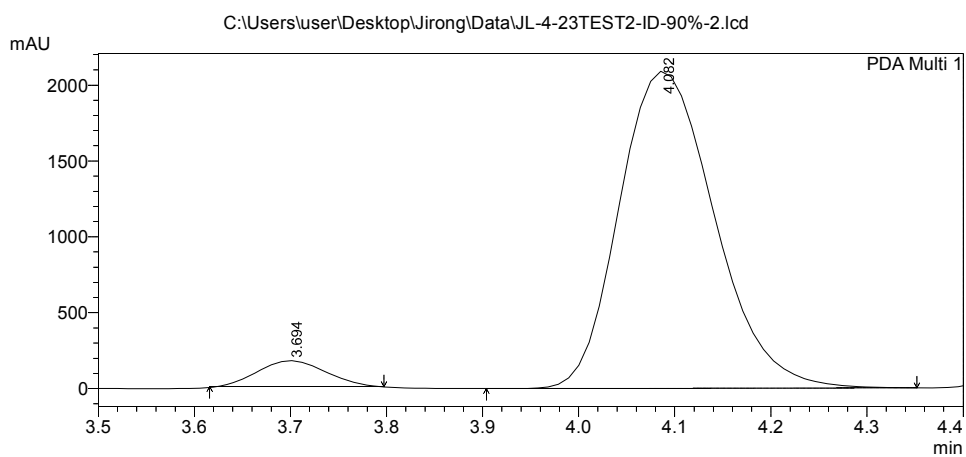
Peak#	Ret. Time	Area	Height	Area %	Height %
1	3.672	2056356	376481	49.651	53.479
2	4.062	2085251	327501	50.349	46.521
Total		4141606	703981	100.000	100.000



## ==== Shimadzu LcSolution Analysis Report ====

C:\Users\user\Desktop\Jirong\Data\JL-4-23TEST2-ID-90%-2.lcd  
 Acquired by : Admin  
 Sample Name : JL-4-23TEST2-ID-90%-1  
 Sample ID : JL-4-23TEST2-ID-90%-1  
 Tray# : 1  
 Vial # : 15  
 Injection Volume : 10 uL  
 Data File Name : JL-4-23TEST2-ID-90%-2.lcd  
 Method File Name : pos3-90%\_10MIN\_1\_d2.lcm  
 Batch File Name : Batch table C3\_90%\_10min\_1.0\_D2.lcb  
 Report File Name : Default.lcr  
 Data Acquired : 9/17/2021 11:06:07 AM  
 Data Processed : 9/17/2021 11:16:10 AM

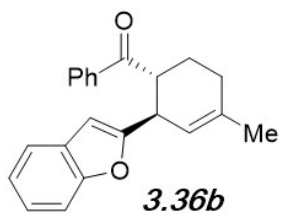
### <Chromatogram>

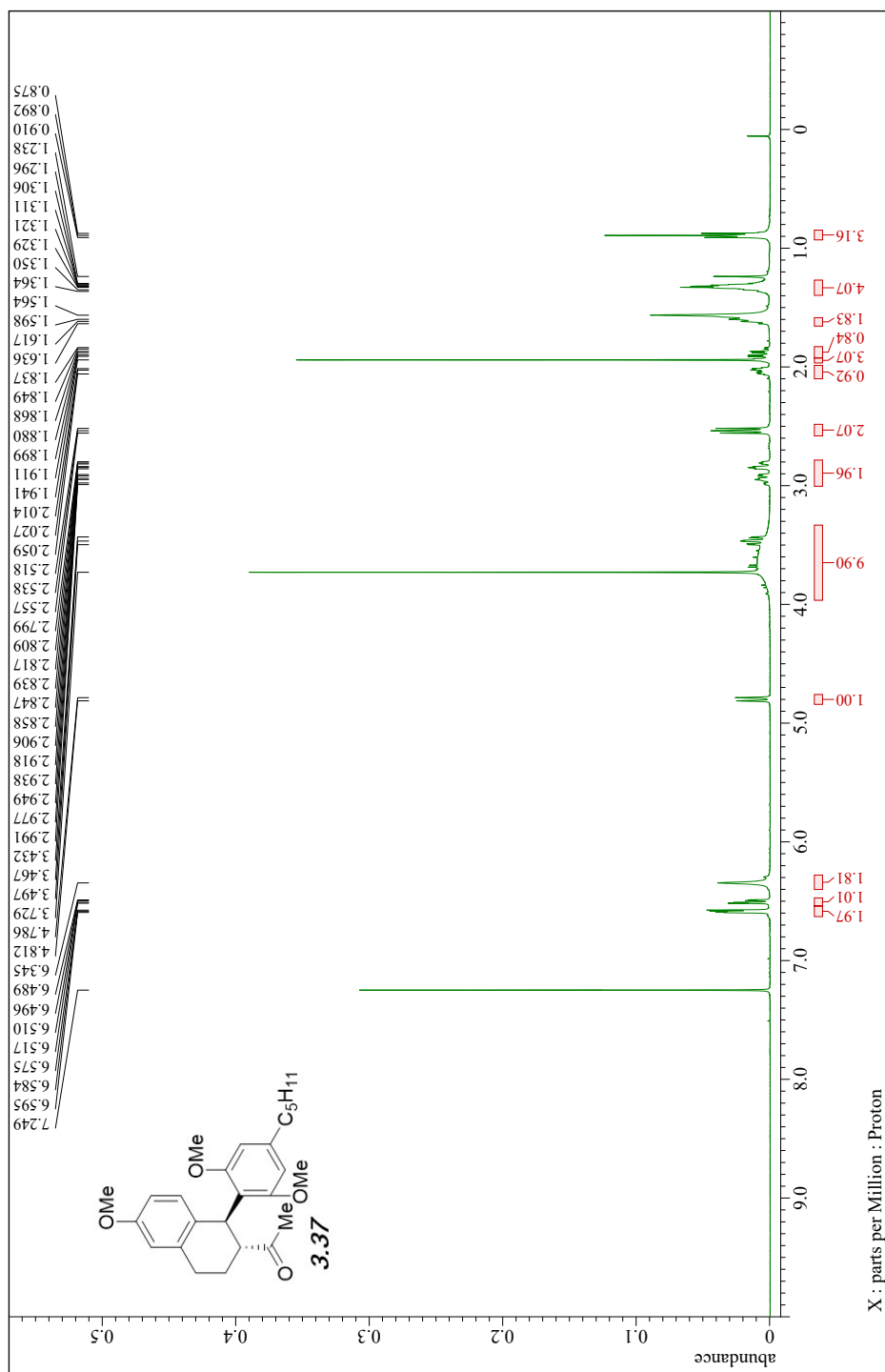


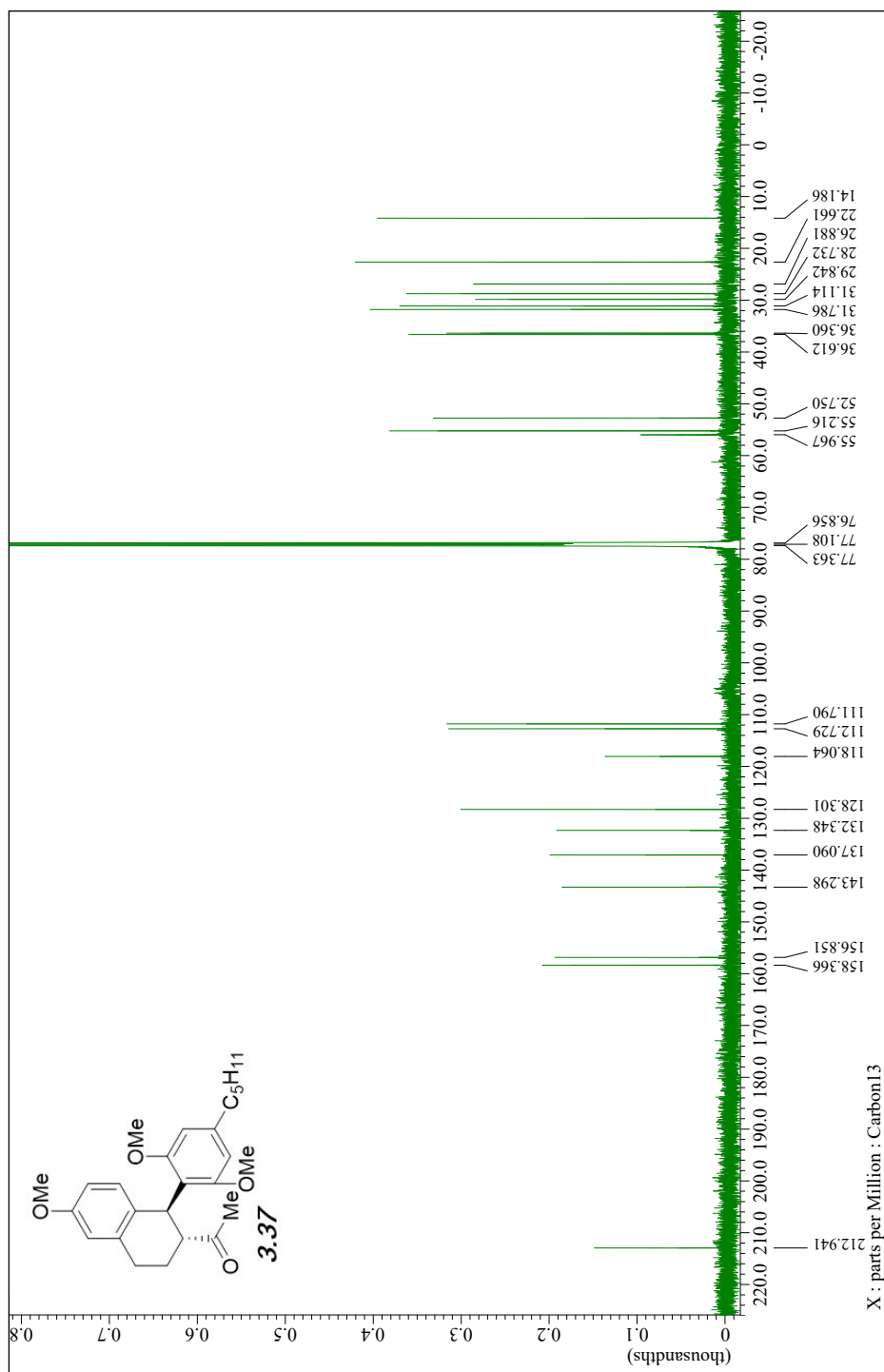
PeakTable

PDA Ch1 254nm 4nm

Peak#	Ret. Time	Area	Height	Area %	Height %
1	3.694	851353	171912	5.584	7.605
2	4.082	14393733	2088574	94.416	92.395
Total		15245086	2260486	100.000	100.000



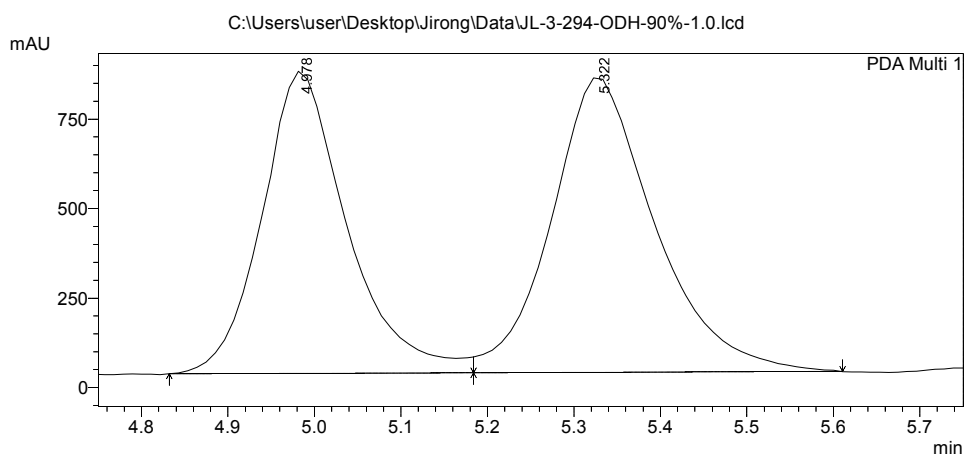




## ==== Shimadzu LCsolution Analysis Report ====

C:\Users\user\Desktop\Jirong\Data\JL-3-294-ODH-90%-1.0.lcd  
 Acquired by : Admin  
 Sample Name : JL-3-294-ODH-90%-1.0  
 Sample ID : JL-3-294-ODH-90%-1.0  
 Tray# : 1  
 Vial # : 15  
 Injection Volume : 10 uL  
 Data File Name : JL-3-294-ODH-90%-1.0.lcd  
 Method File Name : pos5\_90%\_60min\_1.0\_D2.lcm  
 Batch File Name : Batch\_table\_C5-90\_60min\_1.0\_d2.lcb  
 Report File Name : Default.lcr  
 Data Acquired : 8/12/2021 11:49:11 AM  
 Data Processed : 8/12/2021 12:14:19 PM

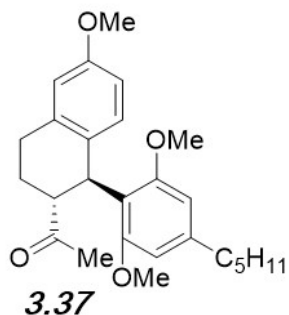
### <Chromatogram>



1 PDA Multi 1/190nm 4nm

Peak Table

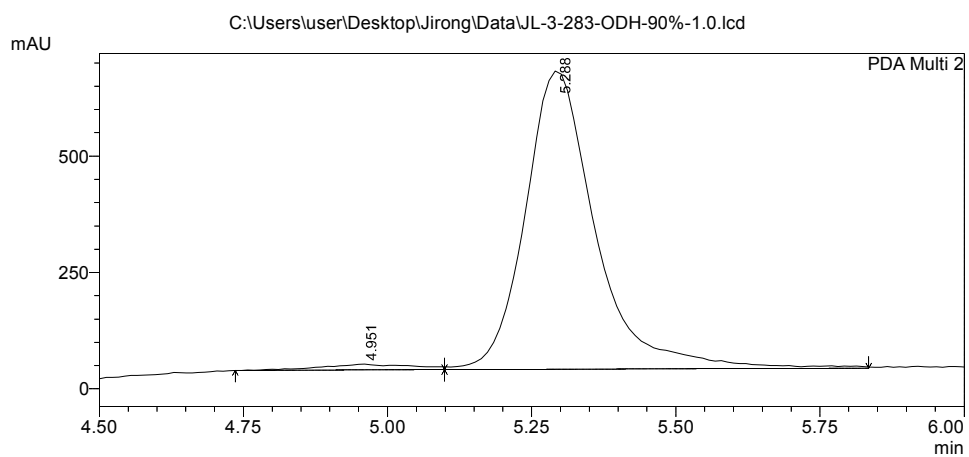
Peak#	Ret. Time	Area	Height	Area %	Height %
1	4.978	5795129	843943	45.893	50.641
2	5.322	6832280	822570	54.107	49.359
Total		12627409	1666513	100.000	100.000



## ==== Shimadzu LCsolution Analysis Report ====

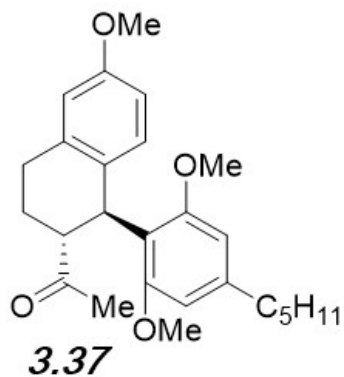
C:\Users\user\Desktop\Jirong\Data\JL-3-283-ODH-90%-1.0.lcd  
 Acquired by : Admin  
 Sample Name : JL-3-283-ODH-90%-1.0  
 Sample ID : JL-3-283-ODH-90%-1.0  
 Tray# : 1  
 Vial # : 15  
 Injection Volume : 10 uL  
 Data File Name : JL-3-283-ODH-90%-1.0.lcd  
 Method File Name : pos5\_90%\_60min\_1.0\_D2.lcm  
 Batch File Name : Batch\_table\_C5-90\_60min\_1.0\_d2.lcb  
 Report File Name : Default.lcr  
 Data Acquired : 8/12/2021 2:32:23 PM  
 Data Processed : 8/12/2021 2:42:03 PM

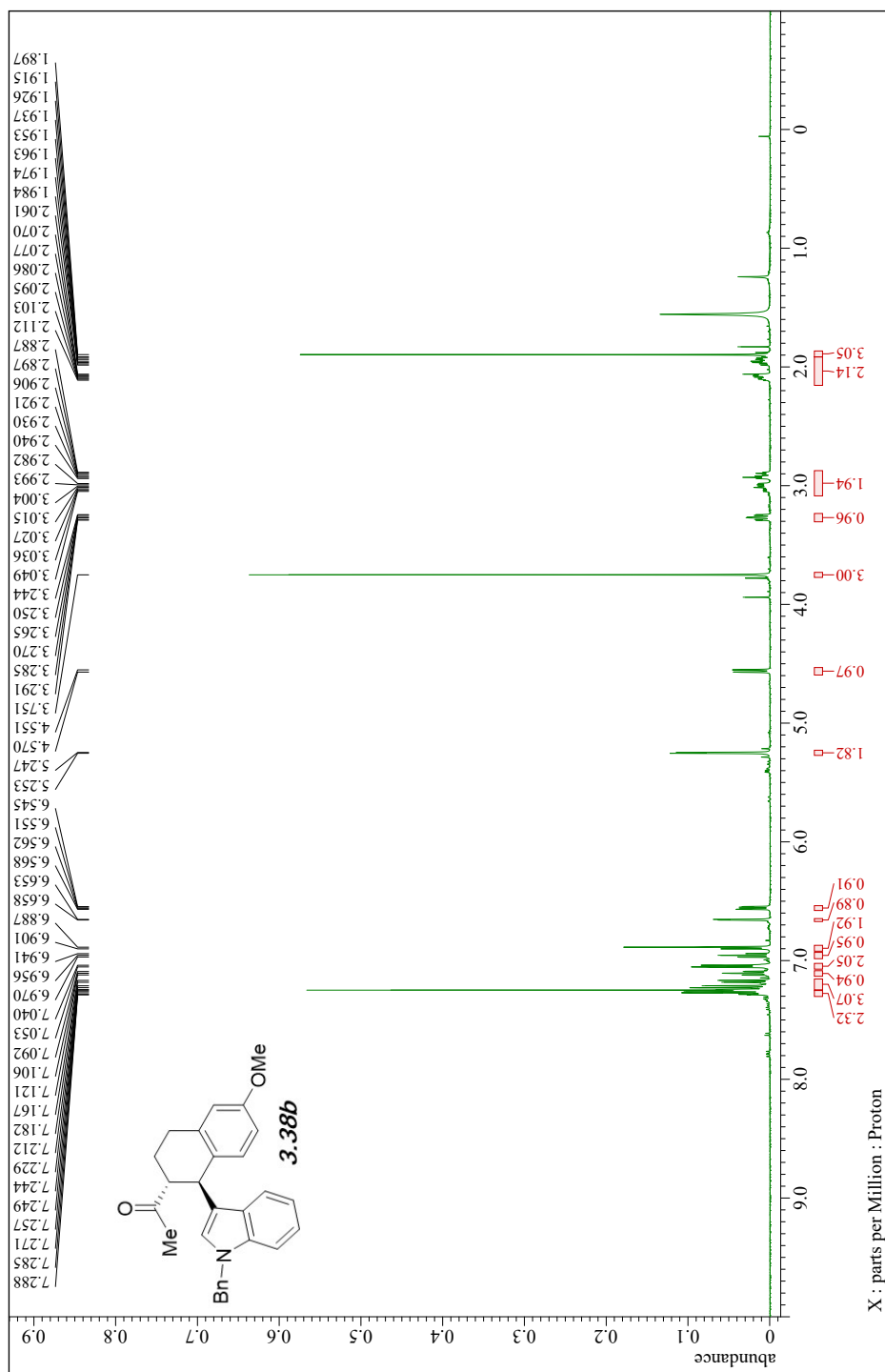
### <Chromatogram>

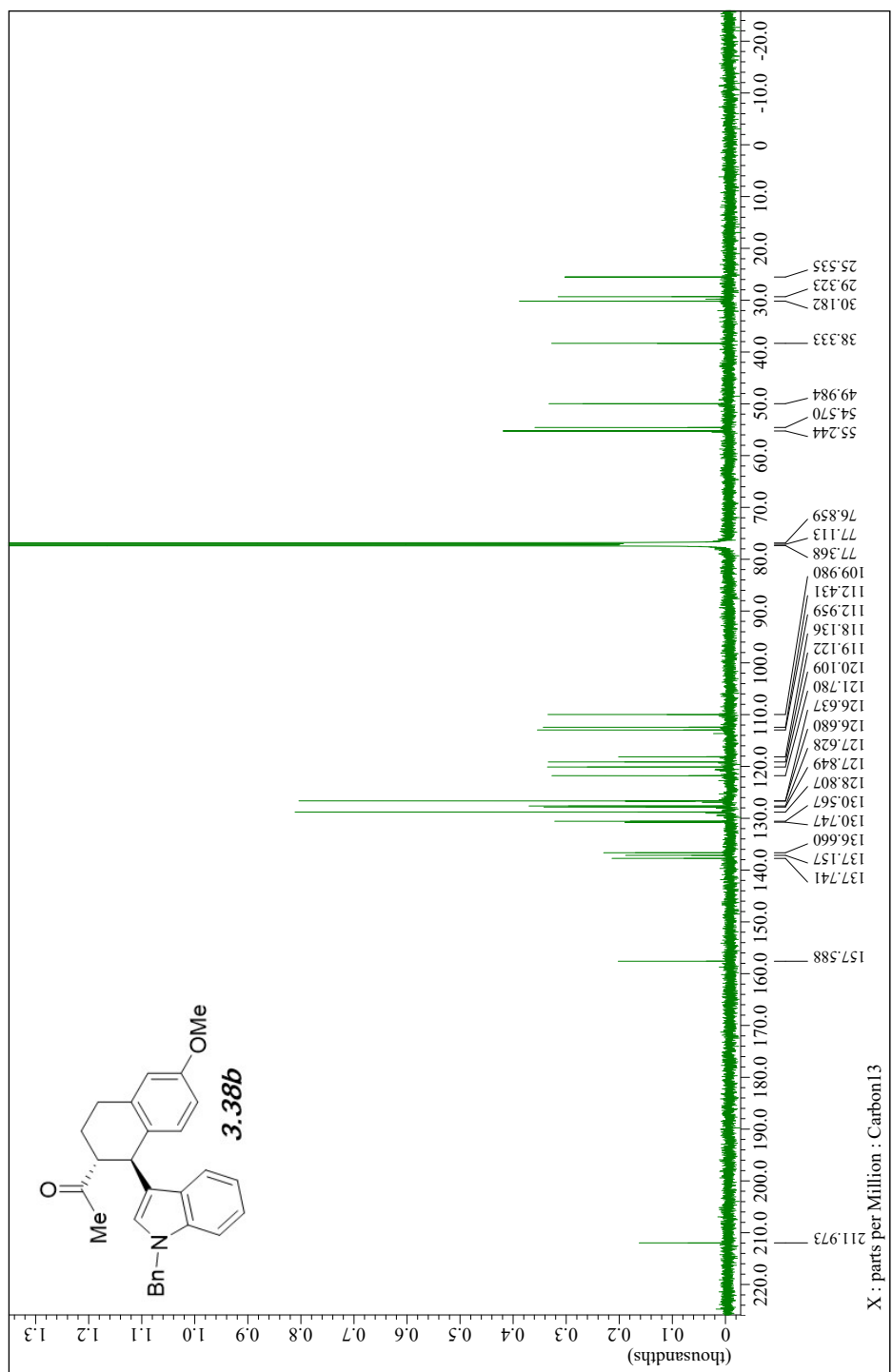


PeakTable

Peak#	Ret. Time	Area	Height	Area %	Height %
1	4.951	130871	12517	2.346	1.918
2	5.288	5448775	640124	97.654	98.082
Total		5579646	652641	100.000	100.000



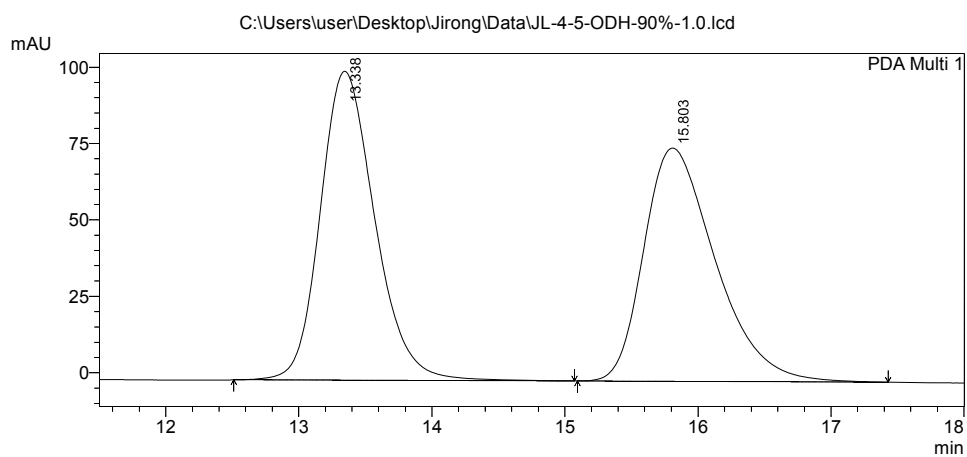




## ==== Shimadzu LCsolution Analysis Report ====

C:\Users\user\Desktop\Jirong\Data\JL-4-5-ODH-90%-1.0.lcd  
Acquired by : Admin  
Sample Name : JL-4-5-ODH-90%-1.0  
Sample ID : JL-4-5-ODH-90%-1.0  
Tray# : 1  
Vial # : 15  
Injection Volume : 10 uL  
Data File Name : JL-4-5-ODH-90%-1.0.lcd  
Method File Name : pos5\_90%\_60min\_1.0\_D2.lcm  
Batch File Name : Batch\_table\_C5-90\_60min\_1.0\_d2.lcb  
Report File Name : Default.lcr  
Data Acquired : 8/19/2021 10:37:51 AM  
Data Processed : 8/19/2021 11:21:03 AM

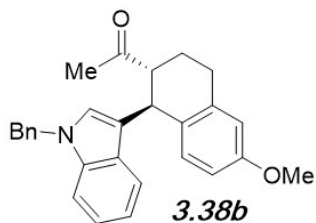
### <Chromatogram>



1 PDA Multi 1/254nm 4nm

PeakTable

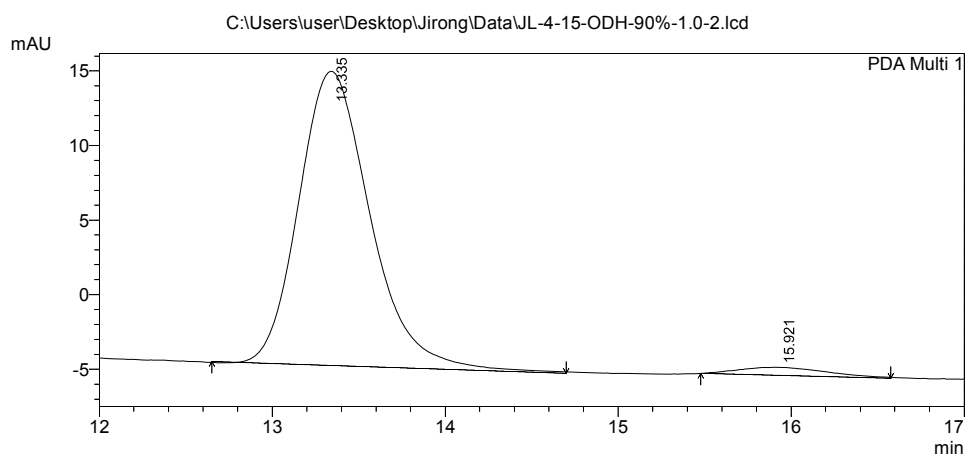
Peak#	Ret. Time	Area	Height	Area %	Height %
1	13.338	2887295	101146	50.298	56.973
2	15.803	2853128	76388	49.702	43.027
Total		5740423	177534	100.000	100.000



## ==== Shimadzu LCsolution Analysis Report ====

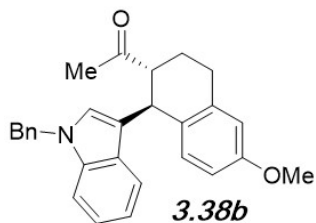
C:\Users\user\Desktop\Jirong\Data\JL-4-15-ODH-90%-1.0-2.lcd  
 Acquired by : Admin  
 Sample Name : JL-4-15-ODH-90%-1.0  
 Sample ID : JL-4-15-ODH-90%-1.0  
 Tray# : 1  
 Vial # : 15  
 Injection Volume : 10 uL  
 Data File Name : JL-4-15-ODH-90%-1.0-2.lcd  
 Method File Name : pos5\_90%\_60min\_1.0\_D2.lcm  
 Batch File Name : Batch\_table\_C5-90\_60min\_1.0\_d2.lcb  
 Report File Name : Default.lcr  
 Data Acquired : 9/2/2021 3:03:12 PM  
 Data Processed : 9/2/2021 3:24:12 PM

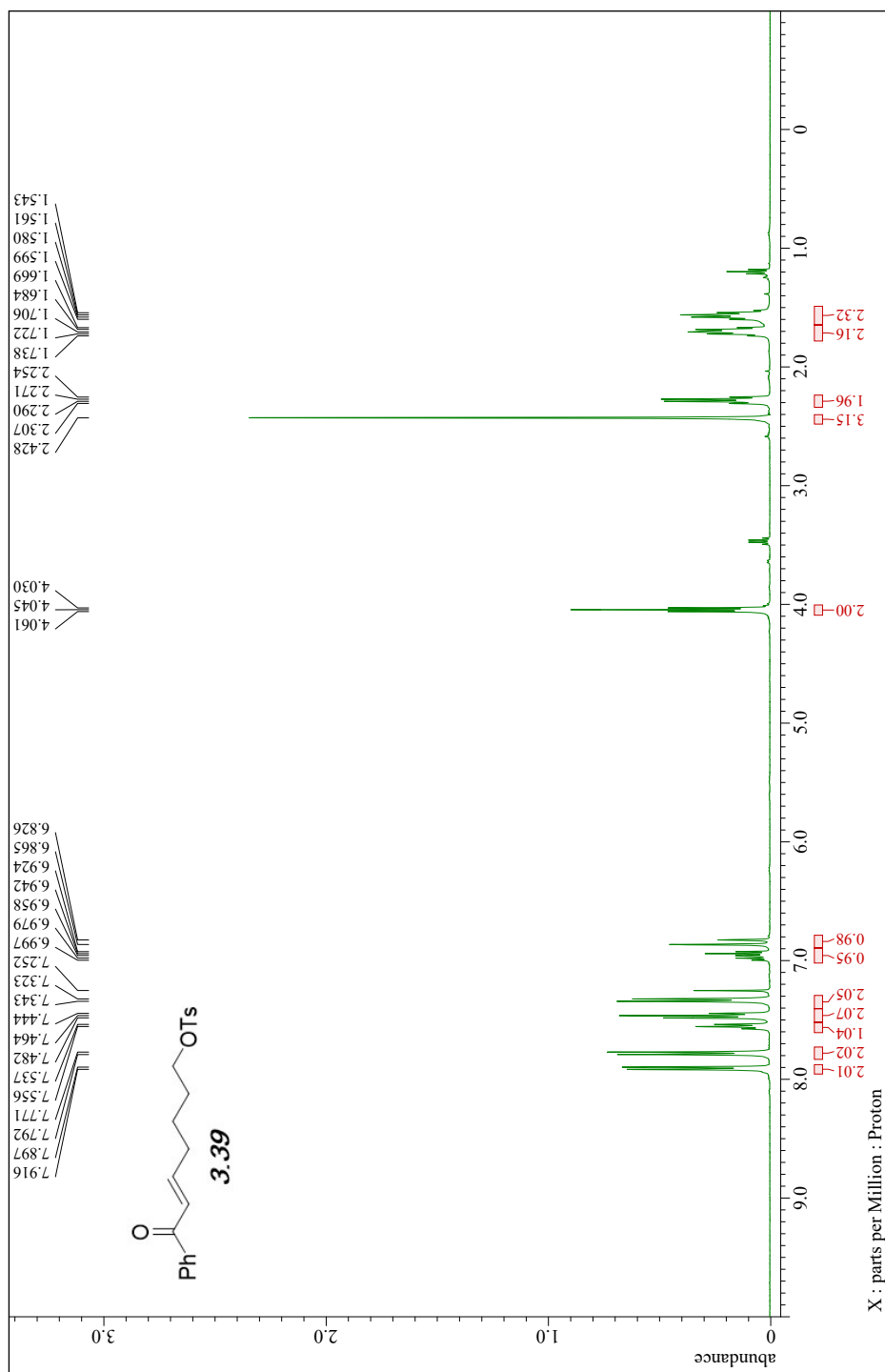
### <Chromatogram>

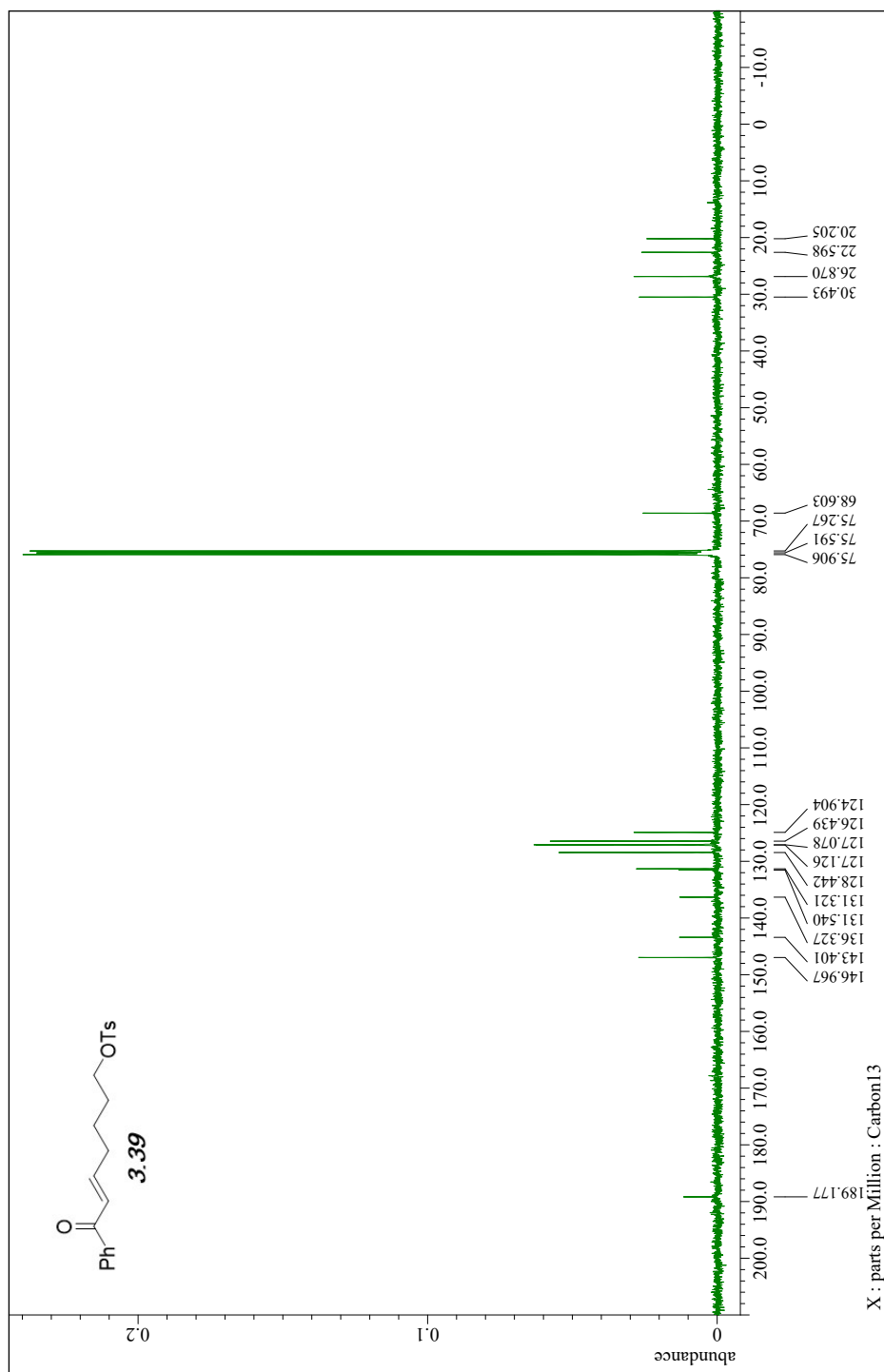


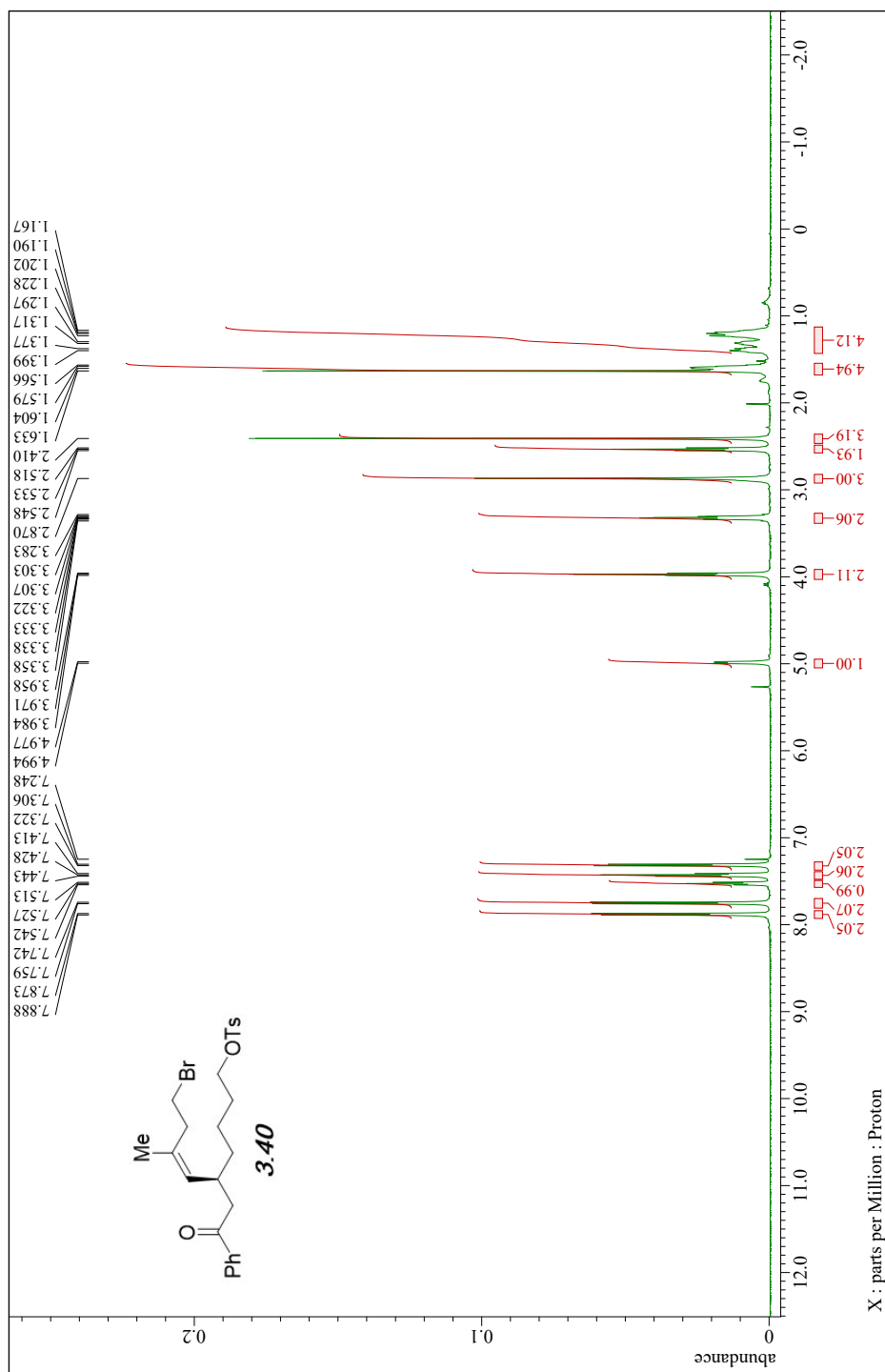
PeakTable

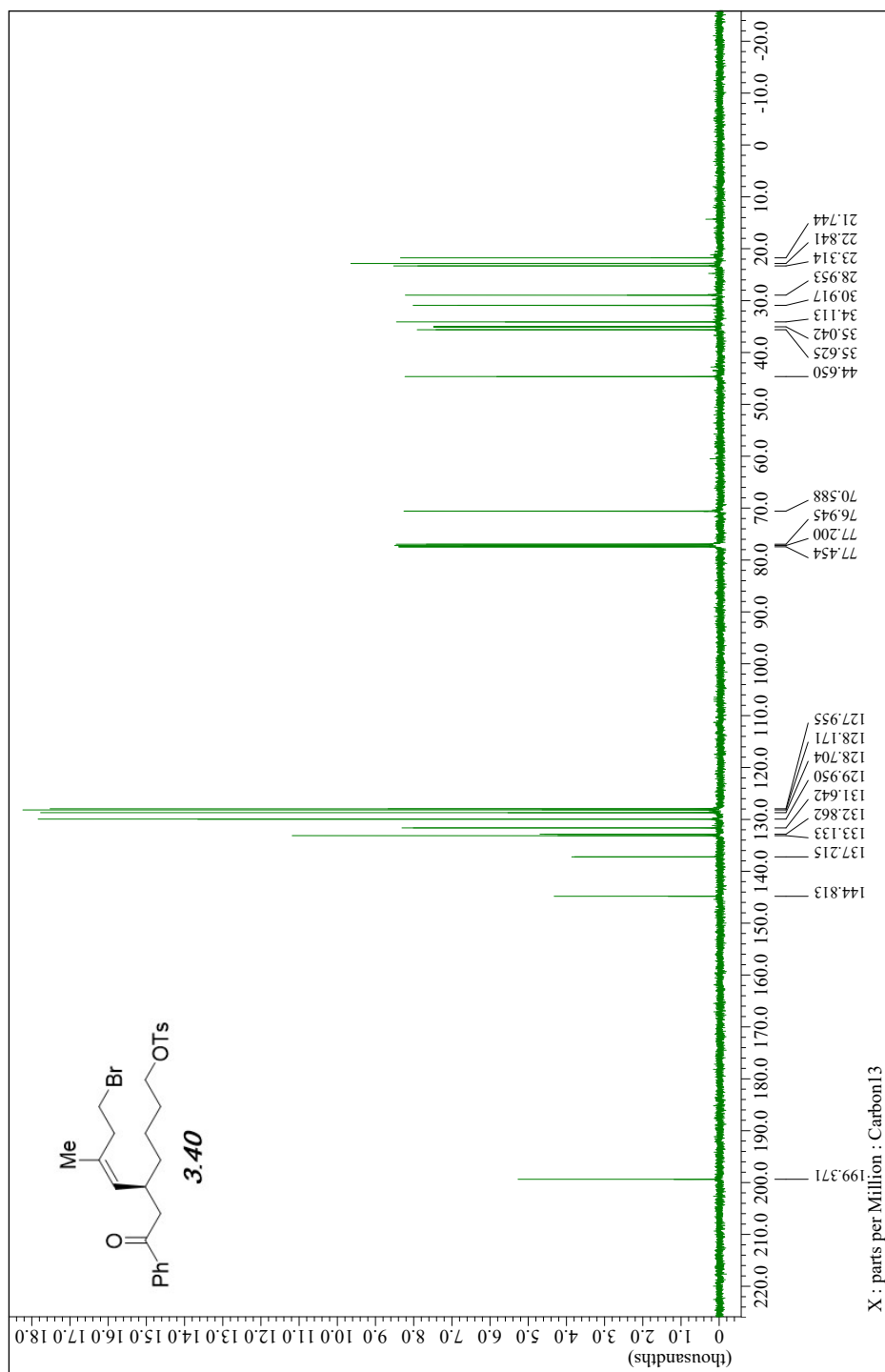
Peak#	Ret. Time	Area	Height	Area %	Height %
1	13.335	566163	19732	96.710	97.275
2	15.921	19262	553	3.290	2.725
Total		585425	20285	100.000	100.000







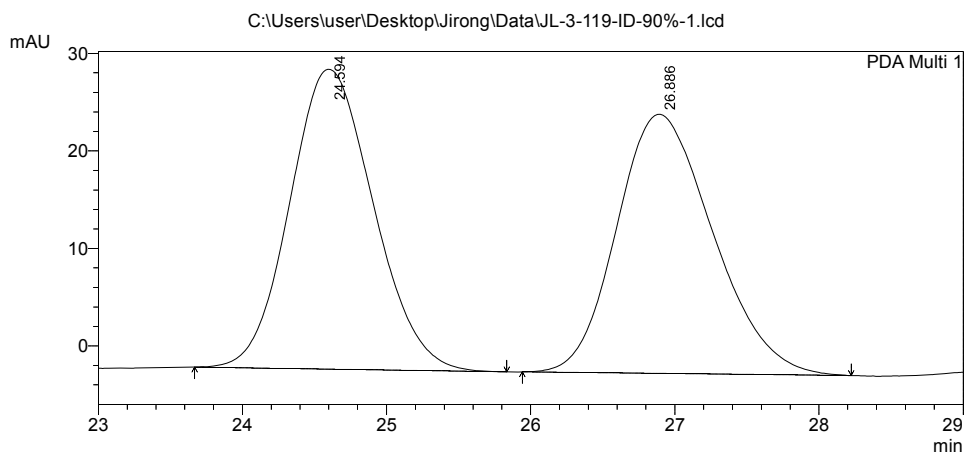




# ==== Shimadzu LCsolution Analysis Report ====

C:\Users\user\Desktop\Jirong\Data\JL-3-119-ID-90%-1.lcd  
Acquired by : Admin  
Sample Name : JL-3-119-ID-90%-1  
Sample ID : JL-3-119-ID-90%-1  
Tray# : 1  
Vial # : 1  
Injection Volume : 10 uL  
Data File Name : JL-3-119-ID-90%-1.lcd  
Method File Name : pos3-90%\_60MIN\_1.0\_D2.lcm  
Batch File Name : Batch table C3\_90%\_60min\_1.0\_D2.lcb  
Report File Name : Default.lcr  
Data Acquired : 4/15/2021 3:15:00 PM  
Data Processed : 4/15/2021 5:02:25 PM

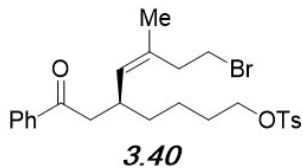
## <Chromatogram>



1 PDA Multi 1/254nm 4nm

PeakTable

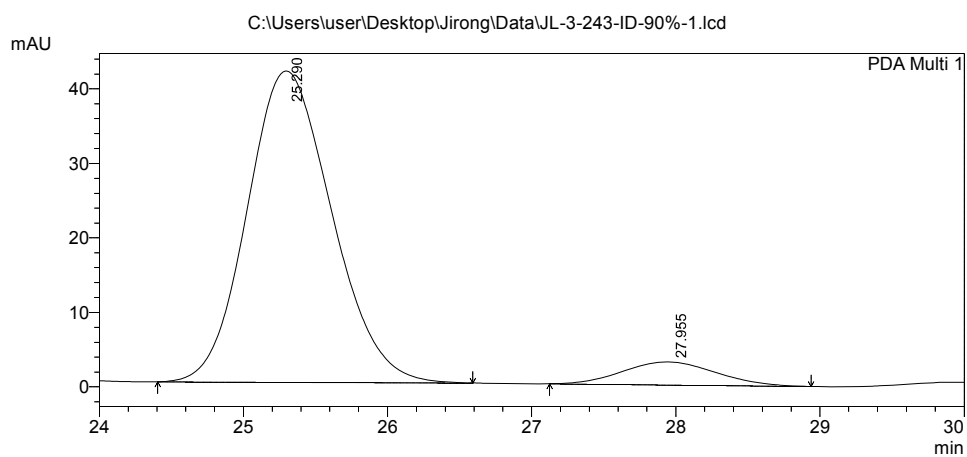
Peak#	Ret. Time	Area	Height	Area %	Height %
1	24.594	1239643	30753	50.139	53.625
2	26.886	1232760	26595	49.861	46.375
Total		2472403	57348	100.000	100.000



# ==== Shimadzu LCsolution Analysis Report ====

C:\Users\user\Desktop\Jirong\Data\JL-3-243-ID-90%-1.lcd  
Acquired by : Admin  
Sample Name : JL-3-243-ID-90%-1  
Sample ID : JL-3-243-ID-90%-1  
Tray# : 1  
Vial # : 15  
Injection Volume : 10 uL  
Data File Name : JL-3-243-ID-90%-1.lcd  
Method File Name : pos3-90%\_60MIN\_1.0\_D2.lcm  
Batch File Name : Batch table C3\_90%\_60min\_1.0\_D2.lcb  
Report File Name : Default.lcr  
Data Acquired : 5/24/2021 7:06:23 PM  
Data Processed : 5/24/2021 7:46:34 PM

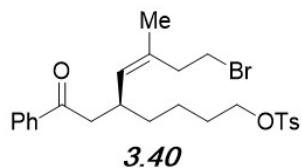
## <Chromatogram>

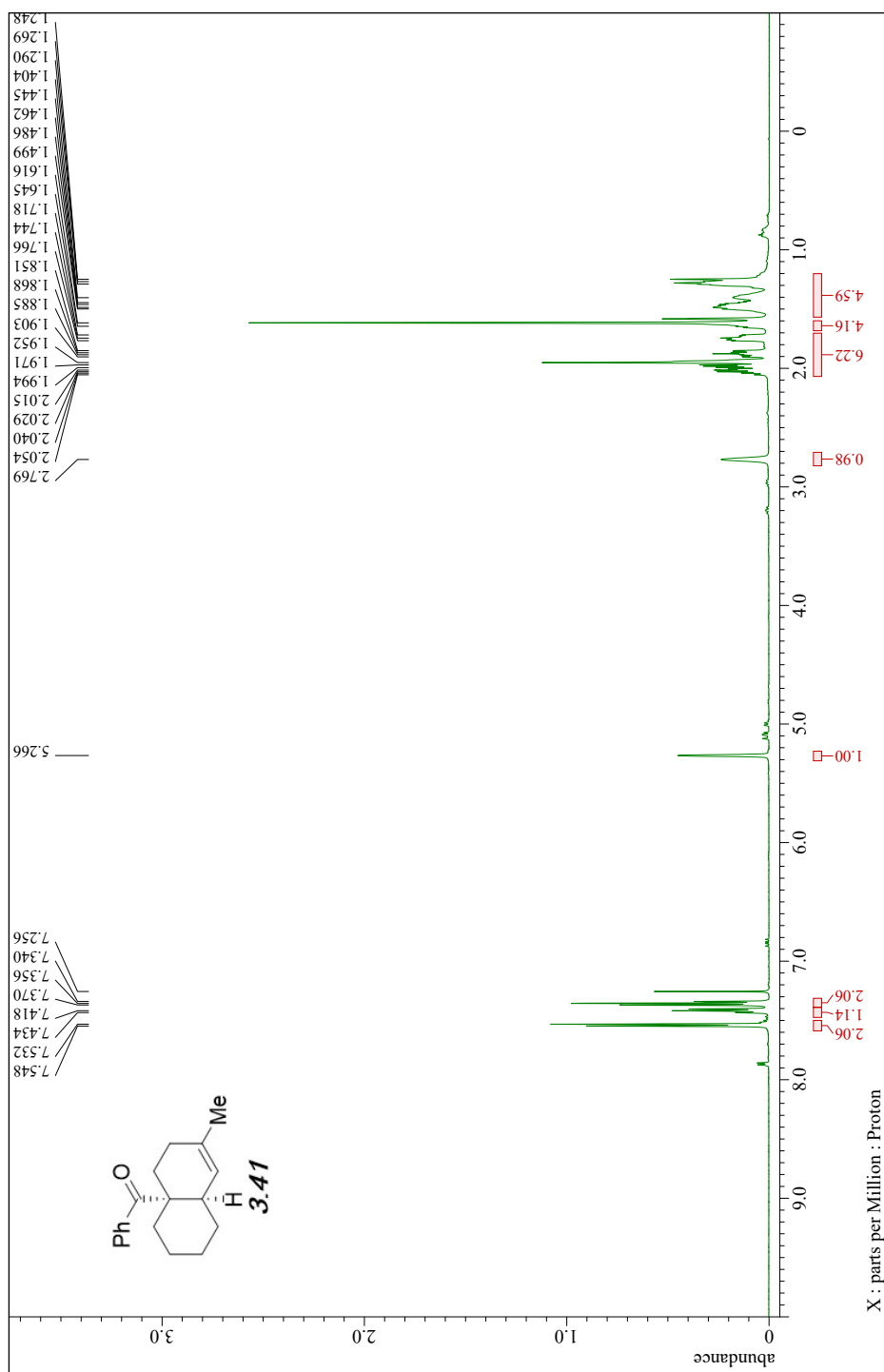


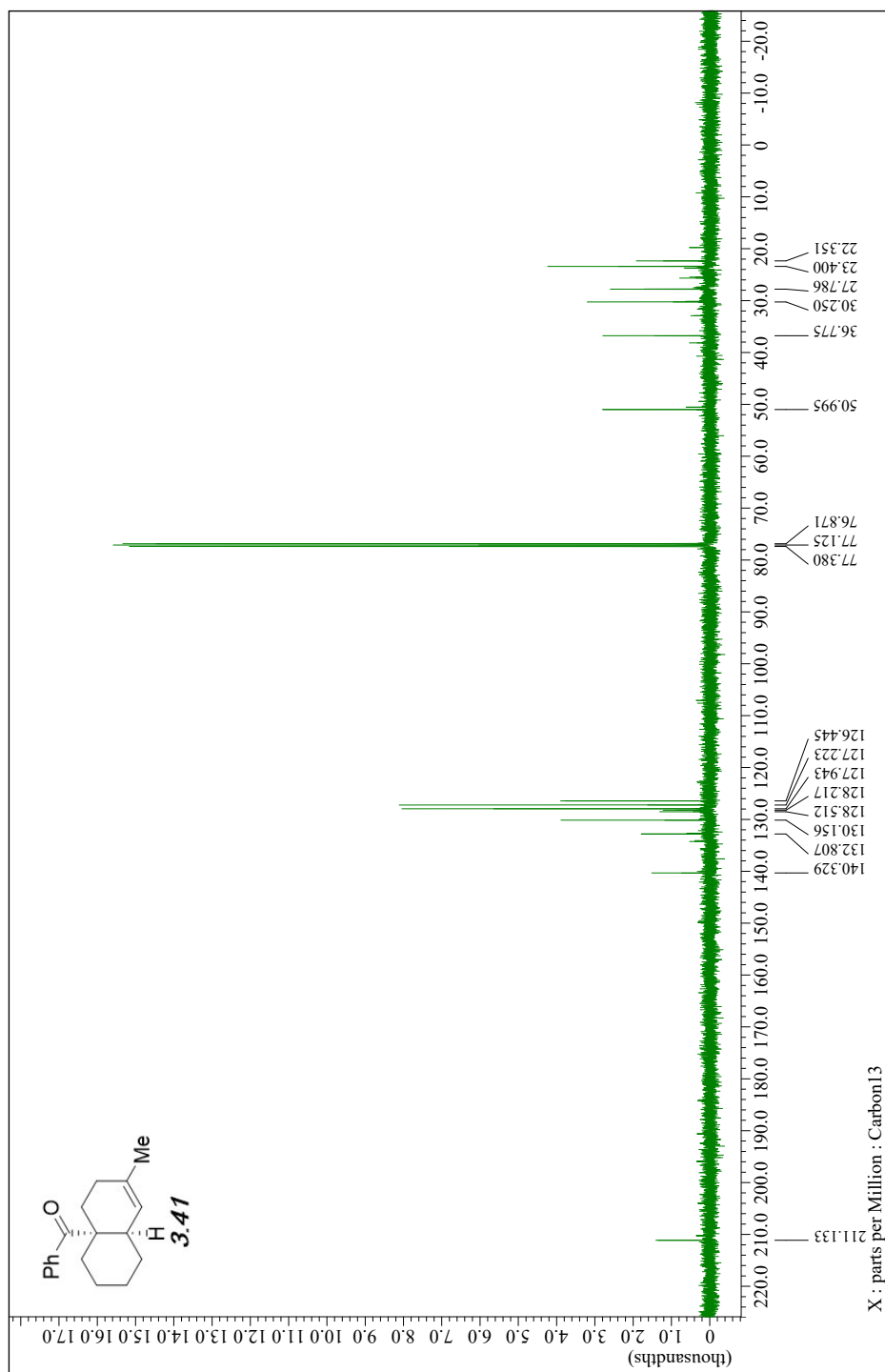
1 PDA Multi 1/254nm 4nm

PeakTable

Peak#	Ret. Time	Area	Height	Area %	Height %
1	25.290	1702476	41782	92.429	93.094
2	27.955	139450	3100	7.571	6.906
Total		1841925	44882	100.000	100.000



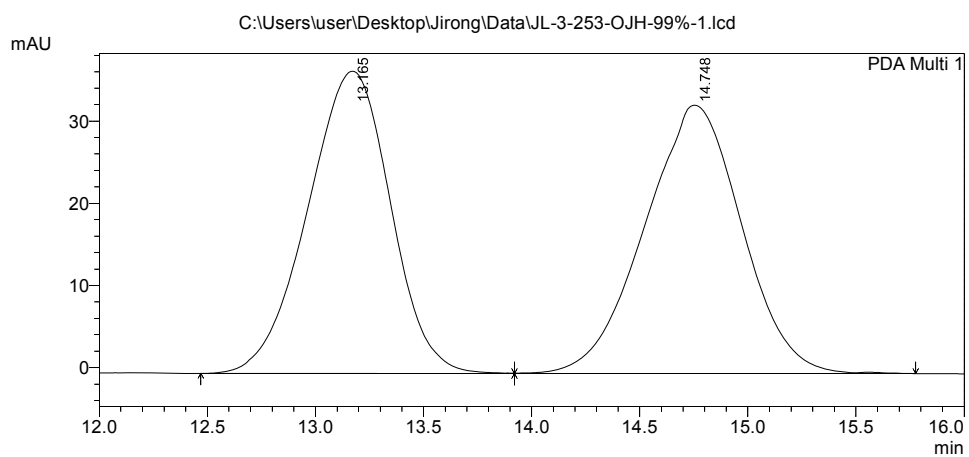




# ==== Shimadzu LCsolution Analysis Report ====

C:\Users\user\Desktop\Jirong\Data\JL-3-253-OJH-99%-1.lcd  
Acquired by : Admin  
Sample Name : JL-3-253-OJH-99%-1  
Sample ID : JL-3-253-OJH-99%-1  
Tray# : 1  
Vial # : 15  
Injection Volume : 10 uL  
Data File Name : JL-3-253-OJH-99%-1.lcd  
Method File Name : pos4\_99%\_60min\_1\_D2.lcm  
Batch File Name : Batch\_table\_C4-99\_60min\_1\_D2.lcb  
Report File Name : Default.lcr  
Data Acquired : 6/9/2021 12:20:52 PM  
Data Processed : 6/9/2021 1:37:26 PM

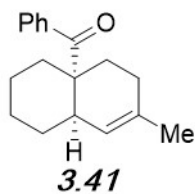
## <Chromatogram>



PeakTable

PDA Ch1 254nm 4nm

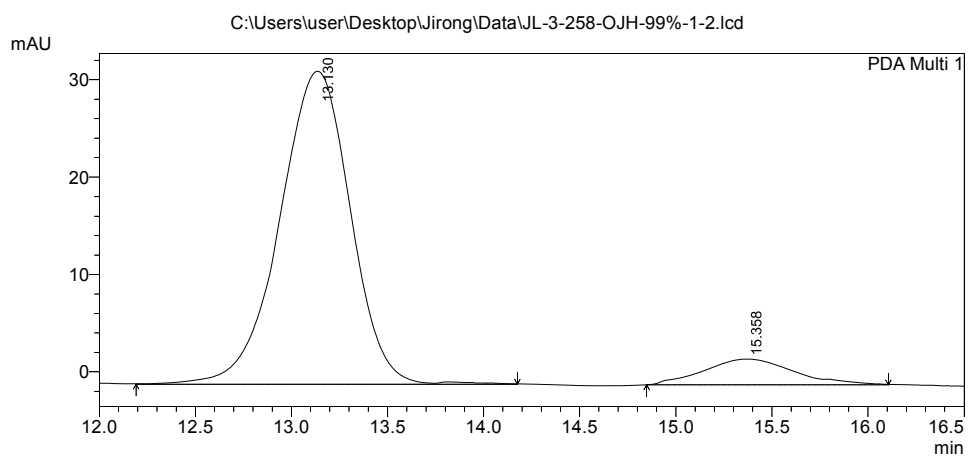
Peak#	Ret. Time	Area	Height	Area %	Height %
1	13.165	979650	36776	49.011	52.971
2	14.748	1019185	32650	50.989	47.029
Total		1998835	69426	100.000	100.000



## ==== Shimadzu LCsolution Analysis Report ====

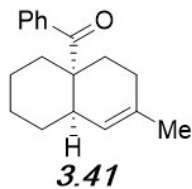
C:\Users\user\Desktop\Jirong\Data\JL-3-258-OJH-99%-1-2.lcd  
 Acquired by : Admin  
 Sample Name : JL-3-258-OJH-99%-1  
 Sample ID : JL-3-258-OJH-99%-1  
 Tray# : 1  
 Vial # : 15  
 Injection Volume : 10 uL  
 Data File Name : JL-3-258-OJH-99%-1-2.lcd  
 Method File Name : pos4\_99%\_30min\_1\_D2.lcm  
 Batch File Name : Batch\_table\_C4-99\_30min\_1\_D2.lcb  
 Report File Name : Default.lcr  
 Data Acquired : 6/21/2021 3:11:06 PM  
 Data Processed : 6/21/2021 4:10:08 PM

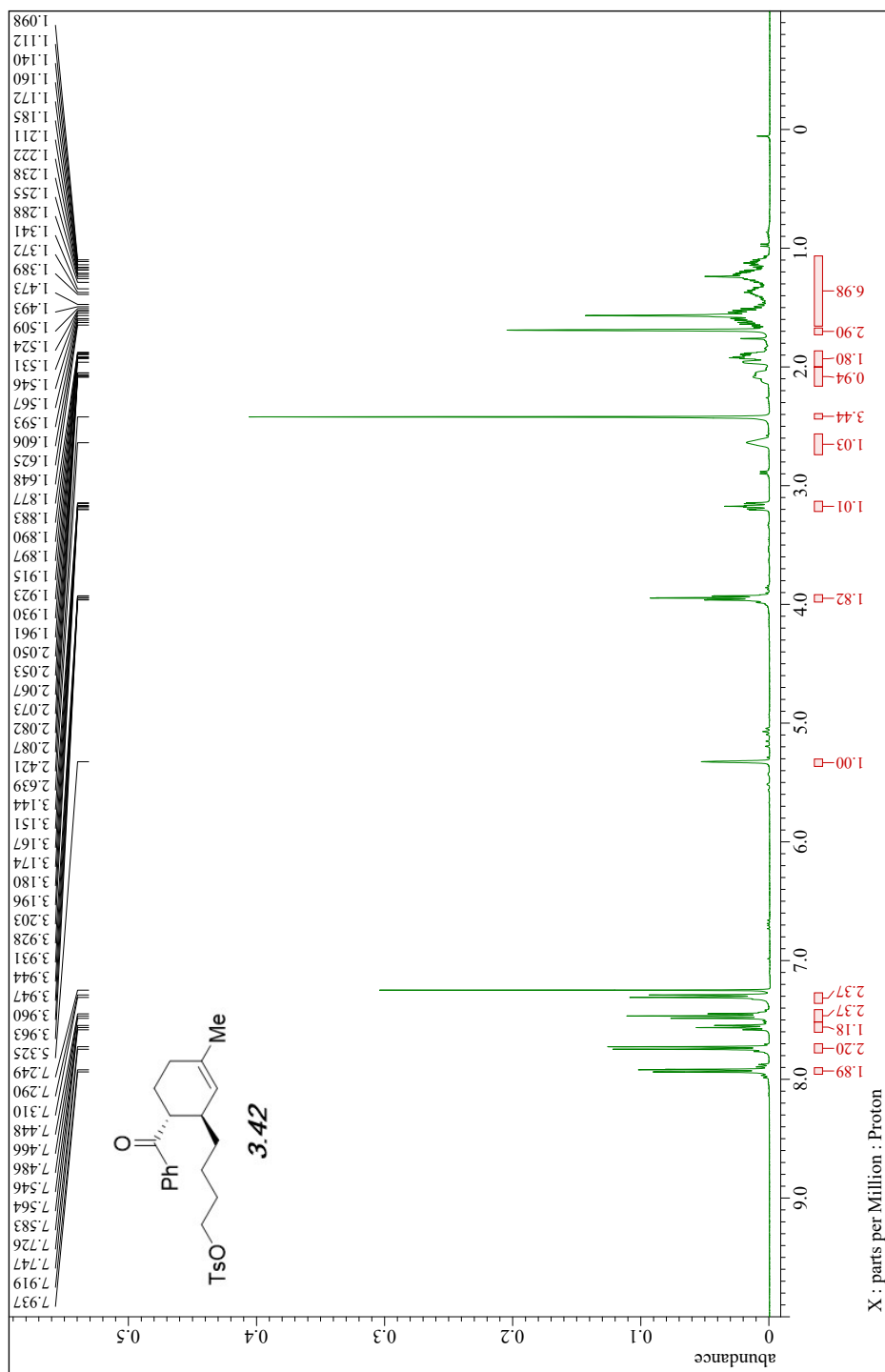
### <Chromatogram>



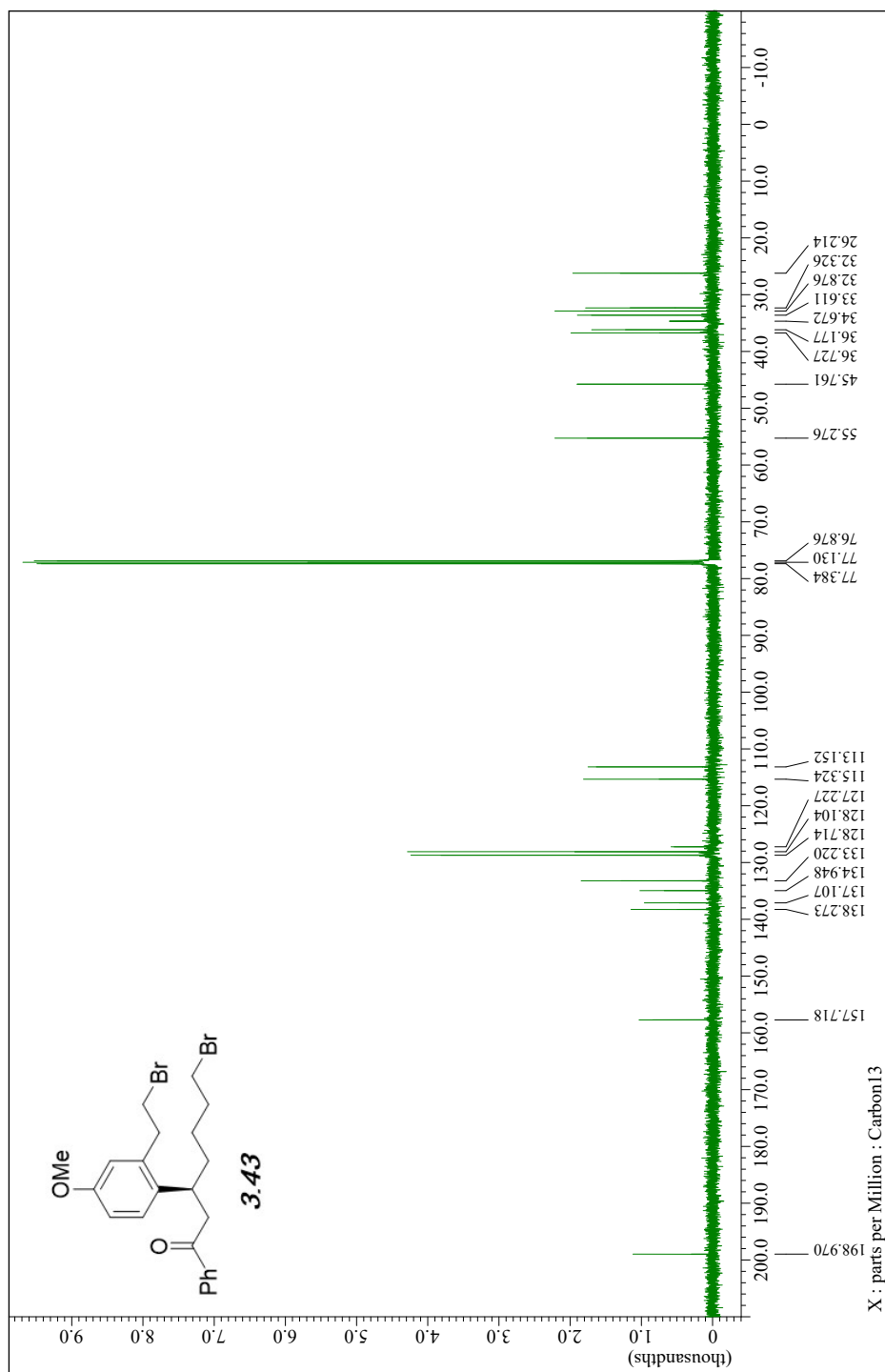
PeakTable

Peak#	Ret. Time	Area	Height	Area %	Height %
1	13.130	822315	32143	90.458	92.395
2	15.358	86744	2646	9.542	7.605
Total		909059	34789	100.000	100.000





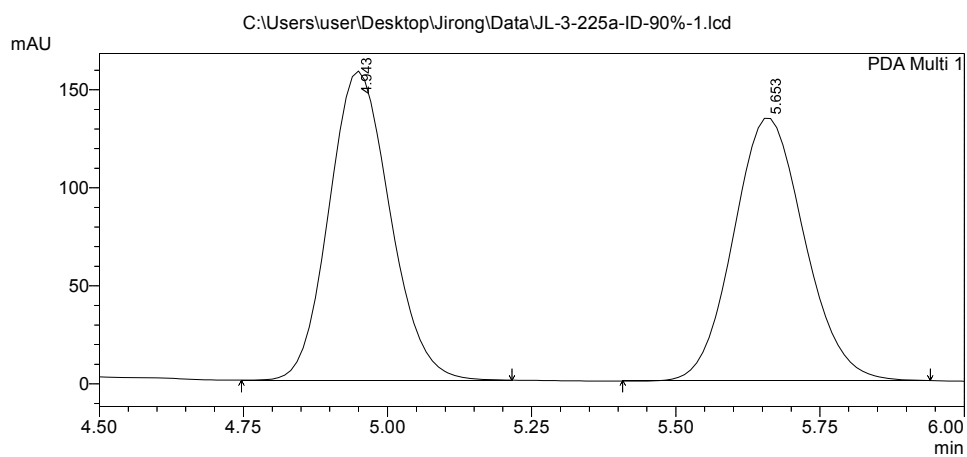




## ==== Shimadzu LcSolution Analysis Report ====

C:\Users\user\Desktop\Jirong\Data\JL-3-225a-ID-90%-1.lcd  
 Acquired by : Admin  
 Sample Name : JL-3-225a-ID-90%-1  
 Sample ID : JL-3-225a-ID-90%-1  
 Tray# : 1  
 Vial # : 15  
 Injection Volume : 10 uL  
 Data File Name : JL-3-225a-ID-90%-1.lcd  
 Method File Name : pos3-90%\_10MIN\_1\_d2.lcm  
 Batch File Name : Batch table C3\_90%\_10min\_1.0\_D2.lcb  
 Report File Name : Default.lcr  
 Data Acquired : 6/25/2021 12:07:42 PM  
 Data Processed : 6/25/2021 12:17:27 PM

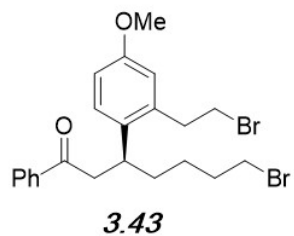
### <Chromatogram>



PeakTable

PDA Ch1 254nm 4nm

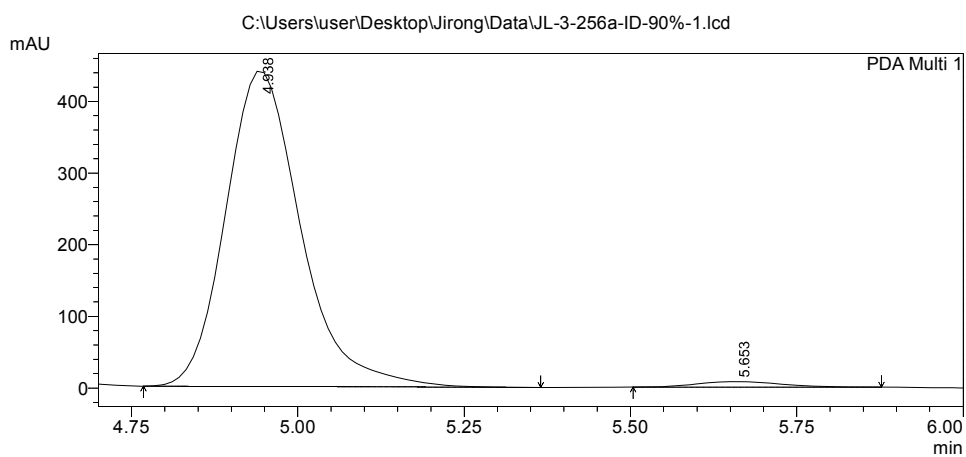
Peak#	Ret. Time	Area	Height	Area %	Height %
1	4.943	1165092	157845	50.429	54.136
2	5.653	1145253	133726	49.571	45.864
Total		2310345	291570	100.000	100.000



## ==== Shimadzu LCsolution Analysis Report ====

C:\Users\user\Desktop\Jirong\Data\JL-3-256a-ID-90%-1.lcd  
 Acquired by : Admin  
 Sample Name : JL-3-256a-ID-90%-1  
 Sample ID : JL-3-256a-ID-90%-1  
 Tray# : 1  
 Vial # : 15  
 Injection Volume : 10 uL  
 Data File Name : JL-3-256a-ID-90%-1.lcd  
 Method File Name : pos3-90%\_10MIN\_1\_d2.lcm  
 Batch File Name : Batch table C3\_90%\_10min\_1.0\_D2.lcb  
 Report File Name : Default.lcr  
 Data Acquired : 6/26/2021 12:10:57 PM  
 Data Processed : 6/26/2021 1:06:19 PM

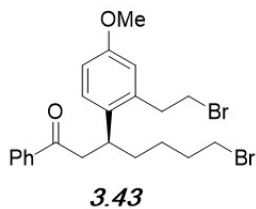
### <Chromatogram>

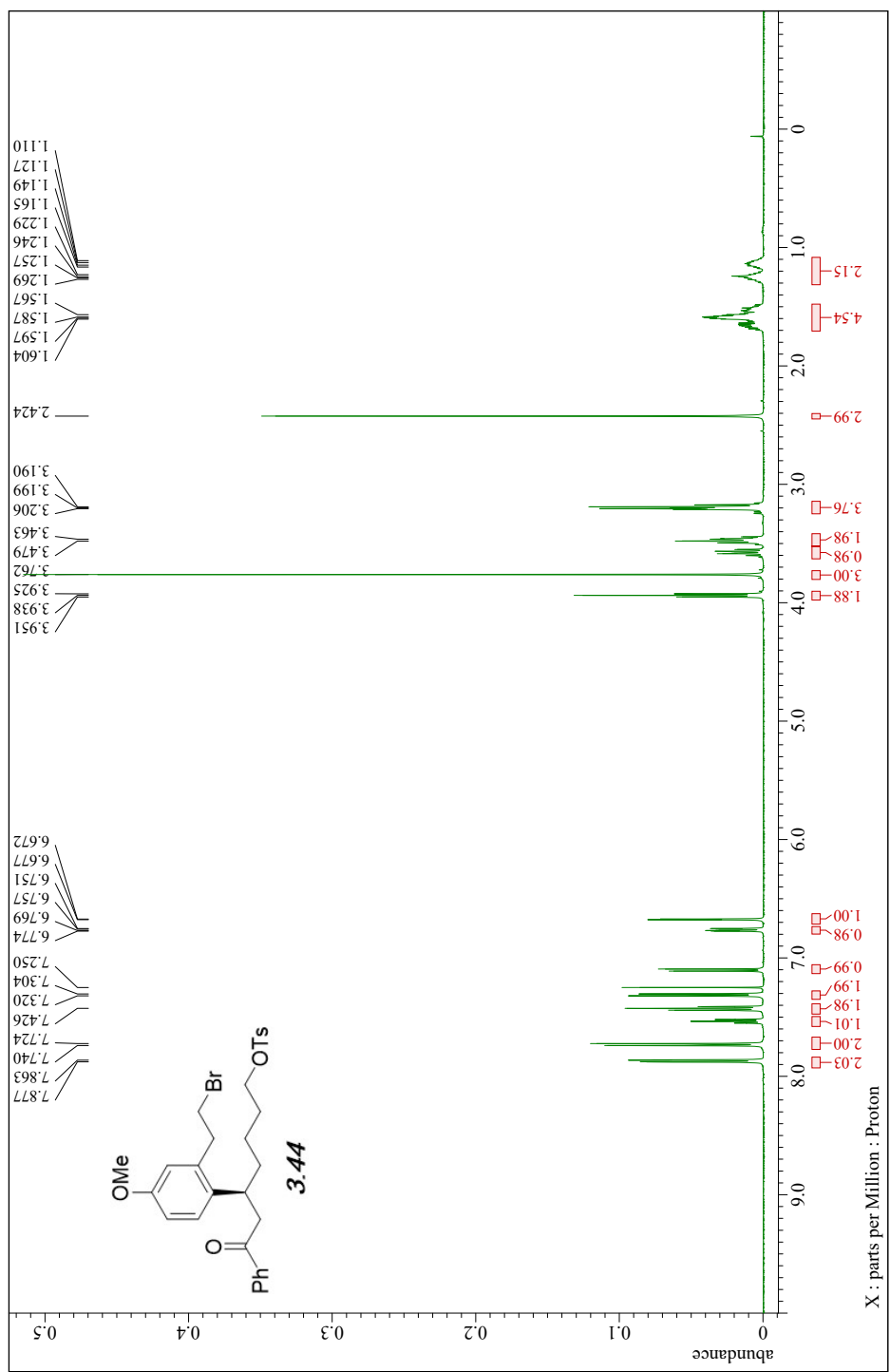


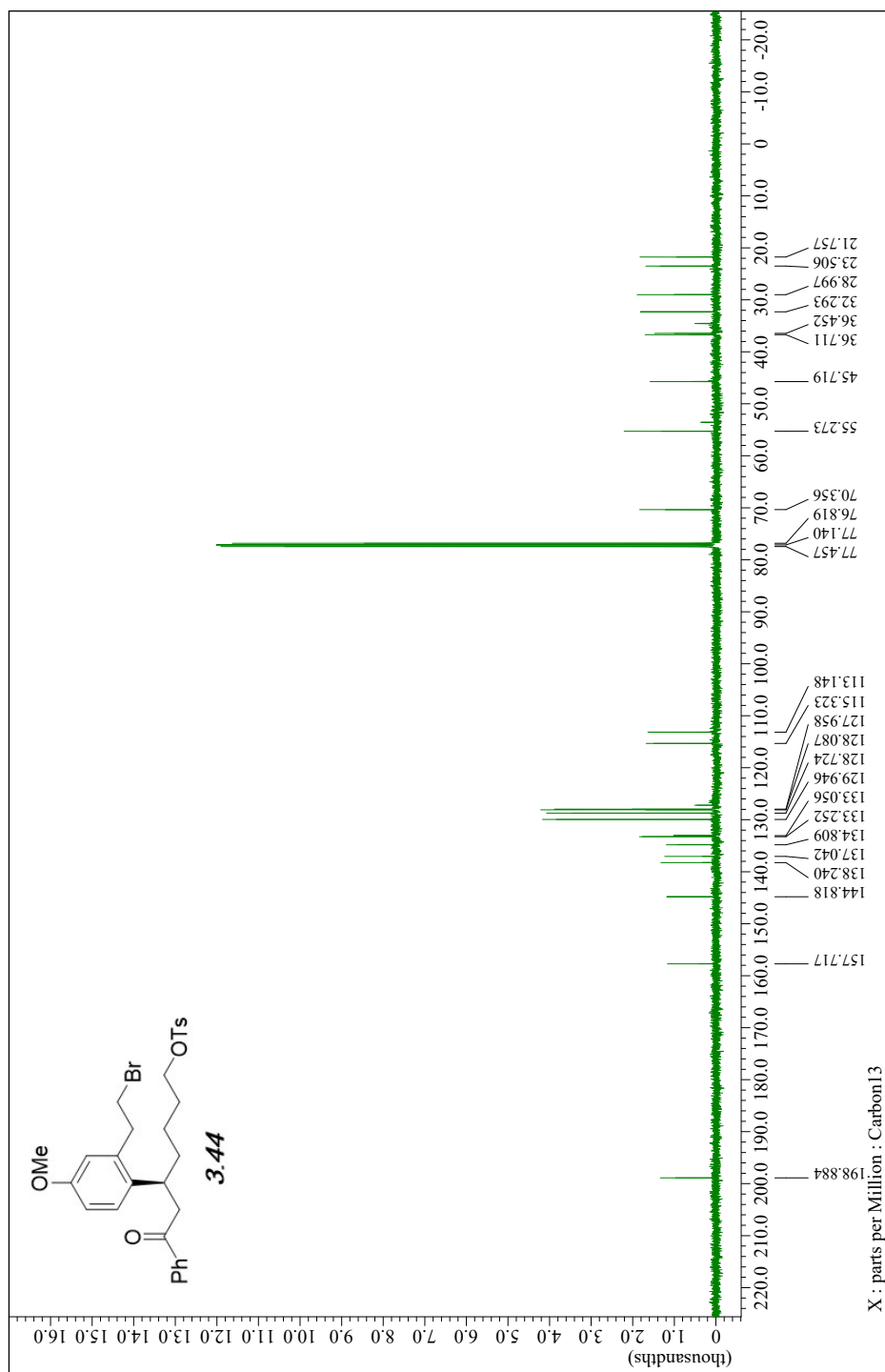
PeakTable

PDA Ch1 254nm 4nm

Peak#	Ret. Time	Area	Height	Area %	Height %
1	4.938	3456772	439990	98.023	98.224
2	5.653	69730	7953	1.977	1.776
Total		3526502	447943	100.000	100.000



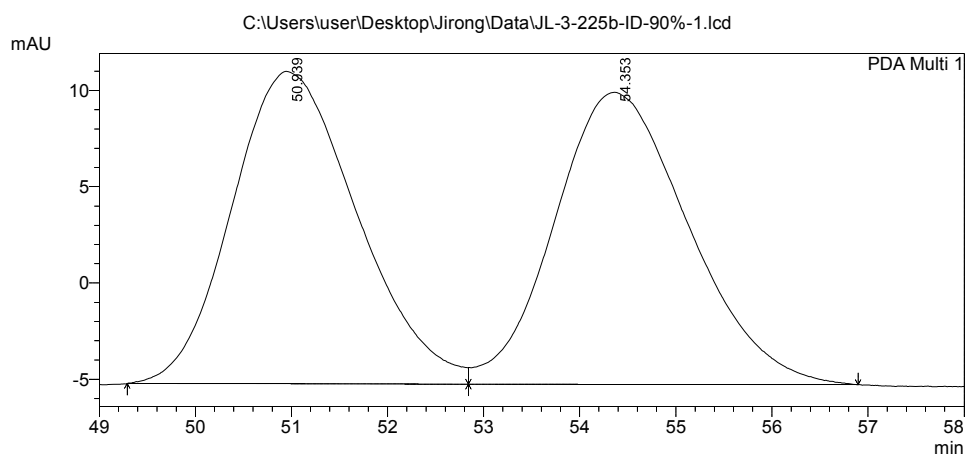




## ==== Shimadzu LCsolution Analysis Report ====

C:\Users\user\Desktop\Jirong\Data\JL-3-225b-ID-90%-1.lcd  
 Acquired by : Admin  
 Sample Name : JL-3-225b-ID-90%-1  
 Sample ID : JL-3-225b-ID-90%-1  
 Tray# : 1  
 Vial # : 15  
 Injection Volume : 10 uL  
 Data File Name : JL-3-225b-ID-90%-1.lcd  
 Method File Name : pos3-90%\_60MIN\_1.0\_D2.lcm  
 Batch File Name : Batch table C3\_90%\_60min\_1.0\_D2.lcb  
 Report File Name : Default.lcr  
 Data Acquired : 6/25/2021 2:25:19 PM  
 Data Processed : 6/28/2021 12:44:37 PM

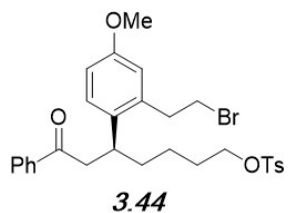
### <Chromatogram>



PeakTable

PDA Ch1 254nm 4nm

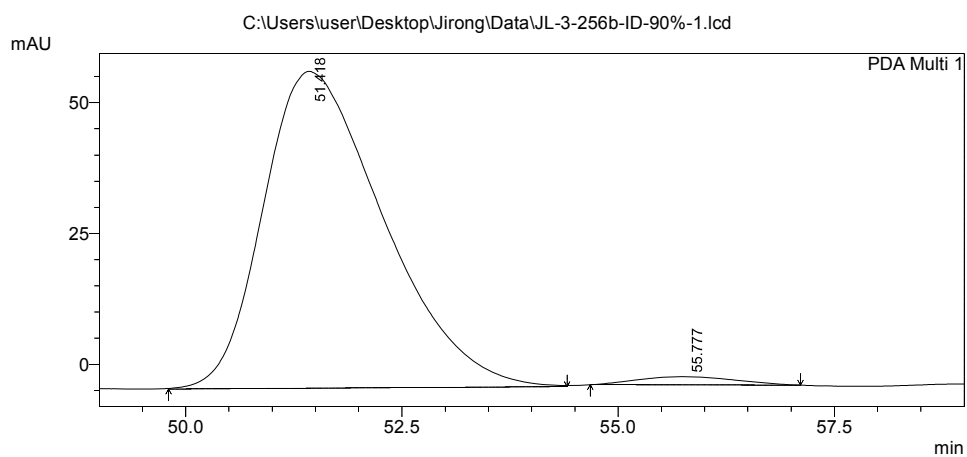
Peak#	Ret. Time	Area	Height	Area %	Height %
1	50.939	1470031	16234	49.994	51.674
2	54.353	1470376	15182	50.006	48.326
Total		2940407	31416	100.000	100.000



## ==== Shimadzu LcSolution Analysis Report ====

C:\Users\user\Desktop\Jirong\Data\JL-3-256b-ID-90%-1.lcd  
 Acquired by : Admin  
 Sample Name : JL-3-256b-ID-90%-1  
 Sample ID : JL-3-256b-ID-90%-1  
 Tray# : 1  
 Vial # : 15  
 Injection Volume : 10 uL  
 Data File Name : JL-3-256b-ID-90%-1.lcd  
 Method File Name : pos3-90%\_60MIN\_1.0\_D2.lcm  
 Batch File Name : Batch table C3\_90%\_60min\_1.0\_D2.lcb  
 Report File Name : Default.lcr  
 Data Acquired : 6/28/2021 11:10:41 AM  
 Data Processed : 6/28/2021 12:43:15 PM

### <Chromatogram>

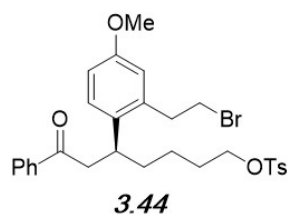


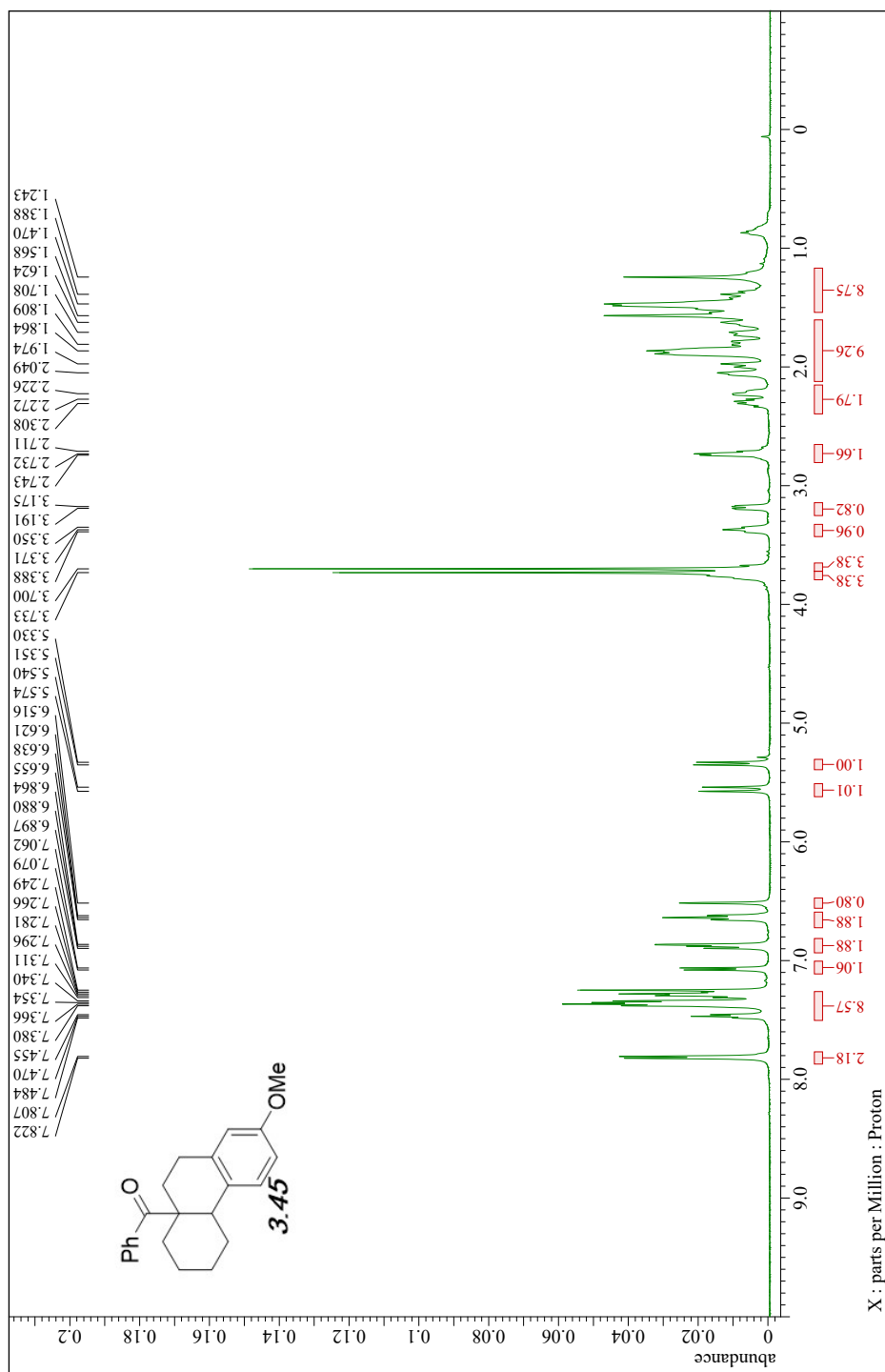
1 PDA Multi 1/254nm 4nm

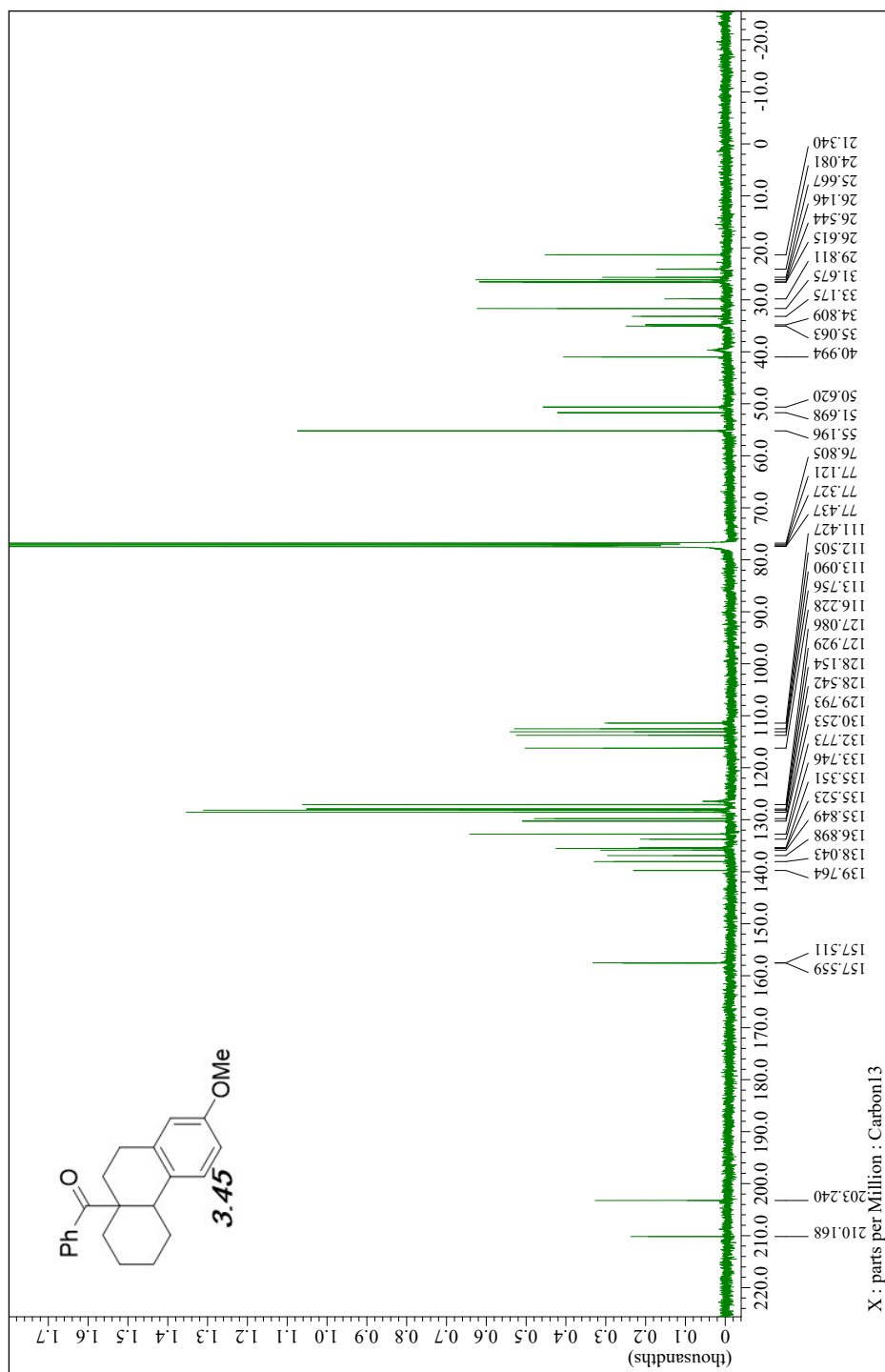
PeakTable

PDA Ch1 254nm 4nm

Peak#	Ret. Time	Area	Height	Area %	Height %
1	51.418	5863406	60558	97.918	97.448
2	55.777	124656	1586	2.082	2.552
Total		5988062	62144	100.000	100.000



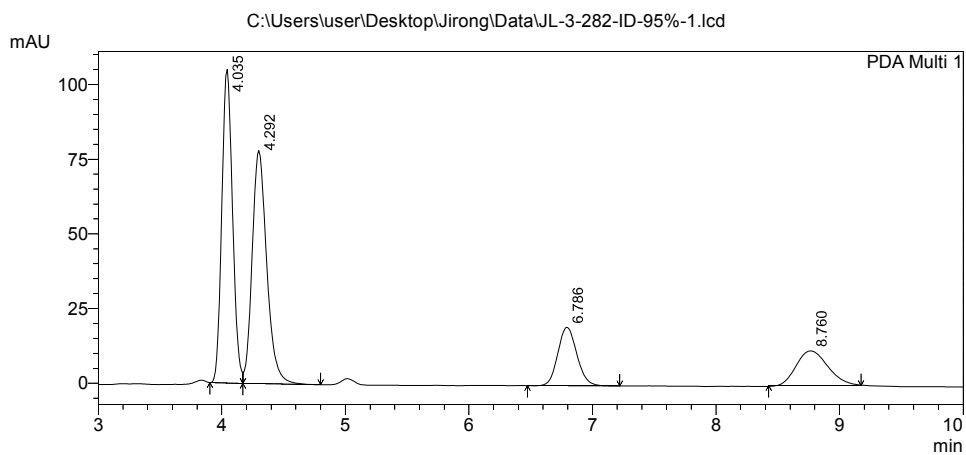




# ==== Shimadzu LCsolution Analysis Report ====

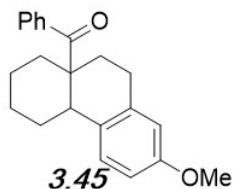
C:\Users\user\Desktop\Jirong\Data\JL-3-282-ID-95%-1.lcd  
 Acquired by : Admin  
 Sample Name : JL-3-282-ID-95%-1  
 Sample ID : JL-3-282-ID-95%-1  
 Tray# : 1  
 Vial # : 15  
 Injection Volume : 10 uL  
 Data File Name : JL-3-282-ID-95%-1.lcd  
 Method File Name : pos3-95%\_60min\_1.0\_D2.lcm  
 Batch File Name : Batch table C3\_95%\_60min\_1.0\_D2.lcb  
 Report File Name : Default.lcr  
 Data Acquired : 8/24/2021 5:52:35 PM  
 Data Processed : 8/24/2021 6:05:40 PM

## <Chromatogram>



PeakTable

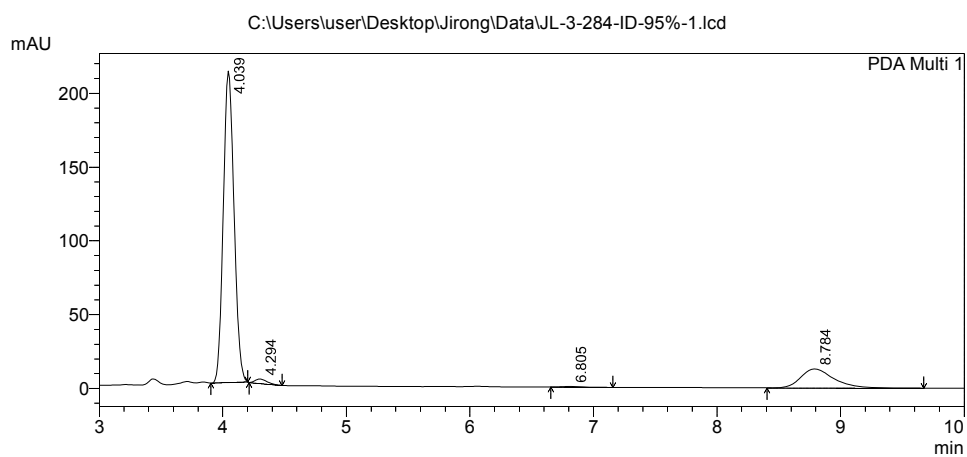
Peak#	Ret. Time	Area	Height	Area %	Height %
1	4.035	635375	105063	37.509	49.002
2	4.292	639160	78032	37.732	36.395
3	6.786	209925	19598	12.393	9.141
4	8.760	209478	11713	12.366	5.463
Total		1693938	214406	100.000	100.000



# ==== Shimadzu LcSolution Analysis Report ====

C:\Users\user\Desktop\Jirong\Data\JL-3-284-ID-95%-1.lcd  
 Acquired by : Admin  
 Sample Name : JL-3-284-ID-95%-1  
 Sample ID : JL-3-284-ID-95%-1  
 Tray# : 1  
 Vial # : 15  
 Injection Volume : 10 uL  
 Data File Name : JL-3-284-ID-95%-1.lcd  
 Method File Name : pos3-95%\_60min\_1.0\_D2.lcm  
 Batch File Name : Batch table C3\_95%\_60min\_1.0\_D2.lcb  
 Report File Name : Default.lcr  
 Data Acquired : 8/24/2021 5:39:19 PM  
 Data Processed : 8/24/2021 6:08:02 PM

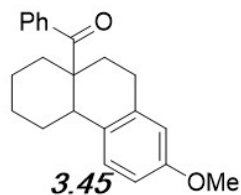
## <Chromatogram>



PeakTable

PDA Ch1 254nm 4nm

Peak#	Ret. Time	Area	Height	Area %	Height %
1	4.039	1273109	211111	82.877	92.865
2	4.294	18605	2894	1.211	1.273
3	6.805	5100	478	0.332	0.210
4	8.784	239328	12848	15.580	5.652
Total		1536141	227331	100.000	100.000



## Chapter 4 Total Synthesis of Cannabinoids

### 4.1 Retrosynthetic Analysis

Based on the successful development of the enantioselective conjugate addition/enolate alkylation annulation method described in Chapter 3, a concise and convergent retrosynthetic analysis of (-)- $\Delta^9$ -tetrahydrocannabinol (THC, **4.1**) and cannabidiol (CBD, **4.2**) was proposed (Figure 4.1).

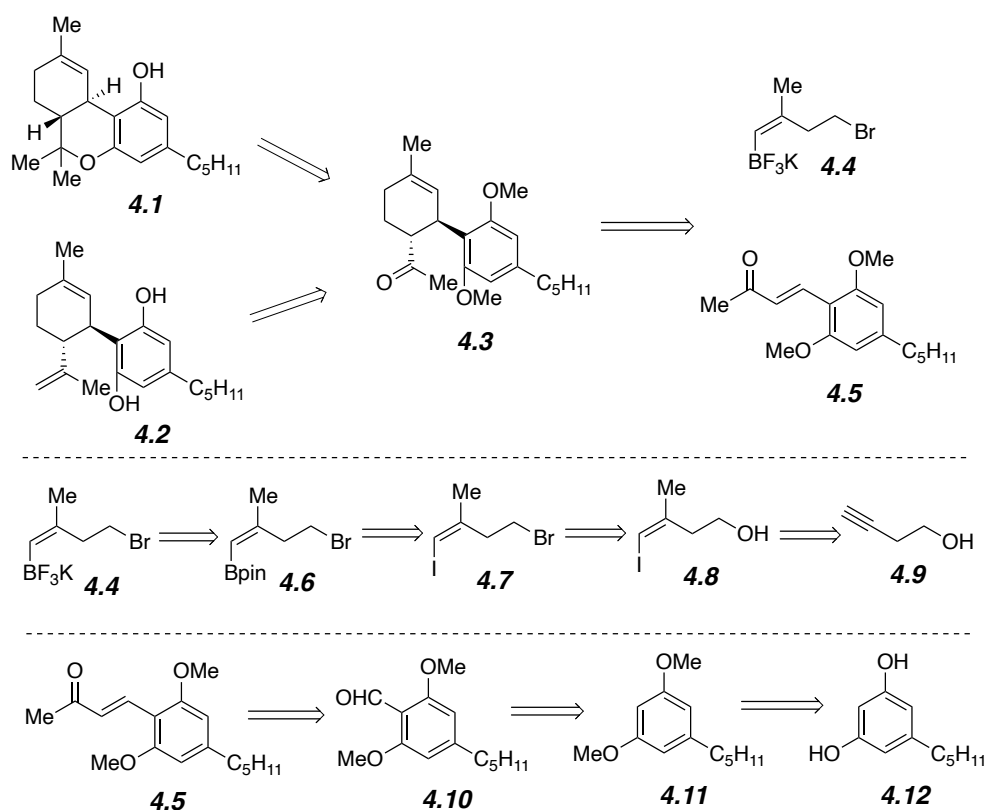


**Figure 4.1.** Retrosynthetic Analysis of THC (**1**) and CBD (**2**)

Both THC (**4.1**) and CBD (**4.2**) could be synthesized from a common intermediate, cyclohexene **4.3**, through methyl magnesium iodide treatment followed by Lewis acid promoted etherification or Wittig olefination followed by the deprotection of phenolic hydroxyls, respectively. Cyclohexene **4.3** could be prepared from building blocks **4.4** and **4.5** via the novel enantioselective conjugate addition/enolate alkylation annulation reaction as demonstrated in the

previous chapter. The synthesis of the unique ambiphilic vinyl trifluoroborate **4.4** was proposed to start from an inexpensive starting material, 3-butyn-1-ol (**4.9**). That synthesis would require alkynyl methylation, Appel reaction, Miyaura borylation, and recrystallization after aqueous  $\text{KHF}_2$  treatment. The enone functionality in **4.5** could be constructed via a Wittig olefination from aldehyde **4.10**, which would be obtained from **4.11** using lithiation chemistry. It was anticipated the ether formation from resorcinol **4.12** should give high yield of **4.11**.

To demonstrate the potential of the annulation for THC analogs that were difficult to synthesize via previous routes, the retrosynthetic analysis of a novel benzofused THC analog **4.13** was also proposed (Figure 4.2). We anticipated that a global deprotection of intermediate **4.14** would also remove the methyl group from the ether on the nucleophile aryl ring, then Lewis acid promoted etherification would form **4.13** in a similar manner as it did in the synthesis of THC (**4.1**). The key benzannulated intermediate **4.14** could be obtained from building blocks **4.15** and **4.5** via enantioselective conjugate addition/enolate alkylation annulation reaction. The novel ambiphilic aryl trifluoroborate **4.15** could be obtained by recrystallization after treating arylboronate **4.16** with aqueous  $\text{KHF}_2$  solution. Aryl bromide **4.17** could be transformed into **4.16** via a modified Miyaura borylation. Appel reaction would provide a reliable route for incorporation of electrophilic functionality to alcohol **4.18**, which would be synthesized by a sequence of bromination of carboxylic acid **4.20** followed by treatment with a strong reductant. Enone **4.5** was proposed to be prepared from olivetol **4.12** as in Figure 4.1.

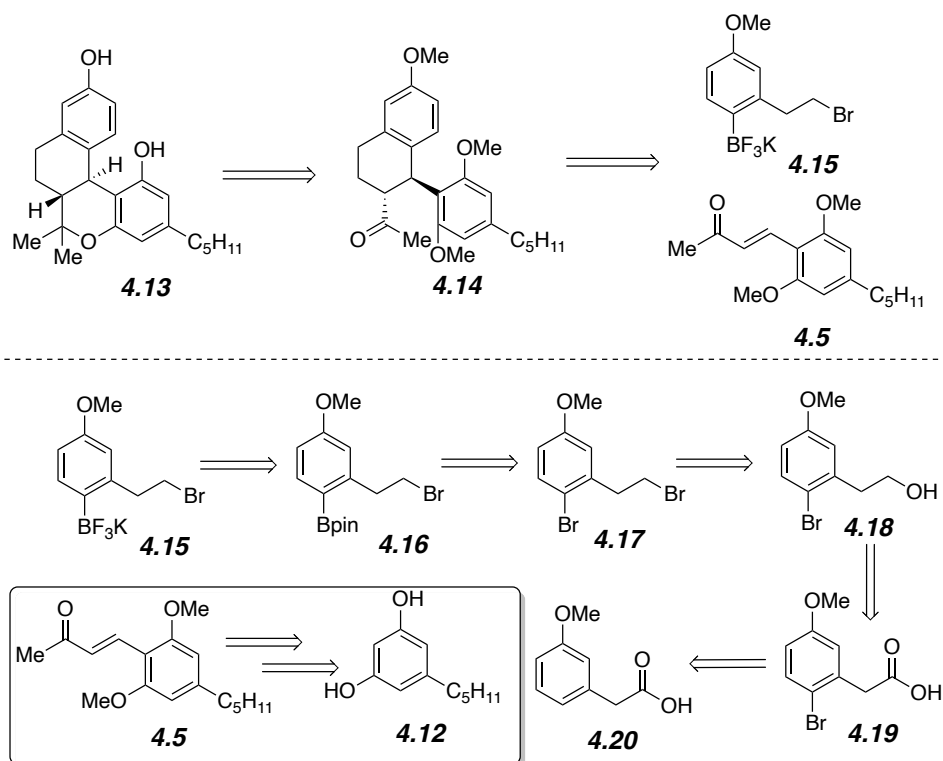
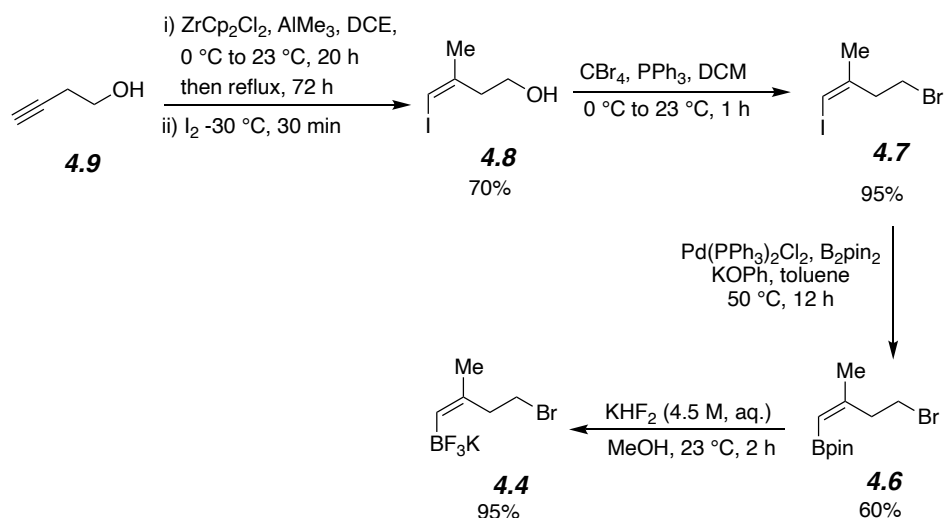


**Figure 4.2.** Retrosynthetic analysis of novel THC analog 13

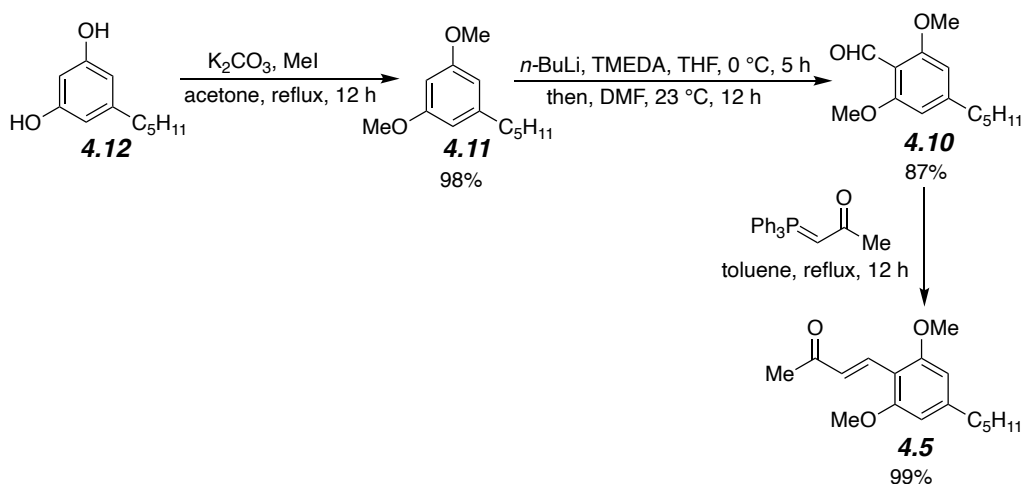
## 4.2 Total Synthesis of THC (4.1) and CBD (4.2)

The total syntheses of THC (4.1) and CBD (4.2) both commenced with the synthesis of the novel ambiphilic vinyl trifluoroborate 4.4 (Scheme 4.1). The vinyl iodide alkyl alcohol 4.8 was successfully obtained from 3-butyn-1-ol in 70% yield using conditions modified from the original report by Negishi.<sup>1</sup> The following Appel reaction efficiently incorporated the electrophilic bromide, transforming alkyl alcohol 4.8 into alkyl bromide 4.7 in 95% yield. After applying modified Miyaura borylation conditions to 4.7,<sup>2</sup> the vinyl boronate 4.6 was obtained in 60% yield. Recrystallization after treating 4.6 with aqueous  $\text{KHF}_2$  solution gave the desired ambiphilic vinyl trifluoroborate 4.4 in 95% as white crystalline solid.



**Scheme 4.1.** Synthesis of ambiphilic vinyl trifluoroborate **4**

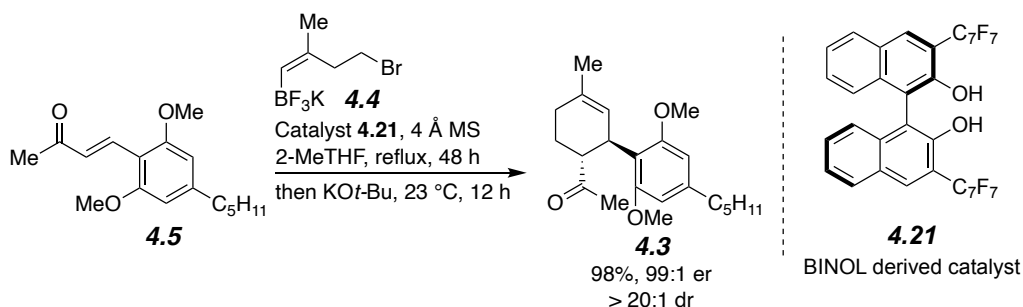
Enone **4.5** was prepared following literature procedures (Scheme 4.2).<sup>3,4</sup> From commercially available olivetol (**4.12**), methyl protection of the both hydroxyls gave bis-ether **4.11** in almost quantitative yield. Aldehyde **4.10** was obtained in 87% yield from bis-ether **4.11** after lithiation and a DMF quench. Enone **4.5** was synthesized via Wittig olefination of aldehyde **4.10** quantitatively.



**Scheme 4.2.** Synthesis of enone **4.5**

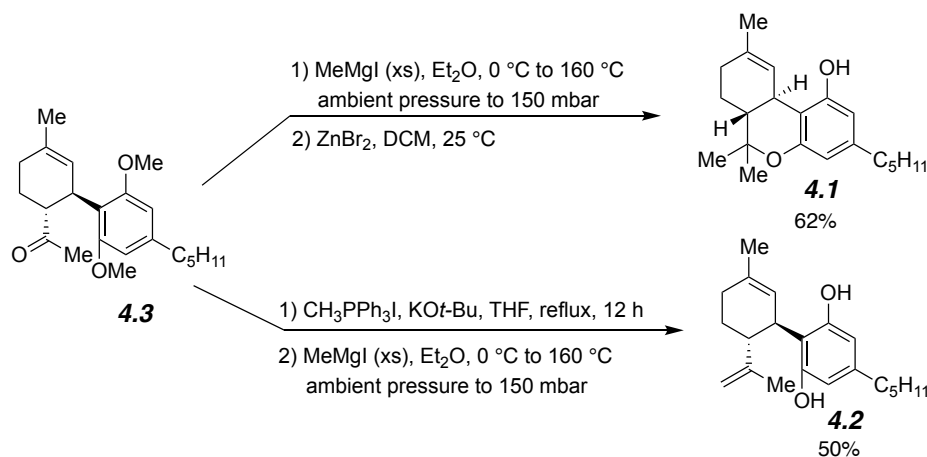
The key cyclohexene **4.3** was then rapidly generated from **4.4** and **4.5** via the 3-3'-perfluorotoluylyl BINOL catalyzed enantioselective conjugate addition/enolate alkylation annulation reaction. This reaction was extremely effective: **4.3** was obtained as a single

diastereomer in 98% yield with 99:1 ee. Notably, this reaction could be scaled up to 1 mmol with only 1.2 equivalent of trifluoroborate **4.4** in 1 M concentration while continuing to provide consistently high yields and selectivity.



**Scheme 4.3.** Synthesis of key intermediate **4.3**

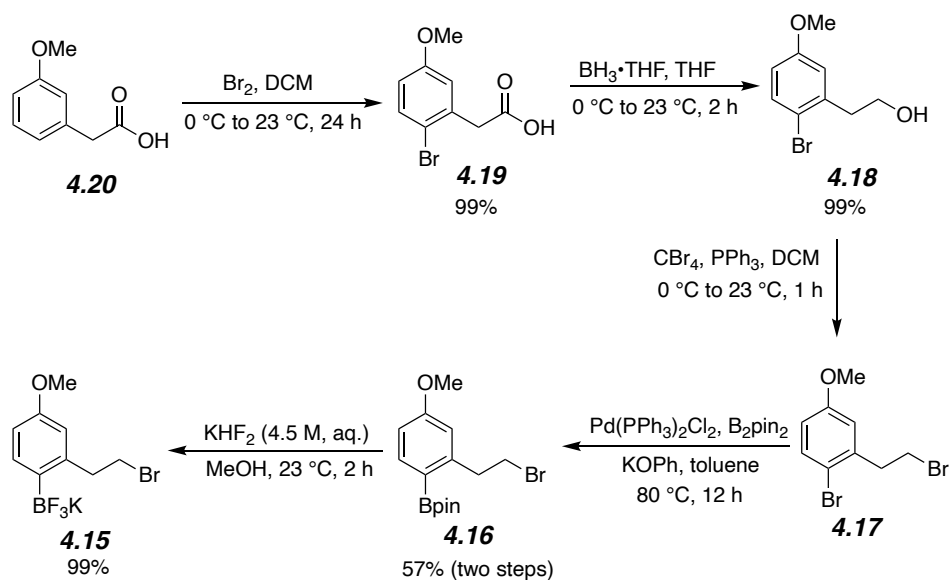
The last step of the THC synthesis was then completed in 62% yield and high enantiopurity after treatment of **4.3** with an excess of methyl magnesium iodide and ZnBr<sub>2</sub> (Scheme 4.4).<sup>Error!</sup> <sup>Bookmark not defined,</sup><sup>5</sup> This synthetic route provided an overall yield of THC in 23% yield for the 7-step longest linear sequence, tying the shortest synthesis reported by the Evans group<sup>6</sup> and doubling their overall yield. CBD was also synthesized from **4.3** by the deprotection of the methoxy groups after a Wittig olefination (Scheme 4.4).<sup>Error!</sup> <sup>Bookmark not defined.</sup>



**Scheme 4.4.** Synthesis of THC and CBD

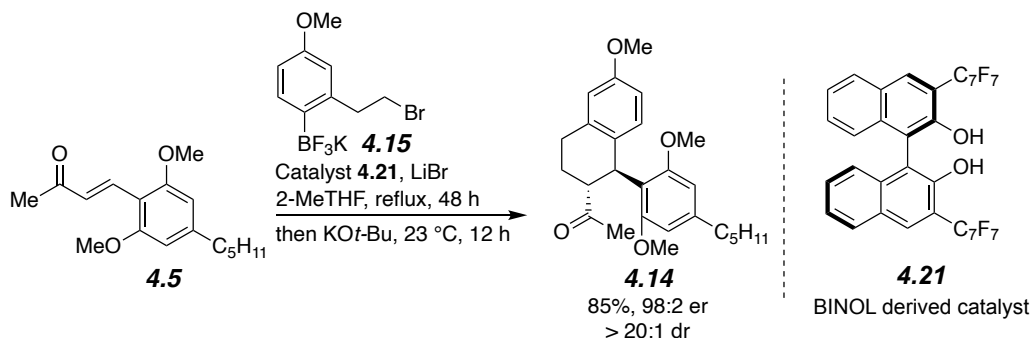
### 4.3 Total Synthesis of Novel THC Analog 4.13

In an approach similar to the syntheses of THC and CBD, the synthesis of analog **4.13** commenced with ambiphilic aryl trifluoroborate **4.15** (Scheme 4.5). Starting with commercially available carboxylic acid **4.20**, aryl bromide acid **4.19** was obtained in almost quantitative yield via bromination. Reduction with borane gave the alcohol **4.18** in 99% yield. Another Appel reaction and Miyaura borylation gave aryl pinacolborane alkyl bromide **4.16** in 57% yield. Treatment with aqueous  $\text{KHF}_2$  synthesized ambiphilic aryl trifluoroborate **4.15** in 99% yield.



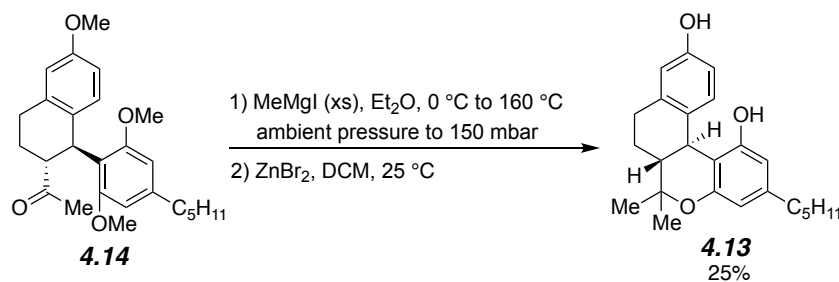
**Scheme 4.5.** Synthesis of ambiphilic aryl trifluoroborate **4.15**

The ambiphilic aryl trifluoroborate **4.15** was then combined with readily synthesized enone **4.5** and utilized in the 3-3'-perfluorotoluylyl BINOL catalyzed enantioselective conjugate addition/enolate alkylation annulation reaction (Scheme 4.6). The aryl-fused intermediate **4.14** was obtained as a single diastereomer in 90% yield with 98:2 ee.



**Scheme 4.6.** Synthesis of aryl-fused intermediate **4.14**

To complete the synthesis of the analog **4.13**, conditions similar to those utilized in the synthesis of THC were applied to the aryl-fused intermediate **4.14** (Scheme 4.7). Because the nucleophile also bore a methyl ether group, we anticipated that it would be deprotected and produce the phenolic hydroxyl. The reaction worked as planned, and the novel THC analog was obtained in 25% yield. This was the first time this analog had ever been made, demonstrating the potential of our methodology to access various analogs that were inaccessible via previous routes.



**Scheme 4.7.** Synthesis of novel THC analog **4.13**

#### 4.4 Conclusion

The total synthesis of THC and CBD was accomplished in high efficiency via a novel conjugate addition/enolate alkylation annulation reaction enabled by sophisticated ambiphilic organoborate alkyl halides, which set two adjacent stereocenters in a single reaction with incredibly high selectivity. This novel arrangement of nucleophilic and electrophilic functionality is impossible for most other nucleophiles, but these ambiphilic boronates are readily synthesized

and bench stable. By simple modification of trifluoroborate ambiphiles, analogs of cannabinoids that were previously inaccessible by prior enantioselective catalytic routes can now be obtained in good yields and excellent enantiopurities. We anticipate more novel analogs will be obtained via this method and we will work promptly to test the potency of their biological activities.

## 4.5 Experimental

### 4.5.1 Methods and Materials

All reactions were carried out in flame- or oven-dried glassware under a positive pressure of argon unless the reaction contained water as a solvent. Dichloromethane, toluene, THF and acetonitrile were purged with argon and dried over activated alumina columns. 1,2-dichloroethane was freshly distilled from CaH<sub>2</sub> before use. 2-Methyl-tetrahydrofuran (2-MeTHF) was purchased from Acros Organics MS as “extra dry 99%+ stabilizer free” in an AcroSeal bottle. Flash chromatography was performed using 60 Å silica gel (Sigma Aldrich). Preparative and analytical plate chromatography was performed on Sigma Aldrich silica gel plates, 250 µm thickness, 60 Å pore size, with UV light at 254 nm used to visualize the plates. Chemical names were generated using Cambridge Soft ChemBioDraw Ultra 12.0. Analysis by HPLC was performed on a Shimadzu Prominence LC (LC-20AB) equipped with an SPD-20A UV-Vis detector (190 nm–400 nm) and a Chiralpak or Chiralcel (250 mm x 4.6 mm) column (see below for column details). The <sup>1</sup>H, <sup>13</sup>C, <sup>11</sup>B, and <sup>19</sup>F NMR spectra were recorded on a JEOL ECA-600, ECA-500, or ECX-400P spectrometer using the residual solvent peak as an internal standard (CDCl<sub>3</sub>: 7.25 ppm for <sup>1</sup>H NMR and 77.00 ppm for <sup>13</sup>C NMR). NMR yields were determined by addition of 1 equivalent of methyl (4-nitrophenyl) carboxylate or *trans*-stilbene as an internal standard to the crude reaction mixture. IR spectra were obtained using a ThermoNicolet Avatar 370 FT-IR instrument. HRMS analyses

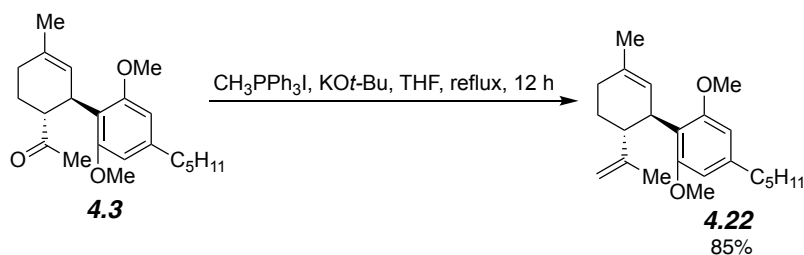
were performed under contract by UT Austin's mass spectrometric facility via an Agilent 6546 Q-TOF LC/MS (high res ESI), Agilent 6530 Q-TOP LC/MS (high resolution CI, APCI or APPI), or Waters Autospec GC/MS (high resolution CI) instrument. Optical rotation was measured by ATAGO PIKAX-2L equipped with a 589 nm light source, and the sample solution was loaded in a 50 mm quartz observation tube.

Commercially available compounds were purchased from Sigma Aldrich, Acros, Combi-Blocks, Oakwood Chemical, Alfa Aesar, Ambeed, ArkPharm, Beantown Chemical, TCI, and Cambridge Isotope Laboratories and were used without further purification.

Experimental procedures for compounds **4.4**, **4.6**, **4.7**, **4.8**, **4.15**, **4.16**, **4.17**, **4.18**, and **4.19** have been reported in experimental section of Chapter 2.

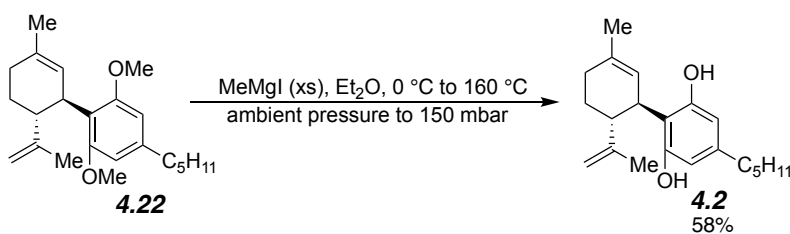
Experimental procedures for compounds **4.3**, **4.5**, **4.10**, **4.11**, and **4.21** have been reported in experimental section of Chapter 3.

#### 4.5.2 Synthesis of CBD **4.2**



In a flame-dried 50 mL round bottom flask equipped with a stir bar, iodo(methyl)triphenylphosphorane (626.2 mg, 1.55 mmol, 2.5 equiv) was dissolved in THF (25 mL). Potassium tert-butoxide (174 mg, 1.55 mmol, 2.5 equiv) was added in one portion. The reaction was stirred at room temperature to form a fine suspension before (*R,R*)-**4.3** (213 mg, 0.62 mmol, 1 equiv) was added. The reaction was then heated to reflux for 12 hours and then cooled to room temperature and quenched by the addition of a saturated aqueous  $\text{NH}_4\text{Cl}$  solution (20 mL).

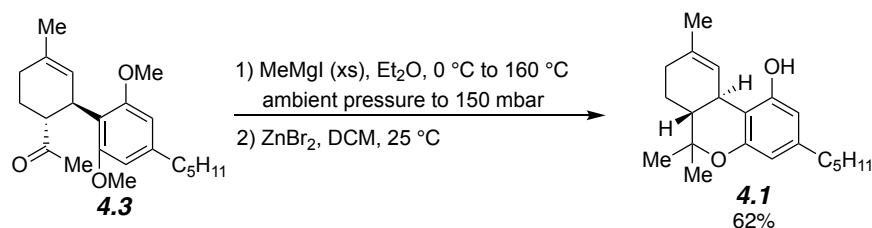
The aqueous layer was extracted with ethyl acetate (10 ml x 3), and the combined organic layers were washed with brine (30 mL) and dried over anhydrous MgSO<sub>4</sub>. The solvent was removed under reduced pressure. The crude product was purified by silica gel column chromatography using 5% ethyl acetate in hexanes to provide **(R,R)-4.22** (180.8 mg, 85% yield) as a light yellow oil. <sup>1</sup>H-NMR (500 MHz, chloroform-d) δ 6.32 (s, 2H), 5.19 (s, 1H), 4.43 (q, *J* = 1.3 Hz, 1H), 4.41 (s, 1H), 3.99-3.96 (m, 1H), 3.72 (s, 6H), 2.89 (td, *J* = 11.0, 3.9 Hz, 1H), 2.52 (t, *J* = 7.9 Hz, 2H), 2.20-2.15 (m, 1H), 1.97 (d, *J* = 16.9 Hz, 1H), 1.76-1.69 (m, 2H), 1.65 (s, 3H), 1.61-1.58 (m, 5H), 1.35-1.28 (m, 4H), 0.89 (t, *J* = 6.9 Hz, 3H). All spectral data match literature report. **Error! Bookmark not defined.**



In a flame-dried 20 mL round bottom flask equipped with a stir bar, **(R,R)-SI-24** (140 mg, 0.4 mmol, 1 equiv) was added in anhydrous ether (4 mL) before being cooled to 0 C°. Methyl magnesium iodide (1.17 mL, 3.5 mmol, 3 M in ether, 8 equiv) was added dropwise. The reaction was allowed to warm up to room temperature and stir for 20 minutes. Then the reaction was heated to 160 C° under reduced pressure (150 mbar) for 1.5 hours. After completion, the reaction was warmed up to room temperature then cooled to 0 C° before being quenched by addition of a saturated aqueous NH<sub>4</sub>Cl solution (5 mL). The aqueous layer was extracted with ether (10 mL x 3). The combined organic layer was washed with brine (15 mL) and dried over anhydrous MgSO<sub>4</sub>. The solvent was removed under reduced pressure. The crude product was purified by silica gel column chromatography using 5-10% ethyl acetate in hexanes to provide **(-)-2** (72.5 mg, 58% yield)

as a light yellow oil.  $^1\text{H-NMR}$  (400 MHz, chloroform- $d$ )  $\delta$  6.27-6.14 (m, 2H), 5.97 (s, 1H), 5.56 (s, 1H), 4.65-4.54 (m, 3H), 3.83 (d,  $J = 8.7$  Hz, 1H), 2.44-2.36 (m, 3H), 2.26-2.19 (m, 1H), 2.10-2.06 (m, 1H), 1.83-1.74 (m, 5H), 1.64 (s, 3H), 1.54-1.48 (m, 2H), 1.31-1.24 (m, 4H), 0.86 (t,  $J = 6.9$  Hz, 3H).  $^{13}\text{C-NMR}$  (101 MHz, chloroform- $d$ )  $\delta$  149.4, 143.1, 140.2, 124.2, 113.8, 111.0, 109.8, 108.1, 46.3, 37.2, 35.6, 31.6, 30.8, 30.5, 28.5, 23.8, 22.6, 20.5, 14.2.  $[\alpha]_{\text{D}}^{20} = -130$  ( $c=1.0$ , EtOH), lit.  $[\alpha]_{\text{D}}^{19} = -129$  ( $c=0.49$ , EtOH).<sup>7</sup> All spectral data match the literature report. **Error! Bookmark not defined.**

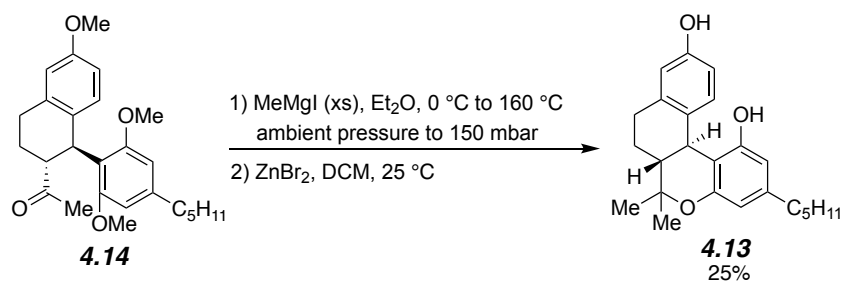
### 4.5.3 Synthesis of THC 4.1



In a flame-dried 10 mL round bottom flask equipped with a stir bar, (*R, R*)-**4.3** (86 mg, 0.25 mmol, 1 equiv) was added to anhydrous ether (1.25 mL) before being cooled to 0 °C. Methyl magnesium iodide (0.85 mL, 2.55 mmol, 3 M in ether, 10 equiv) was added dropwise. The reaction was allowed to warm to room temperature and stirred for 20 minutes. The reaction was heated to 160 °C under reduced pressure (150 mbar) for 50 minutes. After completion, the reaction was allowed to cool to room temperature, then cooled to 0 °C in an ice bath before being quenched by the addition of a saturated aqueous NH<sub>4</sub>Cl solution (5 mL). The aqueous layer was extracted with ether (10 mL x 3). The combined organic layers were washed with brine (15 mL) and dried over anhydrous MgSO<sub>4</sub>. The solvent was removed under reduced pressure. The crude product was dissolved in DCM (3 mL), and then ZnBr<sub>2</sub> (81.1 mg, 0.36 mmol, 1.4 equiv) and anhydrous MgSO<sub>4</sub> (120 mg, 1 mmol, 4 equiv) were added. The resulting suspension was allowed to stir at room temperature for 4 h. The reaction was quenched by the addition of a saturated aqueous NH<sub>4</sub>Cl

solution (10 mL). The aqueous layer was extracted with DCM (10 mL x 3). The combined organic layers were washed with brine (20 mL) and dried over anhydrous MgSO<sub>4</sub>. The solvent was removed under reduced pressure. The crude product was purified by silica gel column chromatography using 5% ether in hexanes to provide (-)-**4.1** (48.4 mg, 62% yield) as a light yellow oil. <sup>1</sup>H-NMR (400 MHz, chloroform-d) δ 6.31 (s, 1H), 6.27 (s, 1H), 6.13 (s, 1H), 4.96 (s, 1H), 3.20 (d, *J* = 10.8 Hz, 1H), 2.44-2.40 (m, 2H), 2.16 (t, *J* = 4.0 Hz, 2H), 1.93-1.89 (m, 1H), 1.72-1.67 (m, 4H), 1.57-1.50 (m, 2H), 1.44-1.37 (m, 4H), 1.27 (t, *J* = 6.6 Hz, 4H), 1.09 (s, 3H), 0.87 (t, *J* = 6.8 Hz, 3H). <sup>13</sup>C-NMR (101 MHz, chloroform-d) δ 154.8, 154.3, 142.9, 134.5, 123.8, 110.1, 109.1, 107.7, 45.9, 35.6, 33.7, 31.6, 31.3, 30.8, 27.7, 25.1, 23.5, 22.7, 19.4, 14.1. [α]<sup>20</sup><sub>D</sub> = -150 (c=1.0, CHCl<sub>3</sub>) lit. [α]<sup>25</sup><sub>D</sub> = -152 (c=1.0, CHCl<sub>3</sub>).<sup>8</sup> All spectral data match the literature reports. **Error! Bookmark not defined.**

#### 4.5.4 Synthesis of Analog 4.13



In a flame-dried 10 mL round bottom flask equipped with a stir bar, (*R, R*)-**4.14** (144 mg, 0.43 mmol, 1 equiv) was added to anhydrous ether (2 mL) before being cooled to 0 °C. Methyl magnesium iodide (2.15 mL, 3 mmol, 3 M in ether, 15 equiv) was added dropwise. The reaction was allowed to warm up to room temperature and stir for 20 minutes. Then the reaction was heated to 160 °C under reduced pressure (150 mbar) for 50 minutes. After completion, the reaction was allowed to cool to room temperature, and then it was further cooled to 0 °C in an ice bath before

being quenched by addition of a saturated aqueous NH<sub>4</sub>Cl solution (5 mL). The aqueous layer was extracted with ether (10 mL x 3). The combined organic layers were washed with brine (15 mL) and dried over anhydrous MgSO<sub>4</sub>. The solvent was removed under reduced pressure. The crude product was dissolved in DCM (3 mL), and then ZnBr<sub>2</sub> (135.0 mg, 0.60 mmol, 1.4 equiv) and anhydrous MgSO<sub>4</sub> (207 mg, 1.72 mmol, 4 equiv) were added. The resulted suspension was allowed to stir at room temperature for 4 h. The reaction was then quenched by the addition of a saturated aqueous NH<sub>4</sub>Cl solution (10 mL). The aqueous layer was extracted with DCM (10 mL x 3). The combined organic layer was washed with brine (20 mL) and dried over anhydrous MgSO<sub>4</sub>. The solvent was removed under reduced vacuum. The crude product was purified by silica gel column chromatography using 15-20% ether in hexanes to provide (*R, R*)-**4.13** (39.6 mg, 25 % yield) as a light yellow sticky oil. This compound will be very quickly oxidized by atmospheric oxygen if not stored in the freezer under an atmosphere of inert gas. **<sup>1</sup>H-NMR** (400 MHz, chloroform-d) δ 6.85 (d, *J* = 8.7 Hz, 1H), 6.73 (s, 1H), 6.59 (d, *J* = 14.7 Hz, 1H), 6.38 (s, 2H), 4.61 (broad, 2H), 3.43 (d, *J* = 9.6 Hz, 1H), 2.93-2.78 (m, 2H), 2.37-2.60 (m, 2H), 1.89-1.81 (m, 1H), 1.63-1.59 (m, 4H), 1.33 (broad, 7H), 1.19 (broad, 3H), 0.89 (m, 3H). **<sup>13</sup>C-NMR** (101 MHz, chloroform-d) δ 155.1, 154.4, 154.3, 144.0, 140.5, 132.0, 124.7, 115.5, 112.3, 110.8, 108.3, 106.8, 48.0, 35.8, 34.0, 31.7, 30.7, 27.5, 27.2, 22.7, 22.3, 18.5, 14.2. **HRMS-ESI m/z** calcd. for C<sub>24</sub>H<sub>30</sub>O<sub>3</sub> [M-H]<sup>-</sup> 365.2122, found 365.2119.

#### 4.6 Bibliography

1. Ma, S.; Negishi, E. *Anti-Carbometalation of Homopropargyl Alcohols and Their Higher Homologues via Non-Chelation-Controlled Syn-Carbometalation and Chelation-Controlled Isomerization*. *J. Org. Chem.* **1997**, *62*, 784–785.

2. Please see Experimental Section in Chapter 2 for details.
3. Trost, B. M.; Dogra, K. Synthesis of (-)- $\Delta^9$ -*trans*-Tetrahydrocannabinol: Stereocontrol via Mo-Catalyzed Asymmetric Allylic Alkylation Reaction. *Org. Lett.* **2007**, *9*, 861–863.
4. Shultz, Z. P.; Lawrence, G. A.; Jacobson, J. M.; Cruz, E. J.; Leahy, J. W. Enantioselective Total Synthesis of Cannabinoids—A Route for Analogue Development. *Org. Lett.* **2018**, *20*, 381–384.
5. Schafroth, M. A.; Zuccarello, G.; Krautwald, S.; Sarlah, D.; Carreira, E. M. Stereodivergent Total Synthesis of  $\Delta^9$ -Tetrahydrocannabinols. *Angew. Chem. Int. Ed.* **2014**, *53*, 13898–13901.
6. Evans, D. A.; Shaughnessy, E. A.; Barnes, D. M. Cationic Bis(oxazoline)Cu(II) Lewis Acid Catalysts. Application to the Asymmetric Synthesis of ent- $\Delta^1$ -Tetrahydrocannabinol. *Tetrahedron Lett.* **1997**, *38*, 3193–3194.
7. Petrzilka, T.; Haefliger, W.; Sikemeier, C.; Ohloff, G.; Eschenmoser, A. Synthese und Chiralität des (-)-Cannabidiols Vorläufige Mitteilung *Helv. Chim. Acta* **1967**, *50*, 719-723.
8. Choi, Y. H.; Hazekamp, A.; Peltenburg-Looman, A. M. G.; Frédérich, M.; Erkelens, C. NMR assignments of the major cannabinoids and cannabiflavonoids isolated from flowers of *Cannabis sativa* *Phytochem. Anal.* **2004**, *15*, 345-354.

## **Chapter 4**

## **Appendix**

